

Unclassified

SECURITY CLASSIFICATION OF THIS PAGE (When Data Entered)

REPORT DOCUMENTATION PAGE		READ INSTRUCTIONS BEFORE COMPLETING FORM
1. REPORT NUMBER Technical Report GL-79-4	2. GOVT ACCESSION NO.	3. RECIPIENT'S CATALOG NUMBER
4. TITLE (and Subtitle) DEVELOPMENT OF A STRUCTURAL DESIGN PROCEDURE FOR RIGID AIRPORT PAVEMENTS	5. TYPE OF REPORT & PERIOD COVERED Final Report	
	6. PERFORMING ORG. REPORT NUMBER	
7. AUTHOR(s) Frazier Parker, Jr., Walter R. Barker, Robert C. Gunkel, and Eugene C. Odom	8. CONTRACT OR GRANT NUMBER(s) Inter-Agency Agreement No. DOT-FA78WAI-377	
9. PERFORMING ORGANIZATION NAME AND ADDRESS U. S. Army Engineer Waterways Experiment Station Geotechnical Laboratory P. O. Box 631, Vicksburg, Miss. 39180	10. PROGRAM ELEMENT, PROJECT, TASK AREA & WORK UNIT NUMBERS Project Nos. 4A762719AT04 and 4A161102B52E	
11. CONTROLLING OFFICE NAME AND ADDRESS Office, Chief of Engineers, U. S. Army, Washington, D. C. 20314; and Federal Aviation Administration, Washington, D. C. 20591	12. REPORT DATE April 1979	
	13. NUMBER OF PAGES 297	
14. MONITORING AGENCY NAME & ADDRESS (if different from Controlling Office)	15. SECURITY CLASS. (of this report) Unclassified	
	15a. DECLASSIFICATION/DOWNGRADING SCHEDULE	
16. DISTRIBUTION STATEMENT (of this Report) Approved for public release; distribution unlimited.		
17. DISTRIBUTION STATEMENT (of the abstract entered in Block 20, if different from Report)		
18. SUPPLEMENTARY NOTES Also published as Federal Aviation Administration Report No. FAA-RD-77-81.		
19. KEY WORDS (Continue on reverse side if necessary and identify by block number)  Airport pavements Pavement design Rigid pavements		
20. ABSTRACT (Continue on reverse side if necessary and identify by block number) The development and formulation of a design procedure for rigid airport pavements are presented. The design criteria used in the procedure are based on the tensile stress in the portland cement concrete (PCC) slab as computed by layered elastic theory and the strength of the PCC slab as measured in the flexural beam test. The criteria were developed by the analysis of some 60 test sections. Procedures are given for the characterization of the pavement materials both by laboratory testing and by typical values and/or correlation (Continued)		

20. ABSTRACT (Continued).

studies. The thickness requirements as determined by the new criteria are compared with the thickness as determined by present Corps of Engineers-Federal Aviation Administration design procedures.



## PREFACE

The study described herein was sponsored by the Federal Aviation Administration as a part of Inter-Agency Agreement No. DOT-FA78WAI-377, "New Pavement Design Methodology," and by the Office, Chief of Engineers, U. S. Army, as a part of Military Construction RDTE Project No. 4A762719AT04, "Pavements, Soils, and Foundations," and Military Engineering RDTE Project No. 4A161102B52E, "Research in Military Engineering and Construction."

The study was conducted under the general supervision of Mr. J. P. Sale, Chief of the Geotechnical Laboratory, U. S. Army Engineer Waterways Experiment Station (WES). This report was prepared by Drs. Frazier Parker, Jr., and Walter R. Barker and Messrs. Robert C. Gunkel and Eugene C. Odom.

Directors of the WES during the study were COL G. H. Hilt, CE, and COL J. L. Cannon, CE. Technical Director was Mr. F. R. Brown.

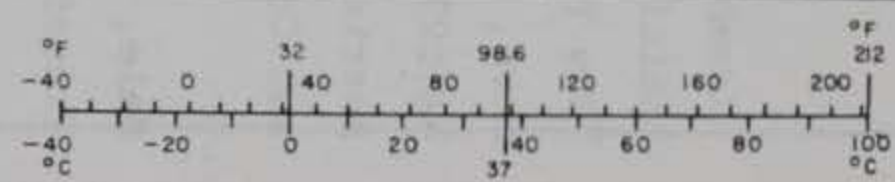
## METRIC CONVERSION FACTORS

### Approximate Conversions to Metric Measures

Symbol	When You Know	Multiply by	To Find	Symbol
<b>LENGTH</b>				
in	inches	*2.5	centimeters	cm
ft	feet	30	centimeters	cm
yd	yards	0.9	meters	m
mi	miles	1.6	kilometers	km
<b>AREA</b>				
in <sup>2</sup>	square inches	6.5	square centimeters	cm <sup>2</sup>
ft <sup>2</sup>	square feet	0.09	square meters	m <sup>2</sup>
yd <sup>2</sup>	square yards	0.8	square meters	m <sup>2</sup>
mi <sup>2</sup>	square miles	2.6	square kilometers	km <sup>2</sup>
	acres	0.4	hectares	ha
<b>MASS (weight)</b>				
oz	ounces	28	grams	g
lb	pounds	0.45	kilograms	kg
	short tons (2000 lb)	0.9	tonnes	t
<b>VOLUME</b>				
tsp	teaspoons	5	milliliters	ml
Tbsp	tablespoons	15	milliliters	ml
fl oz	fluid ounces	30	milliliters	ml
c	cups	0.24	liters	l
pt	pints	0.47	liters	l
qt	quarts	0.95	liters	l
gal	gallons	3.8	liters	l
ft <sup>3</sup>	cubic feet	0.03	cubic meters	m <sup>3</sup>
yd <sup>3</sup>	cubic yards	0.76	cubic meters	m <sup>3</sup>
<b>TEMPERATURE (exact)</b>				
°F	Fahrenheit temperature	5/9 (after subtracting 32)	Celsius temperature	°C

### Approximate Conversions from Metric Measures

Symbol	When You Know	Multiply by	To Find	Symbol
<b>LENGTH</b>				
mm	millimeters	0.04	inches	in
cm	centimeters	0.4	inches	in
m	meters	3.3	feet	ft
m	meters	1.1	yards	yd
km	kilometers	0.6	miles	mi
<b>AREA</b>				
cm <sup>2</sup>	square centimeters	0.16	square inches	in <sup>2</sup>
m <sup>2</sup>	square meters	1.2	square yards	yd <sup>2</sup>
km <sup>2</sup>	square kilometers	0.4	square miles	mi <sup>2</sup>
ha	hectares (10,000 m <sup>2</sup> )	2.5	acres	
<b>MASS (weight)</b>				
g	grams	0.035	ounces	oz
kg	kilograms	2.2	pounds	lb
t	tonnes (1000 kg)	1.1	short tons	
<b>VOLUME</b>				
ml	milliliters	0.03	fluid ounces	fl oz
l	liters	2.1	pints	pt
l	liters	1.06	quarts	qt
l	liters	0.26	gallons	gal
m <sup>3</sup>	cubic meters	35	cubic feet	ft <sup>3</sup>
m <sup>3</sup>	cubic meters	1.3	cubic yards	yd <sup>3</sup>
<b>TEMPERATURE (exact)</b>				
°C	Celsius temperature	9/5 (then add 32)	Fahrenheit temperature	°F



\*1 in. = 2.54 (exactly). For other exact conversions and more detailed tables, see NBS Misc. Publ. 286, Units of Weights and Measures, Price \$2.25, SD Catalog No. C13.10-286.



## TABLE OF CONTENTS

	<u>Page</u>
INTRODUCTION . . . . .	1
BACKGROUND . . . . .	1
PURPOSE . . . . .	2
SCOPE . . . . .	2
APPROACH . . . . .	3
SELECTION OF RESPONSE MODEL . . . . .	4
GENERAL . . . . .	4
COMPARISONS OF AVAILABLE MODELS . . . . .	4
SELECTION OF COMPUTATIONAL PROCEDURE . . . . .	11
MODIFICATION OF MODEL FOR FINITE SUBGRADE DEPTHS . . . . .	15
SELECTION OF MATERIAL CHARACTERIZATION PROCEDURES . . . . .	28
GENERAL . . . . .	28
EFFECTS OF LOAD REPETITIONS . . . . .	32
MODULUS OF ELASTICITY AND POISSON'S RATIO . . . . .	35
SUMMARY . . . . .	38
DEVELOPMENT OF PERFORMANCE CRITERIA . . . . .	41
GENERAL . . . . .	41
FULL-SCALE ACCELERATED TEST . . . . .	46
ASSIGNMENT OF MATERIAL PROPERTIES TO TEST PAVEMENTS . . . . .	48
LIMITING STRESS CRITERIA . . . . .	53
VERTICAL DEFLECTION CRITERIA . . . . .	57
CRITERIA FOR OVERLAY AND REINFORCED SLAB DESIGN . . . . .	64
ASSEMBLY OF PROCEDURE FOR DESIGN . . . . .	72
GENERAL . . . . .	72
MATERIAL SAMPLING . . . . .	72
MATERIAL CHARACTERIZATION . . . . .	74
LAYERED SYSTEM DESIGN . . . . .	78
COMPARISON OF CRITERIA . . . . .	98
JOINT DESIGN . . . . .	107
TRANSLATION FROM DESIGN TO CONSTRUCTION . . . . .	108
CONCLUSIONS AND RECOMMENDATIONS . . . . .	110
APPENDIX A: DEVELOPMENT OF MATERIAL CHARACTERIZATION PROCEDURES . . . . .	A-1

	<u>Page</u>
APPENDIX B: DESCRIPTION OF TEST PAVEMENTS . . . . .	B-1
APPENDIX C: LABORATORY PROCEDURE FOR DETERMINING THE FLEXURAL MODULUS OF BOUND BASES . . . . .	C-1
APPENDIX D: LABORATORY PROCEDURE FOR DETERMINING THE RESILIENT MODULUS OF GRANULAR BASE MATERIALS . . . . .	D-1
APPENDIX E: LABORATORY PROCEDURE FOR DETERMINING THE RESILIENT MODULUS OF SUBGRADE SOILS . . . . .	E-1
APPENDIX F: APPENDIX F: USER INFORMATION FOR THE BISAR COMPUTER PROGRAM . . . . .	F-1
APPENDIX G: REFERENCES . . . . .	G-1



## INTRODUCTION

### BACKGROUND

The motivation for developing a new structural design procedure for rigid airport pavements is that currently available procedures<sup>1-5</sup> have several weaknesses. This does not imply that the existing procedures are not valid, nor does it imply that any proposed new procedure will alleviate all of the weaknesses of the existing procedures.

Rather, the proposed procedure will permit consideration of several design aspects that are ignored or approximated in available procedures.

The procedures described in References 1-5 are similar in approach with variations only in certain details. Of interest is the common approach to modeling the pavement and characterizing the supporting characteristics of the material beneath the portland cement concrete (PCC) surface layer. In all five procedures, the pavement is modeled as a two-layer system, i.e., the PCC surface layer is described as a thin elastic plate, and the underlying material is described as a dense liquid (Winkler) foundation.<sup>6,7</sup> Other important common features of all five procedures are: (a) the supporting characteristics of underlying materials are quantified by a single constant, referred to as the modulus of soil reaction; and (b) this constant is determined with plate load tests conducted on in situ materials.<sup>8,9</sup>

The validity of using a two-layer model and a plate load test for quantifying the supporting characteristics of the underlying material are questionable for pavements with relatively thin layers of bound material and for vehicle gears with large, widely spaced wheel loads. The procedure developed herein utilizes a layered elastic system for modeling the pavement and should improve the validity of the computed pavement response parameters (stress, strain, and deflection) for all layered systems and loads.

The characterization of each layer with fundamental material properties obtained from laboratory tests, as opposed to field tests on in situ material, will permit more flexibility for testing the material



at a range of field conditions. The use of a layered model and laboratory tests to determine properties of the pavement layers will permit trial of a range of types of materials arranged in various layering schemes in order to determine an optimized design. The use of laboratory tests rather than field plate load tests should permit more tests and, therefore, a better representation of the subgrade.

A final reason for developing a new design procedure for rigid pavements is the belief among some engineers involved in pavement design, evaluation, and research that there should be a universal system applicable to design and evaluation of all types of pavements, rather than separate procedures for rigid, flexible, or unsurfaced pavements. From a philosophical point of view, this goal certainly is desirable and is worth pursuing; but from a practical point of view, there are a number of obstacles that will only be overcome by advances in the state of the art of pavement technology. However, there are many more similarities between the design procedure contained herein for rigid pavements and the design procedure contained in Reference 10 for flexible airport pavement than there are between currently used procedures for rigid and flexible airport pavements. Thus, this design procedure represents a step toward achieving the goal of a universal design procedure.

#### PURPOSE

The purpose of this study was to develop a new, practical, and implementable procedure for the structural design of rigid airport pavements. This report documents the development of the methodology contained in the procedure and presents the procedure in a stepwise manner for implementation.

#### SCOPE

The study was limited to the structural design of the pavement section, i.e., the selection of required thickness of pavement layers to carry the design traffic (magnitude and number of loads) under field conditions. The key words, rigid, practical, implementable, and



design, are reflected in the selection of an available linear elastic response model, available procedures and specific conditions for material characterizations, and simplified alternatives for accounting for traffic and environmental conditions. Certainly more sophisticated response models (finite element) and/or more sophisticated material characterizations (nonlinear, nonelastic, or viscoelastic) are available, but these are more readily applicable to analysis rather than routine design. Available test data were used to establish performance criteria and conditions for material characterization.

No innovations are offered in the treatment of joints in the PCC surface layer, although joints are the critical location in the pavement and models are available for providing at least a rudimentary treatment. It was believed that these models had not been developed to the point where they could be used in routine design. Jointing is considered by specifying certain minimum requirements.

No new methods are offered for the design of overlays. Although the use of the basic methodology for design of new pavements appears valid for design of overlays, no acceptable procedure was found to quantify either the load deformation response of in-place pavements or interface conditions so that the structural condition of the pavement would be reflected in the required overlay thickness, or conversely the performance of the overlay.

## APPROACH

The basic approach taken in the study is outlined in the following four tasks:

- a. Selection of a response model.
- b. Selection of material characterization procedures.
- c. Development of performance criteria.
- d. Assembly of the methodology into a practical, implementable, design procedure.



## SELECTION OF RESPONSE MODEL

### GENERAL

The layered elastic model<sup>11</sup> was selected for computing pavement response parameters. By changing from the presently used model (Westergaard idealization), implications are that the presently used model is inadequate and that the layered model offers significant improvements.<sup>6,7</sup> These implications may not be totally true and may, in fact, be completely erroneous in certain respects and for certain conditions. The problem stems from the judgment of adequacy or what is best. Such judgment is oftentimes subjective, based on opinion rather than fact, and in many cases, based on only a limited range of circumstances. Nevertheless, the selection of the layered elastic response model was based on what was believed to be sound, rational, and practical considerations.

### COMPARISONS OF AVAILABLE MODELS

Crawford and Katona<sup>12</sup> have prepared a state-of-the-art report on the prediction of pavement response. In their discussions, they refer to three types of idealizations of pavement structures. These are the Westergaard, layered elastic, and finite element idealizations. To these primary idealizations should be added several significant mutations and combinations of the three primary idealizations.

Hudson and Matlock<sup>13</sup> developed a model that essentially follows the Westergaard idealization but uses a numerical technique for solving the equations of bending for the thin elastic slab representing the surface layer. The numerical technique is based on finite difference approximations of continuous functions, and the corresponding physical idealization of the elastic slab is similar to the finite element idealization. This idealization will be referred to as the discrete element idealization. A model developed by Saxena<sup>14</sup> combines the discrete element idealization of the elastic slab with an elastic solid idealization of the underlying material rather than a dense liquid idealization. The elastic solid idealization (Boussinesq) is a



simplified version of the layered elastic idealization (Burmister<sup>11</sup>) in that only one semi-infinite layer is considered.

Huang and Wang<sup>15</sup> developed a model that combines the finite element idealization for the thin elastic slab with the dense liquid idealization for the underlying material. A model developed by Eberhardt and Willmer<sup>16,17</sup> is similar to that developed by Huang and Wang, but with an additional feature, such that an intermediate layer can be considered. A procedure was developed in which the top two layers are modeled as an equivalent thin elastic plate. The finite element idealization is then used for the equivalent plate, and the dense liquid idealization for the remainder of the structure.

As stated previously, these four models are simply mutations or combinations of the three primary idealizations and are subject to similar limitations. Therefore, the following discussions are limited to the three primary idealizations.

Crawford and Katona<sup>12</sup> provide detailed discussions of the three primary idealizations and include discussions of various material characterization procedures that are necessary for quantification of properties of the pavement structures. For the reader interested in an in-depth comparison, Reference 12 is recommended. However, a brief comparison follows in which the primary reasons are outlined for selecting a response model based on the layered elastic idealization.

For the layered elastic idealization (Figure 1), the pavement structure is represented as a series of horizontal, uniform, elastic layers with properties defined by (a)  $E_i$ , the modulus of elasticity of the  $i^{\text{th}}$  layer; (b)  $\nu_i$ , the Poisson's ratio of the  $i^{\text{th}}$  layer, and (c)  $h_i$ , the thickness of the  $i^{\text{th}}$  layer. Furthermore, the layers extend horizontally to infinity in all directions, and the  $n^{\text{th}}$  layer extends vertically to infinity. The Westergaard idealization (Figure 2) represents the PCC slab as a thin elastic plate with properties defined by  $E_p$ ,  $\nu_p$ , and  $h_p$ , over a dense liquid (Winkler) foundation. The liquid foundation is characterized as a bed of springs having a certain stiffness. Each individual spring represents the effect of the support



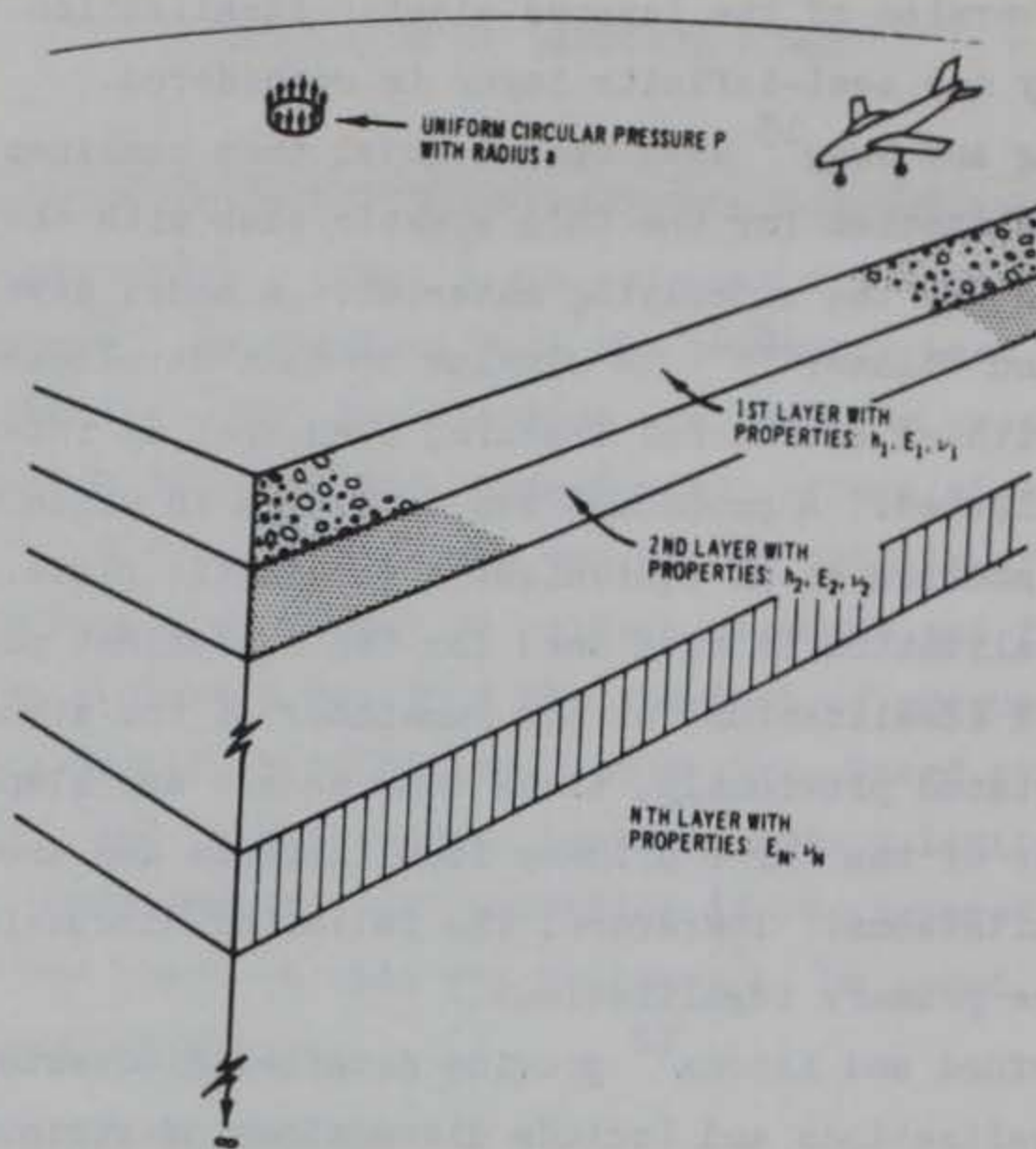


Figure 1. Elastic layered pavement idealization (from Crawford and Katona<sup>12</sup>)

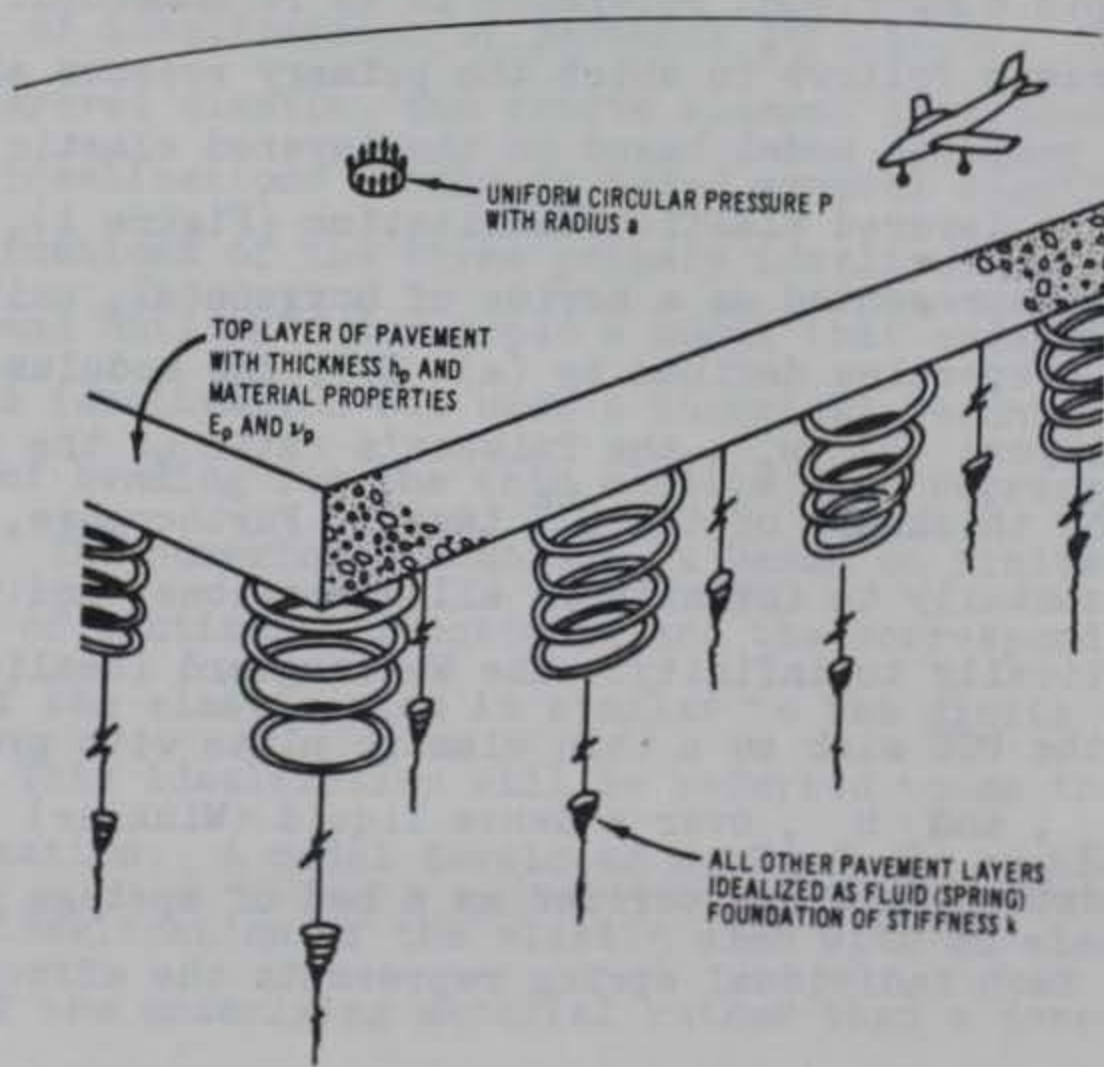


Figure 2. Westergaard pavement idealization (from Crawford and Katona<sup>12</sup>)



provided over a unit area and is quantified by a constant  $k$ , which is the ratio of pressure on the unit area divided by the deflection. In the basic Westergaard idealization, loads were represented as uniform circular pressure distributions, but procedures developed by Pickett et al.<sup>18</sup> and Pickett and Ray<sup>19</sup> permit uniform pressure distributions with any shape to be readily handled.

The elastic layered idealization would appear to be a more realistic representation of a real pavement structure since PCC pavements are truly layered systems, although the materials may not be truly elastic. For practical loadings, however, the materials can be represented by quasi-elastic properties. The representation of the top layer as a thin elastic plate (Westergaard idealization) or as an elastic layer is really not that different when the top layer is a PCC slab, as in rigid pavements. The major difference lies in the representation of the remainder of the structure. The use of fundamental constants  $E$  and  $\nu$  to represent the properties of underlying layers is theoretically sounder than a single constant  $k$ . From a practical standpoint, it is also more valid, considering that the determination of  $k$  is made with a plate test and represents the response of the material to a particular loading condition (i.e., 30-in.\*-diam plate and 10-psi vertical pressure), which may be different from that actually experienced in the pavement.

Experience has shown that, for single, dual, and even dual-tandem gears with closely spaced wheels on relatively thin slabs (less than about 15 in.) laid either directly on the subgrade or on granular layers, quantification of the supporting characteristics of the underlying layer with a modulus of soil reaction produces reasonable computations of the response of the pavement. However, for larger loads transmitted to the pavement through a number of widely spaced wheels, for relatively thin, high-strength (large stiffness) base courses, and for thick PCC slabs, the validity of the idealization decreases. For the thicker slabs and

---

\* A table of factors for converting units of measurement is presented on page iv.



widely spaced wheels, the zone of influence (stresses in the underlying material) becomes much larger than that under a 30-in.-diam plate, although a 10-psi contact pressure may in fact be valid for both conditions. The effect of a thin, high-strength (stiffness) base course will be more pronounced on the load deformation response of a 30-in.-diam plate than on the load deformation response of a thick PCC slab. The response of the 30-in.-diam plate will be significantly reduced by the thin base, whereas the reduction in the response of the pavement will not be as significant.

Another situation in which the use of an elastic layered idealization may be more representative occurs when there exists within the subgrade different types of materials at relatively shallow depths (less than 20 ft). For instance, a stiff or a soft layer in the subgrade may not significantly affect the load deformation response of a 30-in.-diam plate, but the effect may be significant on the load deformation response of a thick slab loaded with a large load on widely spaced wheels.

Characterization of each layer with elastic constants obtained from laboratory tests, rather than one elastic constant obtained from field tests, provides the designer greater flexibility. At this point, it should be noted that it is recognized that the materials in pavements behave neither elastically nor linearly but that the assumption of linear elasticity is necessary for practical application. The state of stress under which the material is tested in the laboratory may be changed to conform to the most critical state of stress under which it may exist in the pavement. This is contrasted with the constant state of stress at which the modulus of soil reaction is selected. There is also the flexibility of being able to readily change the physical condition of the specimen (moisture, pore pressures, density, etc.), whereas this cannot be so easily accomplished on in situ material. Thus, the use of an indirect correction for saturation of the modulus of soil reaction<sup>8</sup> is not necessary.

The use of laboratory procedures makes it possible to test a more representative sample of the existing subgrade and a larger variety



of available base course materials. With the present design procedure, extensive plate bearing tests are the exception rather than the rule. Another factor to be considered is the repetitive nature of the loads applied to a pavement. Certainly, the use of laboratory tests will more readily permit consideration of the effects of repeated load applications than will field plate bearing tests.

In addition to the necessary and practical assumptions of linear elasticity, the layered elastic model has one major weakness when applied to rigid pavements, i.e., the inability to treat discontinuities (cracks and joints) primarily in the PCC layer. In this regard, the Westergaard idealization is better because it does permit a rudimentary treatment of the joints. With the Westergaard idealization, bending stresses in the slab, the vertical slab deflections, or the vertical reactive pressures may be computed at or near the corner or edge of a slab that is semi-infinite in the horizontal direction. Empirical adjustments to these response parameters may then be made to account for the reduction due to support provided by adjacent slabs.

The assumption of completely bonded or completely frictionless layer interfaces is not considered to be a significant weakness. A similar assumption is made by the Westergaard idealization in which the interface between the PCC slab and the underlying material is assumed to be frictionless. The interface between a PCC slab and the second layer is most likely intermediate between a completely bonded and completely frictionless condition. Between all other layers, the assumption of full bonding is probably more valid, being dependent on the type material and construction procedure. However, no data exist to adequately quantify the interface conditions, although the response model does exist that can analytically consider intermediate conditions. The computation of the various response parameters will certainly be affected by the selection of the interface condition. For computation of the design parameters, it was assumed that no bond existed at the interface beneath the PCC slab and that full bond existed at all other interfaces.

The comparison of the finite element idealization with the Westergaard and elastic layered idealizations may not be valid since it



refers basically to a computation procedure rather than to a mathematical representation of the physical structure. As has been noted previously, the finite element idealization may be employed for the upper layer with a dense liquid or elastic solid representation for the remainder of the structure. Nevertheless, consideration as a separate idealization has merit for comparisons between available techniques for computing the response of a pavement to load. As discussed herein, the finite element representation will mean that the entire structure will be broken into a number of finite elements (Figure 3).

In the finite element idealization, the continuous pavement structure is broken into a number of elements connected at nodal points. The material in each element is assigned properties that may vary from element to element. The number of elements and nodal points that may be considered is limited by computer capacity, and thus boundary conditions must be specified. The loads are applied as concentrated forces at the nodal points. With the aid of special types of elements, discontinuities, special interface conditions, reinforcing steel, and dowel bars may be introduced. Special computational techniques permit consideration of

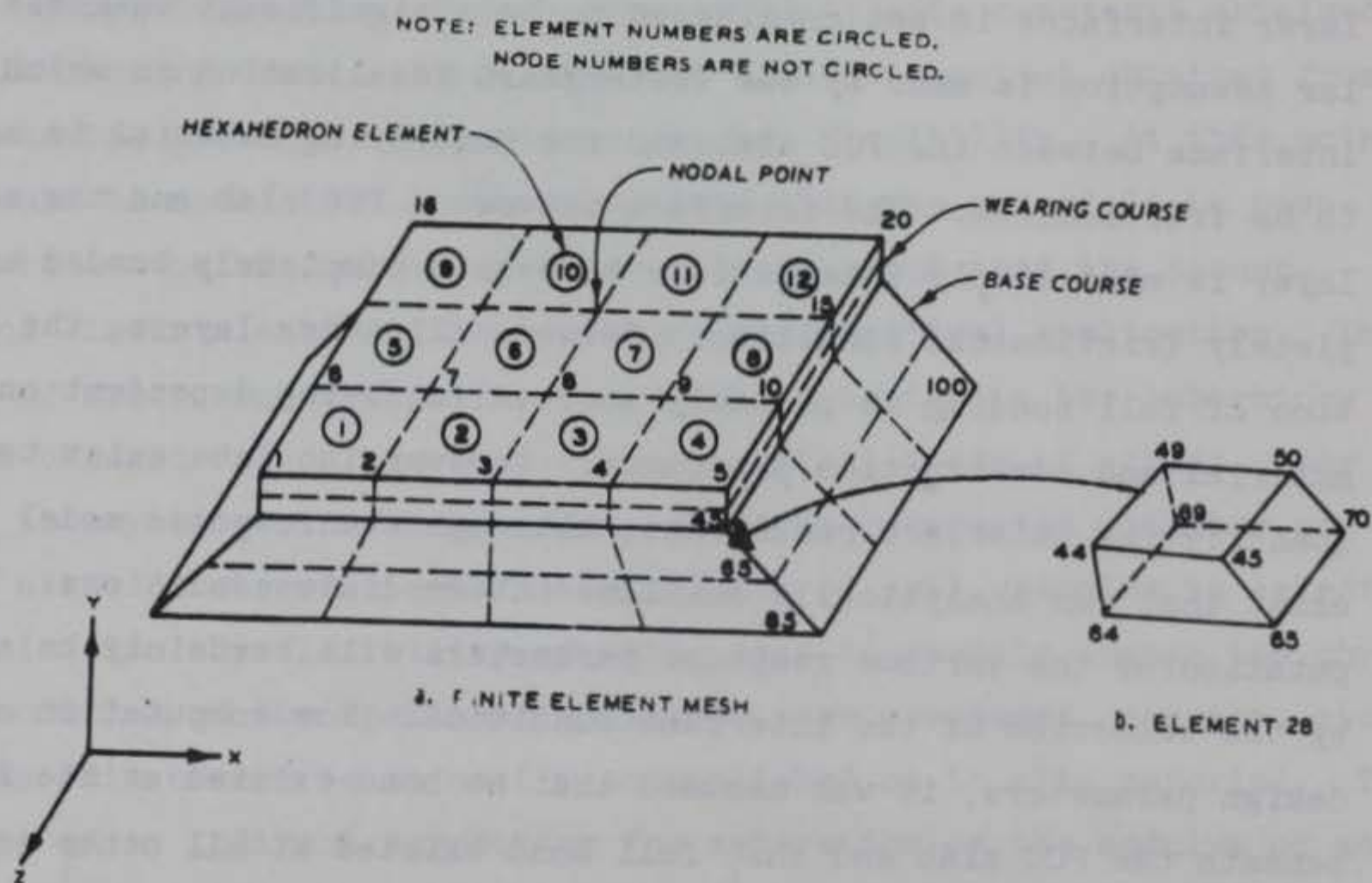


Figure 3. Pavement idealization using the finite element program (from Crawford and Katona<sup>12</sup>)



voids and temperature and moisture gradients within the pavement structure. In addition, variable layer properties (thickness and load deformation properties) and nonlinear material response may also be treated.

However, there are limitations. For a three-dimensional idealization with only a minimum number of elements and refinements (Figure 3), the required time and cost involved in applying the procedure to pavement problems become prohibitive.

There are plane strain, axisymmetric, and prismatic solid finite element idealizations, but with all of these idealizations certain constraints are introduced. If the time, effort, and cost to apply the models are reduced to manageable levels, the applicability to a general design procedure and improvements over simpler models is likewise reduced.

After consideration of all models, the layered elastic model was selected. The model has several weaknesses, and certainly there are more sophisticated models available. However, it offers a viable alternative that can be implemented into a workable design procedure.

Consider the relationship between the interior stress computed by layer theory and 0.75 of the edge stress computed by plate theory (Figure 4). The parameter of 0.75 of the edge stress is the design parameter presently being used for design of rigid airport pavements. Although the relationship in Figure 4 is not one of equality, it is one of strong correlation; thus, if a workable design procedure could be based on edge stress, then it would be expected that a workable procedure could be developed based on the interior stress.

#### SELECTION OF COMPUTATIONAL PROCEDURE

The two most widely used computer codes to solve for the response of a layered elastic pavement idealization are the BISTRO<sup>20</sup> and the CHEVRON<sup>21</sup> codes. In addition, the CRANLAY<sup>22</sup> and the BISAR<sup>23</sup> codes have been used but not as extensively as the BISTRO or CHEVRON codes. From these, the BISAR code was selected to develop the performance criteria because of the author's confidence in the accuracy of the program and



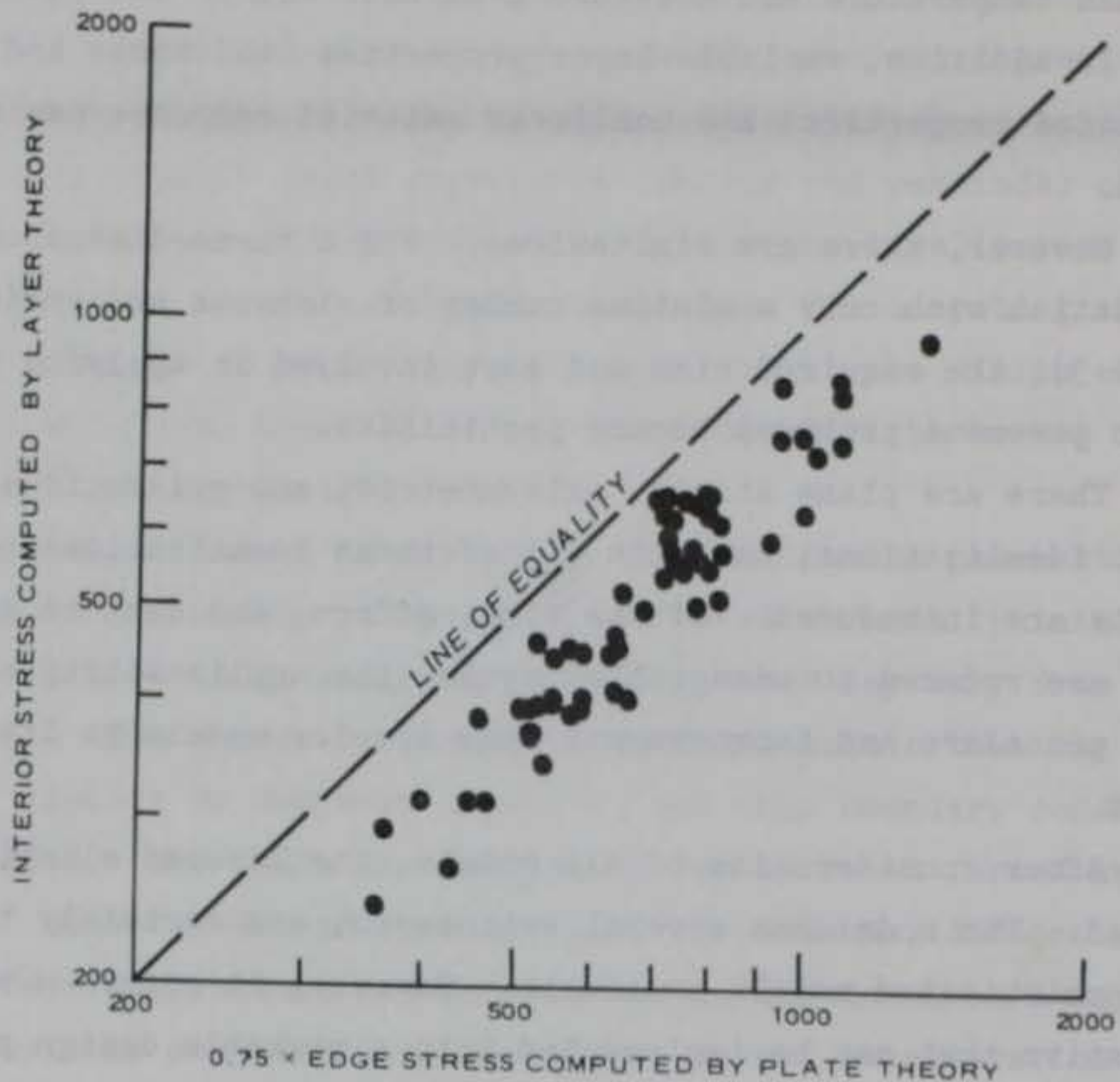


Figure 4. Comparison of stresses computed from test section data (Appendix B)

the ability of the program to consider different interface conditions. The BISAR program is an advanced version of the BISTRO program and has capabilities that, while not necessary for the use of the design procedure developed in the study, may be useful in the future for pavement analysis. The CHEVRON program does offer some advantages in terms of operation cost and may, in some design situations, be a completely adequate program. As an example, the CHEVRON code has been modified for multiple wheels and is recommended by Barker and Brabston<sup>10</sup> for flexible airport design. In order to maintain as much consistency between pavement types, it was the original intent to use the same code for rigid pavements.

However, for rigid pavements that have a subgrade of a low resilient modulus, the deflection basin computed with the CHEVRON



computer code becomes very distorted in the area beneath and immediately adjacent to the loaded area. This distortion is evident when compared with the deflection basins computed using the BISTRO/BISAR computer program (Figure 5). The distortion of the CHEVRON-computed basin is much greater for low subgrade moduli with the distortion decreasing as the subgrade modulus increases until for a subgrade modulus of 7000 psi the basins computed are nearly identical. The distortion is caused by inaccuracies in the numerical solution procedures for various integral equations and Bessel functions for large  $E_p/E_s$  ratios. The distortion in the curves in Figure 5 are accentuated by the location of a stiff layer ( $E = 1,000,000$  psi) at a depth of 240 in. below the bottom of the slab (reasons for this will be discussed in the following section). When the subgrade is assumed infinite in depth, the distortion is not as severe with the CHEVRON code, i.e., there is no hump where the deflections near the load are smaller than those further removed from the load (Figure 6).

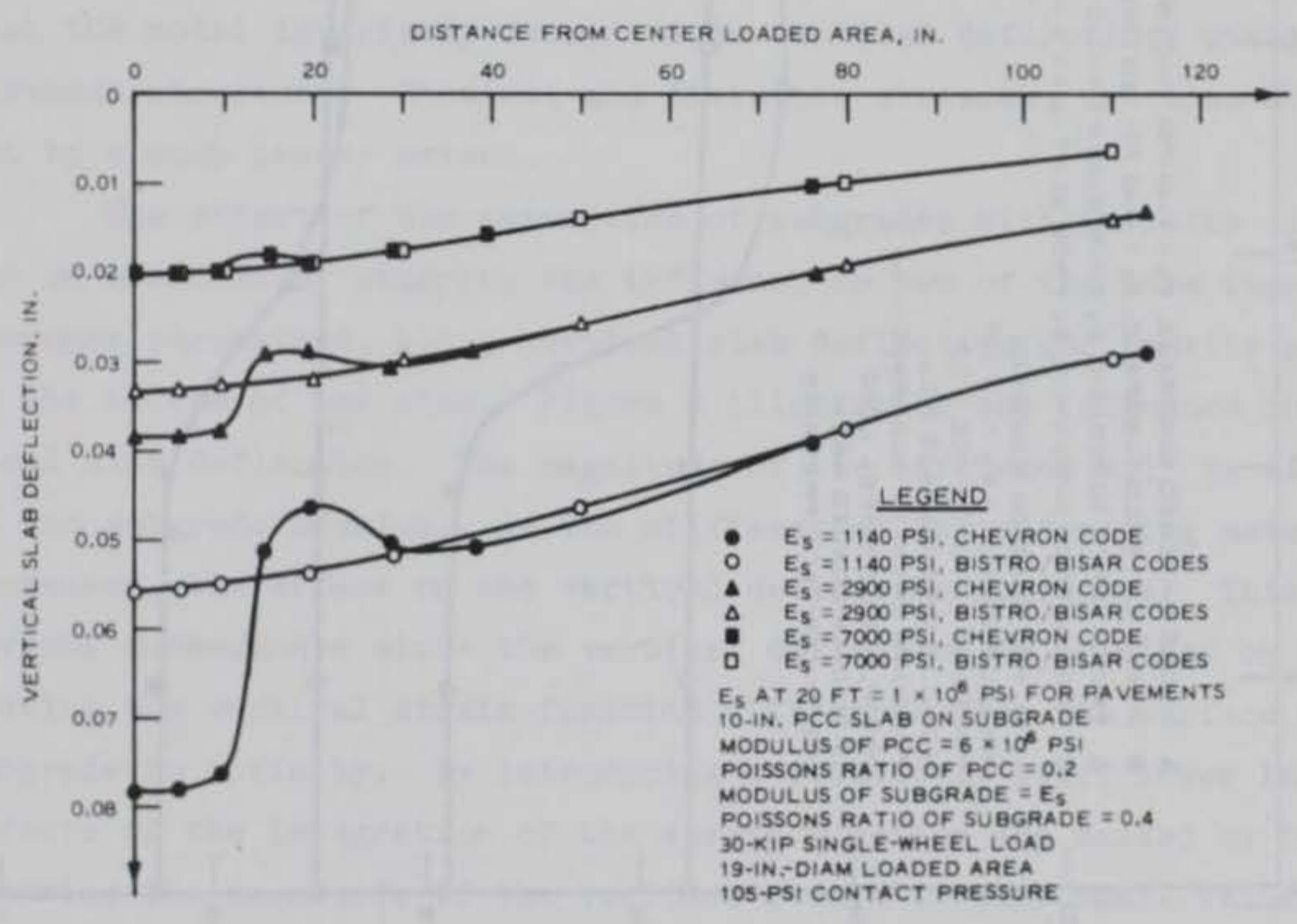


Figure 5. Deflection basins computed with the CHEVRON code compared with the deflection basins computed with the BISTRO/BISAR codes



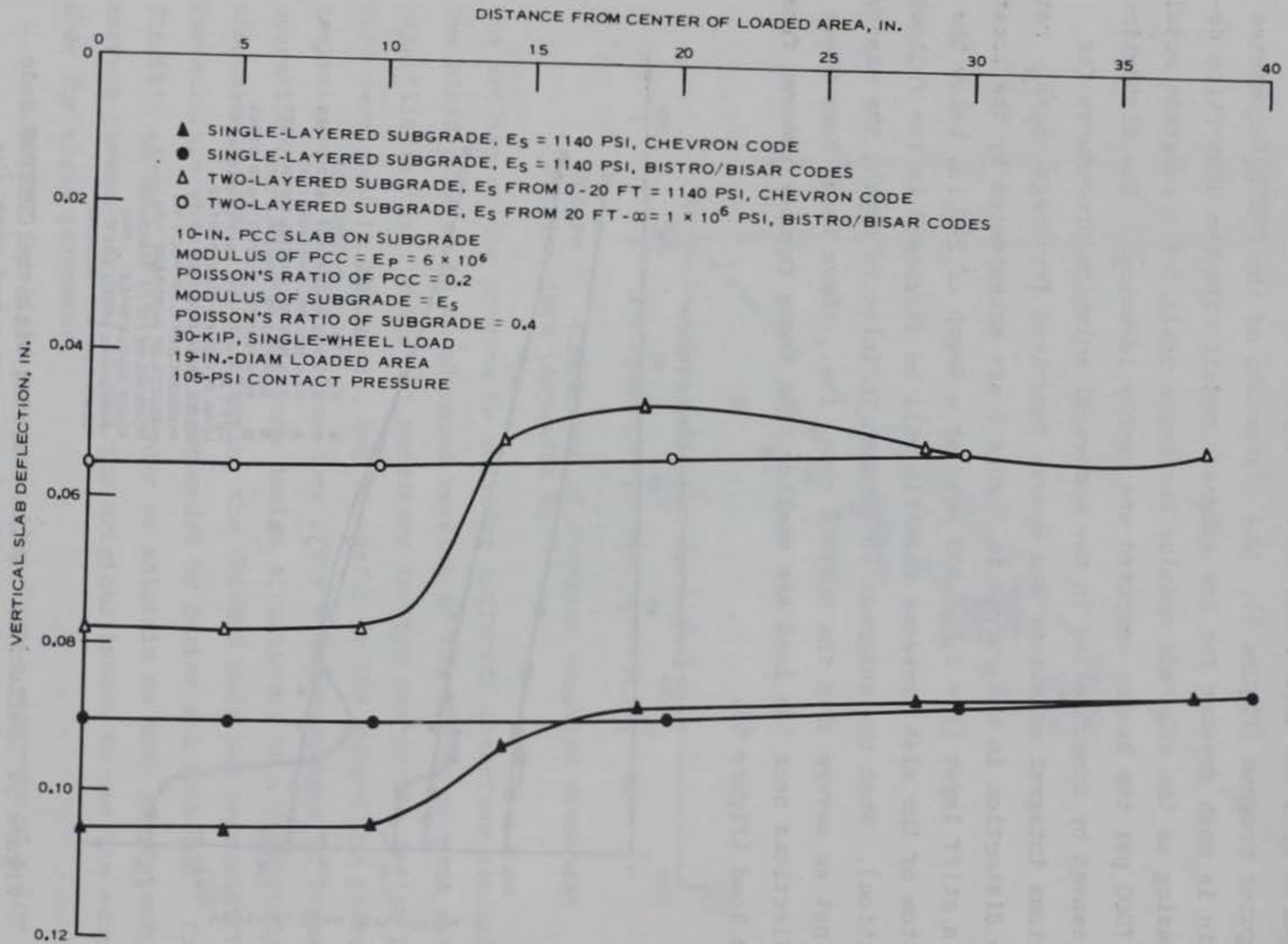


Figure 6. Illustration of effects of stiff layer on shape of deflection basin computed with CHEVRON code compared with that computed with BISTRO/BISAR codes



A much smaller effect on the stresses is apparent, as illustrated by the plot of radial tensile stress in the bottom of the PCC slab in Figure 7. However, it was believed that the additional accuracy of the BISTRO/BISAR computer codes was desirable. Because of the cost benefit and additional capabilities of the BISAR code, this program was chosen over the BISTRO code.

#### MODIFICATION OF MODEL FOR FINITE SUBGRADE DEPTHS

The layered elastic idealization assumes that the bottom layer extends vertically to infinity. This, along with the assumption that the layers extend horizontally to infinity, is a necessary condition for solving the integral equations and Bessel functions to obtain the pavement response. From a practical standpoint, borings are not usually made to depths sufficient to establish the location of layers below a 10-ft depth,<sup>1,24</sup> and the most common situation encountered is one in which the stiffness of the soil increases with depth. The results are that the model invariably overpredicts vertical deflections within the pavement structure. Strains, and therefore stresses, are also affected but to a much lesser extent.

The effect of the assumption of subgrades with infinite extent may be examined by studying the influence on two of the more important response parameters, i.e., vertical slab deflection and tensile stress in the bottom of the slab. Figure 8 illustrates the influence on vertical slab deflection. The magnitude of the influence will be affected by the subgrade modulus. As the stiffness of the underlying material(s) decreases, the effect on the vertical deflection increases. This is an obvious consequence since the vertical deflection is obtained by integrating the vertical strain function with depth from the surface of the subgrade to infinity. By introducing a relatively stiff lower layer, the effects of the integration of the strain function are masked by decreasing the magnitude of the vertical strain to very small values.

Figure 9 illustrates the influence on radial stress in the bottom of the slab. The stress is not significantly affected by the presence



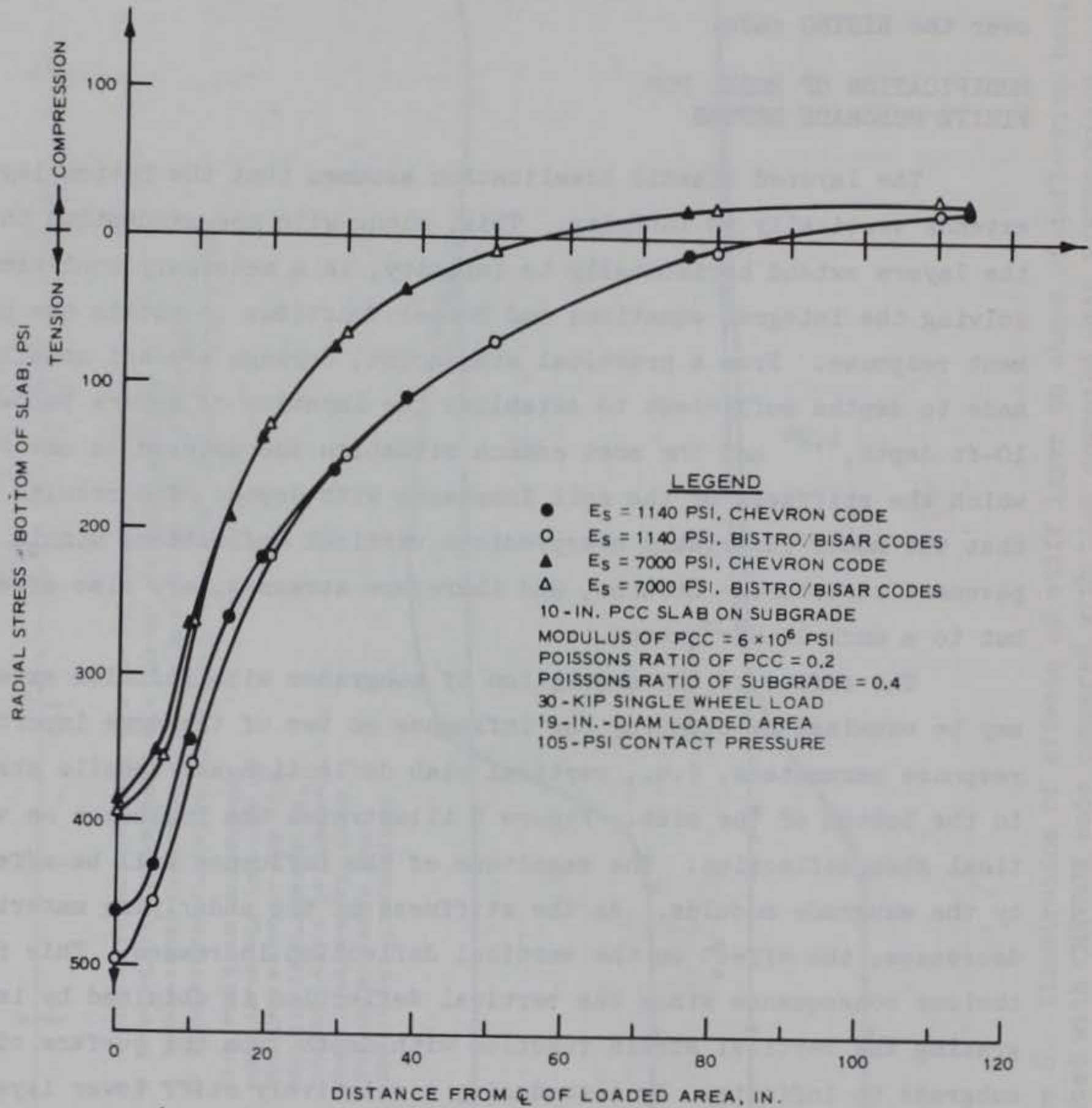


Figure 7. Comparison of tensile stress in bottom of PCC slab computed with CHEVRON and BISTRO/BISAR codes



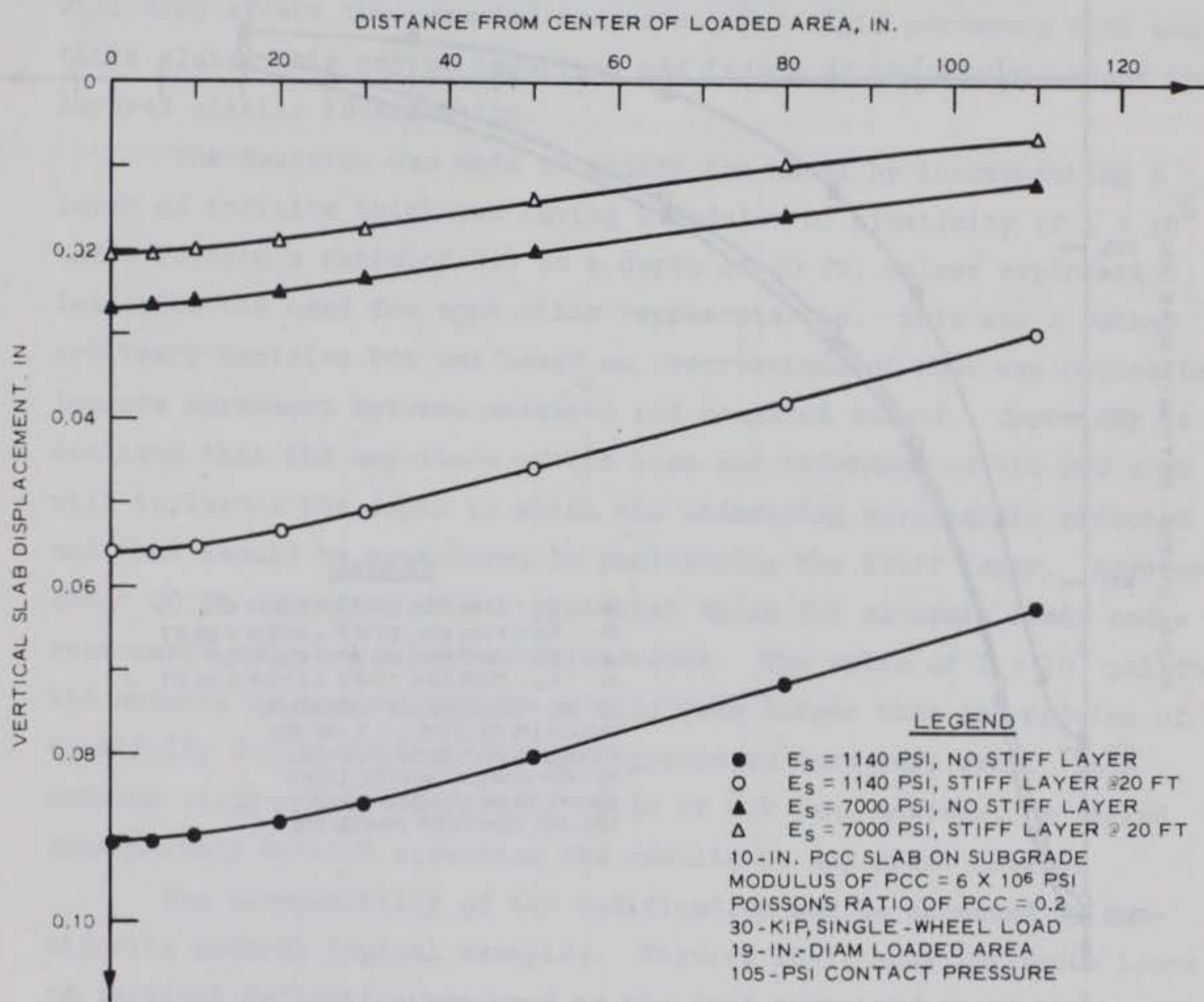


Figure 8. Effect of infinite subgrade depth of vertical slab deflection



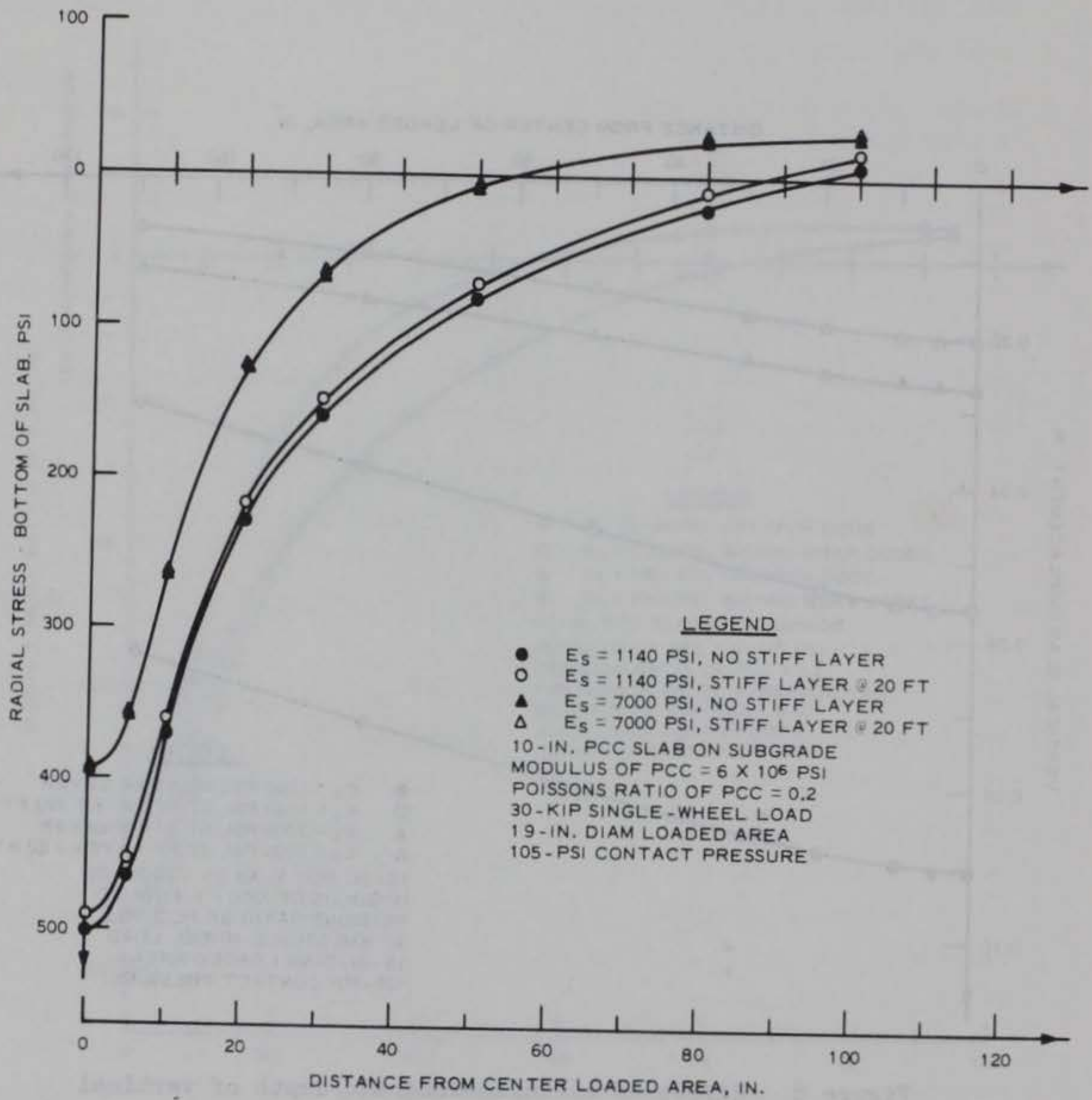


Figure 9. Effect of infinite subgrade depth on stress in bottom of slab



of the stiff layer. This is typical of not only the radial stress (Figure 9) and the tangential stress but also the vertical stress. The components of strain are affected by the assumptions of infinite layers, but since they are computed directly from the stresses and involve no integration or summation process, the effect is small. The effects of small differences are not cumulative as they are for computations of deflections. The assumption of layers of infinite horizontal extent will also affect the computed response. For rigid pavements with small thick slabs, this may be important and is one of the weaknesses of the layered elastic idealization.

The decision was made to modify the model by incorporating a layer of infinite thickness having a modulus of elasticity of  $1 \times 10^6$  psi and a Poisson's ratio of 0.4 at a depth of 20 ft, unless exploration indicates the need for some other representation. This was a rather arbitrary decision but was based on observations of what was needed to improve agreement between measured and computed values. Certainly it is realized that the magnitude of the load and thickness of the PCC slab will influence the depth to which the underlying material is affected and thus should be considered in positioning the stiff layer. However, about 20 ft appeared to be a practical value for aircraft loads and a reasonable range of pavement thicknesses. The value of  $1 \times 10^6$  psi for the modulus is several orders of magnitude larger than the modulus of elasticity for most subgrades and appears to work very well. This modulus value and the Poisson's ratio of 0.4 can, however, be varied considerably without affecting the results to any great extent.

The acceptability of the modification may be enhanced by considering several typical examples. Figures 10-12 show influence lines of vertical deflection measured as the load traveled across the pavement and deflection basins computed with the BISTRO code with and without a stiff layer. The difference in an influence line and a deflection basin is that data for the influence lines were obtained from a gage at a fixed location in the pavement as the load moved and the deflections for the basin were computed for various locations in the pavement with the load located at a fixed position, i.e., center of loaded area located at point



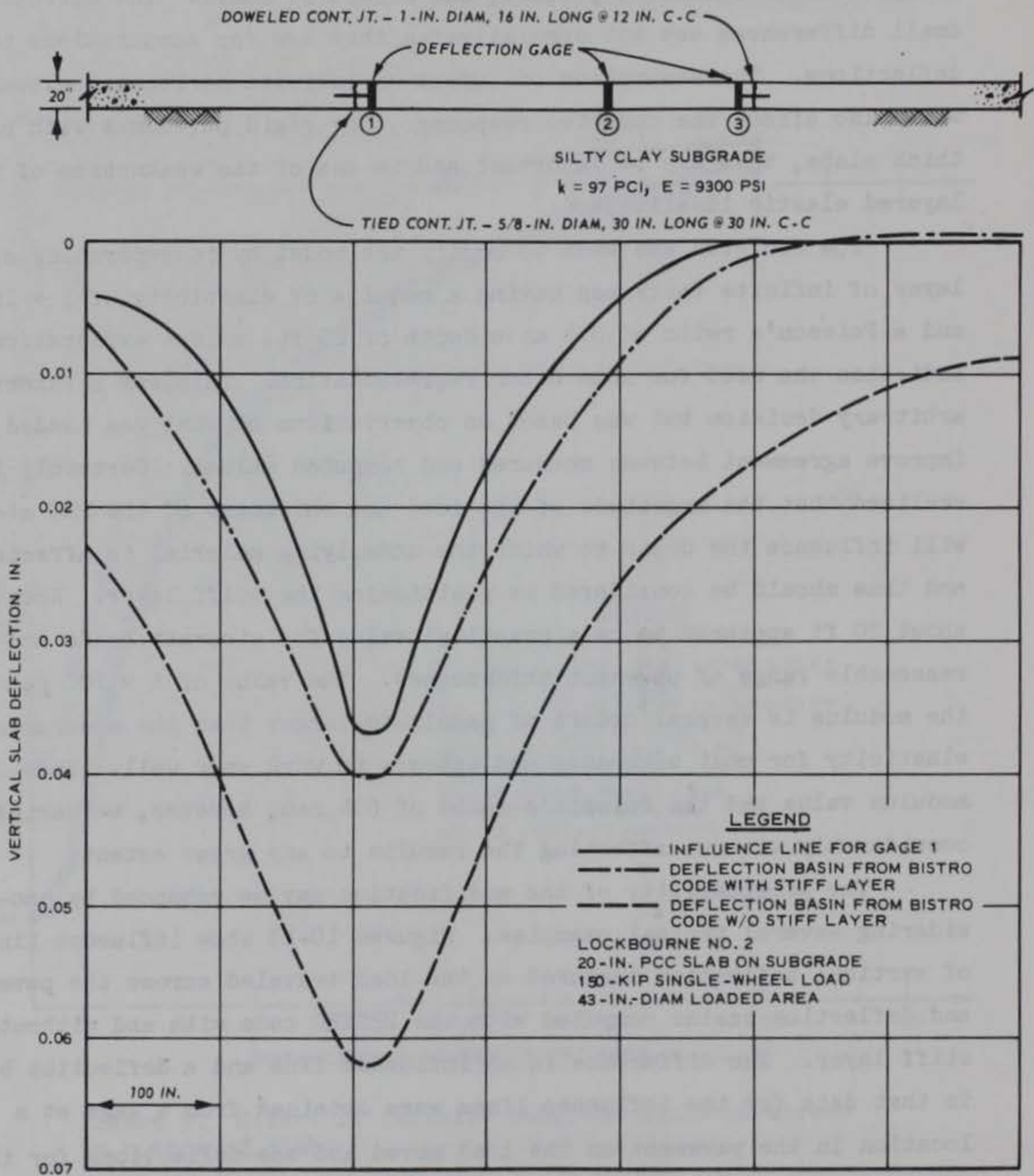


Figure 10. Comparison of measured deflection influence lines with computed deflection basins - Gage 1



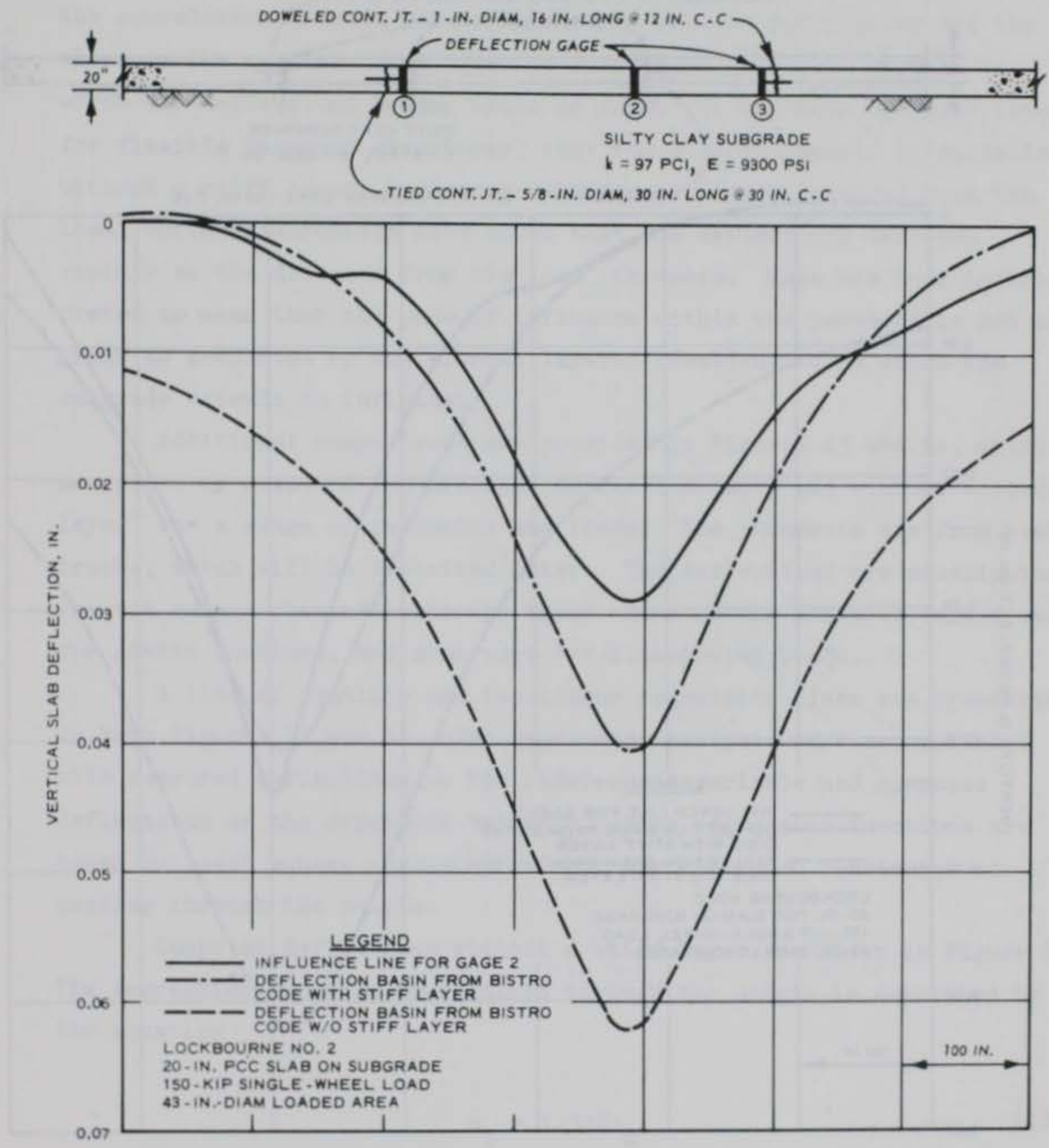


Figure 11. Comparison of measured deflection influence lines with computed deflection basins - Gage 2

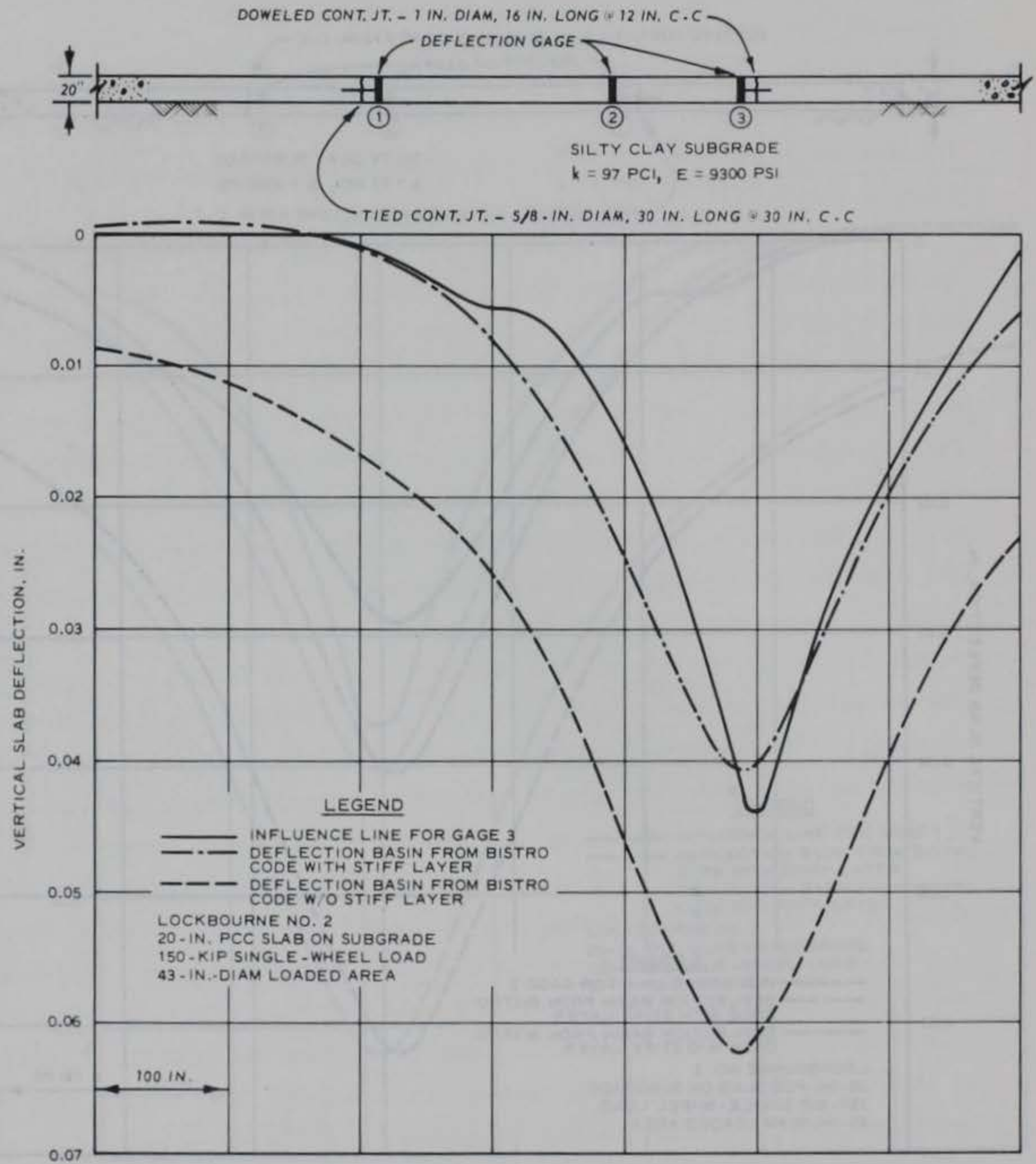


Figure 12. Comparison of measured deflection influence lines with computed deflection basins - Gage 3



of maximum response. Because of the approximations of linearity, elasticity, and time independency, the two are relatively compatible for pavements.

The results shown in Figures 10-12 are typical of the results observed for rigid pavements. The inclusion of the stiff layer improves the correlation between the measured and computed deflections and the shape of the curves. Of particular significance is the location at which the deflections become small or zero. It has been observed (even for flexible pavement structures) that the elastic layered idealization, without a stiff layer, indicates significant deflections far from the load, while measurements have shown that the deflections decrease rapidly as the distance from the load increases. This has been interpreted to mean that the zone of influence within the pavement is not as great as predicted by the elastic layered idealization in which the subgrade extends to infinity.

Additional comparisons are provided in Figures 13 and 14, which are plots of computed and measured deflection (with and without a stiff layer) for a range of pavements and loads. The pavements are from test tracks, which will be described later. The deflections are usually the largest values obtained with the load. Some of the measured values were for static loadings, and some were for slow-moving loads.

A line of equality and two linear regression lines are presented in both Figures 13 and 14. The regression analyses were accomplished with measured deflections as the independent variable and computed deflections as the dependent variable. Both regression functions are based on least square criteria, and one has the added constraint of passing through the origin.

Computed deflections without a stiff layer are shown in Figure 13. The regression function constrained through the origin is described by the equation

$$\Delta_c = 1.338\Delta_m \quad (1)$$

and the unconstrained regression function is described by the equation

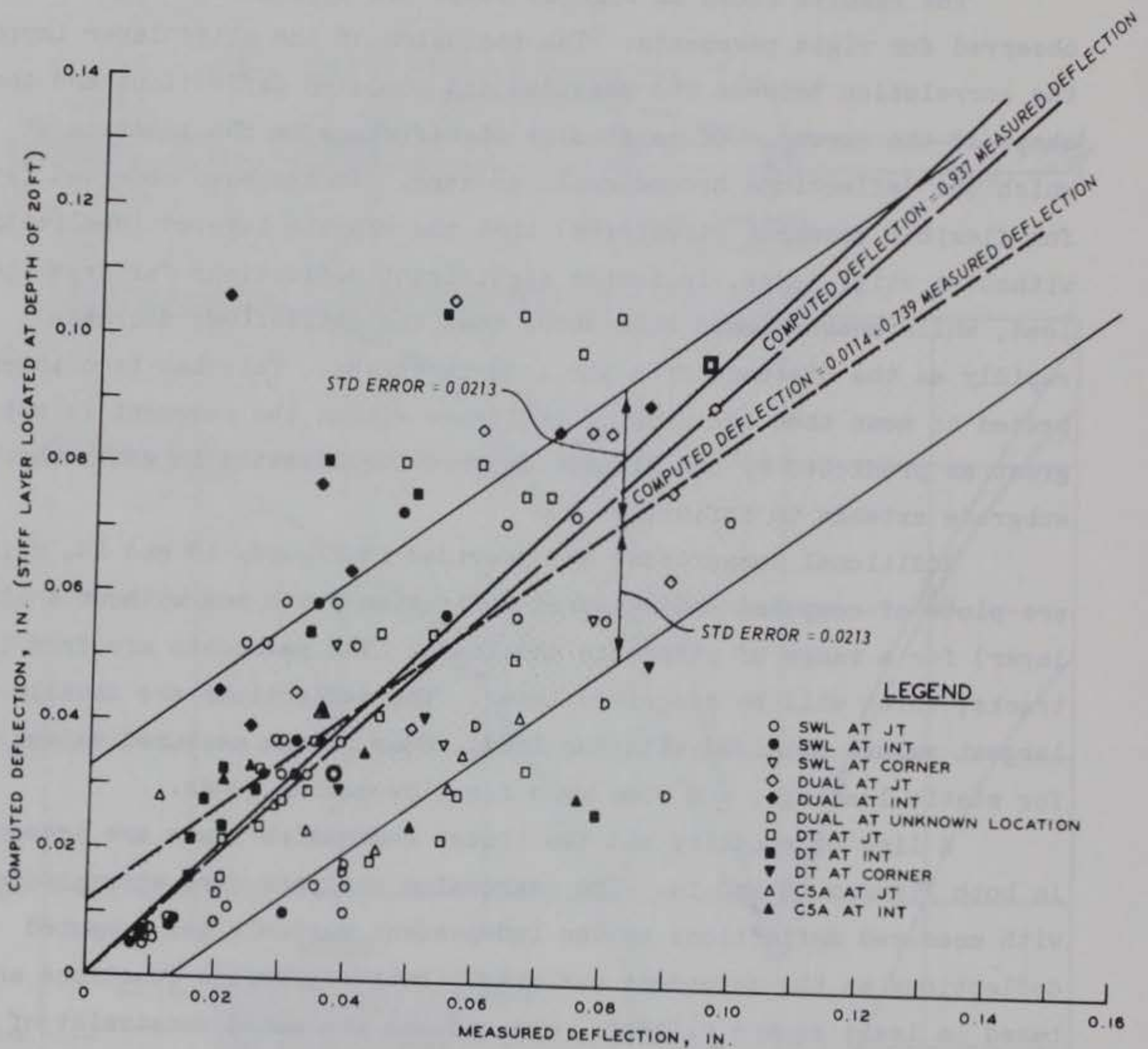


Figure 13. Comparison of measured deflections with deflections computed without a stiff layer



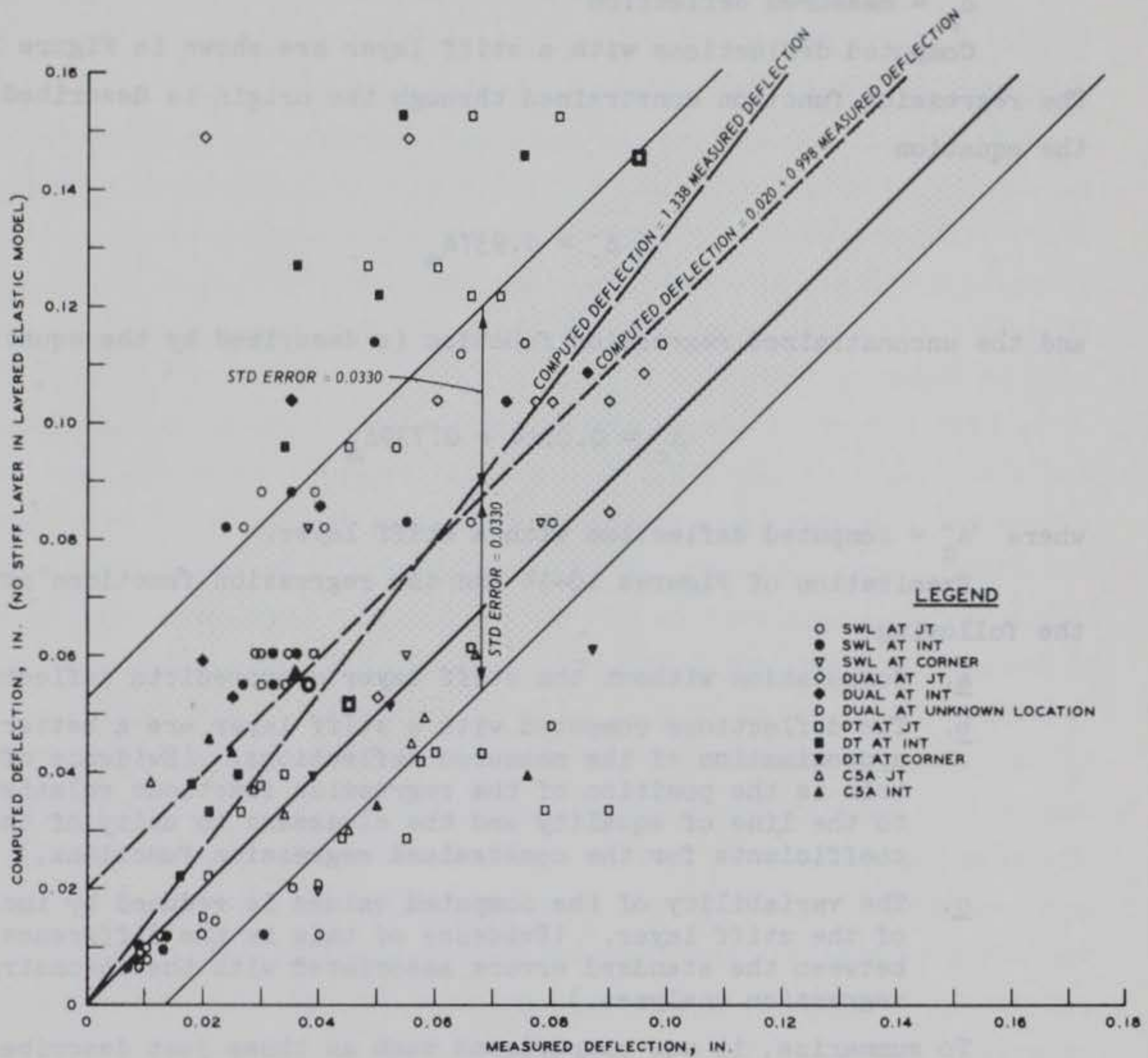


Figure 14. Comparison of measured deflections with deflections computed with a stiff layer

$$\Delta_c = 0.20 + 0.998\Delta_m \quad (2)$$

where

$\Delta_c$  = computed deflection without a stiff layer

$\Delta_m$  = measured deflection

Computed deflections with a stiff layer are shown in Figure 14. The regression function constrained through the origin is described by the equation

$$\Delta'_c = 0.937\Delta_m \quad (3)$$

and the unconstrained regression function is described by the equation

$$\Delta'_c = 0.0114 + 0.739\Delta_m \quad (4)$$

where  $\Delta'_c$  = computed deflection with a stiff layer.

Examination of Figures 10-14 and the regression functions reveal the following:

- a. Computation without the stiff layer overpredicts deflections.
- b. The deflections computed with a stiff layer are a better approximation of the measured deflections. (Evidence of this is the position of the regression functions relative to the line of equality and the closeness to unity of the coefficients for the constrained regression functions.)
- c. The variability of the computed values is reduced by inclusion of the stiff layer. (Evidence of this is the difference between the standard errors associated with the unconstrained regression analyses.)

To summarize, it was comparisons such as those just described that led to the decision to make the rather arbitrary modification to the elastic layered idealization. Although computations of stress and strain do not appear to be affected to the extent that the deflections are affected, it is believed that the modification improves the overall acceptability of the model. From a practical standpoint, it minimizes the need to explore and characterize the subgrade to large depths unless the geology of the area indicates that a soft or stiff layer is probable



between the normal exploration limits and about 20 ft or a soft layer below 20 ft.

## SELECTION OF MATERIAL CHARACTERIZATION PROCEDURES

### GENERAL

The amount of research that has been directed toward characterizing paving materials and subgrades with a test that is more accurate and more fundamental than a plate bearing or CBR (California Bearing Ratio) test is truly prodigious. Conversely, the formulation and application of practical, usable, widely accepted procedures for the routine design of rigid pavements is truly meager. Chou<sup>25</sup> has prepared a state-of-the-art report on the characterization of pavement materials including subgrades. Much of the discussion in this chapter will be based on this study.

The materials composing a rigid pavement respond neither linearly nor elastically to load, but in a complex manner. Generally, the response is nonlinear and nonelastic for a rather wide range of stress and strain conditions. The approximation of linear elasticity is more valid for such materials as PCC and bound bases (subbases) than it is for granular bases (subbases) and subgrades. PCC and bound bases (stabilized with PC or lime) tend to be more brittle and have more linear stress-strain relationships as illustrated in Figure 15. The response of many of the materials is highly dependent on the state of stress and the number of load repetitions to which the material has been subjected. Although the response of rigid pavements is not as sensitive to time and temperature\* as flexible pavement, temperature and rate of loading will have an influence on the characterization of materials in which a bituminous binder is used or in other layers where freezing occurs.

The pavement designer must then approximate the complex response of materials in order to use a simple analytical procedure to obtain the response of a pavement. As it turns out, many of the necessary approximations are not nearly so drastic as might be suspected from consideration of the total response of the materials. The states of stress

---

\* That is, if the effects of temperature gradients within the PCC slab are ignored.



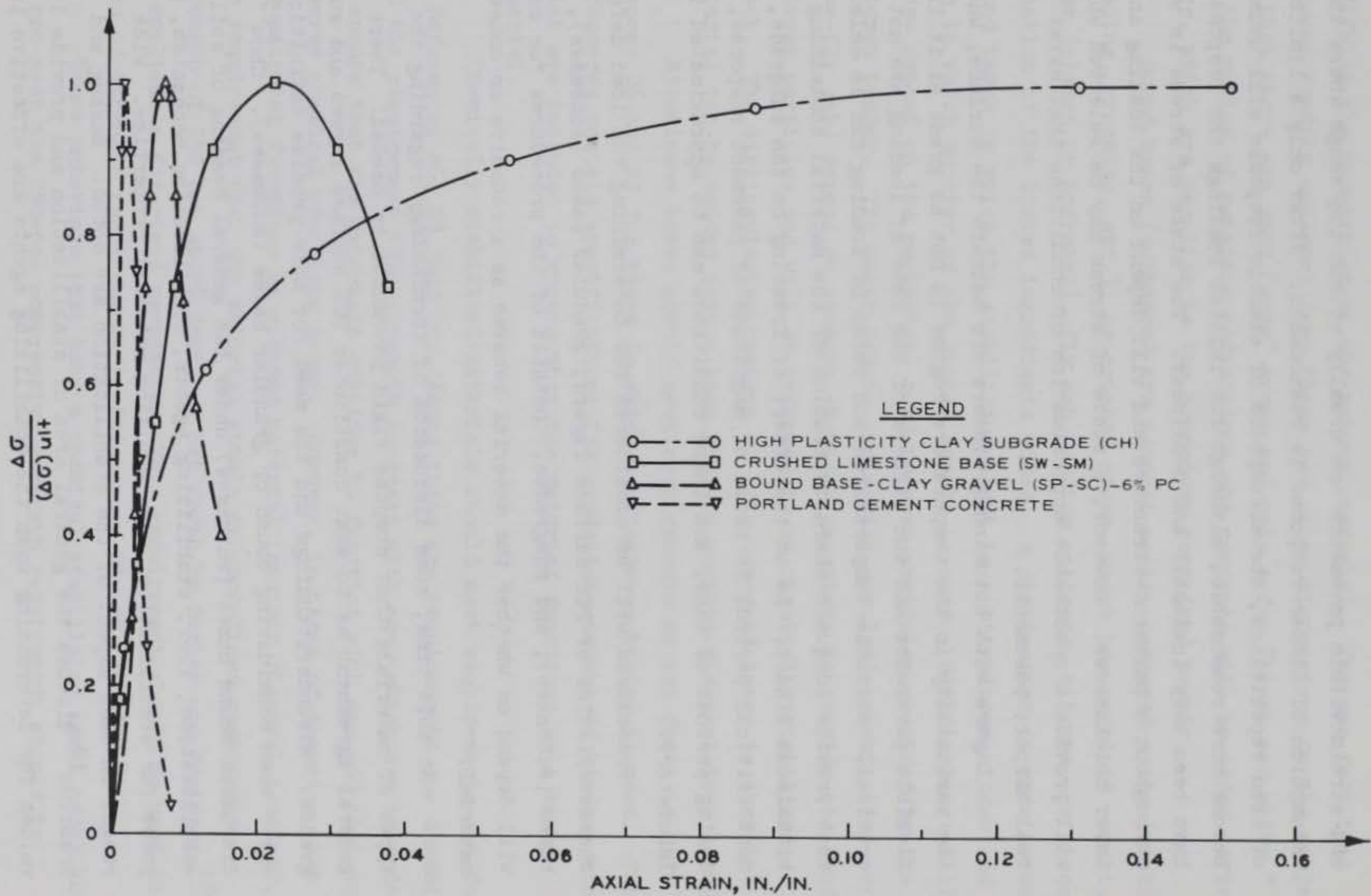


Figure 15. Comparison of typical stress-strain response of types of materials in rigid pavements

and strain within pavements are usually within the range where the assumption of linear response is reasonable. After only a limited number of load repetitions, the assumption of elastic response will usually become more reasonable, although for initial loadings the response may have been very inelastic and nonlinear. The state of stress is variable throughout a pavement structure and will depend on the loading and layer thicknesses. However, a state of stress may be selected which will provide a reasonable approximation of conditions that exist in real airport pavements.

Layers with bituminous binders are beneath the surface, where the variability in the temperature regime is not as great as it is for flexible pavements and the effects of the rate of loading are not as critical. Suitable temperatures and rates of loading can be selected that provide adequate characterization of the material containing a bituminous binder. As to the effect of freezing on the subgrade, the most critical period, in terms of magnitude of pavement response, is during periods of thaw, and these conditions can be approximated in the laboratory.

Procedures will be considered for determining the load deformation characteristics of PCC surface layers, granular bases (subbases), bound bases (subbases), and subgrades. Details of the procedures for subgrades will depend on whether the material behaves as a cohesive or cohesionless material.

At this time, some discussion of terminology regarding the four types of materials that compose rigid pavements is needed. There is general agreement as to what constitutes PCC surface layers and subgrades. Misunderstandings and the need for more precise definitions arise when considering bound or granular bases (subbases). Chou<sup>25</sup> discusses bound bases (subbases) under the general heading of soil stabilization, i.e., stabilizing agents, stabilization mechanism, purposes for stabilization, and resulting material properties. Wide ranges in each aspect of the stabilization are noted. Barker and Brabston<sup>10</sup> discuss the general area of stabilization and provide limiting values for determining when the stabilizing agents are effective in



modifying the properties of the natural material. The one fact that becomes readily apparent from these and other discussions on the subject is that there are many "gray" areas and only a few "black and white." To the myriad of existing definitions and concepts will be added several more, which are peculiar to the procedure contained herein.

Bound bases (subbases) are natural soils, prepared soils (washing, grading, crushing, etc.), or crushed stone, which has portland cement, lime (slaked or hydrated), fly ash, sodium silicate, bitumen, or a combination of the listed ingredients added. A distinction is made between bound bases in which the stabilizing agent is a bituminous binder and one in which another of the listed agents is used. Bituminous stabilized bases depend on the mechanical bond between particles provided by the bitumen binder. The other agents (primarily portland cement, lime, or lime-fly ash) depend on certain chemical reactions to provide the bond between particles and will be referred to as chemically stabilized bases. The distinguishing feature of both types of bases is that the material can be molded into a beam and can sustain flexural-type loadings.

Bituminous bases should meet requirements as set forth in References 26 and 27 for bases in which a bituminous binder is used. The references contain specifications for gradation, amount of binder, etc., which are intended to ensure that the material functions as a bound material.

Chemically stabilized materials should meet requirements set forth in References 26, 28, and 29. Among these are requirements for durability and the requirement that strength increase with age, which are intended to ensure that the materials continue to function with age and that no adverse chemical reactions occur. However, in terms of ensuring that the material functions as a bound material (sustain flexural loading), the requirement that the material attain an unconfined compressive strength of 250 psi at 28 days, as set forth by Barker and Brabston,<sup>10</sup> is applicable for rigid pavements. This requirement should be used in lieu of strength requirements in References 26, 28, and 29.

Those materials that have a chemical stabilizing agent added but do not meet the 250-psi compressive strength requirement should be



characterized with procedures for granular bases (subbases) or subgrades, depending on the nature of the natural material. For instance, a clay subgrade to which lime has been added but which does not meet the 250-psi strength requirement should be characterized and considered simply as part of the subgrade. The general rule is that the material should be characterized and used in the design as if no stabilizing agent had been added when the compressive strength requirement is not met.

Granular bases (subbases) are natural soils, prepared soils (washing, grading, crushing, etc.), or crushed stone, which meets gradation and durability requirements as set forth in References 1-3, 24, and 26. The characteristic of granular bases (subbases) that distinguishes them from bound bases (subbases) is that they do not possess and/or will not maintain the ability to sustain flexural loading.

The elastic constants defined for each layer will be the modulus of elasticity and Poisson's ratio. The modulus of elasticity will receive the greater attention for several practical reasons. One is that, in terms of response of the pavement, the modulus of elasticity is the dominant of the two parameters. A second is that Poisson's ratio varies only within a limited range for the different types of materials composing a pavement structure. Finally, it is difficult to accurately determine Poisson's ratio from laboratory tests.

The strength of the PCC surface layer will be defined by the flexural strength. This parameter is required in current design procedures, and the same well-established characterization procedures will be used.

#### EFFECTS OF LOAD REPETITIONS

To examine the effects of repetitive load applications on the response of rigid pavements, study the vertical deflection patterns that occur as a typical rigid pavement is trafficked. The total vertical slab deflection can be broken into transient (elastic) and permanent components. For rigid pavements, the elastic component remains relatively constant or decreases somewhat with traffic (Figure 16). After cracking is initiated, the elastic deflection will increase as the result of the overall decreased stiffness of the entire system.



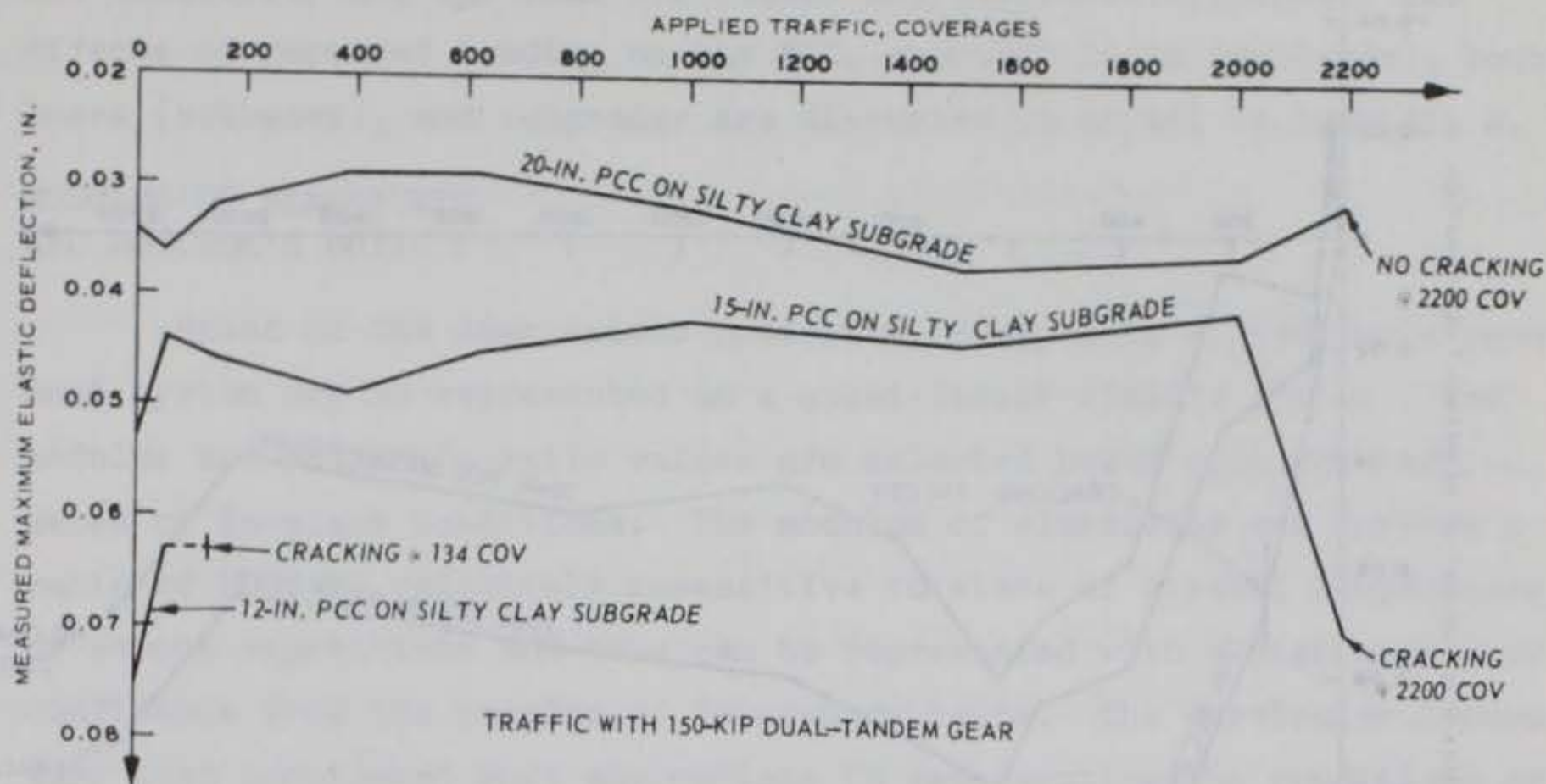


Figure 16. Elastic slab deflection versus traffic

Permanent deformation initially occurs as the slabs become seated and additional densification of loose material occurs. This deformation is rapid at first but then decreases as traffic is applied and essentially decreases to zero. Figure 17 shows that the cumulative deformation becomes relatively constant and remains so until cracking begins. In fact, Figure 17 indicates that between 600 and 2000 coverages there is a decrease in the permanent deformation, i.e., the pavement surface appears to rise. It is not known if this decrease is traffic-related or due to other causes. The only significant decrease in permanent deformation occurred between 600 and 800 coverages for the 20-in. pavement and between 600 and 1000 coverages for the 15-in. pavement. The fact that the decrease in the permanent deformation is greater for the 20-in. pavement than for the 15-in. pavement and occurred between two consecutive readings indicates that the decrease is not related to traffic; thus, it is concluded that after the initial permanent deformation, the traffic-induced permanent deformation remains relatively constant until the onset of cracking. As cracking progresses, permanent deformation again begins to increase.



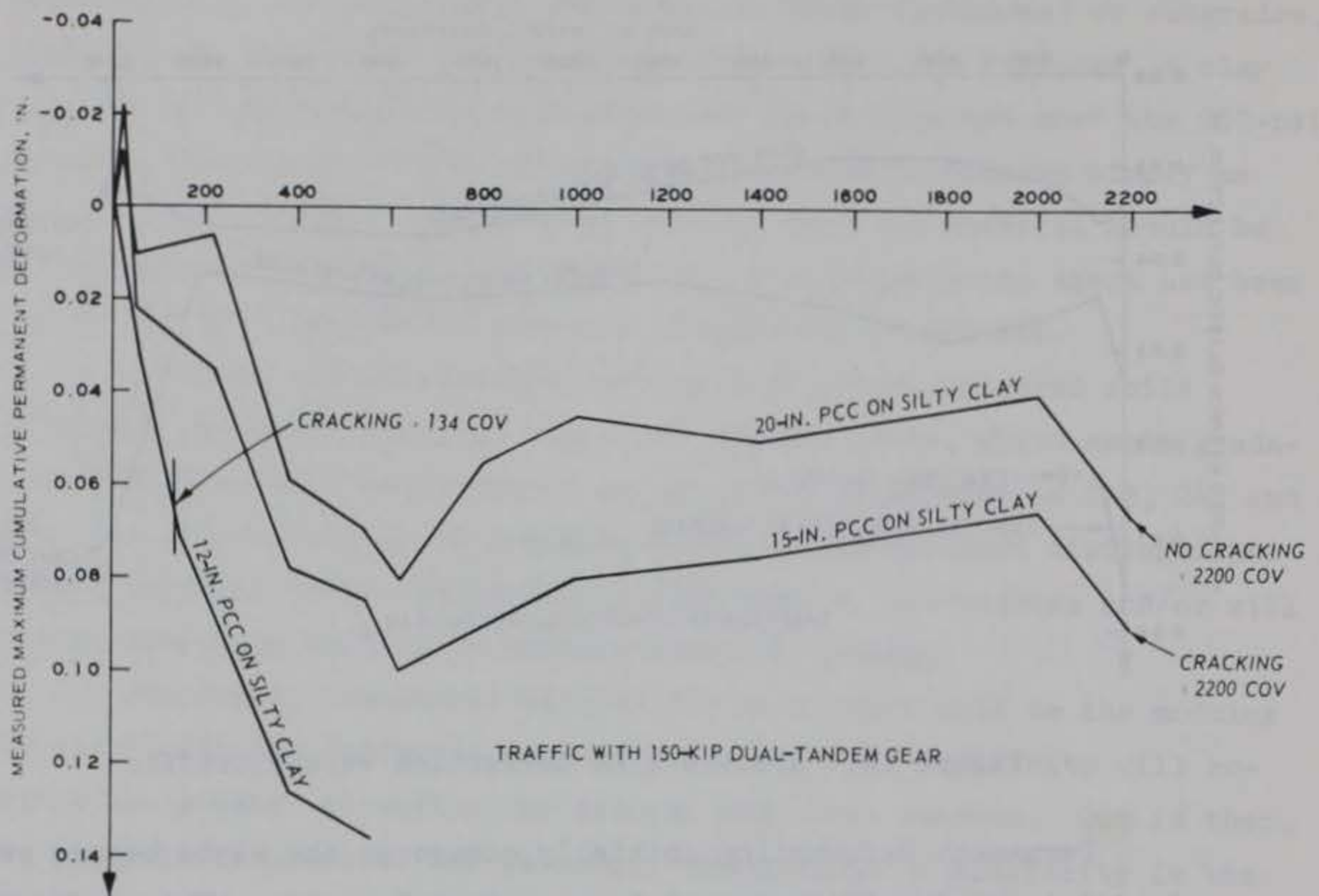


Figure 17. Cumulative permanent deformation versus traffic

The pattern of the total deflection will be similar to that for the permanent deformation since the total is the sum of the permanent and the relatively constant elastic components. The total deflection will then become practically equal to the elastic deflection after initial conditioning. For pavements designed for realistic volumes of traffic, this situation exists for a large portion of the life of the pavement.

Pavement response is a composite of the responses of the various layers. The difference in the response of the four different types of materials to static compression loading (triaxial tests) is illustrated in Figure 15. Although these results are from static tests, the same effects exist for repetitive loads. The effects of repeated loading are more pronounced for subgrades and granular materials than for PCC and bound bases. The relative influence of the assumptions of linearity



and elasticity are the same for static and resilient response. The effects of repeated loading on the PCC, granular bases (subbases), bound bases (subbases), and subgrades are discussed in detail in Appendix A.

#### MODULUS OF ELASTICITY AND POISSON'S RATIO

Based on the discussions presented in Appendix A, the rigid pavement system may be represented on a quasi-linear elastic system. The modulus and Poisson's ratio values are selected based upon best estimates of in-place conditions. The modulus of elasticity and Poisson's ratio of PCC are relatively insensitive to state of stress, temperature, or stress repetitions and thus can be represented with a high degree of confidence from the results of laboratory tests. The particular laboratory test considered most appropriate in representing the conditions of the PCC in a pavement system is the flexural beam test, and thus it is the flexural modulus to be used for design. This is not to eliminate the use of other testing procedures for determining a modulus, but it should be stressed that these design criteria are based upon the flexural modulus and that other modulus values should be related to the flexural modulus. There have been numerous studies relating the modulus values obtained from other test procedures, such as the uniaxial compression test, split tensile test, and resonant column test. If the designer has confidence in the correlations to the flexural modulus, then the results of these tests can be used; but the designer should also realize that the level of confidence of the design systems may be somewhat reduced by such correlations. The usage of Poisson's ratio is relatively narrow, and the effects of varying Poisson's ratio over this range on the computed response is almost negligible. Considering the difficulty in measuring Poisson's ratio, a fixed value of 0.2 for PCC will be adequate for design purposes. Thus, this has been the value of Poisson's ratio selected for development of the design criteria.

The modulus and Poisson's ratio values of base material vary over a wide range. A compensating factor is that the principal strength of rigid pavement is derived from the concrete surfacing, and thus relatively large variations in the moduli of the base can be tolerated.



For bound bases, since the properties in flexure are considered to be appropriate, the beam test as given in Appendix A should be employed. Bituminous bound bases in particular are subject to a variation in modulus and Poisson's ratio due to differences in binder type, binder content, temperature, and rate of loading. There are procedures, as discussed by Barker and Brabston<sup>10</sup> and Chou,<sup>25</sup> for estimating the modulus and Poisson's ratio of bituminous bound bases that can be used for design. Such procedures would certainly be appropriate for designs that employ bituminous bases primarily for waterproofing and not as a structural element. Bases stabilized with cement and/or lime will be similar in behavior to PCC, i.e., the modulus will depend on the strength of the material with Poisson's ratio relatively constant. As with PCC, correlations between the properties in flexure and the properties as determined by other laboratory tests have been developed. As with the bituminous bound bases, the modulus of relatively thin bound bases can be crudely estimated without seriously compromising the pavement design. Published values of the modulus of chemically stabilized materials vary over a wide range, i.e., from less than 100,000 to that approaching the modulus of lean concrete. For development of these criteria, a modulus value of 250,000 psi was used. This modulus may be considered typical of what may be expected from a stabilized base. Poisson's ratios for chemically stabilized bases vary over a wider range than the values for PCC, but 0.2 would still be an adequate estimation.

The properties of granular bases are very dependent on the state of stress, state of compaction, moisture content, and to some lesser degree on the aggregate quality. By specifying the material quality and compaction requirements and dealing with moisture conditions through assuming a nearly saturated condition or by applying some rationale for arriving at a design moisture content, the remaining variable influencing the modulus is the state of stress. Since this particular parameter does have such an important effect on the modulus of base materials, a detailed discussion is presented in Appendix A on the state of stress under rigid airport pavements. The study indicates that the first stress invariant in bases does not vary greatly and that a value of 10 psi would



be a typical value applicable for pavement design. The repetitive triaxial test is considered to be the laboratory test that can best be used to establish the characteristics of a particular granular material. Other approximate methods have been developed that do yield reasonable modulus values, but care should be exercised in the use of either the typical state of stress or the approximate methods of determining the modulus. For these procedures to be appropriate, the pavement design should be a typical design and the materials should meet the specified quality and compaction requirements.

Poisson's ratio of granular materials varies with the shear stress. In the range of stress normally encountered in rigid pavement, the value of 0.3 is an appropriate value for design. In the repetitive triaxial test, the Poisson's ratio is particularly difficult to measure and is subject to a high degree of error; thus, in most design situations, no attempt would be made to measure this material property.

Characterization of subgrade soils is normally considered much more crucial than characterization of the bases, primarily because of the relative thickness between the two and because of greater variation, which can occur in subgrade materials. In many ways, characterization of the subgrade materials is very similar to characterization of unbound granular, i.e., the material must be characterized with respect to a state of stress, moisture condition, and material density. As with the unbound base, the repetitive triaxial test is considered to be the appropriate laboratory test for characterizing the material. For the cohesionless subgrade, the characterization procedure is the same as for the unbound base, except the material quality and material densities will not meet the requirements for base materials; thus, some of the appropriation procedures will not be valid. For cohesive soils, the modulus is more a function of the deviator stress than the first stress invariant; hence, this is the stress parameter used in characterization of the cohesive subgrades. Based on the discussions in Appendix A, a 5-psi deviator stress is considered to be an adequate estimation for design of a typical airport pavement. As with the bases, since these values of stress are estimates for a typical pavement, it may be



desirable to check these estimates through computation of the stresses before the design is finalized.

As discussed in Appendix A, the moisture content at which the laboratory tests are conducted is very critical. Studies of the moisture content in airport subgrades have indicated that in most cases the subgrade material is near saturation. In selecting a moisture content at which the laboratory tests are to be conducted, the final or equilibrium water content should be considered. In some design situations, the designer may have information indicating that this final moisture content would be less than saturated. For such cases, savings may be realized by designing the pavement on the expected subgrade moisture content rather than the saturated water content.

Much effort has been applied toward developing correlations between other material parameters and resilient modulus. A study conducted by the U. S. Army Engineer Waterways Experiment Station (WES) for correlating modulus of subgrade reaction as determined by the plate bearing test is discussed in Appendix A. Such correlations can be useful in estimating the resilient modulus of the subgrade, but as with any empirical correlation care must be exercised in their use. Particular care must be taken in the case of field tests conducted to ensure that the moisture conditions at the time the tests are conducted will be representative of the final water content of the subgrade.

When the moisture content of the subgrade approaches the saturation moisture content, the Poisson's ratio of the material will approach 0.5. In the study at the WES, 0.4 has been found to be a representative value for most subgrades. For subgrades that are to be considered near saturation, it is suggested that 0.4 would be an adequate estimation of Poisson's ratio. If some lesser moisture content is considered applicable for design, then Poisson's ratio should be measured, or some lesser value of Poisson's ratio should be appropriate.

#### SUMMARY

Table 1 provides a summary for determining the modulus and Poisson's ratio for use in the analysis of rigid pavements. The column



Table 1

Summary Chart for Material Characterization

<u>Material</u>	<u>Referenced Laboratory Test</u>	<u>Influencing Parameters</u>	<u>Expected Range for Modulus</u>	<u>Other Methods of Estimating Modulus by Correlations</u>	<u>Typical Values or Range for Poisson's Ratio</u>
PCC	Flexural beam	Age	$3 \times 10^6$ - $6 \times 10^6$	Split tensile Unconfined compression	0.2
Bituminous concrete	Flexural beam	Temperature, rate of loading	$1 \times 10^5$ - $1.5 \times 10^6$	Split tensile Triaxial compression	0.3-0.5
39 Granular base	Triaxial compression	First stress invariant, density, moisture content	$1 \times 10^4$ - $6 \times 10^4$	Empirical charts	0.3
Cohesionless subgrade	Triaxial compression	First stress invariant, density, moisture content	$1 \times 10^4$ - $3 \times 10^4$	Plate bearing	0.3-0.5
Cohesive subgrade	Triaxial compression	Deviator stress, density, moisture content	$4 \times 10^3$ - $3 \times 10^4$	Plate bearing	0.4



entitled "Influencing Parameters" may need additional explanation since the parameters listed are by no means all of the parameters that influence the modulus of a material. First, the table assumes that the material tested is used in the pavement and meets the material specifications. For example, for the bituminous concrete, it is assumed that the aggregate, bitumen, moisture, and density are the same as to be used and do meet the specifications. Thus, in setting up the laboratory tests many influencing parameters will be fixed but others, i.e., those parameters listed, will be variable, and particular care must be exercised in the control of these test parameters.

## DEVELOPMENT OF PERFORMANCE CRITERIA

### GENERAL

Historically, performance criteria for rigid pavements have been based on limiting the tensile stress in the PCC slab to levels such that failure occurs only after the pavement has sustained a number of load repetitions. Cracking or other forms of pavement distress are attributed to the repeated application of loads, and the process and criteria are referred to as fatigue and fatigue criteria. The fatigue process for rigid pavements is assumed to be similar to that for a PCC beam, and the criteria are presented in the same manner as the results of fatigue testing of concrete beams, i.e., a plot is made of the ratio of the applied stress to the strength of the PCC versus the number of stress repetitions applied.

Yimprasert and McCullough<sup>30</sup> prepared a plot comparing performance (will not be referred to as fatigue herein) criteria from several sources. These comparisons (Figure 18) are based on both laboratory tests of beams and the results from the American Association of State Highway Officials (AASHO) road tests. The performance criteria recommended by the Portland Cement Association<sup>5</sup> (Figure 19) are based on laboratory tests of beams. The performance criteria developed by the Corps of Engineers are based on results of full-scale test pavements subjected to controlled accelerated simulated aircraft traffic. The evolution of these criteria is described in References 31-35. One version of these criteria is shown in Figure 20. This curve<sup>35</sup> is a plot of the design factor (DF) versus coverages from the equation

$$DF = R/0.75\sigma_e \quad (5)$$

where

DF = design factor

R = PCC flexural strength

$\sigma_e$  = tensile stress in the bottom of the PCC slab computed with the Westergaard edge-load idealization



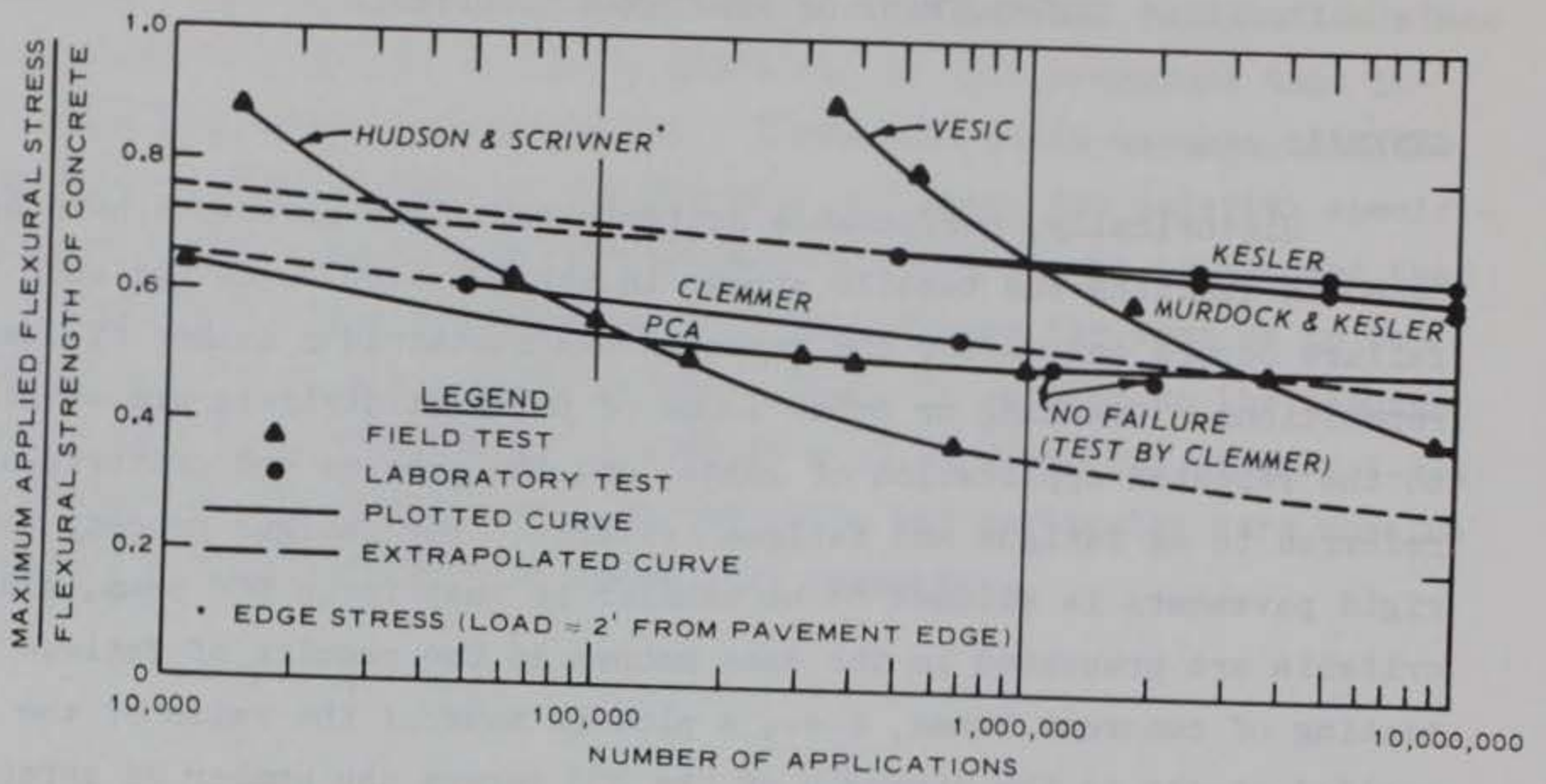


Figure 18. Comparison between field and laboratory tests on fatigue of concrete<sup>30</sup>

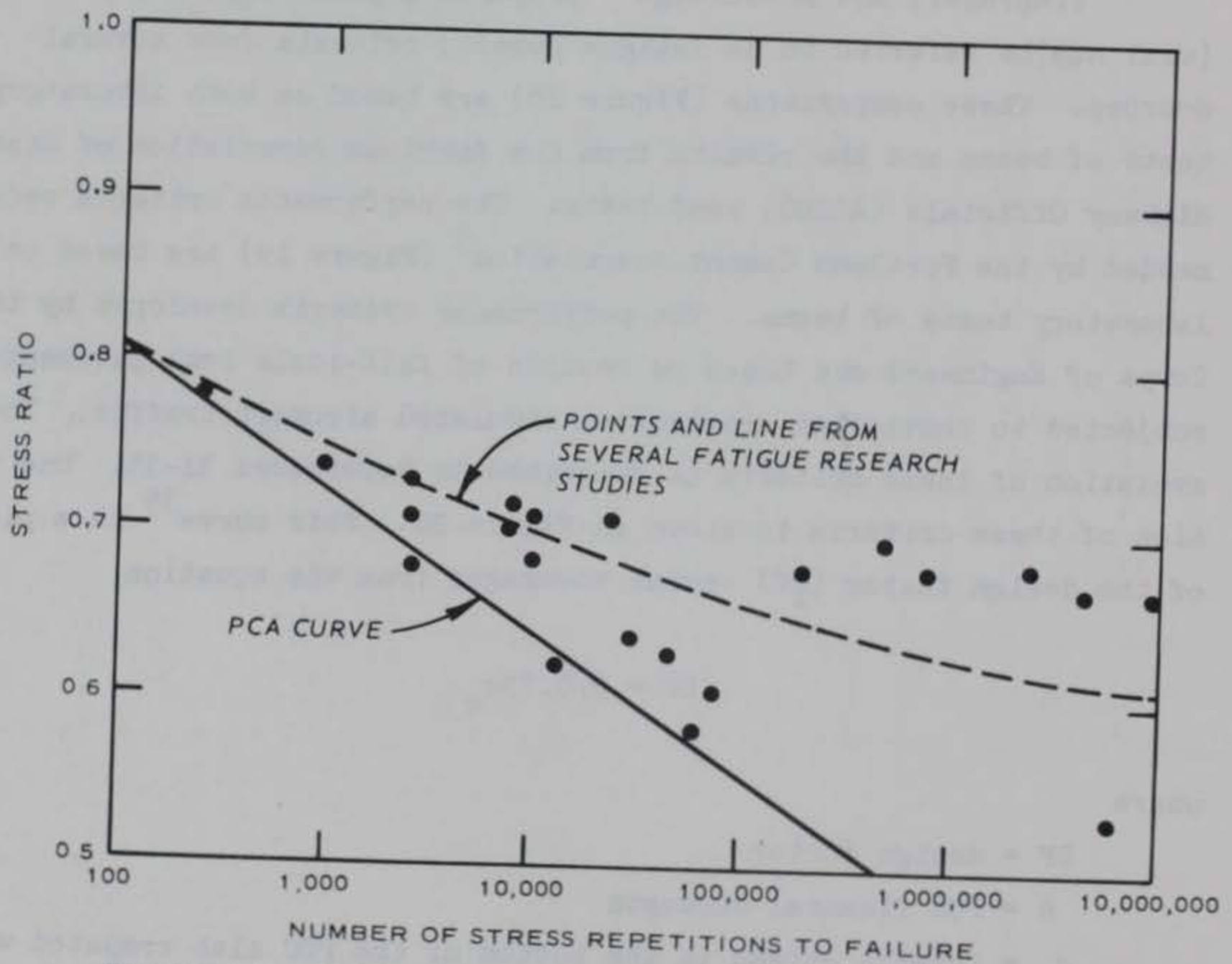


Figure 19. Fatigue curve for concrete subjected to flexural stresses<sup>5</sup>

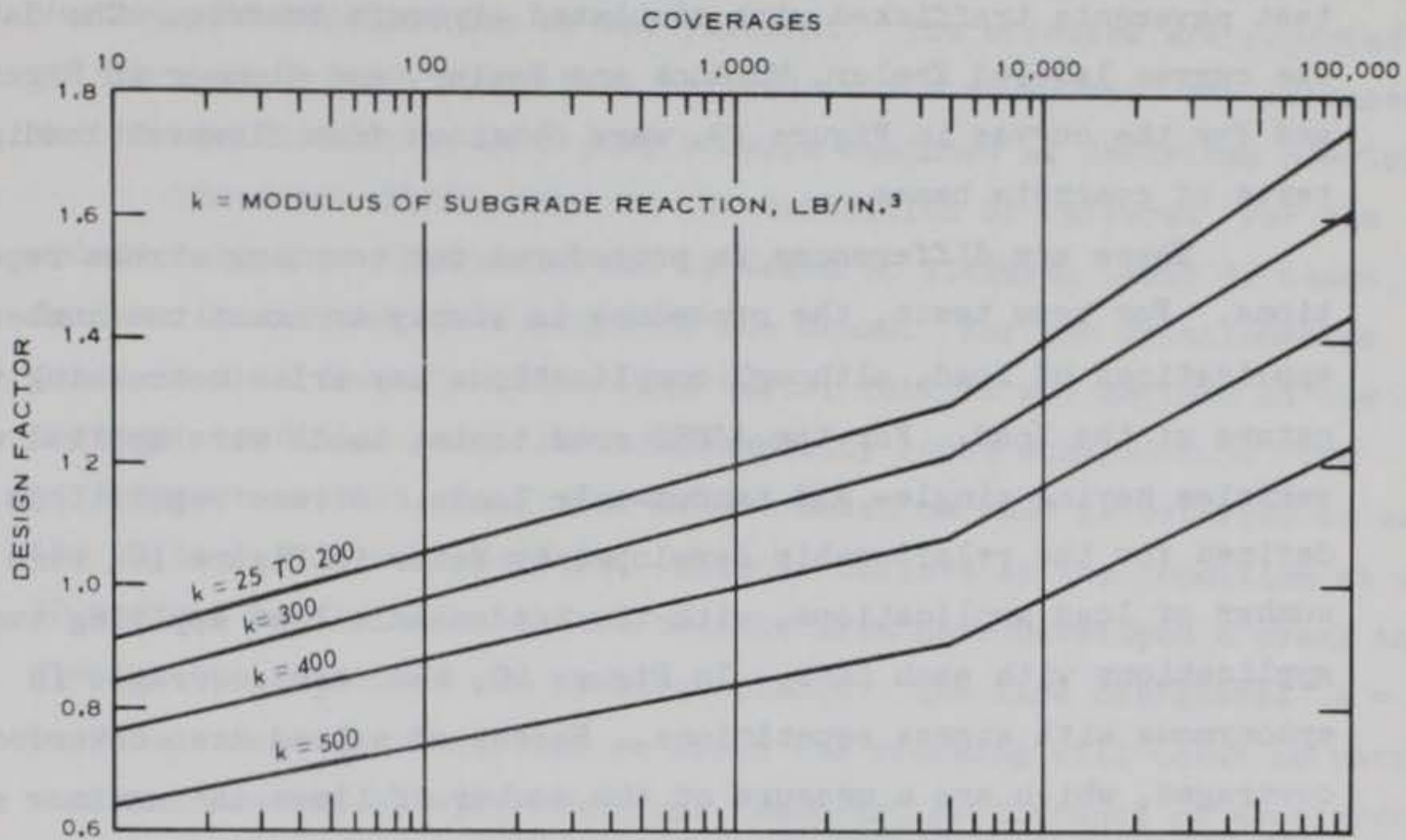


Figure 20. Current Corps of Engineers limiting stress performance criteria

The factor of 0.75 is used to account for the reduction in the edge stress resulting from the support provided by adjacent slabs. Coverages are a measure of the number of repetitions of the maximum stress occurring at a particular location in the pavement. The definition and method for converting actual aircraft operations to coverages is contained in Reference 36. The criteria developed by the Corps of Engineers are often presented in the form of a plot of percent of a standard thickness versus coverages.<sup>37</sup>

Upon detailed examination of the various fatigue criteria, it becomes apparent that while the basic concept and form are the same, many details are different. The data for the criteria are derived from two sources: controlled traffic tests of actual pavements, and laboratory flexural tests on concrete beams (fatigue in compression is described by compressive loading of cylinders or cubes). The data for the curves labeled Hudson and Scrivner and Vesic in Figure 18 were



developed from an analysis of data from the AASHO road tests. In Figure 20, the data for the curves resulted from an analysis of data from test pavements trafficked with simulated aircraft traffic. The data for the curves labeled Kesler, Murdock and Kesler, and Clemmer in Figure 18, and for the curves in Figure 19, were obtained from flexural loading tests of concrete beams.

There are differences in procedures for counting stress repetitions. For beam tests, the procedure is simply to count the number of applications of load, although complications may arise concerning the nature of the load. For the AASHO road tests, loads were applied with vehicles having single- and tandem-axle loads. Stress repetitions, as defined for the relationship developed by Vesic in Figure 18, were the number of load applications, with the tandem-axle load applying two-load applications with each pass. In Figure 20, the term coverages is synonymous with stress repetitions. Passes of a load are converted to coverages, which are a measure of the number of times the maximum stress will occur at a particular location in the pavement. To convert actual aircraft traffic to coverages (stress repetitions), the random lateral movement of the load across the pavement is considered. A factor, referred to as the pass-to-coverage ratio, converts the number of aircraft passes (may be referred to as operations or departures) to the number of coverages that occur at the location of maximum accumulation within the pavement.

The computation of stress is accomplished by different procedures. For laboratory beam tests, the maximum bending stress is easily calculable from simple equations of bending. For the relationship labeled Hudson and Scrivner (from AASHO road test) in Figure 18, the stresses are essentially maximum stresses measured along the pavement edge, with the loads located near the pavement edge. The word "essentially" is used, since the stresses used were not measured directly. Rather, a series of strains were measured, then converted to stresses, and an empirical relationship developed. From this relationship, the stress was computed to develop the performance relationship. The curve labeled Vesic in Figure 18 was also derived from an analysis of the AASHO road test data,



but stresses were computed using the finite element model with the Westergaard idealization of the pavement. The stresses are reported as the maximum that could have existed in the pavement. The stresses for the relationships in Figure 20 were computed as described previously.

There are differences in the definition of failure. For the relationships in Figures 18 and 19 based on flexural tests of beams, failure is defined as fracture of the beams. For the relationships based on data from the AASHO road tests, failure was defined as the pavement condition when the serviceability index equaled 2.5. The performance criteria in Figure 20 are based on what is referred to as the initial failure condition. This is defined as the condition at which 50 percent of the slabs in the traffic area have developed a crack that divides the slab into two or three pieces. The line designated  $k = 25$  to 200 defines the condition at which the cracking will occur no matter what the modulus of soil reaction. However, performance of accelerated traffic tests and results of condition surveys indicated that pavements with high-strength foundations continued to satisfactorily carry loads after cracking, but that pavements with low-strength foundations developed multiple cracking and differential displacements soon after initial cracking. For this reason, additional relationships were added to relax the criterion for defining failure for pavements on high-strength foundations and thus in essence permit additional traffic after initial cracking.

For the performance criteria contained herein, the basic data will be developed from test pavements subjected to controlled accelerated simulated aircraft traffic. The term coverages<sup>36</sup> will serve as the measure of traffic or stress repetitions. The elastic layered idealization and in particular the BISAR computer code will compute the limiting stress. The maximum principal tensile stress occurring in the bottom of the PCC slab and the vertical PCC slab deflection were selected as the critical response parameters. The initial crack definition of failure selected stated that a pavement was considered failed when approximately 50 percent of the slabs in the traffic area had cracked.



No allowances were made for satisfactory performance after initial cracking for pavements on high-strength foundations.

#### FULL-SCALE ACCELERATED TEST

The pavements from which the performance criteria were developed are described in Appendix B. These pavements were constructed and tested by the Corps of Engineers from 1943 to 1973. The procedures followed in each of the test tracks were basically the same. The pavement sections were designed to answer specific questions or to solve certain problems; the pavements were constructed and the as-constructed properties measured; the type of traffic needed to answer the specific questions or to solve the specific problems was applied to the pavement; the volume of traffic and pavement condition were monitored until failure of the pavement was achieved; and the after-traffic properties of the pavement were measured.

Certain details of each test were different. The construction procedures, time of construction, geographic location, type subgrade, type joints, type load, distribution of loading, extent and type of testing, etc., varied. Although extrapolation to a general design procedure is considered justifiable, it should be recognized that the entire range of conditions that might be experienced by a pavement has not been covered. Another factor to be recognized is that although the volume of data may seem substantial, it is not sufficient to define a complete set of criteria. The relationships presented are simplifications of what are probably more extensive and complex families or systems of relationships. Because of the limited data available for each range of conditions, the relationships provided are agglomerations of a group of relationships. For example, the limiting stress criteria are defined by a single relationship. If more data had been available, it may have been possible to define a family of relationships for different loadings or possibly foundation stiffnesses.

The use of data from actual traffic tests permits a number of factors to be considered indirectly in the design. The performance is directly related to traffic, and the resulting criteria are for the



entire pavement rather than for one component or material, such as fatigue of the PCC as obtained from beam tests. Environmental effects are not considered in the computation of the response parameters for developing the criteria. Although the full-scale pavements experienced the effects of temperature and moisture changes and gradients, frictional restraint forces, etc., the range of conditions experienced was not all-inclusive.

The accelerated traffic tests were conducted over short periods of time, and the detrimental effects of exposure to the environment are not experienced. However, the beneficial effects of time are not considered either. PCC gains strength with time; the strength of cohesive subgrades does not reach the minimum strength until saturation occurs (which takes time), nor do the minimum strength conditions prevail all the time. However, the detrimental and beneficial effects of time may, to a certain extent, counterbalance each other.

The effects of joints are not considered directly although it is recognized that joints are a point of weakness in rigid pavements and the distress is usually initiated at joints. The effects of joints are handled in the following manner:

- a. The test pavements all had joints and slab sizes that were similar to the standard types used in airfield pavements.
- b. The traffic was applied in the most critical manner with respect to the joints.
- c. The use of the criteria will result in adequate pavements provided that the standard joint types and similar slab sizes used ensure adequate vertical forces transmitted between slabs.

Each test pavement was limited in size; therefore, construction procedures and equipment were not of the size and complexity used for constructing large amounts of aircraft pavements. More manual operations were involved in the construction of the test pavements than would normally be involved in the construction of a complete runway or taxiway. This must have affected the variability and the quality of pavement. Many of the test items were only 2, 3, or 4 slabs in size. On full-scale paving jobs, the pavement at the start of a job or even at



the start of a day's operations is normally of a poorer quality than the pavement constructed after the "bugs" are worked out of the system. There are other factors, such as the difference in the consolidation of PCC with hand-held vibrators as compared with the consolidation with a slip-form paver. The question of the difference in the test pavements and actual airport pavements is unanswerable, and it must be assumed that the test pavements were representative of real pavements.

The size of the test pavements, some of which were only one slab in size, presents another problem. Considering the variability that naturally occurs, the number of additional slabs needed for a truly representative sample is not known. In assigning traffic at failure, average conditions were selected when possible.

The volume of traffic applied to the test pavements was small as compared with the volume of traffic that would be used to design pavements for today's major civil airports or the larger military facilities. The primary reason for this is the cost involved in applying large amounts of traffic. Another reason is that a number of the tests were conducted during the 1940's and 1950's when pavements were designed for much lower traffic volumes. The net result of the low applied traffic volumes is that the results from the tests will have to be extrapolated to higher traffic volumes in order to be used to design for current and projected traffic.

In summary, the use of data from full-scale accelerated traffic tests has certain disadvantages. However, when the complexity of the problem of designing pavements and alternative sources of data are considered, it apparently is the best alternative for producing criteria that are generally applicable and implementable.

#### ASSIGNMENT OF MATERIAL PROPERTIES TO TEST PAVEMENTS

For the test pavements described in Appendix A, the elastic properties of the various layers shown include moduli of elasticity, Poisson's ratio, and modulus of soil reaction values. For the Multiple-Wheel Heavy Gear Load,<sup>35</sup> Keyed Longitudinal Construction Joint,<sup>38</sup> and



Soil Stabilization Pavement Study<sup>39</sup> pavements, the values shown for all types of materials were obtained from laboratory and field tests of the various materials. However, for the remainder of the pavements (Lockbourne 1-3,<sup>40-46</sup> Sharonville Channelized,<sup>34,47</sup> and Sharonville Heavy Load<sup>48</sup>), the load deformation properties of the foundation material were described solely by the modulus of soil reaction obtained from static plate load tests. The modulus of elasticity for the subgrades for these pavements was obtained from the correlation between modulus of elasticity and static modulus of soil reaction (Figure 21). Values of Poisson's ratio were selected from values presented by Barker and Brabston.<sup>10</sup>

Data from which the correlation in Figure 21 was developed are shown in Table 2. These data were obtained by conducting static plate bearing tests<sup>8</sup> on in situ soils and repeated load triaxial tests (Appendix D) on "undisturbed" samples of cohesionless soils or samples prepared in the laboratory to approximate field conditions for cohesionless soils. Two points in Figure 21 were not used in establishing the correlation since the laboratory specimens did not represent the in situ conditions.

The general application of a relationship, such as shown in Figure 21, to a wide range of conditions is questionable on several accounts. However, for the purpose for which it was developed and used herein, it did appear to provide reasonable estimates for the modulus of elasticity of the subgrade in the earlier test tracks. The credibility of the correlation is enhanced by the comparisons presented in Figure 22. The three points represented three conditions in which both types of tests had been performed. Points 1 and 2 were for a high plasticity clay (CH) and point 3 was for a low plasticity clay (CL). The second curve in Figure 22 was taken from Reference 49. The proximity of the three additional data points and the additional curve to the established relationship indicates that the correlation should provide reasonable estimates of the resilient modulus of subgrade soils. It should be noted that the laboratory tests were conducted according to procedures outlined in Appendix D and that moduli for cohesive soils



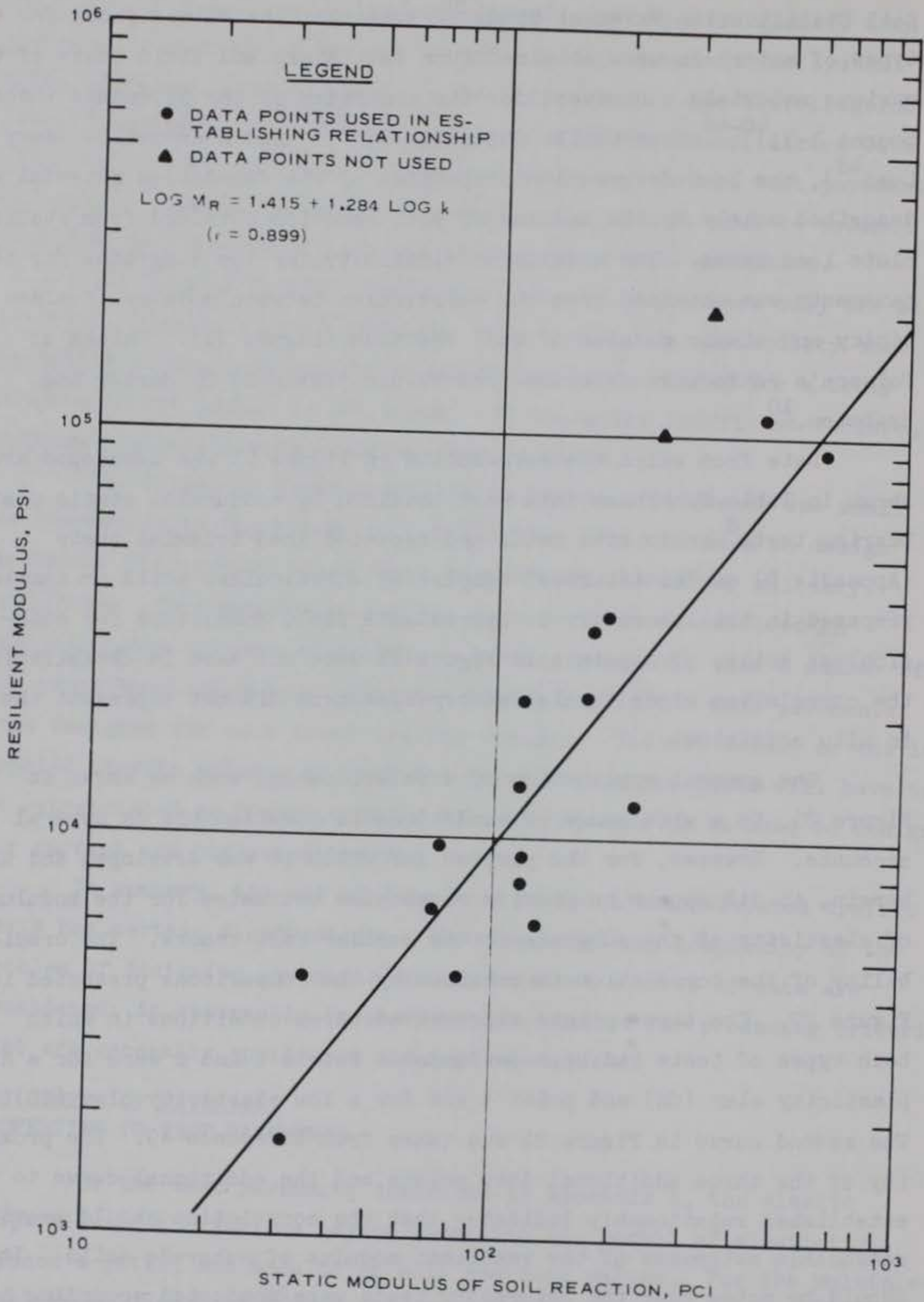


Figure 21. Correlation between resilient modulus of elasticity and static modulus of soil reaction



Table 2

Data for Correlation Between Static Modulus of Soil  
Reaction and Resilient Modulus

<u>Soil Identification</u>				<u>Modulus of Soil Reaction</u>	
<u>No.</u>	<u>Class</u>	<u>LL</u>	<u>PI</u>	<u>pci</u>	<u>Resilient Modulus, psi</u>
1	CL	36	12	35	4,500*
2	CH	50	32	170	22,000*
3	CH	58	33	32	1,700*
4	SM	N.P.		116	21,500**
5	CL	49	25	75	9,400*
6	ML	27	3	225	12,000**
7	SW-SM	N.P.		190	35,000**
8	SW-SM	N.P.		450	112,500**
9	SP	N.P.		630	91,000**
10	CL	43	21	175	32,500*
11	CH	73	48	85	4,500*
12	CH	73	48	118	13,200*
13	CH	73	48	120	7,625*
14	CH	73	48	120	9,000*
15	CH	73	48	130	6,213*
16	CH	73	48	72	6,500*
17	CH	53	34	325	200,000†
18	CH	64	42	250	102,500†

\* Resilient modulus determined at deviator stress of 5 psi.

\*\* Resilient modulus determined at first stress invariant of 10 psi.

† Points not used to establish correlation. Laboratory specimens were not representative of in situ material.



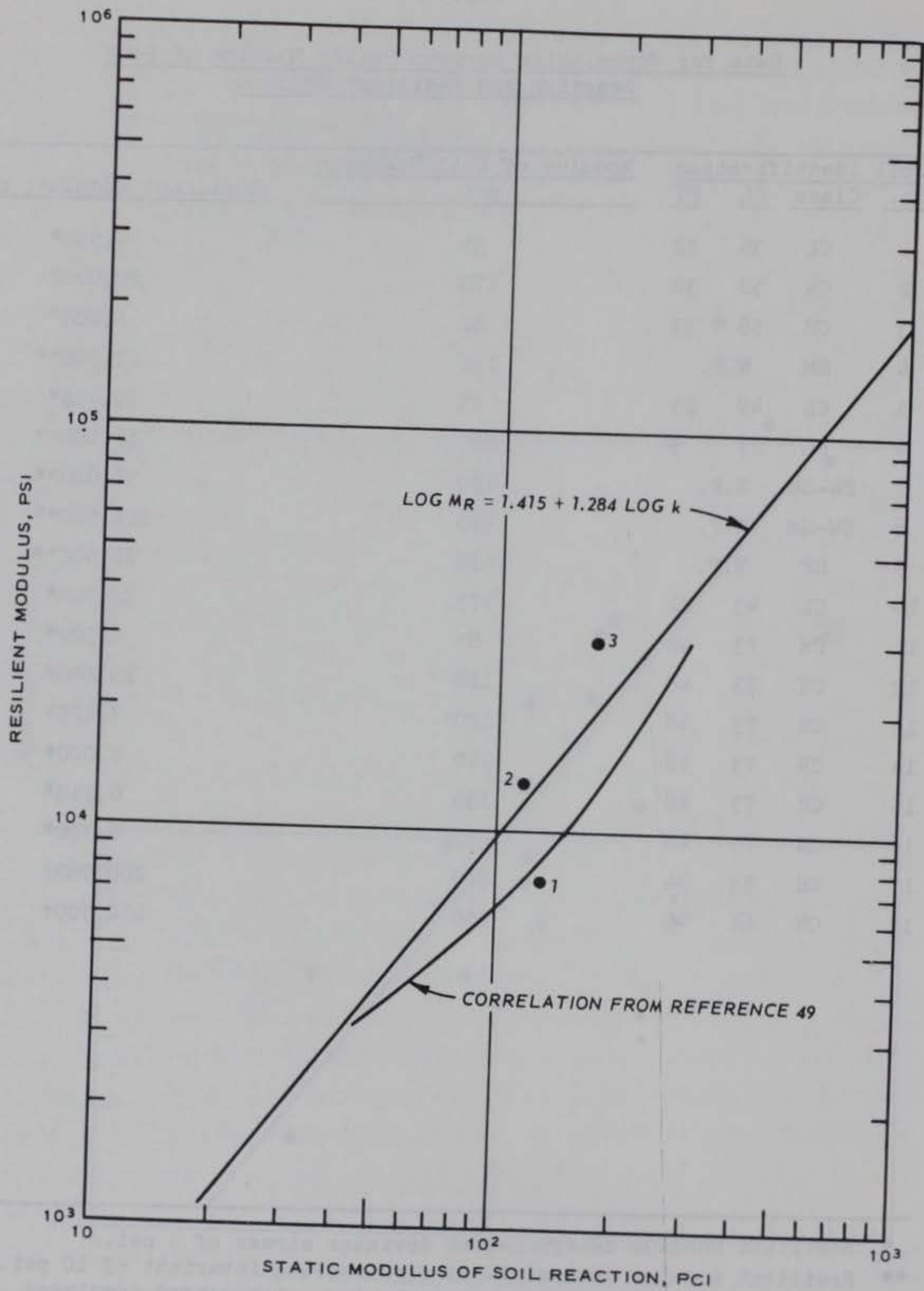


Figure 22. Comparison of correlation with measured values and correlation from Reference 49



were selected at a deviator stress of 5 psi and at a first stress invariant of 10 psi for cohesionless soils.

The moduli of elasticity for the granular base materials in the earlier test sections were selected using data from the previously described correlation (when plate bearing tests were conducted on top of the base courses), combined with information from other sources. This additional information was obtained from procedures for determining moduli of granular materials described by Barker and Brabston (Appendix G<sup>10</sup>) and Chou,<sup>50</sup> and from test results for similar materials presented by Chisolm and Townsend<sup>51</sup> and Hicks.<sup>52</sup> Values for Poisson's ratio were assigned from values recommended by Barker and Brabston.<sup>10</sup> The earlier test pavements did not contain bound base courses.

#### LIMITING STRESS CRITERIA

The limiting stress (fatigue) criteria are presented as a relationship between design factor and coverages. The basic definitions of coverages and design factor are the same as used previously for Corps of Engineers criteria. The one difference in detail is that stress as computed with elastic layered theory is substituted for the stress computed with the Westergaard idealization, and the factor to account for stress reduction due to shear between slabs is omitted. Design factor is now defined as

$$DF' = R/\sigma \quad (6)$$

where

DF' = design factor for stress computed with elastic layered theory

R = PCC flexural strength

$\sigma$  = maximum principal tensile stress at bottom of PCC slab computed with elastic layered model

The limiting stress criteria are illustrated in Figure 23. The data points in this figure are listed in Table 3. The plus signs after coverages in Table 3 and the arrows on the data points in Figure 23



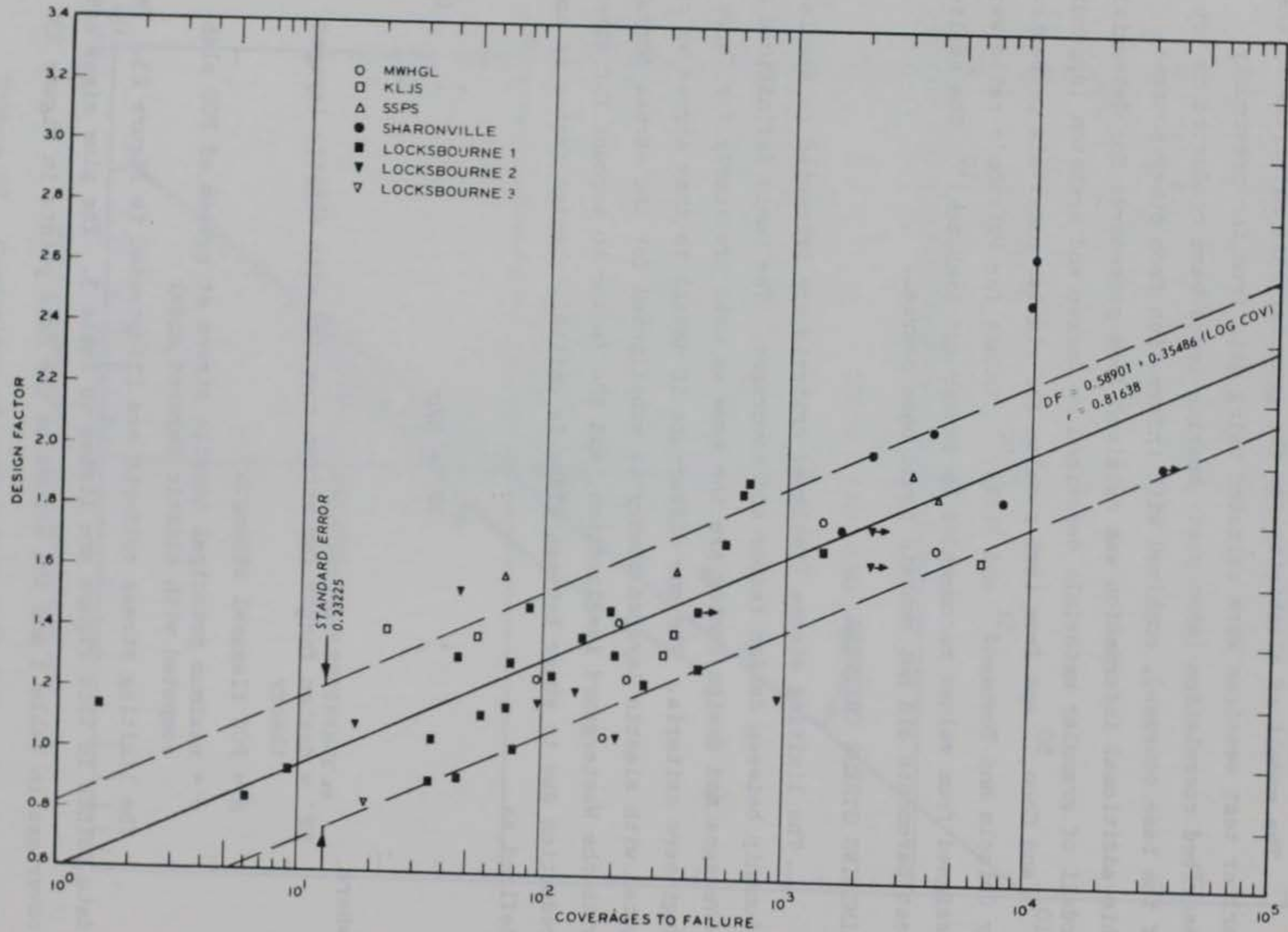


Figure 23. Performance criteria based on design factors listed in Table 3



Table 3

## Data for Development of Performance Criteria

Site Location	Item Identification	Type Load	Traffic, Coverages	Design Factor	Vertical Deflection, in.	
Lockbourne No. 1	A	Dual-Wheel	390+*	1.84	0.0206	
	A		45	1.31	0.0356	
	B		187	1.47	0.0322	
	B		35	1.03	0.0558	
	C		200	1.33	0.0437	
	C		44	0.92	0.0757	
	D		450	1.30	0.0498	
	D		33	0.89	0.0863	
	E		430+	1.48	0.0409	
	E		77	1.02	0.0712	
	F		550+*	1.87	0.0446	
	F		111	1.25	0.0770	
	K		72	1.29	0.0634	
	K		700	1.91	0.0393	
	N		150	1.39	0.0653	
	N		9	0.94	0.105	
	O		573	1.70	0.0575	
	O		72	1.14	0.0928	
	P		262	1.24	0.0894	
	P		6	0.84	0.144	
Q	1,390	1.68	0.0657			
Q	57	1.12	0.106			
U	88	1.51	0.04			
U	1.5	1.16	0.0625			
A (Reconstr.)	Dual-Wheel	658	1.87	0.0435		
Lockbourne No. 2	E1	Single-Wheel	97	1.15	0.0641	
	E2		942	1.19	0.0584	
	E3		17	1.07	0.0808	
	E4		203	1.07	0.0786	
	E5		43	1.53	0.0479	
	E6		2,204+	1.77	0.0407	
	E7		2,204+*	2.44	0.0346	
	M1		Dual-Tandem	134	1.21	0.104
	M2		Dual-Tandem	2,204+	1.63	0.0807
M3	Dual-Tandem	2,204+*	2.46	0.0562		
Lockbourne No. 3	1	Dual-Wheel	18	0.82	0.0903	
Sharonville Channelized	57	Dual-Wheel	34,650+*	2.35	0.04	
	58		34,650+	1.98	0.044	
	59		7,600	1.86	0.03	
	60		1,674	1.80	0.018	
	61		3,867	2.13	0.017	
	62		10,082	2.72	0.013	
Sharonville Heavy Load	71	Dual-Tandem	9,680+*	3.28	0.0295	
	72	Dual-Tandem	9,680	2.53	0.0413	
	73	Dual-Tandem	2,115	2.00	0.0507	
MWHGL	1	C-5A	221	1.25	0.0579	
	2		4,230	1.69	0.0502	
	2		Dual-Tandem	95	1.24	0.0537
	3		Dual-Tandem	205	1.43	0.0454
	3		C-5A	1,400	1.78	0.0433
	4		C-5A	180	1.05	0.0683
KLJS	1	C-5A	54	1.39	0.0589	
	2		344	1.40	0.0530	
	3		22	1.40	0.0579	
	4		6,336	1.76	0.0530	
	4		Dual-Tandem	320	1.43	0.0591
SSPS	3	Dual-Tandem	3,215	2.00	0.0478	
	3		350	1.62	0.058	
	4		4,660	2.00	0.0478	
	4		70	1.61	0.0574	

Note: The plus sign (+) indicates that traffic stopped prior to item failure.

\* Data points not used in analysis.

indicate that the pavements did not fail at the stated traffic level. Of the 10 data points that had not failed, six were considered invalid since these six points had not approached failure. These six points are shown in Table 3 with an asterisk preceding the coverage level.

Several curve fitting techniques were tried on the remaining 54 data points. The one finally selected was a linear relationship fitted to the data by means of least squares with the design factor as the dependent variable and the logarithm\* of the coverages as the independent variable. The resulting relationship in Figure 23 is described by the equation

$$DF' = 0.58901 + 0.35486 \log(\text{Cov}) \quad (7)$$

where  $\log(\text{Cov})$  equals the logarithm of the traffic in terms of coverages. The standard error from the regression in terms of the design factor is 0.23225. The band width of two standard deviations about the regression line is shown as the shaded area in Figure 23. The correlation coefficient from the regression analysis was 0.81638.

Several factors considered in the selection of the particular relationship in Figure 23 should be briefly noted. The selection of the design factor as the dependent variable was made for the purpose of producing a relationship that would minimize (based on least squares criteria) the variability in the required thickness, stiffness, and strength of pavement to carry a certain load. The alternative would have been to select coverages as the dependent variable and design factor as the independent variable. This solution would then minimize the variability with respect to coverages. The choice between the two relationships is subjective in nature, and only through examination of both relationships was the choice made to use the relationship having the design factor as the dependent variable for the design criteria.

---

\* Unless otherwise denoted, all logarithms will be to the base ten.



A single relationship, rather than multiple relationships for several ranges of conditions, was selected because of insufficient data for a range of groupings and from visual inspection of the plot, which showed no well-defined groupings of data points. Groupings according to load and foundation stiffness were tried. A linear regression was selected because its simplicity was commensurate with the nature of the data in the sense that each data point is reflective of numerous factors of a complex problem. In addition, the absence of visual trends in the data did not suggest the applicability of a more complex relationship.

The absence of data points for traffic volumes greater than 10,000 coverages should be noted. Only one point is shown for coverage levels greater than 10,000, and this pavement did not reach failure at the indicated traffic level. Use of the relationship to design for traffic volumes greater than 10,000 coverages (which will frequently be the case for current traffic volumes) will require extrapolation of the linear relationship. There is nothing to suggest that this should not be the case.

#### VERTICAL DEFLECTION CRITERIA

The vertical deflection criteria are presented as relationships between vertical slab deflection and traffic in terms of coverages. The vertical slab deflection data in Table 3 were computed with the elastic layered theory using the BISAR program. For each aircraft gear, the deflection was computed under each tire and under the centroid of the gear. The maximum deflection at these points is shown in Table 3.

Several types of curve-fitting techniques were tried to determine the best fit curve through the 54 data points in Table 3 that were used to develop the design factor criteria. The one finally selected was a power curve fit to the data by means of least squares with the vertical deflection as the dependent variable and the number of the coverages as the independent variable. The resulting relationship in Figure 24 is described by the equation

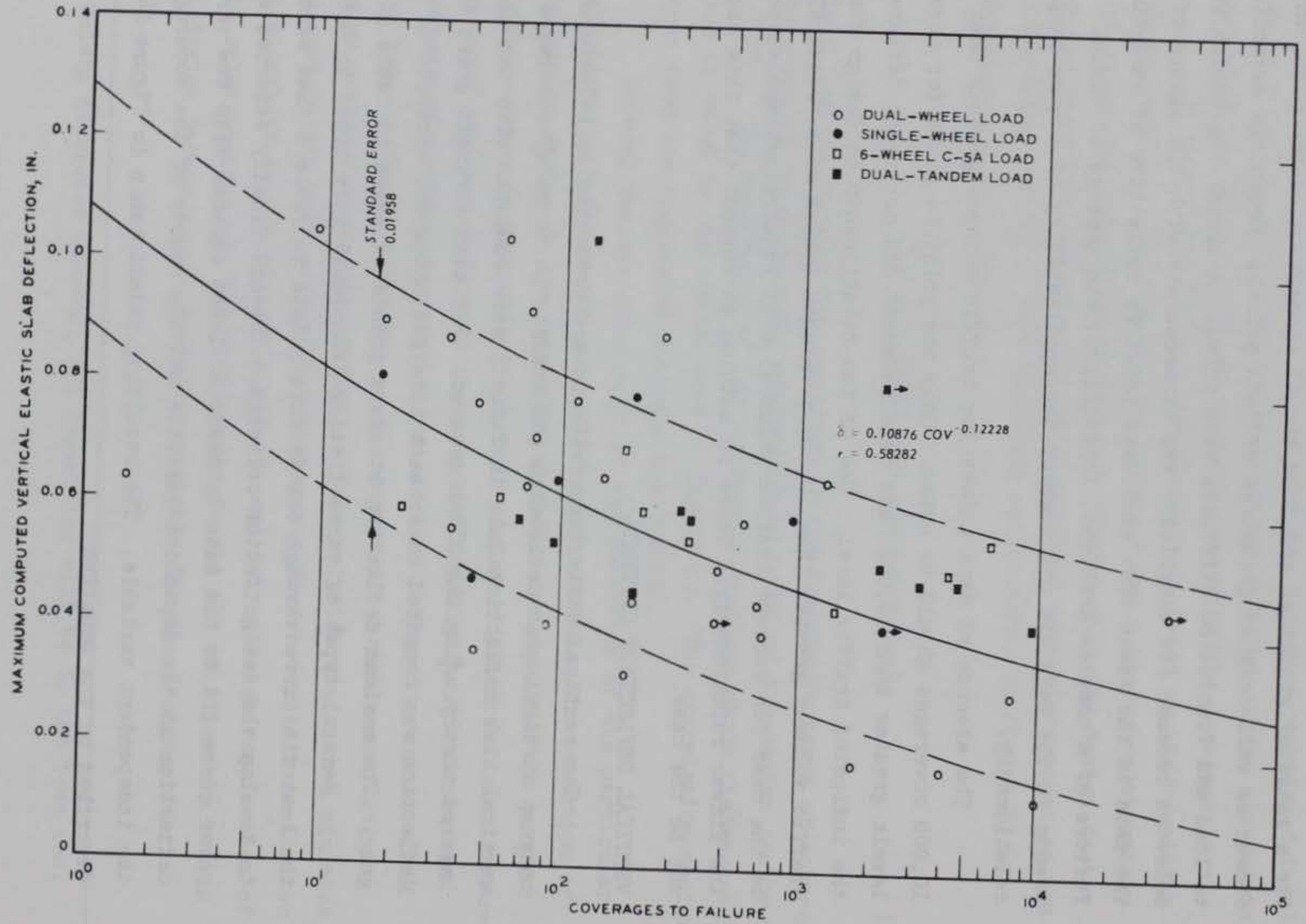


Figure 24. Performance criteria based on vertical deflections presented in Table 3



$$\delta = 0.10876(\text{Cov})^{-0.1228} \quad (8)$$

where  $\delta$  represents the computed vertical elastic slab deflection. The standard error for Equation 8 is 0.01958 in. A band, two standard errors wide, is shown in Figure 24. The correlation coefficient of -0.58282 from the regression analysis signifies that deflection is a poor indicator of pavement performance.

To improve the relationship between computed deflection and pavement performance, an attempt was made to identify particular test sections that may have failed due to excessive deflection. In the plot of the test data (Figure 23), 24 test sections failed at coverage levels less than the coverage level predicted by Equation 7. If the assumption is made that the premature failure of these 24 sections may have been due to excessive deflection, a reason exists for examining these test sections alone. It still must be realized that in most of the test sections the overprediction of Equation 7 will be caused by inherent variability of the test data. Therefore, an analysis of the 24 points was conducted to see where these points were with respect to the best fit deflection curve (Figure 24). The failure coverage for 16 data points is less than the coverage predicted from the deflection-coverage relationship in Figure 24. Thus, no conclusions can be drawn from the failure of these 16 sections, but the remaining 8 test sections did indicate excessive deflection. From this analysis, it was postulated that the eight test sections failed due to excessive deflection and that deflection criteria could be obtained from these data.

A regression analysis was run on these eight points, and the curve selected as the best fit (Figure 25) is described by the equation

$$\delta = 0.098738 (\log \text{Cov})^{-0.57910} \quad (9)$$

This curve was selected as the limiting deflection criterion. Equation 9 has a standard error of 0.00356 and a correlation coefficient of -0.98720.

As an additional analysis, the deflection data were divided into two groups: (a) 35 points in the group for single- and dual-wheel gears

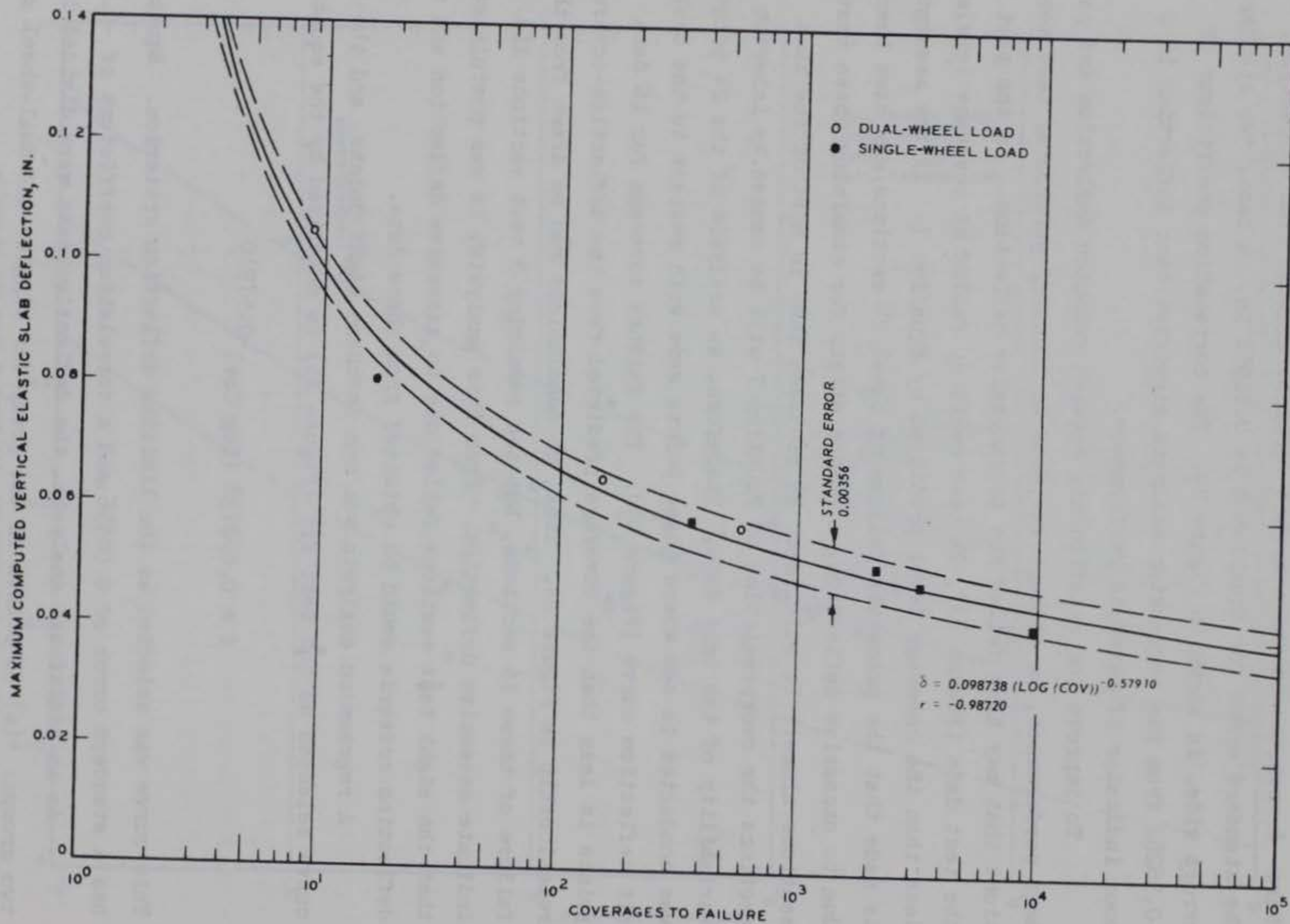


Figure 25. Performance criteria based on vertical deflections assumed to have failed because of excessive deflection



(Figure 26); and (b) 19 points in the group for dual-tandem and C-5A gears (Figure 27). The best fit curve for each group is also shown in the respective figure. The best fit equation for single- and dual-wheel gears is given by

$$\delta = 0.12657(\text{Cov})^{-0.16314} \quad (10)$$

where

$$\text{SE} = 0.02085$$

$$r = -0.67485$$

The best fit equation for multiple-wheel gears is expressed as

$$\delta = 0.077005(\text{Cov})^{-0.049191} \quad (11)$$

where

$$\text{SE} = 0.01355$$

$$r = -0.41200$$

The difference in the two curves in Figures 26 and 27 indicates that the vertical slab deflection varies more with the type of aircraft gear than with the performance of the pavement. Two different aircraft gears could produce about the same stress on a single pavement, but the deflection caused by the aircraft gears could vary greatly. As an illustration, consider the case of a Boeing 747 aircraft with a maximum ramp weight of 713 kips and a Boeing 727 aircraft with a maximum ramp weight of 173 kips. Both of these aircraft produce wheel loads of about 42 kips. Computations for an 18-in.-thick PCC slab ( $E = 4 \times 10^6$  psi,  $\nu = 0.2$ ) on a 12-in.-thick base ( $E = 30,000$  psi,  $\nu = 0.3$ ) over a subgrade with  $E = 10,000$  psi and  $\nu = 0.4$  yield maximum tensile stresses in the slab and maximum vertical slab deflections of 294 psi and 0.0435 in. for the Boeing 747 and 262 psi and 0.0238 in. for the Boeing 727. As noted, the stresses are almost the same, but the deflection produced by the Boeing 747 is almost twice that produced by the Boeing 727. The use of a single relationship for deflection criteria

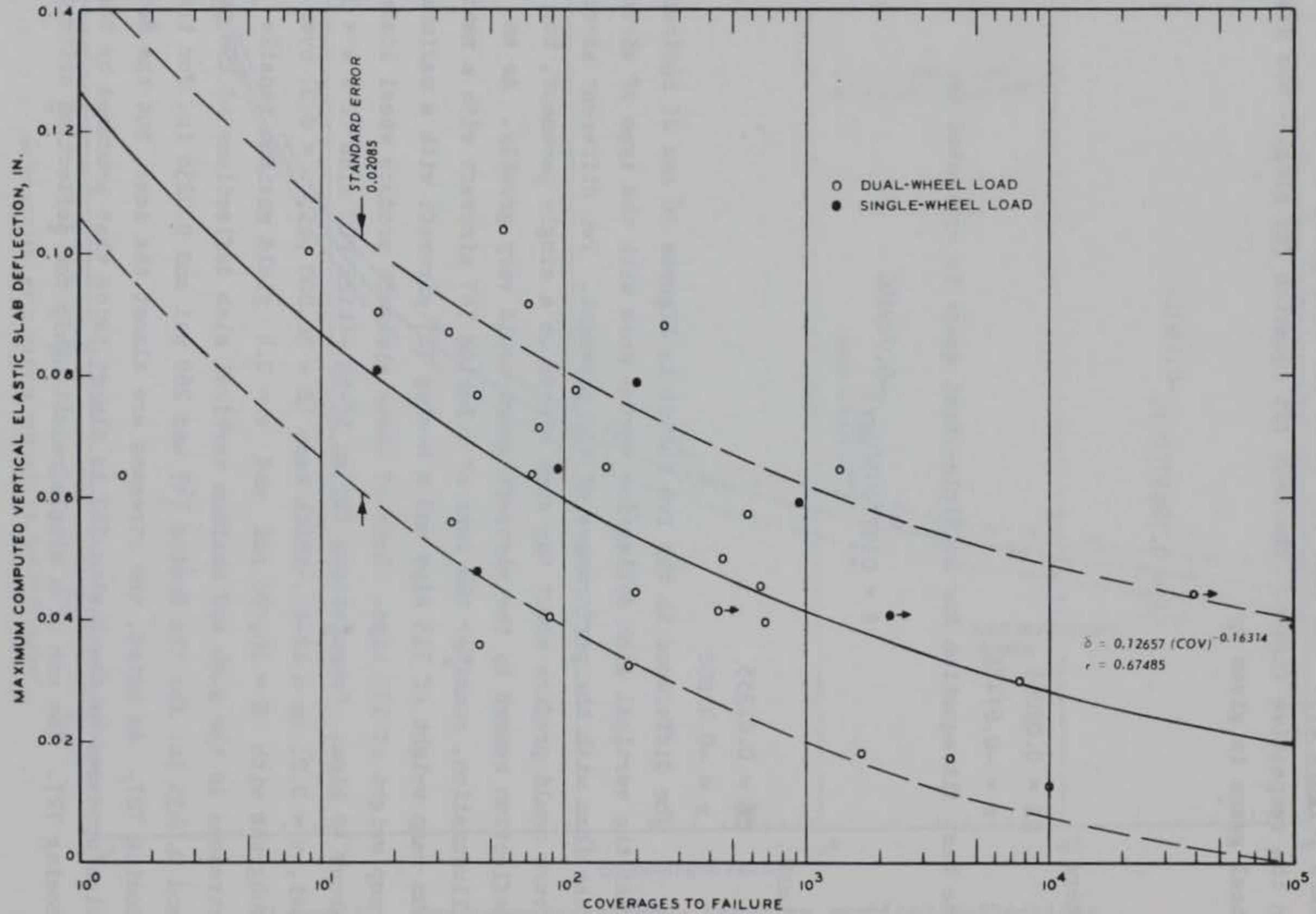


Figure 26. Performance criteria for single- and dual-wheel gears based on vertical deflections



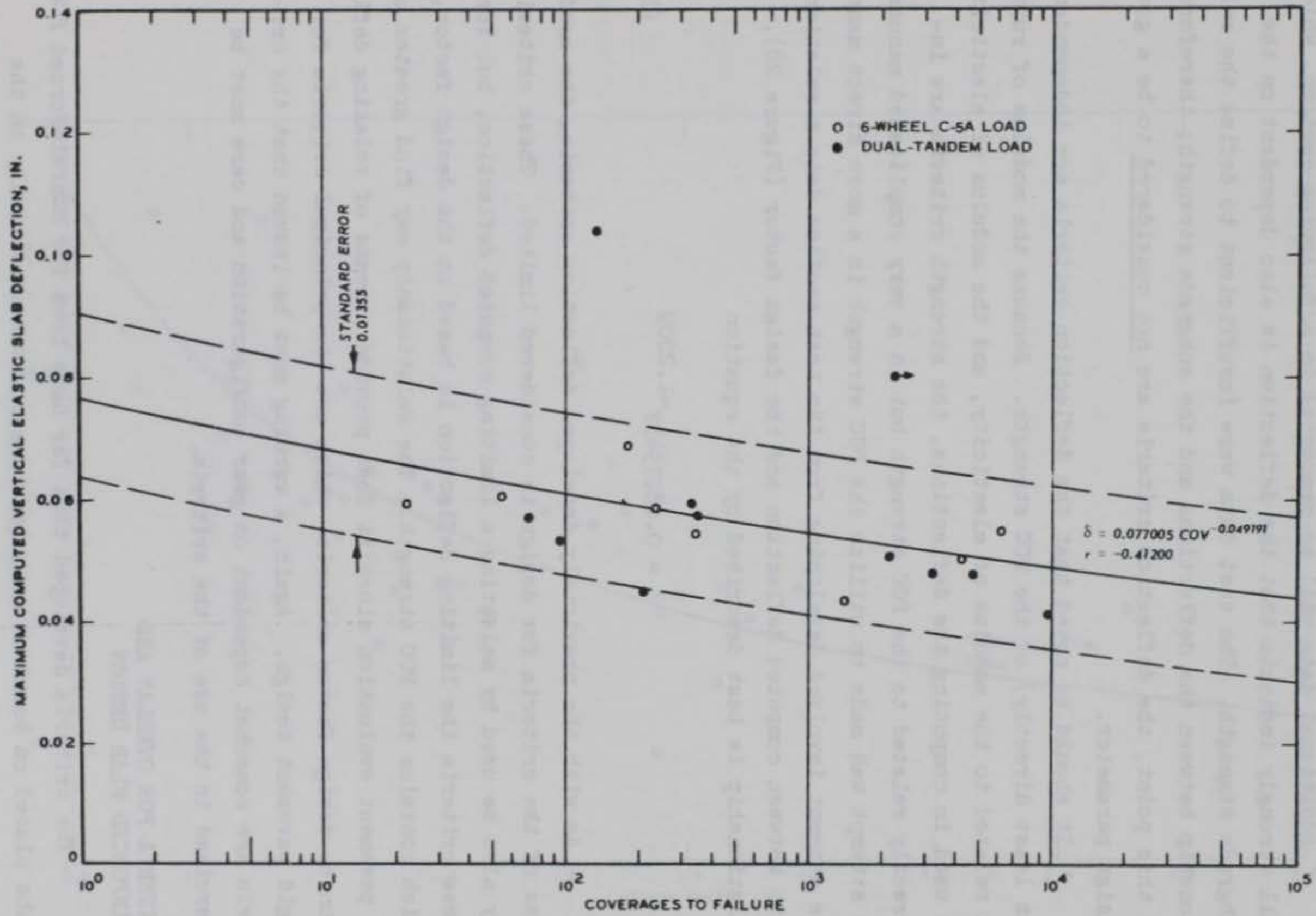


Figure 27. Performance criteria for six-wheel C-5A and dual-tandem gears based on vertical deflections

would be either too severe for the Boeing 747 or unconservative for the Boeing 727.

Additional data will be presented in a following section, which will strongly indicate that the deflection is also dependent on the subgrade strength. The test data were insufficient to define the relationship between the deflections and the subgrade strength; therefore, at this point, the deflection criteria are not considered to be a good design parameter.

It should be noted that the deflection criteria are independent (at least directly) of the PCC strength. Because the modulus of rupture is related to the modulus of elasticity, and the modulus of elasticity is used in computing the deflections, the strength criteria are indirectly related to the PCC strength but in a very complicated manner. An attempt was made to utilize the PCC strength in a more direct manner. The attempt involved developing from the test section data a relationship between computed deflection and the design factor (Figure 28). The relationship is best described by the equation

$$\delta = 0.082794DF^{-1.2209} \quad (12)$$

As with the previously developed deflection criteria, the usefulness of the criteria for design is considered limited. These criteria may also be used by selecting a limiting computed deflection, but for these criteria the limiting deflection is based on the design factor, which contains the PCC strength. The relationship may find greater use in pavement evaluation since it does provide a means of relating deflection to design factor criteria, which are the principal criteria for rigid pavement design. Again, a warning must be issued that the criteria are somewhat dependent on gear configuration and care must be exercised in the use of the criteria.

#### CRITERIA FOR OVERLAY AND REINFORCED SLAB DESIGN

The criteria developed thus far have been for nonreinforced PCC slabs placed on bound or granular base courses or directly on the



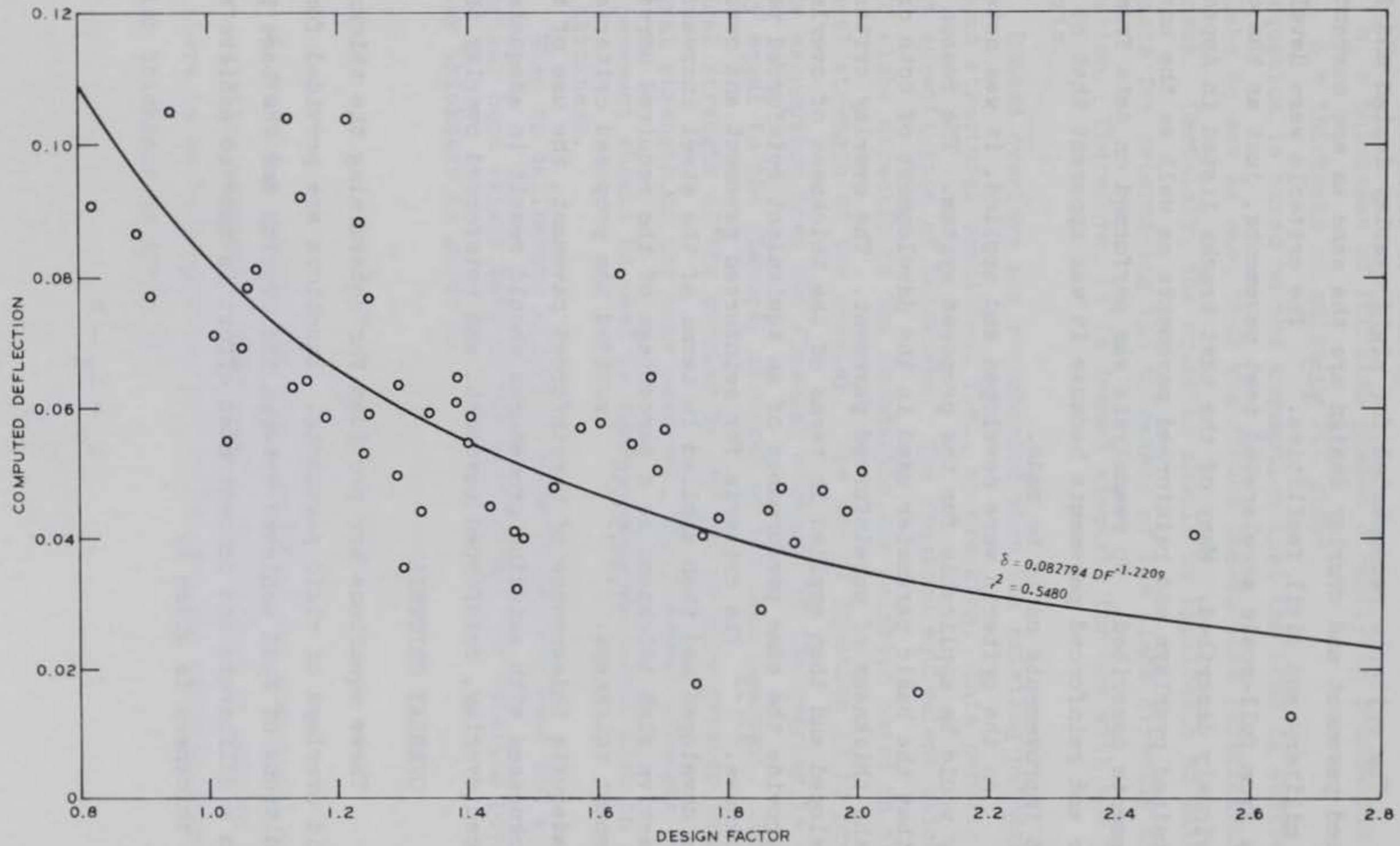


Figure 28. Relationship of computed deflection versus design factor as developed from test section data

subgrade. Criteria for unreinforced rigid overlays and reinforced pavements and overlays will be considered in this section.

The criteria recommended for rigid overlay design and for reinforced pavement and overlay design are the same as are currently employed for military and civil facilities.<sup>1-3</sup> The criteria were developed from data from full-scale accelerated test pavements, just as the criteria previously described. Many of the test tracks listed in Appendix A contained overlays and reinforced pavements as well as the unreinforced pavements described. No reanalysis was performed on data from the overlays and reinforced pavements because it was apparent that no significant improvements could be made.

As the criteria were developed and applied, it was noted that they would be applicable for the proposed system. The reason for this is that the basic parameter used in the development of both criteria is the thickness of unreinforced pavement. The overlay criteria were developed and then applied in terms of the thickness of overlay needed to provide the same performance of an equivalent reinforced pavement thickness.<sup>33,53</sup> The criteria for reinforced pavement and overlay design were developed and then applied in terms of the steel increasing the effective slab thickness as a percentage of the required unreinforced pavement thickness.<sup>33,34,53,54</sup> Provided the proposed criteria result in adequate thicknesses of unreinforced pavement, the use of these thicknesses with existing procedures should result in adequate unreinforced overlay, reinforced pavement, and reinforced overlay thicknesses.

#### OVERLAY CRITERIA

Three equations are provided for determining the thickness of rigid overlays of rigid pavements. Equations are provided for the three conditions of bond achieved between the overlay and the base pavement. When a deliberate and concentrated effort is made to achieve bond, overlay thickness is given by

$$h_o = h_d - h \quad (13)$$



where

$h_o$  = thickness of overlay

$h_d$  = thickness of PCC slab placed directly on foundation

$h$  = thickness of existing PCC slabs

This equation is based on the assumption that the bond is sufficient for two slabs to act as one, thus the direct one-for-one relationship in thickness. Certainly, the equation should be applicable no matter what the basis for determining the thickness of the slabs directly on the foundation. Therefore, it is deemed adequate for use with the proposed criteria.

Bonded overlays are recommended when the existing pavement is in sound structural condition, i.e., no cracking. This permits the direct substitution of thickness. The required equivalent thicknesses of PCC slabs directly on the foundation are selected based on the flexural strength of the overlay. The use of Equation 13 is predicated on the assumption that the flexural strength of the overlay is approximately equal to the flexural strength of the base pavement. Should the flexural strength of the overlay be 100 psi or more greater than the flexural strength of the base pavement, the flexural strength of the base pavement should be used to compute the equivalent slab on foundation thickness.

When no deliberate effort is made to achieve bond and a condition of partial bond exists between the overlay and the existing pavement, overlay thickness is given by

$$h_o = \sqrt[1.4]{h_d^{1.4} - Ch^{1.4}} \quad (14)$$

where  $C$  equals a coefficient that depends on the structural condition of the existing pavement. When a deliberate effort is made to ensure that there is no bond between the overlay and the existing pavement, overlay thickness is given by

$$h_o = \sqrt{h_d^2 - Ch^2} \quad (15)$$



As based on a visual inspection of the existing pavements, the numerical value of  $C$  is established as follows:

$C = 1.00$  when the slabs are in good condition, with little or no structural cracking.

$C = 0.75$  when the slabs show initial cracking caused by loading, but little or no multiple cracking.

$C = 0.50$  when a large number of slabs show multiple cracking, but the majority of slabs are intact or contain only single cracks.

$C = 0.35$  when the majority of slabs show multiple cracking.

Equations 14 and 15 were developed empirically from the results of full-scale test tracks and adjusted where necessary based on actual performance data. The performance of various overlay items was compared with varying thicknesses of slabs on similar foundations under the same load and traffic. The overlay thickness is related to an equivalent thickness of slab on foundations. Therefore, if it is assumed that the equations establish a valid relationship between overlay and equivalent slab on foundation thickness, then appropriate overlay thicknesses can be determined provided the criteria for selecting the equivalent slab on foundation is adequate. Because of their wide usage, it was assumed that the equations provide adequate overlay design; thus, they are recommended for use with the proposed criteria for overlay design.

Although the presently used overlay design equations are recommended, a design procedure with elastic layered theory as the basic response model provides the framework within which the overlay design may be directly incorporated. This will, however, require development of capabilities in several areas, such as the ability to quantitatively define the load-deformation characteristics of cracked pavements (which will be reflective of support provided and the resulting performance of the overlay), and the ability to quantitatively define the degree of bond developed between the overlay and the existing pavement.

A system, such as that currently existing, might be employed for characterizing cracked pavements, i.e., when  $C = 1.00$ , the modulus of elasticity of the PCC layer is as measured for the intact material; when  $C = 0.5$ , the modulus of the PCC layer might be 0.4 times the measured



modulus of the intact material, etc. Further, the same type system might be used to describe the degree of bond achieved between the overlay and the base pavement. The effect of such a system would be the same as the different exponents in Equations 14 and 15. The BISAR code, as recommended for use with the criteria developed herein, does have the capability of considering variable bond between layers, but the problem is in defining the degree of bond.

The bonded case could be handled with the proposed system, provided it is only applied when the existing pavement is structurally sound. However, the only improvement over Equation 13 that could be effected would be to consider differences in the moduli of the PCC in the overlay and the existing pavement. The effect of different PCC moduli are not considered significant. When the moduli are the same, Equation 13 should give the same results as direct application of the design procedure since the assumption of full continuity between the two PCC layers, which is made in the equation and can be made in the response model (BISAR code).

The currently used procedure for design of rigid overlays of flexible pavements is to design the overlay thickness as a slab on foundation where the load deformation characteristics of the existing flexible pavement are defined by a modulus of soil reaction measured with a plate bearing test. It is recommended that the same procedure be employed with the proposed procedure, i.e., the overlay designed as a slab on foundation. Material characterization procedures discussed previously with test procedures outlined in Appendixes C-E should be followed.

When the asphalt concrete (or other type bituminous material) surface layers of the existing flexible pavement are badly fractured and, in the estimation of the designer, will not behave as a bound material, the designer may characterize with either of the following:

- a. The material may be assigned the same properties as granular base or subbase material in the pavement.
- b. The material may be assumed to be granular, and a modulus may be estimated using the procedure described by Barker and Brabston in Appendix G.<sup>10</sup>



If the bituminous surface course is less than 3 in. thick, it may be assigned the same modulus as the base or subbase course regardless of its structural condition.

Occasionally, the use of a plate bearing test to characterize the load deformation characteristics of flexible pavements provides questionable results. The characterization of the materials composing a flexible pavement with the prescribed procedures and the use of these properties in an elastic layered model should improve the design of rigid overlays of flexible pavements.

#### CRITERIA FOR REINFORCED PAVEMENTS AND OVERLAYS

The basic criterion for the design of reinforced pavements and overlays is shown in Figure 29. This relationship was developed empirically from data from full-scale accelerated traffic tests. The test tracks designated Lockbourne No. 1,<sup>40-42</sup> Lockbourne No. 2,<sup>43,44</sup> and Sharonville Channelized Traffic<sup>34,47</sup> contained reinforced test sections of varying thicknesses and percentages of reinforcement.

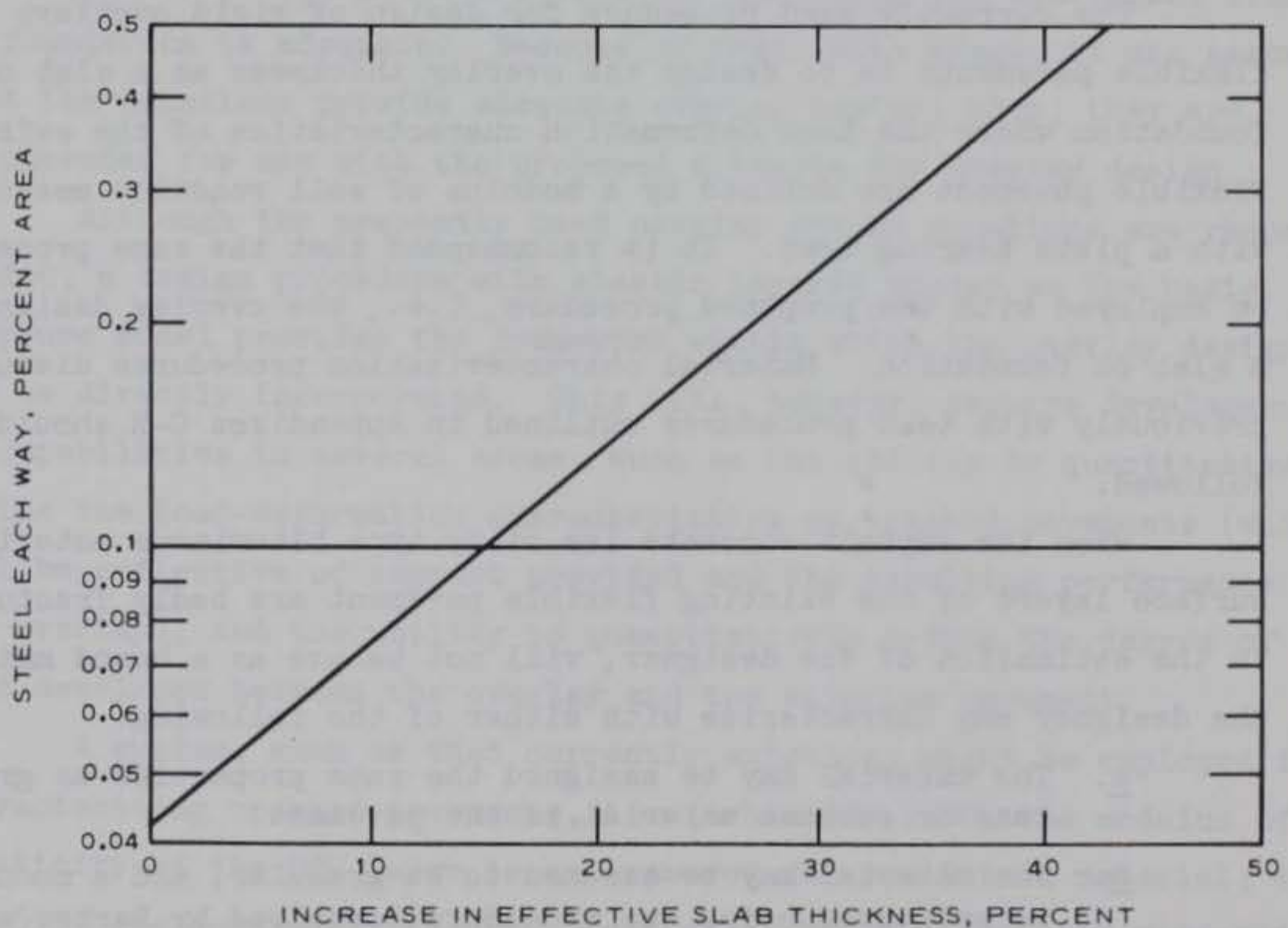


Figure 29. Effect of steel reinforcement on rigid pavements<sup>53</sup>



The relationship in Figure 29 was developed by comparing the performance of plain and reinforced pavements and relating the improvements in performance to the amount of steel. The basis for the comparison was the thickness of unreinforced pavement. Therefore, assuming that the proposed procedure will result in adequate thicknesses of unreinforced pavement, application of the criteria illustrated in Figure 29 should result in adequate thicknesses of reinforced pavements and overlays. Limitations on application of the criteria, as presently employed, should continue to be used.

## ASSEMBLY OF PROCEDURE FOR DESIGN

### GENERAL

Herein, procedures for application of the response model, material characterization tests, and performance criteria to the design of rigid airport pavements will be set forth. Much of the information provided will be general in nature since the problems faced by the engineer will vary widely for each design situation. Although a general procedure is provided by which rigid pavements can be designed, the emphasis has been placed on presenting the development and background in lieu of presenting a cookbook-type design procedure.

### MATERIAL SAMPLING

Only general guidance can be provided for material sampling. The amount accomplished should depend on how much the designer feels he needs to adequately define the properties of the materials so that the resulting pavement will have the desired reliability. The variability of the subgrade, borrow and aggregate sources, number of material sources considered, the type of facility being designed, etc., should determine the extent of the material sampling program.

### SUBGRADE AND BORROW

Guidance for soils investigations for currently used procedures are contained in References 1-3 and 24. Provisions for exploratory surveys and preliminary investigations, as contained in these references, are applicable to the procedures outlined herein. The depth and spacing of borings contained in these references for cut, fill, and borrow areas are applicable. Samples should be obtained from the borings or from pits for classification and development of compaction data.

The extent of undisturbed sampling will depend on the results from the preliminary soil survey. At least four samples of each distinct type of subgrade soil should be obtained for resilient modulus testing. Bag samples of each distinct type of borrow material proposed for use as



fill should be taken to provide for preparation of four samples of each distinct type material for resilient modulus testing.

#### BASE (SUBBASE) MATERIAL

Samples from all sources of aggregate that are to be considered in the design process should be obtained in quantities sufficient to perform classification tests, durability tests, and at least four specimens for resilient modulus testing. If a binder is to be used to produce bound base material, the samples from available sources should be obtained and used in the preparation of specimens for resilient modulus testing. Procedures as currently employed to ensure that binders (cement, lime, fly ash, or bituminous materials) meet required specifications should be employed.

#### PORTLAND CEMENT CONCRETE

Samples from available sources of aggregate, portland cement, and additives should be obtained and tested to ensure compliance with material specifications. In addition, samples of aggregate from available sources and representative samples of portland cement and additives should be obtained for mixture proportioning studies to determine ranges of flexural strength and modulus.

#### EXISTING PAVEMENTS TO BE OVERLAID

The basic requirements for a preliminary survey of pavements to be overlaid is the same as for a new pavement, i.e., to define the materials within the pavement. If as-built plans and specifications are available, the preliminary investigation may be omitted. However, if this information is not available a series of borings will be necessary to determine the layered system comprising the existing pavement. Undisturbed samples, where possible, or disturbed samples for cohesionless materials should be obtained for all materials in quantities sufficient to provide four specimens of each distinct material type for resilient modulus testing.



For rigid pavements, samples should be obtained for the subgrade and base course layers. Condition coefficients should be established, as outlined in References 1-3, to define the structural condition of the PCC surfacing. Beams of the existing PCC should be obtained for flexural testing, or if this is not possible, cores should be obtained for split tensile testing. Procedures for obtaining and testing drilled cores and sawed beams are outlined in ASTM Standard Method C 42-68<sup>55</sup> (CRD-C 27-69<sup>56</sup>).

For flexible pavements, samples should be obtained for the subgrade, subbase course, and base course layers. For bituminous surfacings, layers 3 in. thick or less need not be sampled, and the layer may be included with the base layer when assigning material properties. Likewise, when the bituminous surface layers are cracked to the point where they would not function as a continuous layer of bound material, then the same material properties may be assigned as for the base layer. No specific guidance can be provided to determine the amount of cracking that will destroy the integrity of the bituminous surfacing. It will be a matter of the opinion of the designer.

#### MATERIAL CHARACTERIZATION

The standard tests for classifying materials, establishing compaction requirements, and determining if material specifications are met will be the same as those presently employed.<sup>1-3,24</sup> Procedures, different from those currently used, will be needed to characterize the load deformation properties of each material. These properties will be determined from laboratory tests rather than from field tests.

Variations will be obtained in material properties. For design, it is recommended that the average value of modulus of elasticity be used. The 80 percentile value is recommended for use when determining the design value of flexural strength. Selection of Poisson's ratio will not be so precise. All available data should be studied, including recommended typical values, and a representative value selected.

Procedures are available for estimating modulus values as well as values of Poisson's ratio. The reliability desired in the resulting



design should be considered before relying on a procedure that will result only in an approximation of the material properties. Thickness design is not overly sensitive to Poisson's ratio and approximations are acceptable, although it is recommended that tests be conducted and used in conjunction with typical values for selecting a representative value.

#### SUBGRADE

Test procedures for subgrade soils are outlined in Appendix E. Cohesionless soils will be insensitive to moisture content, but very sensitive to density. Samples should be prepared as close as possible to field densities. Moduli values should be computed at first stress invariants of 10 psi, and average values computed. Computations of Poisson's ratio should be made and compared with typical values for selecting representative values for design.

Cohesive soils are sensitive to moisture content and density and should be tested at the most critical conditions. Normally, this will be in a condition of complete saturation. However, for arid locations where experience indicates that saturated conditions are never attained, moisture contents less than saturation may be used. Undisturbed samples should be used where applicable and where possible. For fill material, specimens should be compacted to simulate field conditions (density and moisture) as close as possible and saturated from the as-compacted condition. Moduli values should be computed at a deviator stress of 5 psi, and the design value selected as the average value from test results.

When the potential for frost action exists and the pavement is to be designed based on zero or partial frost protection, the subgrade should be tested according to procedures outlined in Appendix B of Reference 10. Moduli values should be selected at a deviator stress of 5 psi, and the average value selected for design. When the subgrade is to be protected against frost penetration (even though climatic and soil conditions are conducive to frost action), procedures outlined in Appendix E should be used.



Computations of Poisson's ratio should be made and compared with the typical values to select a representative design value.

Procedures for characterization of subgrades beneath existing pavements for overlay design are basically the same as those described above, exceptions being that the materials should be tested at their in situ moisture and density conditions. Exceptions to this would be conditions where frost penetration may produce higher water contents during thaw periods or special conditions (sample taken near edge of paved area or in areas where the surface was not sealed) where the moisture conditions are not those normally prevailing in the subgrade.

#### BASE (SUBBASE) MATERIAL

Separate procedures are provided for granular and bound base materials. Granular materials should be tested in compression according to procedures outlined in Appendix D. The response of granular bases, while insensitive to moisture, is dependent on the density of the material. Therefore, specimens should be prepared as close as possible to field densities. Moduli values should be selected at first stress invariants of 10 psi, and average values selected for design. Computations of Poisson's ratio should be made and compared with typical values for selecting a representative design value.

Bound base materials should be tested in flexure according to procedures outlined in Appendix C. Separate procedures are provided for chemically stabilized and bituminous stabilized bases. Chemically stabilized materials are sensitive to curing time and conditions and should be moist-cured for 28 days prior to testing. Bituminous stabilized materials are sensitive to temperature, and the design modulus should be selected for average temperature conditions in the base. The average temperature may be selected from available temperature prediction models. The values selected for design should be the average of all values obtained. Poisson's ratio should be selected from the following recommended values:



<u>Material</u>	<u>Poisson's Ratio</u>
Bituminous Stabilized	0.5 for E < 500,000 psi 0.3 for E > 500,000 psi
Chemically Stabilized	0.2

#### PORTLAND CEMENT CONCRETE

Mixture proportioning studies should be conducted to establish a practical range of flexural strength that may be obtained with available materials. Flexural strength tests are conducted according to ASTM Standard Method of Test C 78-75<sup>57</sup> (CRD-C 16-66<sup>56</sup>). During the conduct of flexural tests, deflections should be measured, and moduli of elasticity computed according to procedures outlined in the Corps of Engineers procedure CRD-C 21-58.<sup>56</sup>

The design strengths specified should depend on the method used in the specifications. If mixture proportions are contained in the job specifications, the design strength should be the strength obtainable 80 percent of the time with the specified mixture proportions. If flexural strength is specified in job specifications, the design strength should be the strength reasonably obtainable 80 percent of the time with locally available materials that meet other material requirements. The 80 percentile strength should then be used for construction quality control.

Normally the modulus of elasticity of PCC will not vary over a very wide range for aggregates from a particular locality. For the mixtures meeting strength requirements, a representative value of modulus of elasticity should be selected. Should a range of over 1,000,000 psi exist between the moduli for proposed mixtures, limiting moduli from the ends of the range should be used in the design procedure. Should this result in differences in the required thickness, each thickness design would then have to be tied to particular mixtures. However, situations that require different thicknesses based on the modulus of elasticity of the concrete will, in all likelihood, be rare.

Strength of PCC in existing pavements may be obtained by testing beams sawed from the pavement according to ASTM Standard Method of Test



C 78-75<sup>57</sup> (CRD-C 16-66<sup>56</sup>) or from tensile strength obtained from split tensile tests according to ASTM Standard Method of Test C 496-71<sup>58</sup> (CRD-C 77-22<sup>56</sup>) on cores from the pavement. The split tensile strength should be converted to flexural strength with a correlation recommended by Hammitt<sup>59</sup> or other correlations as available.

#### LAYERED SYSTEM DESIGN

Once the properties of available materials have been determined the optimum (economic and structural considerations) layered system may be selected by a trial-and-error process. PCC slab thickness and base course type and thickness will be the primary parameters that may be varied. The results will be an array of acceptable designs, which are structurally acceptable but must be evaluated economically to determine the optimum design.

The array of acceptable layered systems will be bounded by practical limitations. The minimum thicknesses of bases and PCC slabs are based on structural requirements, construction constraints, thickness limitations based on soil and environmental conditions (swelling soils, frost action, etc.), and limitations of locally available materials. Awareness and adherence to these practical limitations will reduce the effort required by the designer.

The procedures for selecting layered thicknesses, as outlined herein, will be based solely on structural considerations. However, special requirements, as currently specified in References 1-3 and 24, should control when thicker or higher quality layers are indicated.

#### LIMITING STRESS CRITERIA

The limiting stress criteria (Figure 23) are used to select a PCC slab thickness for a given set of foundation conditions. Base course thickness is controlled by the stress criteria, but the control is indirect. Base course thickness will normally be held constant, and the thickness of the PCC slab varied until an acceptable structure is determined. The process can then be repeated with a different base thickness. The entire process may be repeated for all available materials. In areas where frost problems exist, the base course thickness



will probably be controlled by requirements for protection of the subgrade against frost penetration.

The use of the limiting stress criteria can best be demonstrated by a set of example problems. Three foundation conditions are illustrated in the examples. One case will be with the PCC slab directly on the subgrade, a second is with the PCC slab on a 12-in. base course layer with properties similar to a granular material, and a third case is with the PCC slab on an 8-in. base course layer with properties similar to a bound material. Two conditions of traffic are illustrated in each of the examples, one similar to that which might be encountered at a civil aviation facility and a second similar to that which might be encountered at a military installation.

Four procedures for handling traffic or loads are illustrated. For the examples for civil facilities, the procedures recommended in Reference 1 are followed. To determine a pavement thickness, all traffic is equated to equivalent DC-8-61 traffic with the relationship

$$\log R_1 = \left( \log R_2 \right) \left( \frac{W_2}{W_1} \right)^{1/2} \quad (16)$$

where

$R_1$  = equivalent DC-8-61 departures

$R_2$  = adjusted departures of aircraft in question

$W_1$  = wheel load for equivalent DC-8-61

$W_2$  = wheel load for aircraft in question

A second thickness of the pavement is determined only for the wide-body jet aircraft in the traffic mixture. When Equation 16 is used, wide-body jet aircraft are substituted for equivalent DC-8-61 traffic on a one-to-one basis. The number of departures for aircraft with single- or dual-tire gears should be adjusted using the following conversion factors:

<u>To Convert</u>	<u>To</u>	<u>Multiply <math>R_2</math> by</u>
Single wheel	Dual tandem	0.50
Dual wheel	Dual tandem	0.60



For the examples for military installations, the pavements are designed for each aircraft, and the required thickness is selected for the critical aircraft. For both civil and military designs, the cumulative damage concept is applied in a rather crude fashion, and the pavement designed for the entire mixture of traffic.

For the four methods of handling traffic, the proposed criteria will be an approximation. The test pavements were loaded with only one type load, and the loads were applied across the pavements in specific patterns. In many of the earlier tests, the loads were distributed uniformly across the pavements; in the later tests, the loads were applied in a distribution simulating a normal distribution. Interwoven into these criteria is also the concept of "coverages." The concept of coverages as applied herein is discussed in Reference 36. It is a difficult concept to comprehend, and impossible to extend or use with other criteria, such as fatigue data developed from flexural tests of concrete beams. However, conceptually it is analogous to the more general terminology of stress or load repetitions even though the two are not interchangeable. The traffic at failure (in terms of coverages) assigned each of the test pavements was for one type load and is implicitly tied to the manner in which the traffic was applied.

From the standpoint of applied load, the procedure of equating all traffic to equivalent DC-8 traffic and the use of this one load with the criteria is conceptually correct since the test pavements were loaded with only one type load. The assumption necessary is that Equation 16 realistically accounts for the differences in load configuration and distribution of load on the pavement. Certainly the equation provides only an approximation, but as will be seen in the examples, it is an acceptable approximation.

The procedure of designing for only the wide-body jet aircraft and comparing this design with the design for the equivalent DC-8 design is similar to the procedure employed for military design, i.e., the most critical design (thickest slab) is selected. Conceptually the use of this procedure with the proposed criteria is correct from the standpoint of load and load application. However, the assumption necessary is that the pavement life or thickness required is not affected by any loading



except the critical loading, i.e., the loading requiring the thickest pavement. This assumption may not be totally valid, but as will be seen in the examples, it also provides an acceptable approximation.

The use of any of the procedures described has the advantage of simplifying the process of treating a mixture of traffic. This simplification appears to be in order when considering the impreciseness of the performance relationship, the precision of material characterization procedures, and the accuracy of estimates of traffic (both numbers and magnitude of loads).

The use of cumulative damage concepts to account for the effects of mixed traffic is a more complex procedure than those previously described. Conceptually it is a more satisfying procedure since theoretically the effects of each load, the differences in the distribution of each load across the pavement, and their cumulative effects on pavement life (or thickness required) can be considered. However, several factors should be noted to caution the user when using this procedure.

As noted previously, the data for development of the limiting stress criteria (Figure 23) were from pavements where only one load was used, and this load was distributed across the pavement in a particular manner. The effects of different loads are not accounted for in the criteria, and one is forced to make the assumption that each load has a detrimental effect on the pavement and that Miner's hypothesis, in some form, can be used to accumulate the damage from each aircraft. The feeling that most people have is that each aircraft operation does have some detrimental effect on the pavement; however, no definitive data exist to show this (to the author's knowledge). Conversely, there is a certain amount of evidence available from laboratory tests to indicate that the fatigue strength or life of concrete is not adversely affected by loads less than some fraction of a failure load and that they may even have a beneficial effect.<sup>60,61</sup> Certainly a pavement is a more complex system than a beam or cylinder, and in addition to fatigue of the concrete, such things as foundation support are affected by load repetitions. However, because of the lack of definitive data to prove



or disprove its validity, the use of Miner's hypothesis must be considered only as a rough approximation.

When cumulative damage concepts are applied, one is faced with the task of choosing the complexity of the analysis to be performed. The limiting stress criteria (Figure 23) are based on the maximum stress existing in the pavement, i.e., design factor is defined as the ratio of flexural strength of concrete to the maximum induced stress. Stresses less than the maximum do exist in the pavement, and one must decide whether to include their effects in the analysis. Similarly, the location of the maximum stress will vary as the position of the gear varies. In addition, the peak of the load distribution for each aircraft will vary. This can best be illustrated by considering Figure 30. This figure illustrates, conceptually, two distributions of loads across a pavement and the distribution of stress within the pavement for loads located at the center of the distribution, i.e., the location where they are most likely to occur. The criteria, as developed, are based only on the maximum stress that occurs, and through the concept of coverages, the critical location within the pavement, i.e., the location (one tire width wide) where the maximum number of maximum stress repetitions will occur. When an accumulated damage approach is used, one must decide whether or not to try to account for the effects of stresses other than the maximum. This is represented by the unshaded area in Figure 30. The next decision that must be made is whether or not to consider the differences in the locations of the center line of the distributions of the various aircraft (aircrafts A and B in Figure 30). With the criteria, as developed, inclusion of either effect will be only an approximation.

In the examples, only the maximum stress is considered, and the location of the center line of the distributions of each aircraft is considered to be coincident, i.e., the pass-to-coverage ratios developed in Reference 36 were used to convert aircraft departures or operations to coverages. This is a rather crude application of cumulative damage concepts but is as complex as can be justified considering the approximations involved.



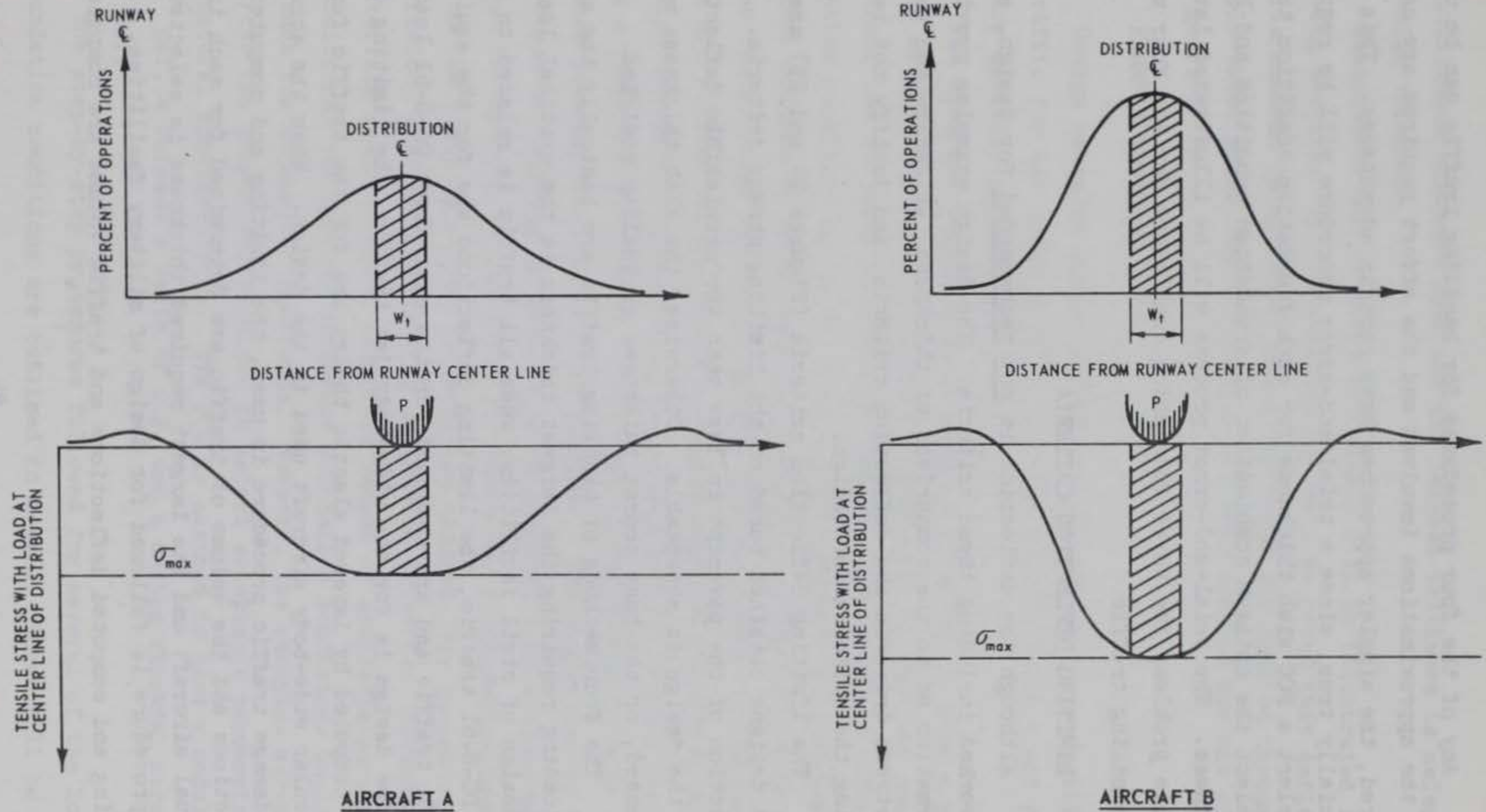


Figure 30. Distribution of aircraft load and stress within pavement



Any of the four procedures for handling traffic can be used. When the approximations involved and the effort required are considered, the simpler approaches have certain advantages. This is especially true, since a trial-and-error procedure will be required to select a PCC slab thickness for each foundation condition tried and to select the optimum combination of foundation condition and PCC slab thickness. The trial-and-error process will be illustrated later with example problems for three foundation conditions for the four methods for handling traffic.

#### LIMITING DEFLECTION CRITERIA

Although the deflection is not recommended for design, examples are worked including these criteria. The design examples provide some information as to the comparison of thickness, as determined by both the stress criteria and deflection criteria, and justify not recommending the criteria for design.

The limiting deflection criteria (Figures 24 and 25) are used to check designs obtained based on the limiting stress criteria. If the deflection of the pavement is less than the permissible deflection, then the design is acceptable. Otherwise, the slab thickness must be increased, or the base course thickness or quality modified.

The four methods of handling traffic are basically the same. The loading requiring the largest thickness is the critical loading. For design of civil facilities, when all traffic is related to equivalent DC-8-61 traffic, the limiting deflections are for the equivalent DC-8-61 traffic and are computed for the equivalent DC-8-61 load. When the design is for the wide-body jet traffic, the limiting deflections computed by layered elastic theory are for the traffic for the particular wide-body aircraft used in the design. When the accumulative damage traffic procedure is used, the limiting and computed deflections and the volume of traffic are determined for each individual aircraft and the largest required thickness is selected. The same procedure is followed for design of military facilities, i.e., limiting and computed deflections and traffic volume are computed for



each individual aircraft load and the largest thickness is selected as the design thickness.

Examples of all of these procedures will be illustrated in the following section. In the examples, it will be noted that deflection criteria control in all cases where the loads are applied through multiple-wheel gears, but the stress criteria control for the single-wheel gears.

#### EXAMPLE PROBLEMS

Design examples follow for both civil and military facilities. The traffic for the civil facility is tabulated in Table 4 and for the military facility in Table 5.

The subgrade soil for the examples is assumed to have a resilient modulus of 10,000 psi and a Poisson's ratio of 0.4. For one foundation condition, the PCC slab is placed directly on the subgrade. The second foundation condition is one in which a 12-in. base course having a resilient modulus of 30,000 psi and a Poisson's ratio of 0.3 is placed between the PCC slab and the subgrade. The properties of the base course are similar to what might be contained with a granular material. The third foundation condition is one in which an 8-in. base course having a resilient modulus of 300,000 psi and a Poisson's ratio of 0.2 is placed between the slab and the subgrade. The properties of this base course are similar to what might be obtained with a bound material. PCC slab thicknesses are selected for these three foundation conditions based on the limiting stress criteria and checked, for purposes of illustration, against the limiting deflection criteria. Assuming that the materials used represent realistic ranges of available materials, then additional designs for different foundation conditions would have to be made for economic comparisons. However, the examples serve to illustrate the procedures required to select acceptable pavements based on structural considerations. The PCC is assumed to have a modulus of  $4 \times 10^6$  psi, a Poisson's ratio of 0.2, and a design flexural strength of 700 psi.

The step-by-step procedures followed for several of the loading and foundation conditions are outlined in detail. These will be typical



Table 4

Traffic for Example of Design for Civil Facility

<u>Aircraft</u>	<u>Traffic Volume Annual Departures</u>	<u>Gross Aircraft Weight, kips</u>	<u>Contact Area, in.<sup>2</sup></u>
DC-9	7000	115	165
B-727	7000	173	237
DC-8	2000	358	209
B-747	1000	713	245

Note: Designs assume 95 percent of gross aircraft weight on main gears.

Table 5

Traffic for Example of Design for Military Facility

<u>Aircraft</u>	<u>Traffic Volume Annual Departures</u>	<u>Gross Aircraft Weight, kips</u>	<u>Contact Area, in.<sup>2</sup></u>
B-52	1000	480	267
KC-135	2000	300	267
C-141	2000	320	208
F-111	4000	110	241

Notes: 1. Designs assume 90 percent of gross aircraft weight on main gears.  
2. Load for B-52 includes 15 percent overload factor.



of the procedures followed for other conditions. The results for all the loading and foundation conditions will then be tabulated and compared.

Design for Civil Facility--Granular Base. For a 20-year design for a civil facility, a 12-in. granular base over the previously described subgrade and all traffic equated to equivalent DC-8-61 traffic, the first step is to convert the annual departures in Table 4 to total departures by multiplying the annual departures by 20. The next step is to apply Equation 16 to convert the total departures to equivalent DC-8-61 departures. This results in the following:

<u>Aircraft</u>	<u>Total Departures</u>	<u>Equivalent DC-8-61 Departures</u>
DC-9	140,000	8,800
B-727	140,000	69,400
DC-8	40,000	40,000
B-747	20,000	<u>20,000</u>
		138,200

The next step is to convert the total equivalent DC-8 departures to coverages by dividing by the pass-to-coverage ratio of 3.35.<sup>36</sup> This results in traffic as expressed in coverages of 41,300. Applying Equations 7 and 9, respectively, results in a required design factor of 2.23 (stress criteria) and a limiting deflection of 0.0407 in.

The next step is to run the BISAR computer program for several trial slab thicknesses. The design factor is computed, and the results may be tabulated in the following manner:

<u>PCC Slab Thickness, in.</u>	<u>Design Factor</u>	<u>Slab Deflection, in.</u>
14	1.52	0.0594
16	1.80	0.0516
18	2.10	0.0453
20	2.44	0.0400
22	2.79	0.0357

These results may be plotted as illustrated in Figure 31, and a required slab thickness of 18.8 in. is selected. A check of deflection criteria reveals that a PCC slab thickness of 19.7 in. would be required to meet the deflection criteria. This completes the structural design for this one load and foundation condition.



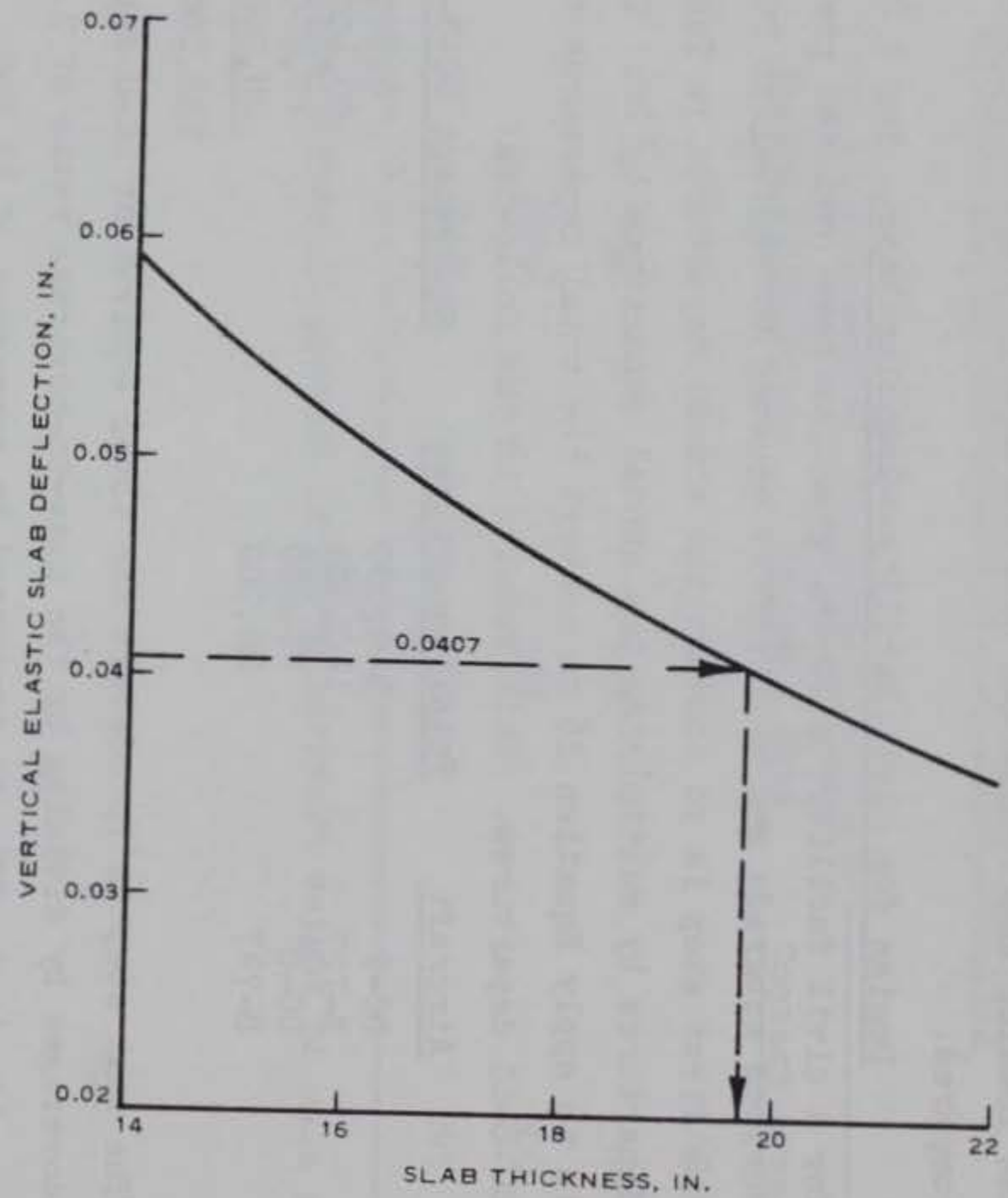
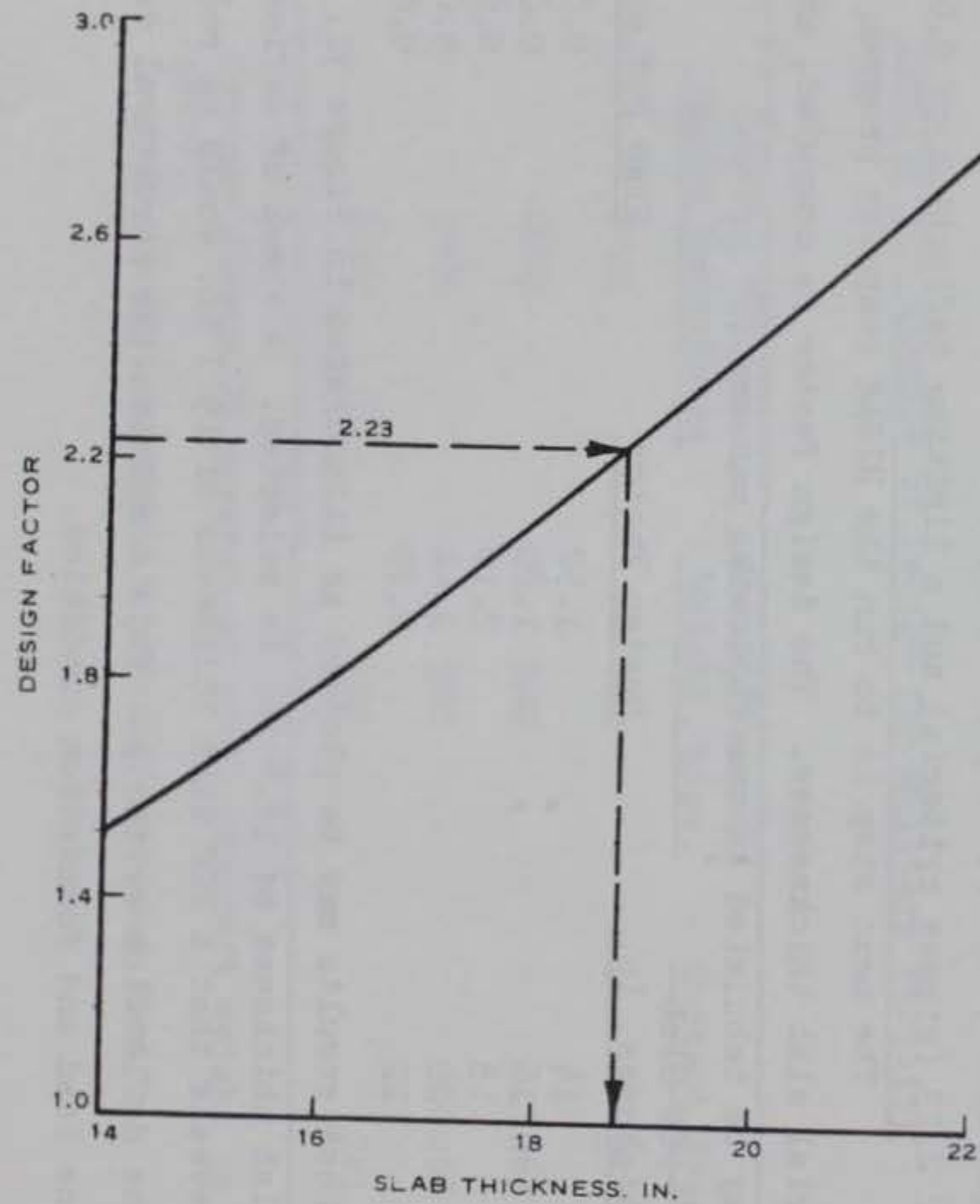


Figure 31. Selection of required slab thickness - civil facility - equivalent DC-8 traffic



The design for the wide-body jet aircraft in the traffic mix is similar. The 20,000 total departures are converted to 5,750 coverages with a pass-to-coverage ratio of 3.48.<sup>36</sup> Applying Equations 7 and 9, respectively, results in a required design factor of 1.92 and a limiting deflection of 0.0459 in. The BISAR computer code was run for several trial slab thicknesses, and design factors computed with the maximum stress. The results are tabulated as follows:

<u>PCC Slab Thickness, in.</u>	<u>Design Factor</u>	<u>Slab Deflection, in.</u>
12	1.45	0.0650
14	1.73	0.0565
16	2.04	0.0494
18	2.38	0.0435
20	2.75	0.0387

These results may be plotted as illustrated in Figure 32, and a required slab thickness of 15.2 in. is selected. A check of deflection criteria reveals that a 17.1-in.-thick PCC slab is required for satisfying the deflection criteria. Thus, the equivalent DC-8-61 traffic is critical, and the design would be based on the slab thickness requirement of 18.8 in. for the DC-8-61.

Design for Military Facility--Bound Base. This example illustrates the procedure for selecting PCC slab thickness for the traffic tabulated in Table 5 and a foundation composed of the 8-in.-thick bound base course ( $E = 300,000$  psi and  $\nu = 0.2$ ) over the previously described subgrade ( $E = 10,000$  psi and  $\nu = 0.4$ ). For a 20-year design for a military facility, the first step is to convert the annual aircraft passes in Table 5 to total passes by multiplying by 20. The next step is to convert the total passes for each aircraft into coverages by the appropriate pass-to-coverage ratios from Reference 36. Equation 7 is then applied to determine the design factor, and Equation 9 is applied to determine limiting deflection. The results of these steps on the traffic in Table 5 are tabulated as follows:

<u>Aircraft</u>	<u>Total Passes</u>	<u>Total Coverages</u>	<u>Design Factor</u>	<u>Design Deflection, in.</u>
B-52	20,000	13,100	2.05	0.0435
KC-135	40,000	12,800	2.05	0.0436
C-141	40,000	11,700	2.03	0.0438
F-111	80,000	14,200	2.06	0.0433



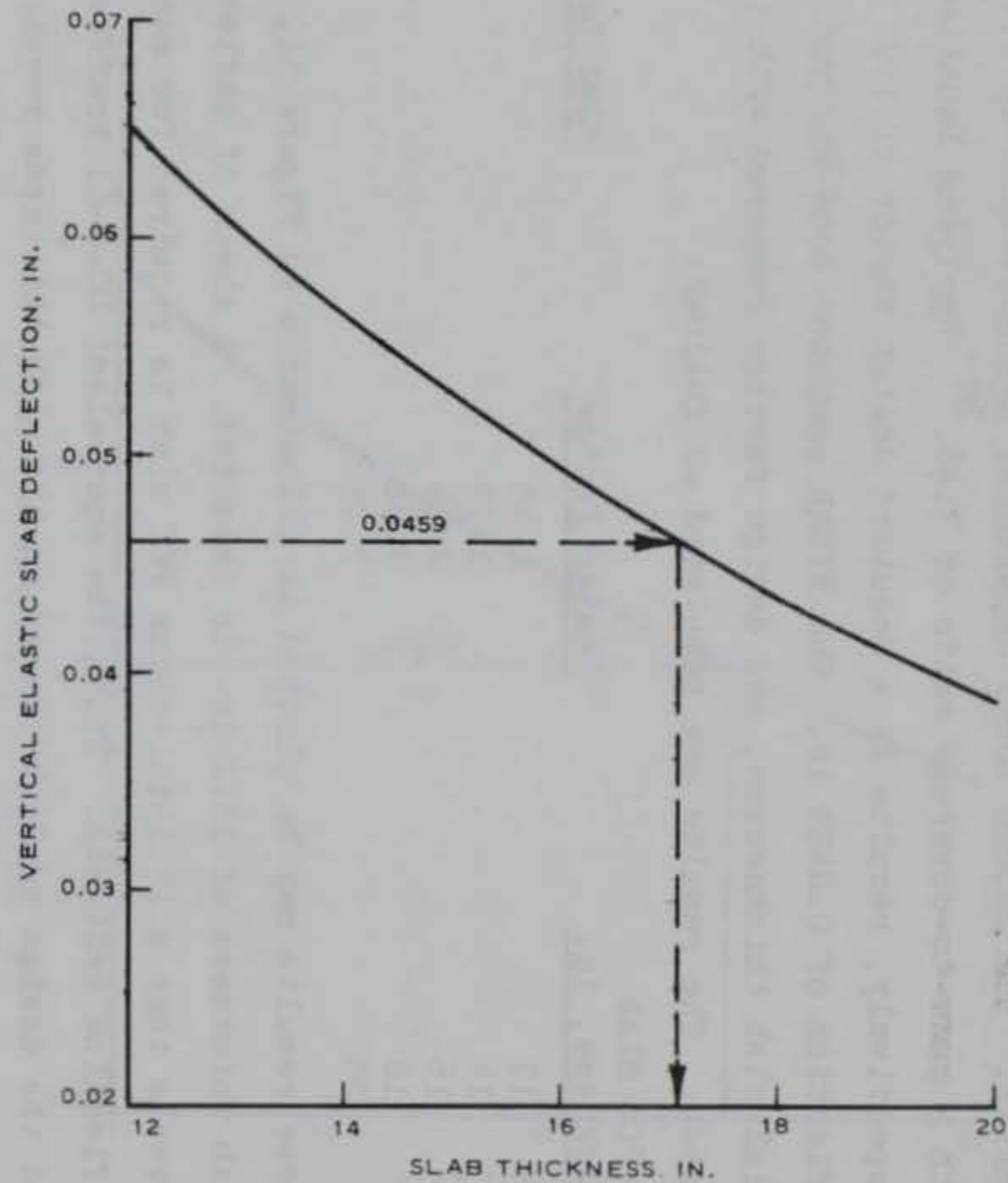
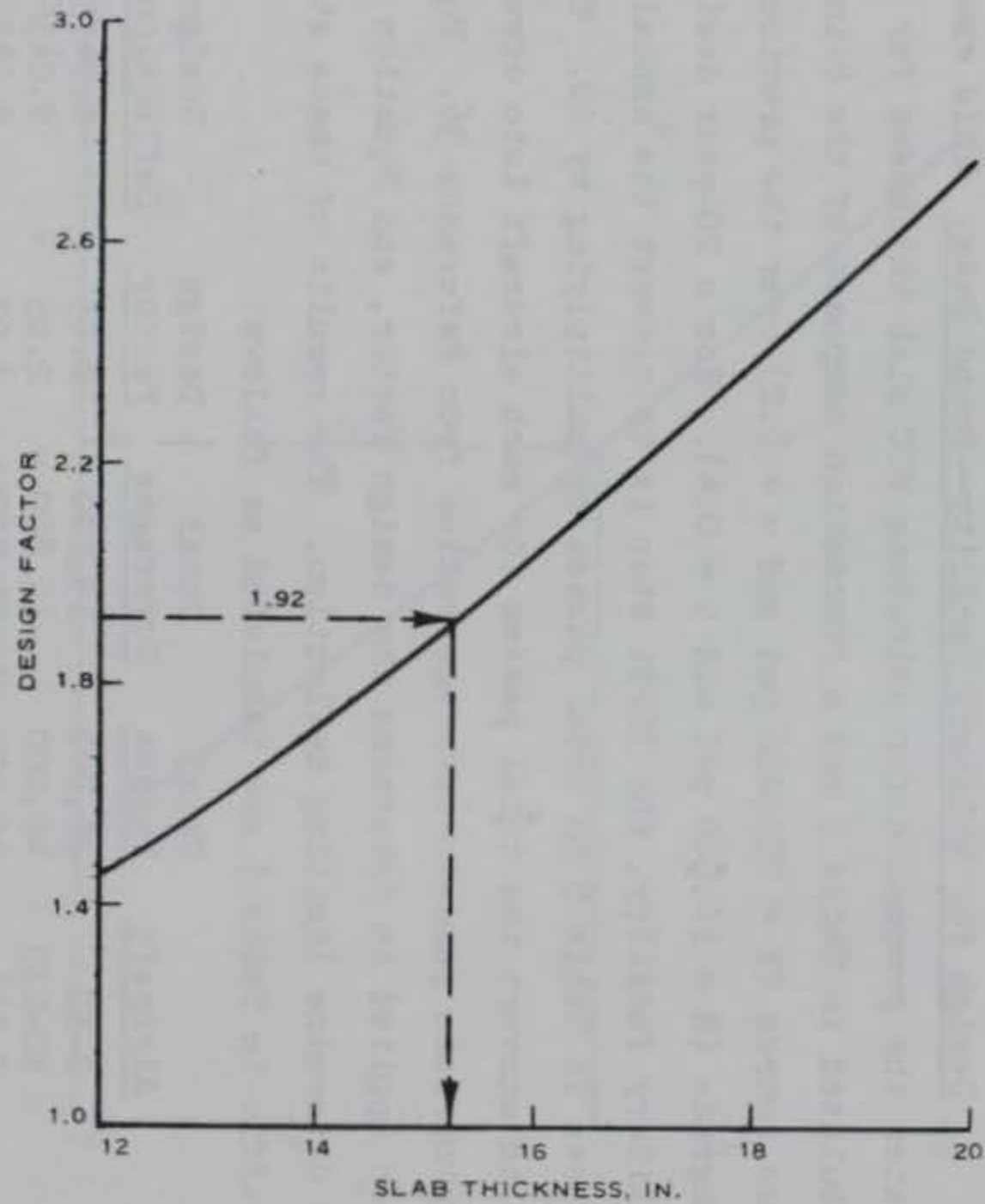


Figure 32. Selection of required slab thickness - civil facility - wide-body jet traffic



The next step is to run the BISAR computer code for several trial slab thicknesses to generate for each aircraft an array of data similar to the following for the B-52 aircraft:

<u>PCC Slab Thickness, in.</u>	<u>Design Factor</u>	<u>Slab Deflection, in.</u>
20	1.56	0.0576
22	1.79	0.0520
24	2.02	0.0472
26	2.27	0.0431

These results are plotted for each aircraft (B-52 aircraft in Figure 33), and a slab thickness is selected based on the limiting stress criteria. Again, for illustrative purposes the thickness is checked against the deflection criteria (Figure 33). The results for all four aircraft are tabulated as follows:

<u>Aircraft</u>	<u>Required Slab Thickness (Stress Criteria), in.</u>	<u>Required Slab Thickness (Deflection Criteria), in.</u>
B-52	24.3	25.8
KC-135	12.6	13.8
C-141	14.7	15.5
F-111	13.3	<10

The design thickness of 24.3 for the PCC slab would then be selected based on the B-52 traffic and the stress criteria.

Design for Civil Facility--Mixed Traffic--Bound Base. This example will illustrate how the criteria can be used with cumulative damage concepts to design the PCC slab thickness to account for the effects of a mixture of traffic. The foundation is composed of the 8-in.-thick bound base layer over the subgrade, and the PCC has the properties previously enumerated.

The first step is to convert the traffic in Table 4 to total departures for a 20-year life and then to convert the total coverages by application of appropriate pass-to-coverage ratios from Reference 36. The next step is to apply Equations 8 and 9 as appropriate to determine the limiting deflections for each aircraft at the applied traffic level. The total coverages and limiting deflection for each aircraft in the mix are tabulated as follows:



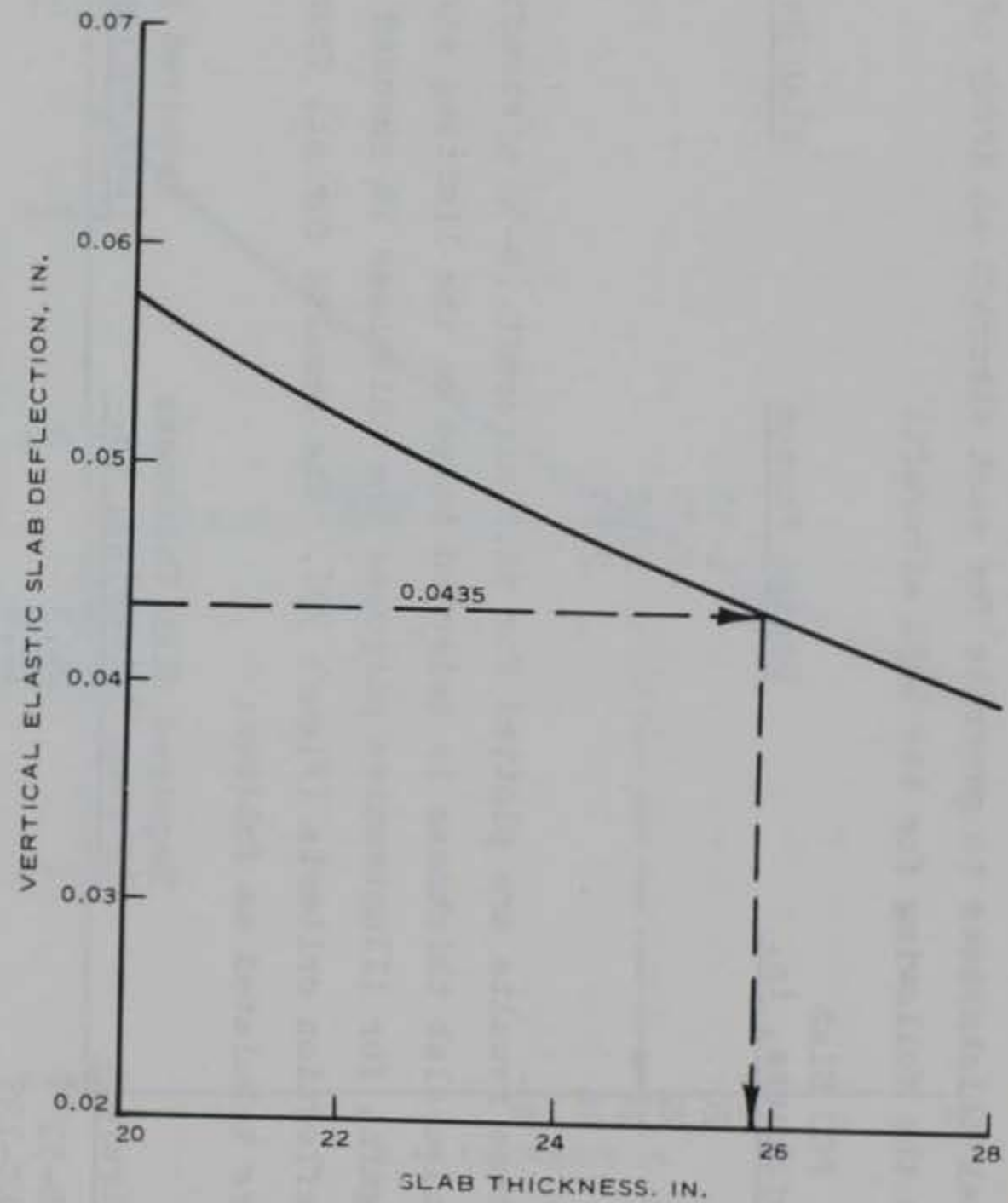
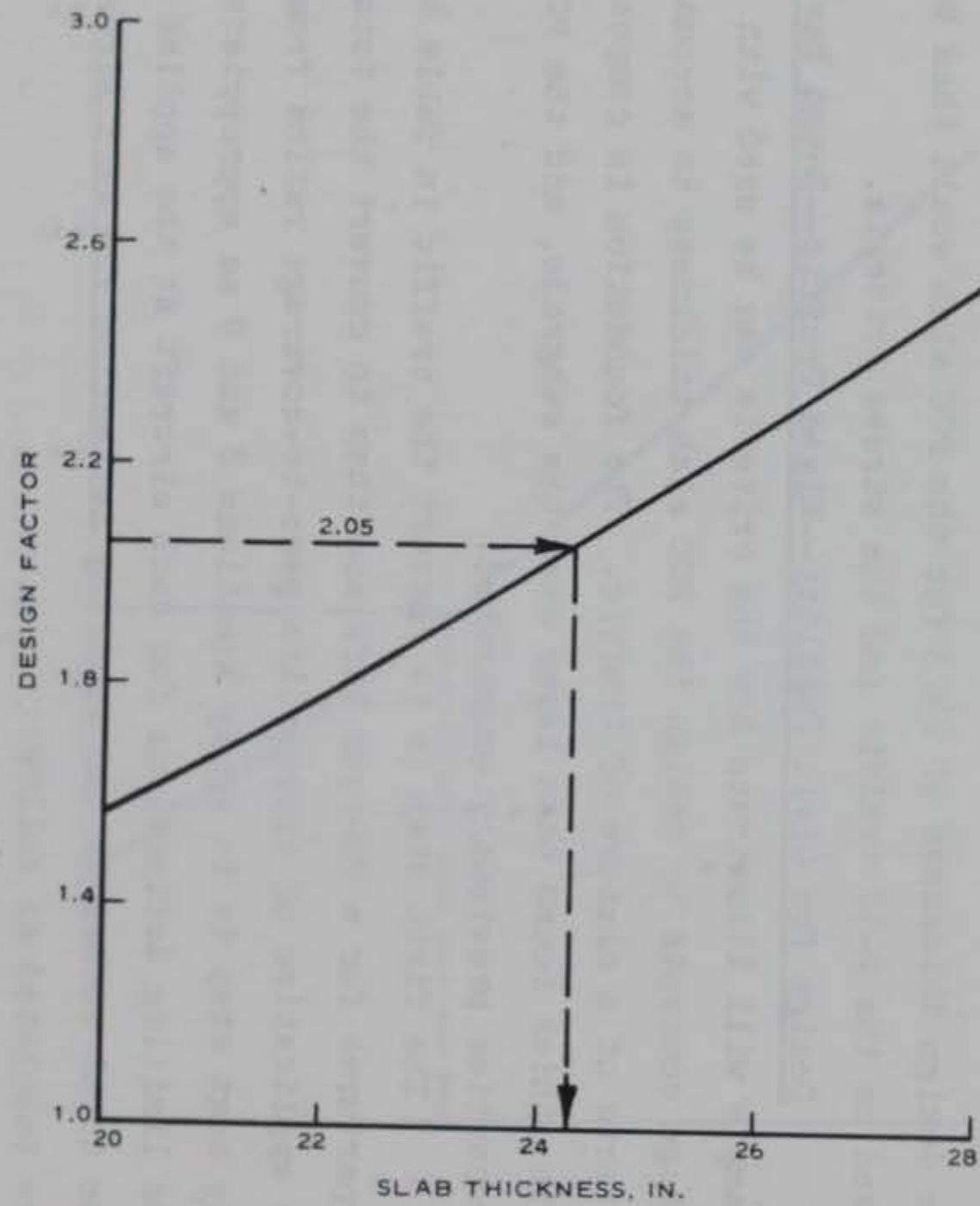


Figure 33. Selection of required slab thickness - military facility - B-52 aircraft



<u>Aircraft</u>	<u>Applied Coverages</u>	<u>Limiting Deflection, in.</u>
DC-9	38,000	0.0409
B-727	42,900	0.0406
DC-8	11,900	0.0438
B-747	5,750	0.0459

The BISAR computer code is run for a number of trial slab thicknesses for each aircraft. Design factors are then computed, and maximum deflections are selected from the results of the computer runs. With the computed design factor, the allowable coverage level for each aircraft for the particular thickness in question may be computed. Finally, the ratio of the applied to allowable coverage level for each aircraft, plus the sum, is computed. The results of this procedure are contained in Table 6. Figure 34 presents a plot of the summation of the ratios of applied to allowable coverages versus thickness. Application of Miner's hypothesis, i.e., failure will occur when the ratio of applied to allowable coverages reaches one, yields a required thickness of 16.8 in. A comparison of limiting deflections for each aircraft listed above with the computed deflections in Table 6 reveals that the computed deflection is less than the limiting deflection for a thickness of 17 in. for all aircraft except the DC-8. For the DC-8, the limiting value is 0.0438 as compared with the computed value of 0.0461. For the 18-in.-thick slab, the computed deflection for the DC-8 is 0.0433. By plotting the deflection versus slab thickness, it is determined that a slab thickness of 17.8 in. would be required to satisfy the deflection criteria. Again, the results indicate that for the twin-tandem gear the deflection criteria would dictate the design and help to confirm the conclusion that design on the basis of deflection would be overly conservative.

By comparing the ratios of applied to allowable coverages in Table 6, it can be noted that the DC-8 aircraft dominates the design. Although the B-747 has about the same gear load, the flotation of the gear is more efficient; therefore, the damaging effect of the B-747 traffic is negligible compared with the effect of the DC-8 traffic.

Summary of Design Examples. The array of designs obtained for the civil facility traffic is shown in Table 7 and for the military facility traffic in Table 8. Presented also in the tables is the slab



Table 6

Mixed Traffic Analysis--Civil Facility--Bound Base

<u>Aircraft</u>	<u>Maximum Deflection, in.</u>	<u>Design Factor</u>	<u>Allowable Traffic, Coverages</u>	<u>Applied Coverages/ Allowable Coverages</u>
<u>Slab Thickness = 16 in.</u>				
DC-9	0.0178	3.26	$3.36 \times 10^7$	0.00
B-727	0.0261	2.39	119,000	0.36
DC-8	0.0491	1.96	7,300	1.63
B-747	0.0471	2.22	39,500	<u>0.15</u>
				2.14
<u>Slab Thickness = 17 in.</u>				
DC-9	0.0165	3.57	$2.51 \times 10^8$	0.00
B-727	0.0243	2.62	529,000	0.08
DC-8	0.0461	2.11	19,300	0.62
B-747	0.0441	2.38	111,000	<u>0.05</u>
				0.75
<u>Slab Thickness = 18 in.</u>				
DC-9	0.0154	3.91	--	0.00
B-727	0.0228	2.86	$2.51 \times 10^6$	0.02
DC-8	0.0433	2.27	54,600	0.22
B-747	0.0416	2.56	358,000	<u>0.02</u>
				0.26
<u>Slab Thickness = 19 in.</u>				
DC-9	0.0145	4.27	--	0.000
B-727	0.0213	3.11	$1.27 \times 10^7$	0.003
DC-8	0.0407	2.44	164,000	0.073
B-747	0.0394	2.75	1,230,000	<u>0.005</u>
				0.081



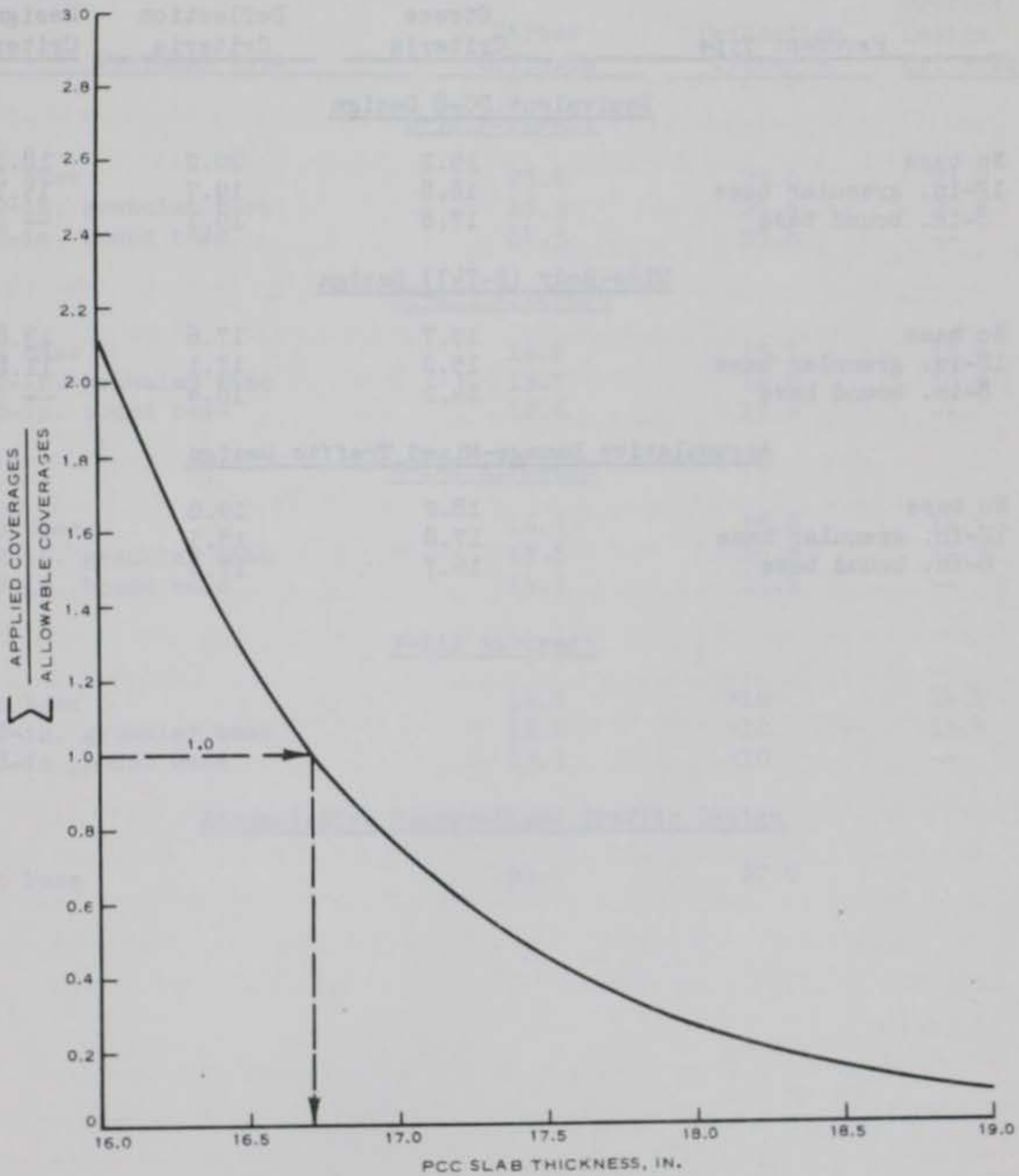


Figure 34. Summation of the ratios of applied to allowable coverages versus slab thickness



Table 7

Slab Thickness for Civil Facility

<u>Pavement Type</u>	<u>Required Slab Thickness, in.</u>		
	<u>Stress Criteria</u>	<u>Deflection Criteria</u>	<u>Present Design Criteria</u>
<u>Equivalent DC-8 Design</u>			
No base	19.2	20.2	18.1
12-in. granular base	18.8	19.7	15.7
8-in. bound base	17.8	19.1	--
<u>Wide-Body (B-747) Design</u>			
No base	15.7	17.6	13.8
12-in. granular base	15.2	17.1	11.8
8-in. bound base	14.2	16.4	--
<u>Accumulative Damage-Mixed Traffic Design</u>			
No base	18.2	19.0	
12-in. granular base	17.8	18.5	
8-in. bound base	16.7	17.8	



Table 8

Slab Thickness for Military Facility

Pavement Type	Required Slab Thickness, in.		
	Stress Criteria	Deflection Criteria	Present Design Criteria
<u>B-52 Aircraft</u>			
No base	25.6	27.0	23.2
12-in. granular base	25.3	26.5	20.8
8-in. bound base	24.3	25.8	--
<u>KC-135 Aircraft</u>			
No base	14.2	15.2	13.0
12-in. granular base	13.7	14.6	10.9
8-in. bound base	12.6	13.8	--
<u>C-141 Aircraft</u>			
No base	16.3	16.8	14.7
12-in. granular base	15.8	16.2	12.7
8-in. bound base	14.7	15.5	--
<u>F-111 Aircraft</u>			
No base	14.2	<10	14.1
12-in. granular base	13.9	<10	13.4
8-in. bound base	13.3	<10	--
<u>Accumulative Damage-Mixed Traffic Design</u>			
No base	25.6	27.0	

thickness as determined by present Corps of Engineers\* design criteria. The comparison between the different slab thicknesses should be noted. Although the design examples provide some comparison between the different criteria, these examples cover only a limited design condition. A more comprehensive comparison is provided in the following section.

#### COMPARISON OF CRITERIA

In working through the design examples, it was obvious (Tables 7 and 8) that the slab thicknesses obtained by applying the stress criteria (Equation 7) or the deflection criteria (Equation 9) were different from the thicknesses obtained from the present Corps of Engineers design procedure. Although the difference due to the dependence of the criteria on the gear was expected in the case of deflection criteria, for the stress criteria the magnitude of the difference was unexpected and felt to be unacceptable. To understand the nature of the differences in the criteria, additional analyses were conducted.

First, the required slab thicknesses for different design situations were computed using each of the design criteria. Figures 35 and 36 present the comparisons of the required slab thicknesses over a range of subgrade strengths for the DC-8 and C-141 aircraft. From these figures, it is seen that the slab thickness determined by the deflection criteria is highly sensitive to changes in subgrade strength. This would strongly indicate these deflection criteria to be dependent on the subgrade strength. It would appear that for weak subgrades, the deflection criteria would be overly conservative. From these studies, the conclusion was reached that the surface deflection would not be a good design parameter. The stress criteria also appeared, at least for the higher levels of traffic, to give slab thicknesses that were significantly greater than those determined from the present design criteria.

For additional comparison between the stress criteria and present design criteria, coverage predictions (Table 9) were made

---

\* These criteria are also the same as FAA design criteria contained in FAA Advisory Circular AC 150/5320-6C. Thereafter, the criteria will be referred to as the present design criteria.



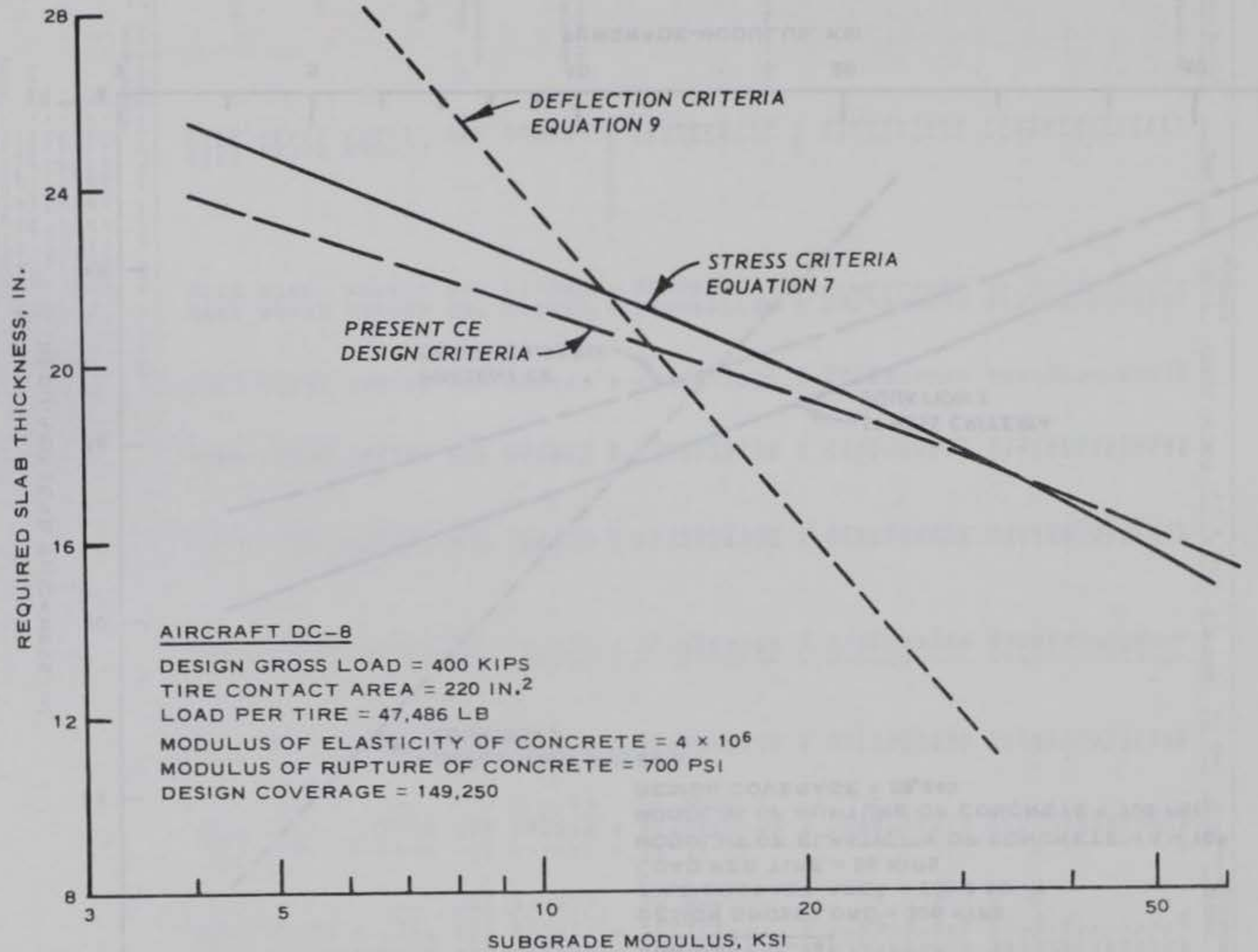


Figure 35. Comparison of deflection and stress criteria with present design criteria - DC-8 aircraft

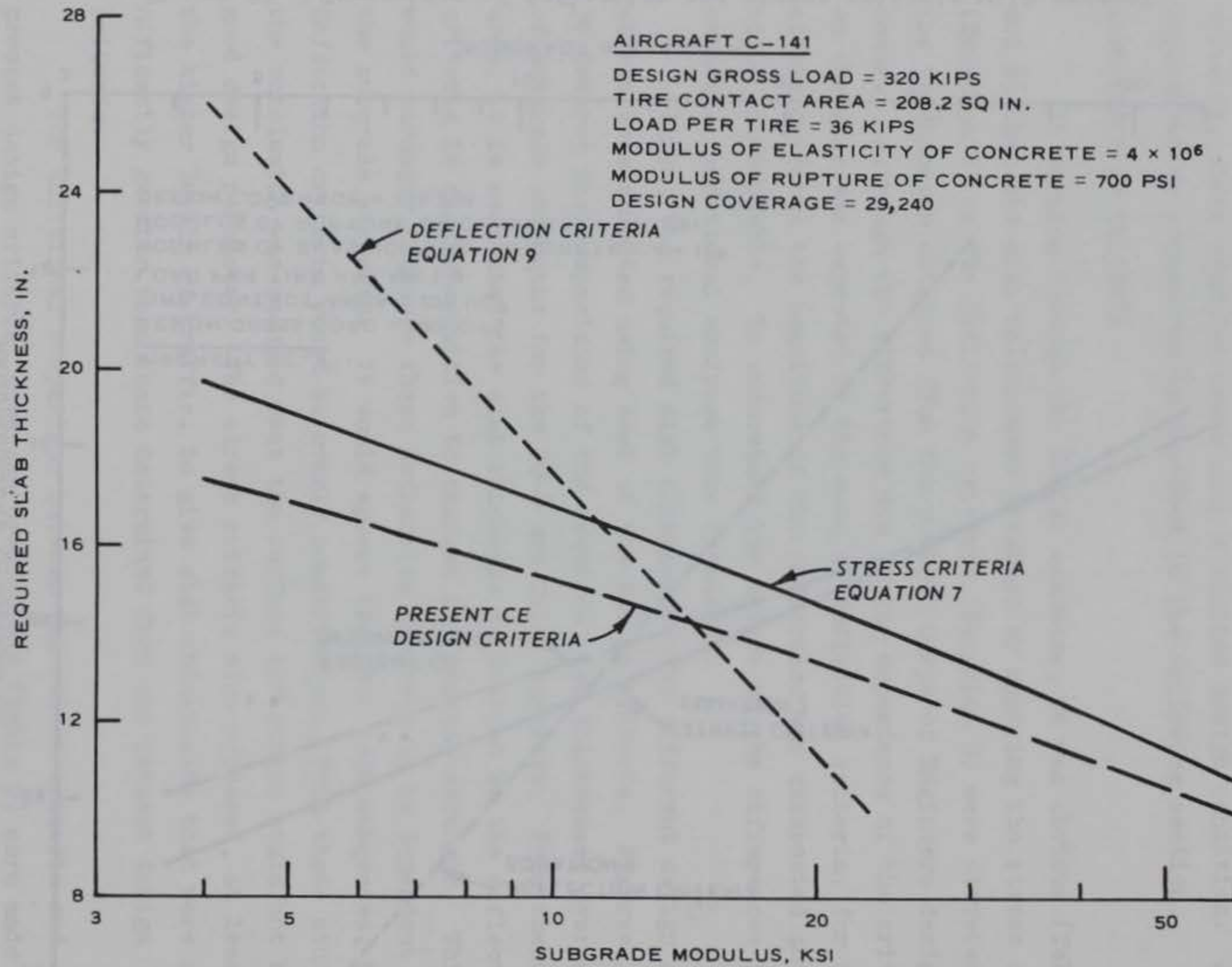


Figure 36. Comparison of deflection and stress criteria with present design criteria - C-141 aircraft



Table 9

## Data for Comparison of Stress and Present Criteria

Test Series*	Test**	Thickness (in.)	K (psi)	R (psi)	0.75 $\sigma_e$ (psi)	H (percent)	$\sigma_{int}$ (psi)	Coverages		
								Actual	Present	Equation 7
Lockbourne No. 1	A-1	5.72	150	740	627	92.7	405	390.0*	461,000	7,885
	A-2	5.72	150	780	911	71.3	599	45.0	0.400	96
	B-1	5.50	75	740	776	79.4	504	187.0	6,000	286
	B-2	5.50	75	780	1145	60.6	759	35.0	0.010	17
	C-1	5.50	70	740	788	78.6	558	200.0	5,000	116
	C-2	5.50	70	780	1165	59.8	853	44.0	0.010	8
	D-1	5.50	75	740	776	79.4	572	450.0	6,000	90
	D-2	5.50	75	780	1145	60.6	877	33.0	0.010	7
	E-1	5.75	104	740	680	87.5	505	430.0*	85,000	286
	E-2	5.75	104	780	998	66.9	771	77.0	0.100	15
	F-1	7.75	52	740	525	106.0	396	550.0*	12,068,000	3,734
	F-2	7.75	52	780	804	80.6	625	111.0	9,000	70
	K-3	9.44	90	735	730	81.4	570	72.0	12,000	90
	K-2	9.44	90	780	547	107.3	410	700.0	14,606,000	4,527
	N-2	8.00	75	780	709	88.1	564	150.0	103,000	161
	N-3	8.06	75	735	936	66.7	785	9.0	0.100	10
	O-2	9.46	75	780	569	104.2	458	573.0	9,265,000	1,253
	O-3	9.46	75	735	764	78.9	647	72.0	5,000	34
	P-2	7.58	95	780	721	86.9	632	262.0	69,000	61
	P-3	7.58	95	735	937	66.0	883	6.0	0.100	5
Q-2	9.44	109	780	524	110.7	465	1,390.0	24,064,000	1,102	
Q-3	9.44	109	735	694	84.4	659	57.0	31,000	30	
U-2	5.83	207	780	818	77.4	527	88.0	3,000	305	
U-3	5.83	207	735	995	60.0	651	1.5	0.100	32	
	A-RBC	9.81	107	725	451	118.3	390	658.0	73,462,000	3,502
Lockbourne No. 2	E-1	15.00	90	725	796	78.5	629	97.0	5,000	37
	E-2	15.00	150	680	721	79.8	574	942.0	7,000	44
	E-3	15.00	99	710	782	78.2	663	17.0	4,000	22
	E-4	15.00	164	680	707	80.7	642	203.0	9,000	21
	E-5	18.75	91	695	573	95.5	454	43.0	1,149,000	421
	E-6	20.26	97	700	505	104.4	397	2,204.0*	9,541,000	1,843
	E-7	24.00	88	760	397	129.2	312	2,204.0*	364,000,000	145,115
	M-1	12.00	55	725	719	81.7	600	134.0	13,000	54
	M-2	15.00	55	725	543	102.1	446	2,204.0*	6,806,000	800
	M-3	20.00	55	725	364	136.1	295	2,204.0*	1,003,000,000	165,000
	Lockbourne No. 3	6.00	62	800	1339	57.3	976	18.0	0.004	4
Sharonville Channelized	57	20.00	27	740	447	116.6	315	34,650.0*	57,233,000	81,420
	58	18.00	30	740	519	105.8	373	34,650.0*	11,718,000	7,567
	59	16.00	47	730	585	97.4	394	7,600.0	2,136,000	3,284
	60	12.00	335	730	654	89.8	416	1,674.0	179,000	1,728
	61	14.00	300	730	538	103.1	349	3,867.0	7,883,000	15,335
	62	16.00	360	730	428	120.9	274	10,082.0	107,620,000	595,949
Sharonville Heavy	71	32.00	100	800	359	145.4	249	9,680.0*	3,900,000,000	20,368,141
	72	28.00	70	800	566	120.9	319	9,680.0	107,620,000	227,465
	73	24.00	70	800	585	103.6	401	2,115.0	8,483,000	8,604
MHWGL	1-C5	10.00	60	725	820	73.6	580	221.0	0.910	70
	2-C5	12.00	70	800	632	97.8	473	4,230.0	2,433,000	1,176
	3-C5	14.00	74	700	510	104.1	394	1,400.0	9,130,000	2,095
	4-C5	8.00	74	775	1014	64.3	735	180.0	0.040	19
	2-DT	12.00	70	700	779	75.5	566	95.0	1.700	65
	3-DT	14.00	74	660	637	85.2	461	205.0	40,000	221
KLJS	1-C5	8.00	250	905	747	94.7	656	54.0	885,000	160
	2-C5	11.00	100	730	641	89.9	522	344.0	185,000	182
	3-C5	10.00	80	810	763	84.8	580	22.0	35,000	182
	4-C5	10.00	235	860	576	112.1	522	6,336.0	29,597,000	909
	4-DT	10.00	235	860	709	94.2	643	320.0	752,000	124
SSPS	3-200	15.00	120	900	621	108.9	463	3,215.0	18,474,000	5,893
	3-240	15.00	120	900	745	94.0	564	350.0	704,000	659
	4-200	15.00	150	870	588	110.5	463	4,660.0	23,368,000	3,982
	4-240	15.00	150	870	706	96.0	555	70.0	1,353,000	544

\* For description of test series, refer to Appendix B.

\*\* Column headings:

- K = the modulus of subgrade reaction
- R = the modulus of rupture for the concrete slab
- $\sigma_e$  = the edge stress as computed by plate theory
- H = the percent standard thickness computed for development of design criteria
- $\sigma_{int}$  = the interior stress as computed by layer theory
- Actual = actual coverage to failure or if a + is used would mean section did not fail and the coverage given is when traffic was terminated
- Present = the predicted coverage to failure as determined from present design criteria
- Equation 7 = the predicted coverage to failure as determined from the design criteria (Equation 9) developed in this study



for the test sections using both criteria. Figure 37 shows the comparison of the two criteria. These data are the evidence that the two criteria are different even though much of the same test data were used in the development of both criteria.

The difference is particularly noticeable at the lower coverages (below 200) and the higher coverages (from 1,000 to 30,000). Figure 38 presents a comparison of both criteria with the actual coverages to failure. The comparison of Figure 38 clearly shows that the stress criteria as developed in this study better predicts the actual performance, at least for the lower and higher coverages, than the present design criteria.

To better understand why the present design criteria are failing to predict performance in certain coverage ranges, the test data were reanalyzed in the same manner, i.e., plate theory was used to compute edge stresses, as was done to develop the original Corps of Engineers design criteria. The data for the analysis are given in Table A1. Also, the present design criteria were used to develop interior stress criteria of the form of Equation 7. This was accomplished by designing, based on present design criteria, a number of pavements covering a range of design conditions. The design factors for these hypothetical sections were computed in the same manner as the design factors for the test sections. The result was interior stress criteria, which best fit the present design criteria.

Figure 39 shows the comparison between the present design criteria and the data developed from the test sections. It should be repeated that these data shown were computed using edge stresses in the same way as was used to develop the present design criteria. The specific reasons for the disparity between the criteria and the test section data are not known. One contributing factor may have been that a considerable amount of the data shown is from test sections constructed and tested after the development of the present design criteria. The lack of data would not completely explain the disparity, but no other explanations can be offered. Figure 40 provides a comparison of stress criteria (Equation 7) with the present design criteria. From this



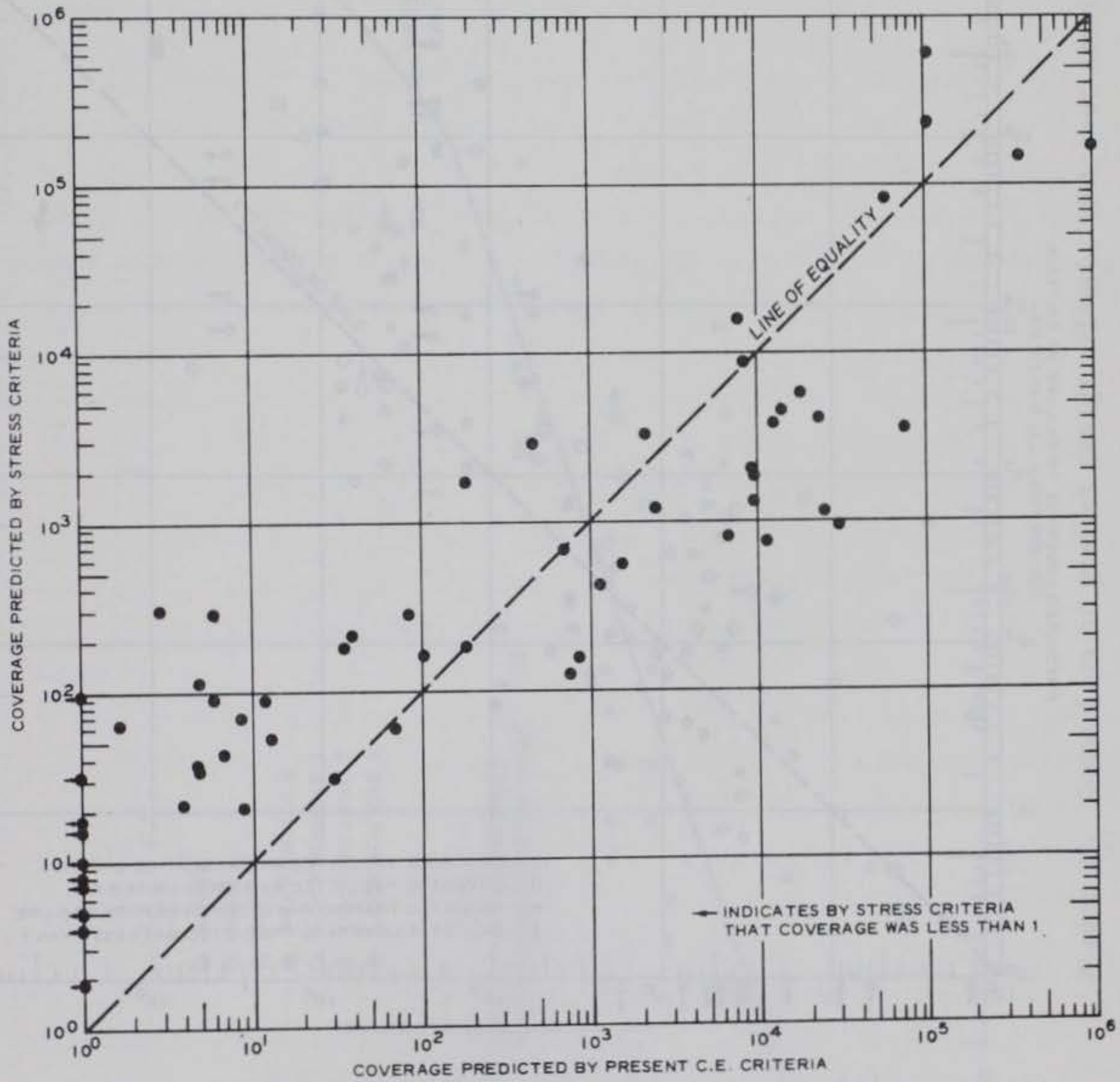


Figure 37. Comparison of coverage predicted by present design criteria with coverage predicted by stress criteria

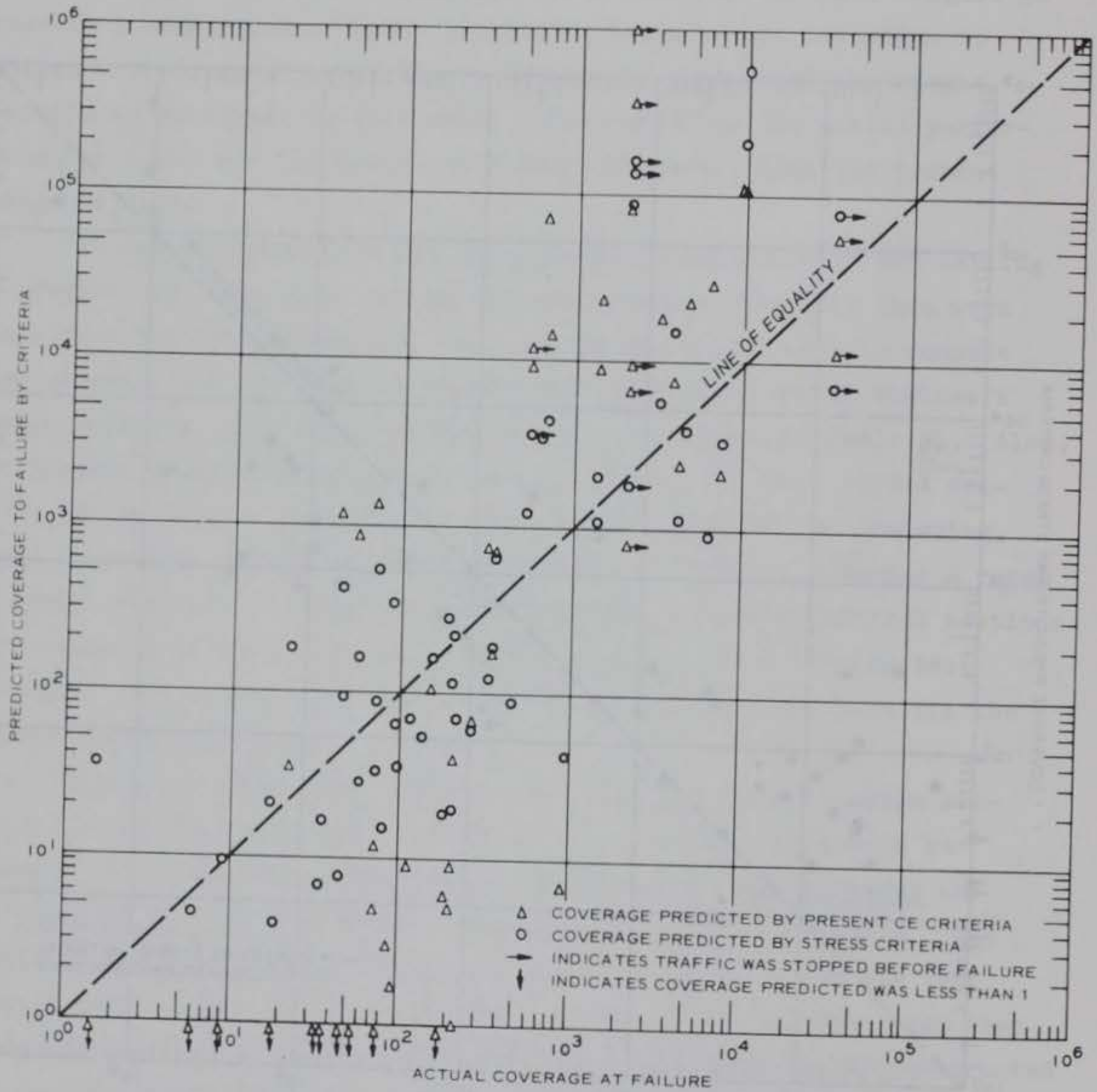


Figure 38. Comparison of actual coverage to failure with predicted coverage to failure



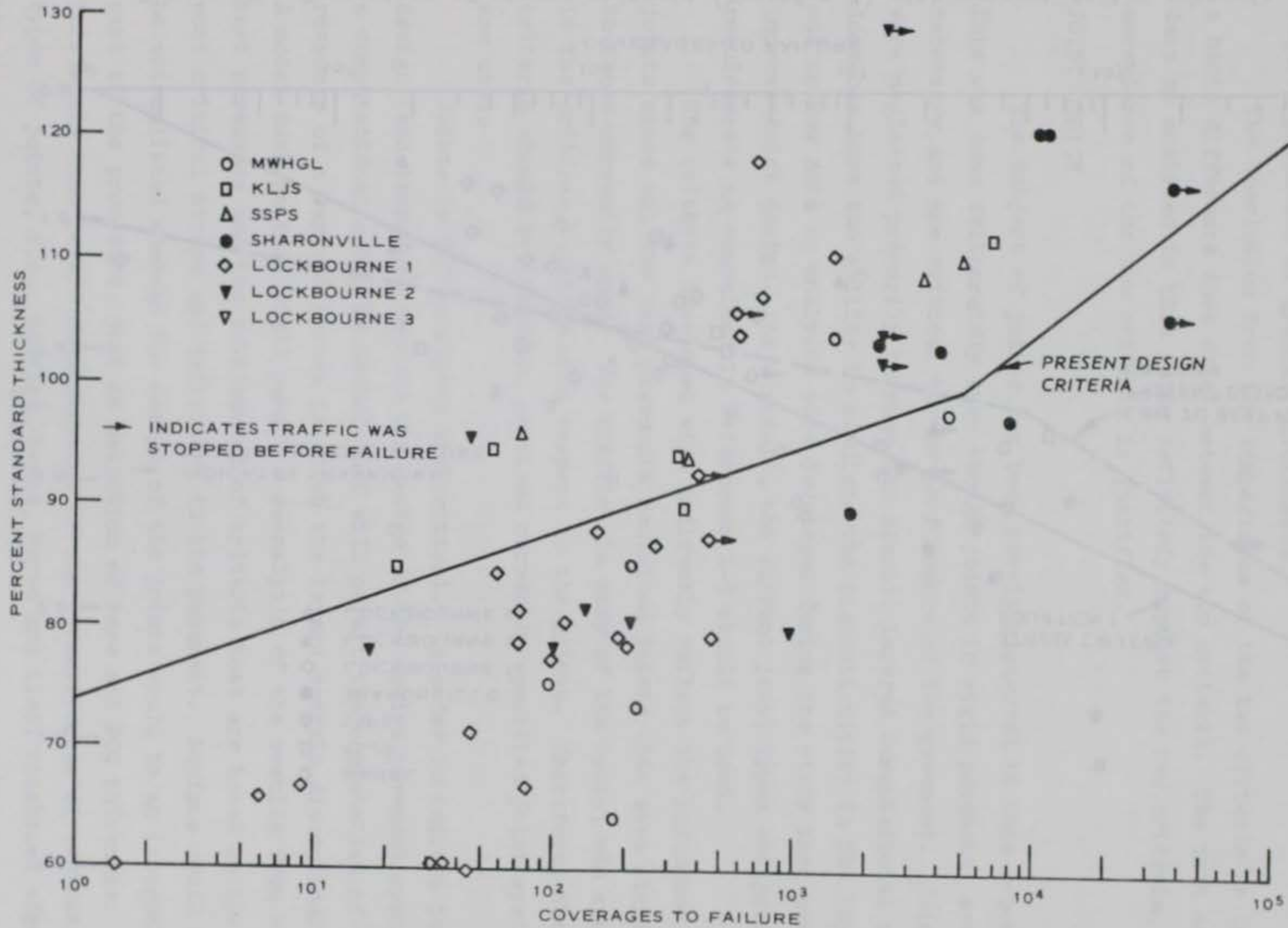


Figure 39. Comparison of present design criteria with test section data

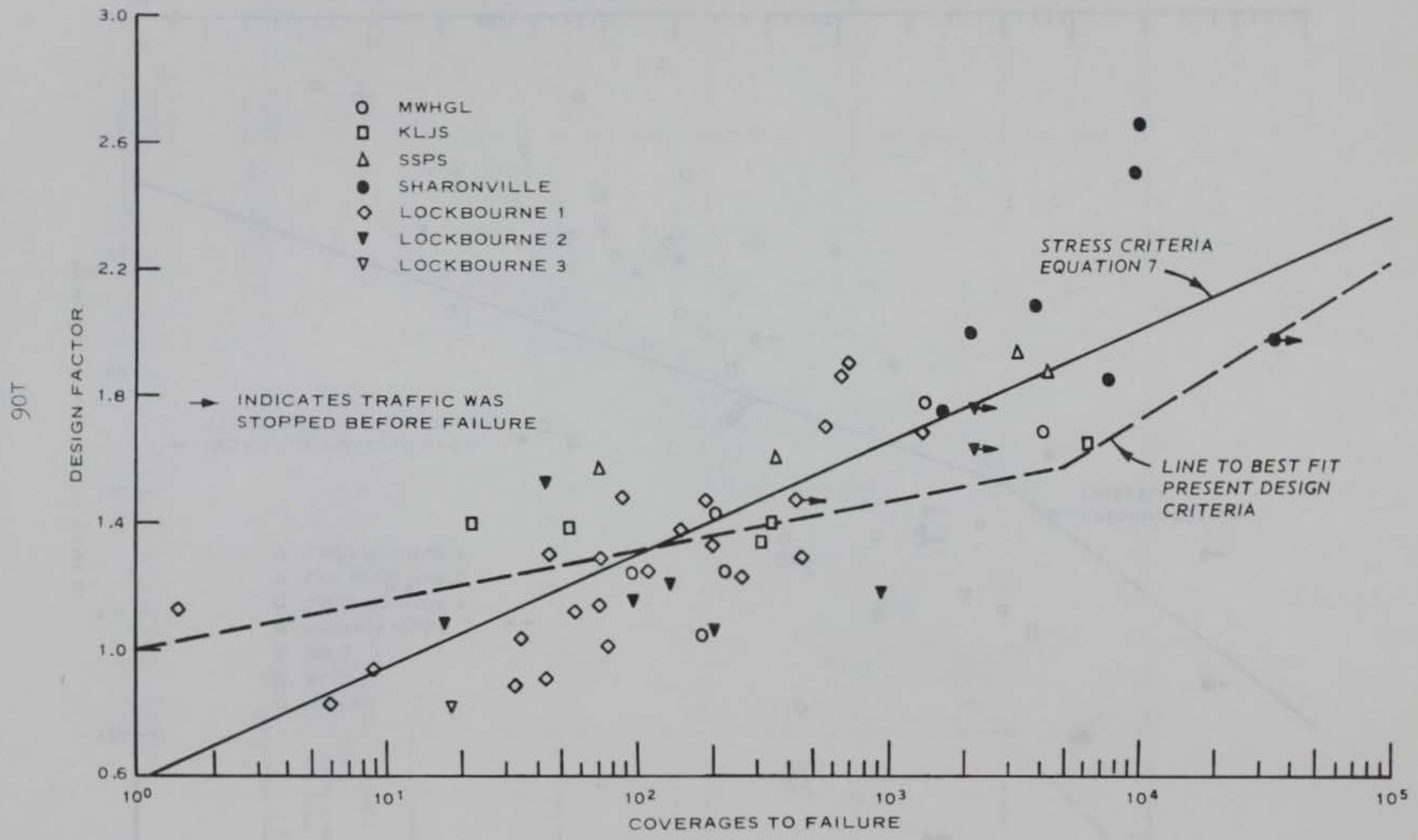


Figure 40. Comparison of stress criteria (Equation 7) with present design criteria



comparison, it is clear that for low coverages the new stress criteria will require pavements of lesser thickness and for high coverages will require pavements of greater thicknesses.

The conclusion from the comparisons of the two criteria is that a basic difference does exist between the two criteria. The test section data as analyzed in this study definitely support the new criteria, and acceptance of the new criteria is justified.

#### JOINT DESIGN

The subject of joints has been sorely neglected in this report. This was done deliberately even though joints in rigid pavements are necessary and are critical to the performance of the pavement. Joints were neglected primarily because the elastic layered computational model does not have the ability to simulate the discontinuities in the layers, and no new data or analyses were developed during the study that would improve joint design. As a result, the current joint types and joint requirements as contained in References 1-3 should be used.

The criteria developed will indirectly reflect the influence of joints since all the test pavements contained joints that were similar to those currently used. The traffic, in many of the tests, was applied in the critical location with respect to the joints. Therefore, the criteria should be adequate, provided currently specified joint systems are used.

Joints in PCC pavements are critical. In order to improve joint design (and therefore improve the design of the entire pavement system), a computational model is needed that will permit the computation of the response of a layered system in which the layers contain discontinuities. A model such as this would permit a reanalysis of the results from the test pavements and the development of criteria that are based on the most critical stress and deflection in the pavement. Designs could then be accomplished wherein the design of the joints would be an integral part of the procedure, just as selection of base and PCC thickness. This would then permit consideration of the effectiveness of various types of joints, i.e., doweled, keyed, keyed and tied, thickened edge, etc.



## TRANSLATION FROM DESIGN TO CONSTRUCTION

The production of plans and specifications for constructing pavements with the design procedure contained herein will require some modifications to presently used procedures. For subgrade soils and borrow material, no changes will be needed. The materials to be used may be identified, and with specifications of thickness of compacted layer, density, and moisture, there is a reasonable degree of certainty that the material constructed will be as intended by the designer.

For bases (subbases) and PCC, changes will be required. For bases, there are several alternatives. One alternative is to completely specify the material as to source, gradation, density, moisture, type and amount of additive, and layer thickness. A second alternative is to specify alternate types (granular, chemically stabilized, or bituminous stabilized) along with the required thicknesses and moduli of elasticity of each type. A third alternative is to specify a relationship between modulus of elasticity and layer thickness. This will permit the contractor to select the type material to use. Certain ranges of acceptable moduli and thicknesses would have to be established, and different quality control measures would be required for the third alternative.

For PCC, the alternatives are similar to those for bases, i.e., a complete description of the material to be used, including source of aggregates, mix design, etc., may be specified, or the desired properties (flexural strength and modulus of elasticity) may be specified, allowing the contractor to select necessary materials and ingredient proportions.

The selection of the procedure to use for translation from design to construction will depend on how and when the economic analysis is to be made. The use of a layered model permits a number of structurally acceptable layered systems to be generated. If the designer performs the economic analysis, then definite narrow specifications should be provided to ensure that the pavement that is built conforms to that which the designer intended. When end-product specifications (such as



the third alternative for bases) are used, it is implicitly assumed that the contractors will consider all possible alternatives in preparation of their bids and thus perform the economic analysis. In this case, the specifications would be very broad.

The user agency should select the type procedure that best fits within its management system. Any of the alternatives discussed above should prove satisfactory.

A final note on translation from design to construction should be made regarding rounding off of thicknesses. Thicknesses of base (sub-base) courses should be considered in increments of 1 in. When fixed side forms are used, the thickness of PCC should be rounded to the nearest full inch. For fractions of an inch equal to or less than 0.25 in., the thickness is rounded down; for fractions of an inch greater than 0.25 in., the thickness should be rounded up. When slip-form pavers are to be used, the thickness of PCC should be rounded to the nearest 0.5 in. with the quarter points (0.25 and 0.75 in.) as the limits for rounding up or down.

## CONCLUSIONS AND RECOMMENDATIONS

The following conclusions and recommendations are offered regarding the design procedure developed herein:

- a. There exists a basic difference in the design criteria developed in this study and the present design criteria. The data from test sections support the acceptance of the stress criteria as developed herein.
- b. The design criteria as developed in this report should be implemented for the design of aircraft pavements. The Shell BISAR computer code should be used for computation of stresses and deflections. Materials should be characterized with procedures recommended in this report.
- c. Data points are needed at traffic volumes greater than 10,000 coverages to verify extrapolation of the limiting stress and limiting deflection performance relationships, or to provide means for modification of the relationships for higher traffic volumes.
- d. Efforts should be continued toward the development of a more generalized computational code, which will permit direct inclusion of the effects of discontinuities in the layers and variable interface conditions between layers.
- e. Efforts should be made to develop procedures for quantifying the load deformation characteristics of deteriorated rigid pavements and interface conditions between PCC layers. Achievement of these goals will permit design of rigid overlays of rigid pavements with same methodology used for new rigid pavements.



APPENDIX A: DEVELOPMENT OF MATERIAL  
CHARACTERIZATION PROCEDURES

CONSIDERATION OF REPEATED LOADING

PORTLAND CEMENT CONCRETE

Chou<sup>25</sup> devotes a chapter to the characterization of PCC. One of the many factors noted by Chou, which affects the modulus of elasticity of concrete, is the repeated application of stresses. The consensus from this review and two additional, rather extensive, reviews of the fatigue of PCC<sup>60,61</sup> is that the stiffness as measured with any of a variety of procedures (flexural, compression, etc.) and as computed by several different methods (secant, tangent, etc.) is decreased by the application of load repetitions. However, as far as is known, it has not been shown that traffic causes a significant reduction in the modulus of in-place PCC. The extensive evaluation program conducted on military airfields has not shown this to be a major factor.<sup>62</sup> This presumes, of course, that the concrete is intact. Exposure to freezing-thawing and deicing salts, aggregate reactivity, sulfate attack, etc., will affect the modulus of elasticity, but this is usually manifest in visible deterioration other than structural cracking.

The complexity of the relationship between modulus of elasticity and repeated loads and the apparently small magnitude of change caused by traffic has led to the omission of the effects of repeated load on PCC modulus of elasticity. There may be some decrease in modulus due to repeated loads or exposure, but conversely there should be some increase because of the effects of long-term hydration. The net result is that the computation of the modulus of elasticity from the stress-strain relationship obtained from the initial loading of a PCC specimen is considered adequate for characterizing the material for the life of a pavement.

Poisson's ratio for PCC normally receives very little attention. This may be unjustified, but as pointed out by Chou,<sup>25</sup> the range of statically determined Poisson's ratio is only from about 0.11 to 0.21,



and the average of dynamically determined values was about 0.24. Added factors are the difficulty of measurement and the relatively small influence that varying Poisson's ratio within a reasonable range has on the computed response. Several studies referenced by Chou show that the value of Poisson's ratio increases with load repetitions, but that this occurs primarily for high stress levels. No evidence was found to indicate that load repetitions should seriously be considered in describing Poisson's ratio for PCC.

The effects of repeated loads on the strength of PCC is a well-established and extensively researched phenomenon.<sup>60,61</sup> It is universally accepted that the magnitude of stress that can be sustained by PCC before cracking is a function of the number of repetitions of the stress and that the magnitude of this stress decreases as the number of stress repetitions increases. The number of stress repetitions of a given magnitude that a material can sustain is dependent on numerous factors, i.e., age, mix proportions, type aggregate, rate of loading, range of loading, etc. The most important, however, is the static strength of the material. Fatigue data are normally presented in the form of a plot of the ratio of the static strength to the applied stress versus the number of repetitions. This would appear to be the characterization needed for PCC and is the approach taken indirectly by several design agencies.<sup>1,4,5</sup> Safety factors are applied to keep stress levels within tolerable limits, and the material is characterized by the static strength.

The approach taken by other agencies<sup>2,3</sup> is similar but the effects of load repetitions on the entire pavement system are considered, and the fatigue relationships used are for the entire pavement system. The number of load repetitions the pavement can sustain is related to the static strength of the PCC and the stress within the pavement. The result is that the effects of load repetitions are handled indirectly and a fatigue relationship for the concrete to be used is not required for each design situation. Rather, the performance of the pavement system is related to the static strength and is the one parameter needed to characterize the material. This is also the



approach taken for the procedure developed herein.

#### BOUND BASES (SUBBASES)

When considering bound bases, chemically stabilized materials (portland cement, lime, fly ash, etc.) and bituminous-stabilized materials need to be discussed separately, even though the conclusions regarding inclusion of effects of repeated loading are the same for both types of bound bases. Due to the viscous and temperature-dependent behavior of the bituminous binder, bituminous-stabilized materials are affected by temperature and rate of loading to a much greater extent than any other component in a pavement structure.

A great deal of the work done on the characterization of bituminous mixtures has been directed toward determining the rather complex response of the material and the effects of temperature and rate of loading. Also, much of the work has been performed for the purpose of characterizing the material for flexible pavements.

Chou<sup>25</sup> has a detailed review of characterization procedures for bituminous mixtures. The various types of available tests are discussed including repeated load flexural tests. The effects of rate of loading and temperature are noted as dominating factors. Therefore, the inclusion of the effects of repeated loading, while important, does not account for other important factors. Complete characterization would require that a different rate of loading be used for various features (runways, taxiways, and aprons) and that a range of temperatures be used for defining the modulus of elasticity and Poisson's ratio. From a practical point of view, the ranges of rates of loading and temperatures encountered are limited, and the inclusion of the effects of repeated flexural loads at approximate temperatures and rates of loading adequately characterizes bituminous bases (subbases) for rigid pavement design.

Chemically stabilized bound bases (subbases) are not as dependent on the rate of loading and the temperature as bituminous bases. They do have an effect, but this effect would be minor in comparison with other factors. Chou<sup>25</sup> cites numerous references of studies made of the load



deformation properties of chemically stabilized material. Emphasis is placed on the modulus of elasticity, and the effects of repeated loads are noted. The effects on compressive, tensile, and flexural loadings are noted and are essentially the same, i.e., the modulus increases with the number of loadings. The magnitude and nature of the increase would be dependent on the type loading, magnitude of applied stress, curing time, etc. Modulus values computed from compressive tests generally appear to be more sensitive to load applications than do modulus values computed from flexural tests.

Static and resilient modulus values for several chemically stabilized bound materials are compared in Table A1. The results shown are averages from tests of several samples. The materials were field-mixed, but the samples were compacted and cured in the laboratory. The larger ratios are for the more flexible materials. Indications are that the consideration of the effects of repeated loading on the modulus of elasticity of chemically stabilized bases is a justifiable requirement.

#### GRANULAR BASES (SUBBASES)

Granular materials are extremely difficult to characterize. For bituminous mixtures, the rate of loading and the temperature are the dominating factors affecting the properties of the material. For granular materials, the state of stress, particularly the confining stress, is the dominating factor in determining load-deformation properties. Repeated loading also affects the modulus of granular materials. In summarizing the results of numerous studies, Chou<sup>25</sup> states: "The consensus from these studies has been that the response of granular materials to repeated loading is different from their response to static loading." The general pattern noted was that repeated loadings increased the stiffness provided shear failure was not progressing. This implies that the modulus of elasticity is increasing.

The effect on Poisson's ratio of repeated loading may be different from the effect of repeated loading on modulus of elasticity. The nature of any change in Poisson's ratio that may occur with repeated



Table A1

Comparison of Static and Resilient Moduli of  
Chemically Stabilized Bound Bases

<u>Material</u>	<u>Loading</u>	<u>Static Modulus, psi</u>	<u>Resilient Modulus, psi</u>	<u>Ratio <math>M_R/E_{static}</math></u>
Low plasticity clay (CL) with 12 percent portland cement	Flexure	200,000	273,000	1.37
Low plasticity clay (CL) with 12 percent portland cement	Compression	79,000	105,000	1.33
Low plasticity clay (CL) with 2 percent portland cement, 3 percent lime, and 10 percent fly ash	Compression	30,000	80,000	2.67
Low plasticity clay (CL) with 10 percent portland cement	Compression	80,000	110,000	1.38
Sandy clay (SC) with 5 percent portland cement	Compression	37,000	125,000	3.38

applications will depend on the initial density of the material. If the relative density is low, then densification may occur and there would be an apparent decrease in Poisson's ratio (possibly negative values) as loads are applied. However, Poisson's ratio would reach a relatively constant value where it would remain unless shear failure began to occur. Then, there would be an apparent increase in Poisson's ratio as the material underwent an increase in volume during shear failure. To summarize, the use of repeated loadings to characterize granular materials is a well-established, generally accepted procedure.

### SUBGRADES

The thickness of the PCC surface layer and the properties of the subgrade are the two most important parameters in determining the response of rigid pavements to loads. As noted previously, subgrades are generally the components of rigid pavements where the assumptions of linearity and elasticity are least valid. The subgrade is also the pavement component that is most affected by repeated load applications.

Subgrades may be divided into the general classes of cohesive and cohesionless soils. The majority of soils possess properties of both, but in a saturated condition, where it is generally appropriate to characterize subgrade soils, most natural subgrade soils behave primarily as a cohesive material. Repeated loading affects both cohesive and cohesionless soils. Cohesionless sands, gravels, or sand-gravel combinations will respond much like granular bases or subbases. Cohesive soils are more sensitive to repeated loadings. The resilient modulus of cohesive subgrades generally increases with load repetitions provided the level of stress is lower than that required to initiate shear failure. However, the number of stress repetitions required before a stable condition is reached may be greater than for bound bases, granular bases, or cohesionless subgrades.

The effects of repeated loadings on the response of cohesive subgrades may be examined by studying the response of several test pavements. These pavements consisted of PCC slabs directly on a prepared clay (CH) subgrade as part of the Multiple-Wheel Heavy Gear Load (MWHGL)

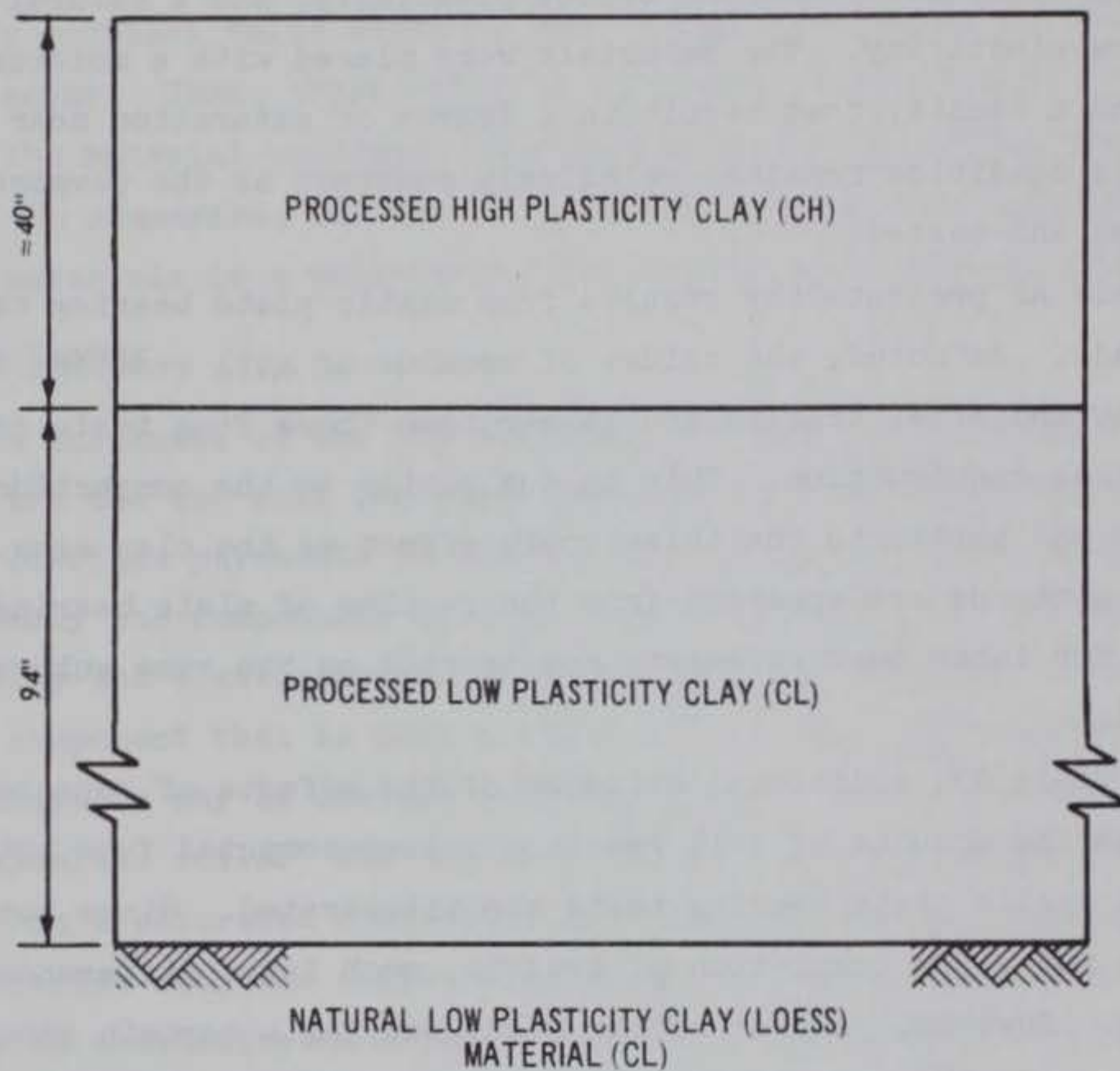


Pavement Tests.<sup>35</sup> The pavements consisted of 8-, 10-, 12-, and 14-in.-thick PCC slabs directly on the prepared clay subgrade. The prepared clay subgrade (Figure A1) was composed of two processed materials (a clay of high plasticity and one of low plasticity) and a natural material of low plasticity. The materials were placed with a moisture content and a density that result in a degree of saturation near 100 percent. This condition remained relatively constant as the pavements were constructed and tested.

Table A2 presents the results from static plate bearing tests on the subgrade. As noted, the values of modulus of soil reaction from the tests conducted after traffic are larger than those from tests conducted prior to slab construction. This is due partly to the compaction effect of traffic and partly to the thixotropic effect as the clay ages. The same type patterns are apparent from the results of plate bearing tests conducted for later test pavements constructed on the same subgrade (Table A2).

In Table A3, additional evidence of the effects of repeated loading and the modulus of soil reaction values computed from both static and cyclic plate bearing tests are illustrated. Since both tests were run after completion of traffic, such large differences were unexpected. However, removal of the slab, causing a certain amount of disturbance and allowing relaxation of stresses within the soil, may account for at least part of the difference between the static and cyclic response.

The difference in the response to moving wheel loads and a cyclic load applied at one location on the pavement may account for part of the difference, i.e., the conditioning or stiffening effects of moving wheel loads distributed across a pavement are different from the effects of a cyclic load applied at one location. Ledbetter<sup>63</sup> investigated the response of pavements to moving loads and showed that the response is rather complex (especially for flexible pavements). Cyclic load tests conducted in test pavements at the WES have shown that the response of the pavement to the first load in a series of loadings is different from the response to subsequent loads in that



CONSTRUCTED - 1968 - MULTIPLE WHEEL HEAVY GEAR LOAD TESTS

DEPTH OF PROCESSED HIGH PLASTICITY CLAY (CH) WILL VARY WITH THICKNESS OF PAVEMENT ABOVE. TOTAL DISTANCE FROM TOP OF PAVEMENT TO NATURAL UNPROCESSED MATERIAL IS 144 IN.

FOR THE KEYED LONGITUDINAL JOINT STUDY AND THE SOIL STABILIZATION PAVEMENT STUDY THE TOP 6 TO 12 IN. OF THE CH MATERIAL WAS REPROCESSED AND MATERIAL CUT OR ADDED AS REQUIRED TO MEET GRADE.

Figure A1. Clay subgrade for WES rigid test pavements



Table A2

Results from Plate Bearing and Field Density  
and Moisture Content Tests

Item	Modulus of Soil Reaction, pci		Dry Density, pcf		Moisture Content percent	
	Before Traffic	After Traffic	Before Traffic	After Traffic	Before Traffic	After Traffic
	<u>Multiple-Wheel Heavy Gear Load Study (Reference 35)</u>					
1	62	154	86	84	32	34
2	70	94	84	83	33	34
3	74	87	86	83	32	35
4	74	125	86	87	32	32
Average	70	115	85	84	32	34
<u>Keyed Longitudinal Joint Study (Reference 38)</u>						
1	70	--	85	--	31	--
2	110	100	92	81	28	36
4	47	--	86	--	30	--
5	40	--	81	--	37	--
Average	67		86		32	
<u>Soil Stabilization Pavement Study (Reference 39)</u>						
1	47	180 & 200	86	89	32	30
2	85	118	89	--	34	--
3	84	164	87	--	32	33
4	40	68	86	86	33	33
5	--	120 & 143	--	87	--	32
Average	64	142	87	88	33	32
Overall Average	67	129	86	85	32	33

Table A3

Results from Cyclic Plate Bearing Tests -  
Multiple-Wheel Heavy Gear Load Study

<u>Item</u>	<u>Cyclic Modulus of Soil* Reaction, pci</u>	<u>Static Modulus of Soil** Reaction, pci</u>	<u>Dry Density, pcf</u>	<u>Moisture Content percent</u>
1	370	169	84	33
2	270	111	85	33
3	300	115	84	33
4	<u>330</u>	<u>128</u>	<u>88</u>	<u>32</u>
Average	318	131	85	33

\* Modulus of soil reaction computed with 10-psi plate pressure after 10 cycles at 5-psi and 10 cycles at 10-psi pressure.

\*\* These values are different from those shown in Table A2, since the values shown in Table A2 are the average of several tests and the values shown here are for one test conducted at the same location as the cyclic tests.



series even though the pavement may have sustained considerable traffic prior to the tests. This indicates that the conditioning effect of traffic is different from a cyclic load at one point. There may also be a time factor involved wherein a certain amount of relaxation occurs when there is a rest period between load applications. Certainly the phenomena of pavement response and material characterization are not thoroughly understood.

Much of the discussion presented thus far appears to be tearing down evidence accumulated to justify the use of repeated load tests for characterizing paving materials. However, this is not the case because the response of a pavement to vehicle loading (Figure 14 in main text) relates well with the response computed with material properties obtained from repeated load tests. The validity of the use of repeated load testing for cohesive subgrades can be illustrated by comparing vertical slab deflections and horizontal bending strains in the PCC slabs in the MWHGL pavement tests with corresponding values computed using moduli of elasticity values computed from various type tests. Poisson's ratio of the clay subgrade was assumed as 0.4, and as discussed previously, a stiff layer ( $E = 1 \times 10^6$  psi) was located at a depth of 20 ft in the elastic layered simulation.

A composite modulus of elasticity for the subgrade was obtained from the static and the cyclic modulus of soil reaction values. An average value was used for all four pavements. The test results shown in Tables A2 and A3 indicate some variability within the test section, but this was probably due to test variability and natural variability within the entire test section rather than a real difference between individual sections. The composite modulus of elasticity was computed with the formula

$$E = 19.8k \quad (A1)$$

where

E = modulus of elasticity, psi

k = modulus of soil reaction computed by dividing plate pressure by plate deflection, pci



Equation A1<sup>64</sup> is derived from Boussinesq's theory for Poisson's ratio of 0.4 and rigid 30-in.-diam plate. Application of Equation A1 yields moduli of 6300 psi for the cyclic tests and 2300 psi for the static tests (after-traffic plate bearing tests).

Static triaxial and unconfined compression tests conducted on undisturbed samples from the subgrade yielded moduli of 1850 psi for the high-plasticity clay (CH) and 1600 psi for the low plasticity clay (CL). Repeated load triaxial tests on companion samples yielded the plots of resilient modulus versus deviator stress shown in Figures A2 and A3. From a composite or average relationship designated by the heavy dashed line in Figures A2 and A3, moduli of 7,500 psi and 13,500 psi were selected for the high plasticity and low plasticity clays, respectively. These were selected at a deviator stress of 5 psi. In a triaxial test, the deviator stress is defined as the difference between the applied axial stress and the confining stress. These tests were run on material sampled during the Soil Stabilization Pavement Study (SSPS),<sup>39</sup> which was conducted several years after the MWHGL tests. However, it is noted that the condition of the material was similar for both test tracks. Table A2 shows the results of plate bearing tests conducted before and after traffic for both the MWHGL and SSPS tests, as well as for the Keyed Longitudinal Joint Study (KLJS),<sup>38</sup> which was conducted between the MWHGL and the SSPS. The average moduli of soil reaction, dry density, and moisture contents are comparable.

In the plots of measured versus computed slab deflections (Figures A4-A7), the computed values were obtained with the subgrade characterized with the different moduli. In addition to the data points, a line of equality and a least-square-regression relationship constrained through the origin are shown. These comparisons indicate that the use of repeated load test characterizations results in underprediction of the deflection and that the use of static load test characterizations results in overprediction of the deflection. The computed values with repeated load characterizations relate more closely with the measured values (Figures A4 and A6). The correlation with the results from the cyclic plate tests produced the relationship



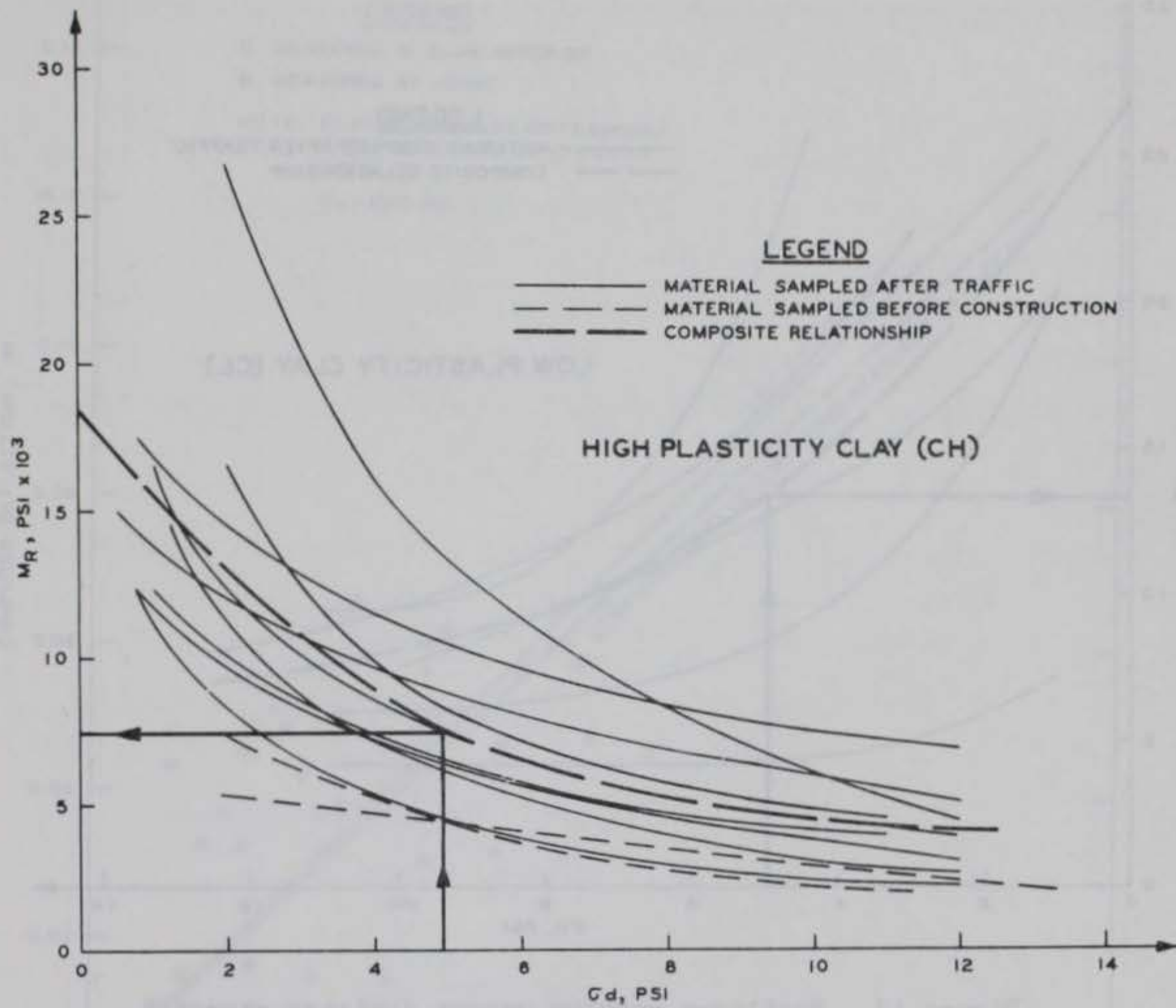


Figure A2. Resilient modulus versus deviator stress for high plasticity clay

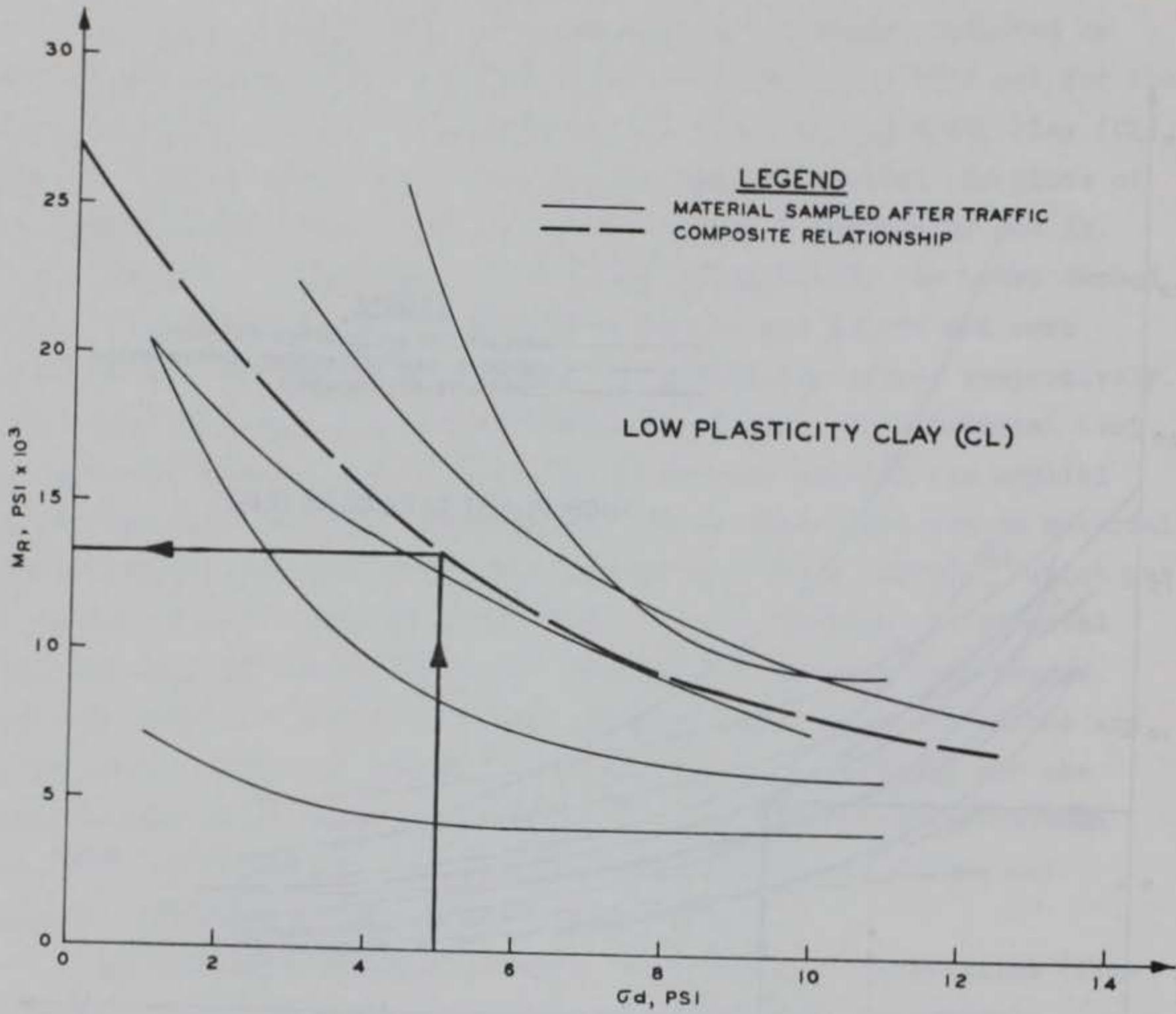


Figure A3. Resilient modulus versus deviator stress for low plasticity clay



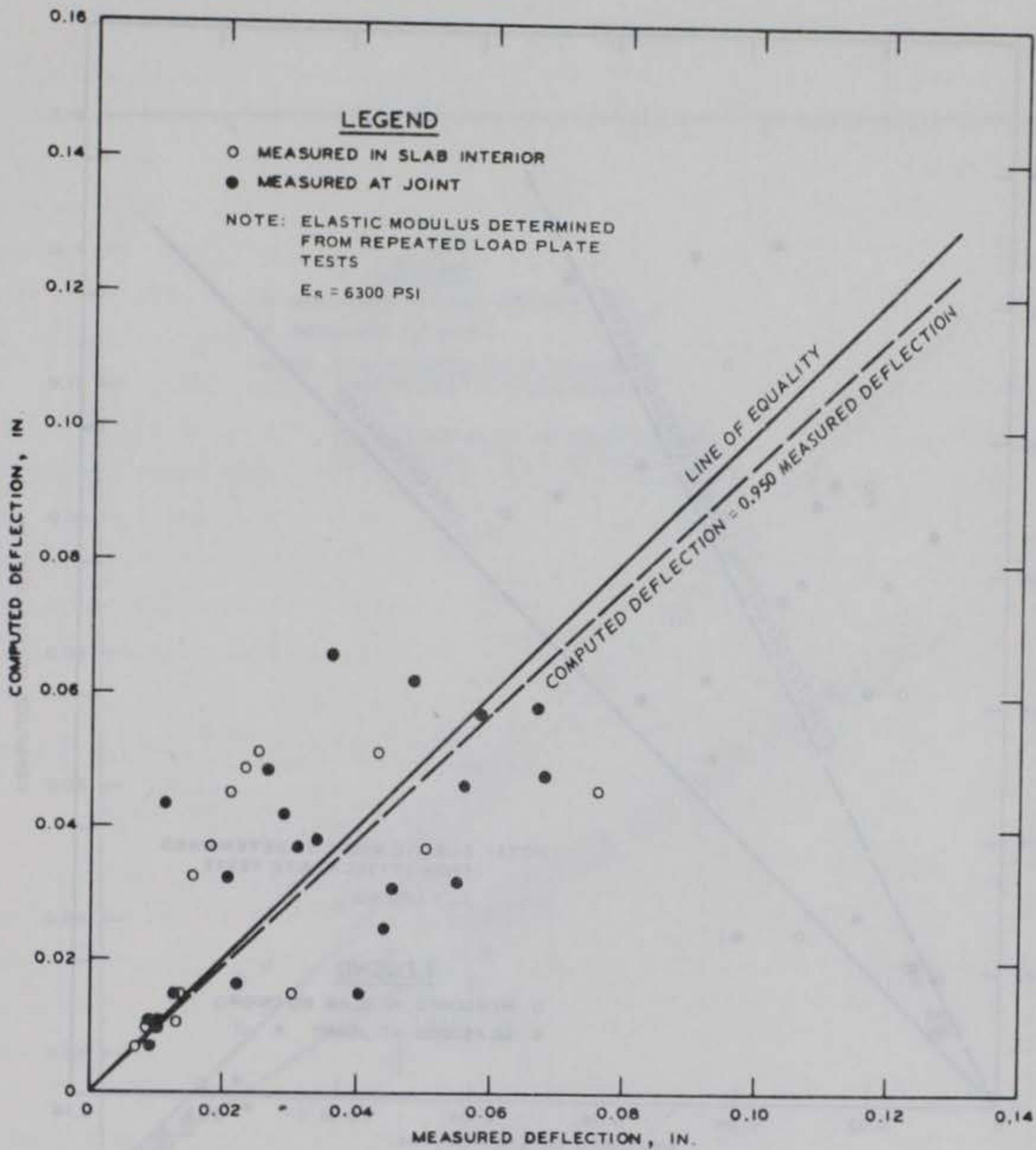


Figure A4. Comparison of measured slab deflection and deflections computed with the subgrade characterized with cyclic plate bearing tests

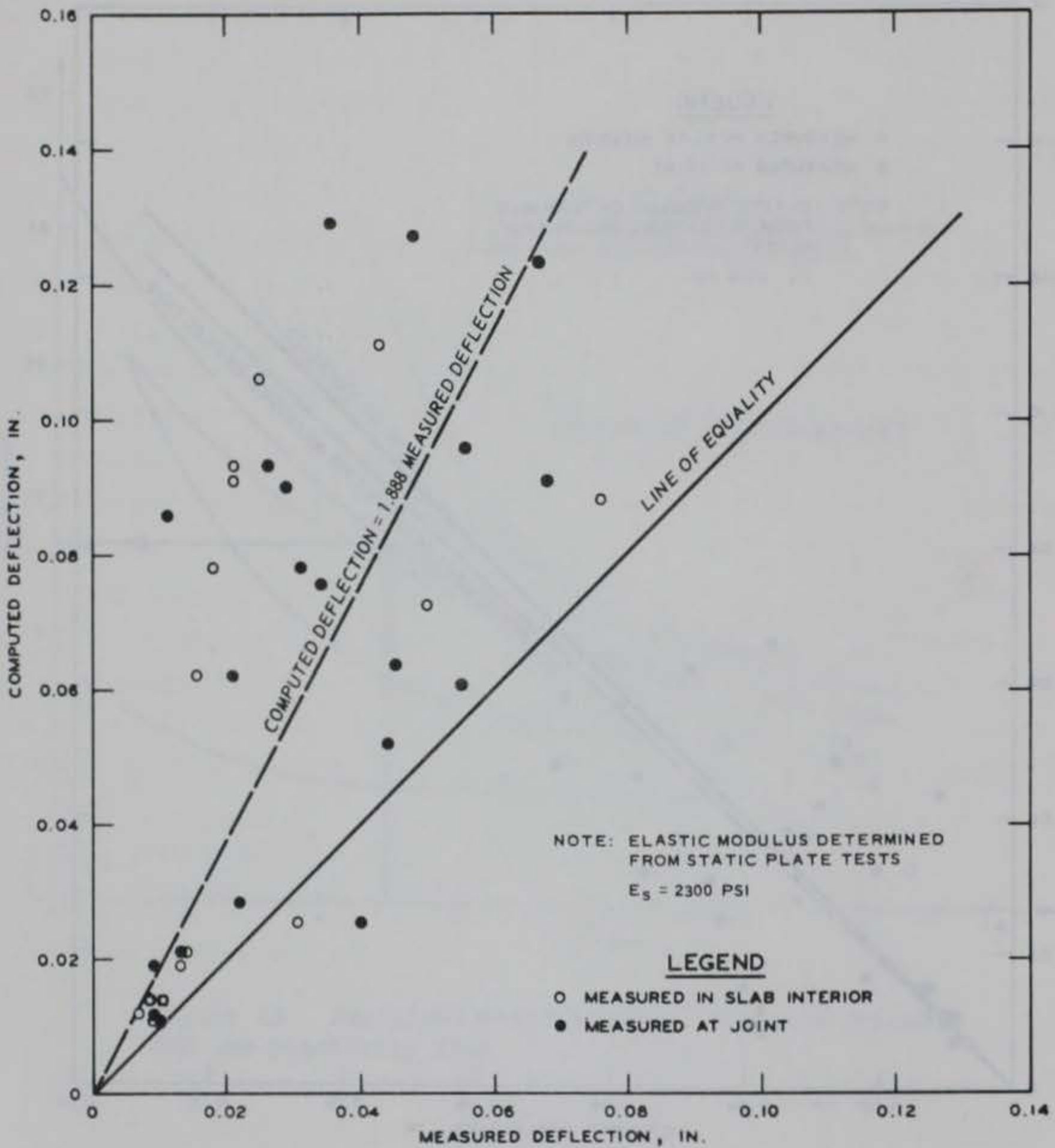


Figure A5. Comparison of measured slab deflection and deflections computed with the subgrade characterized with static plate bearing tests



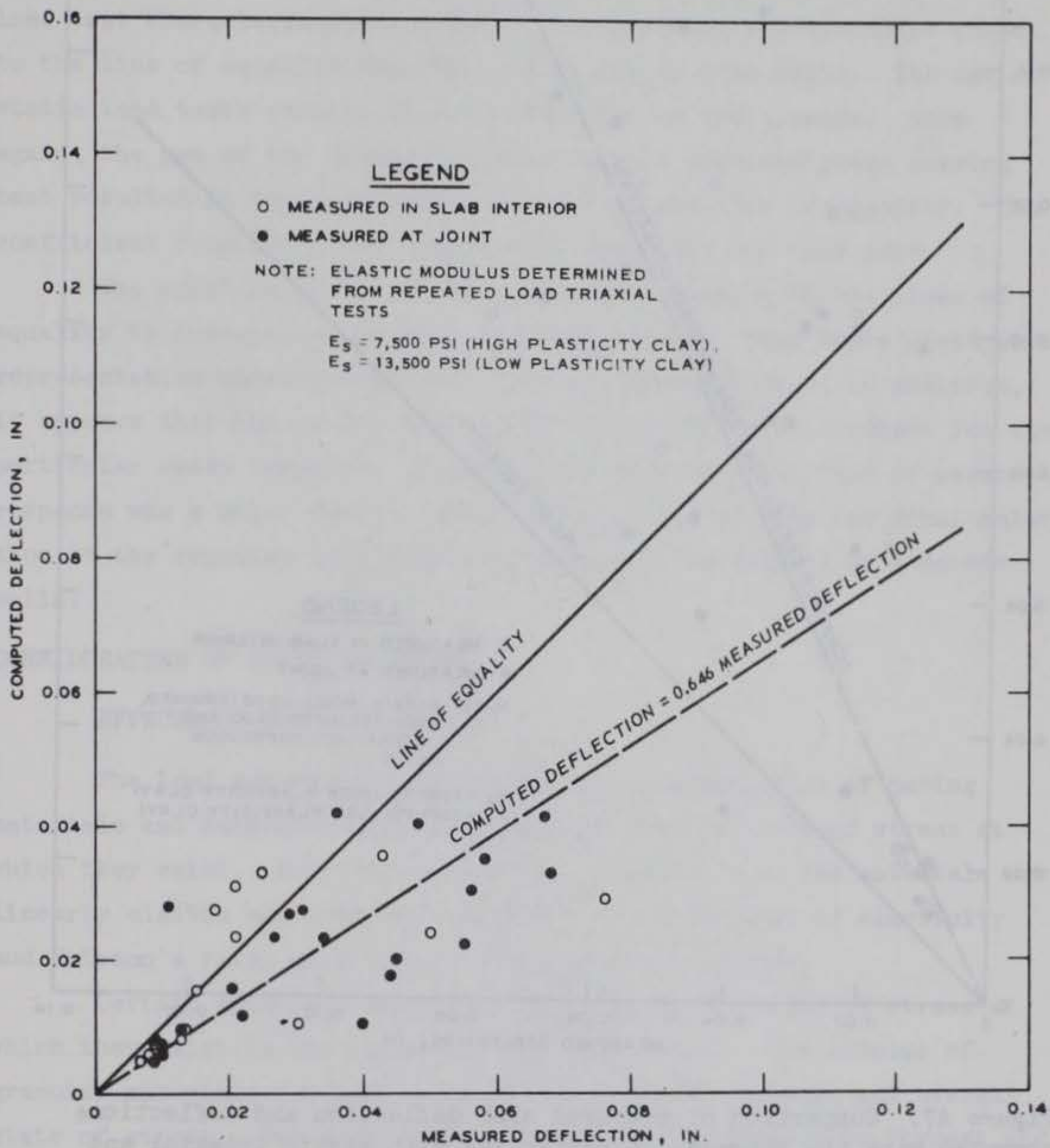


Figure A6. Comparison of measured slab deflection and deflections computed with the subgrade characterized with repeated load triaxial tests

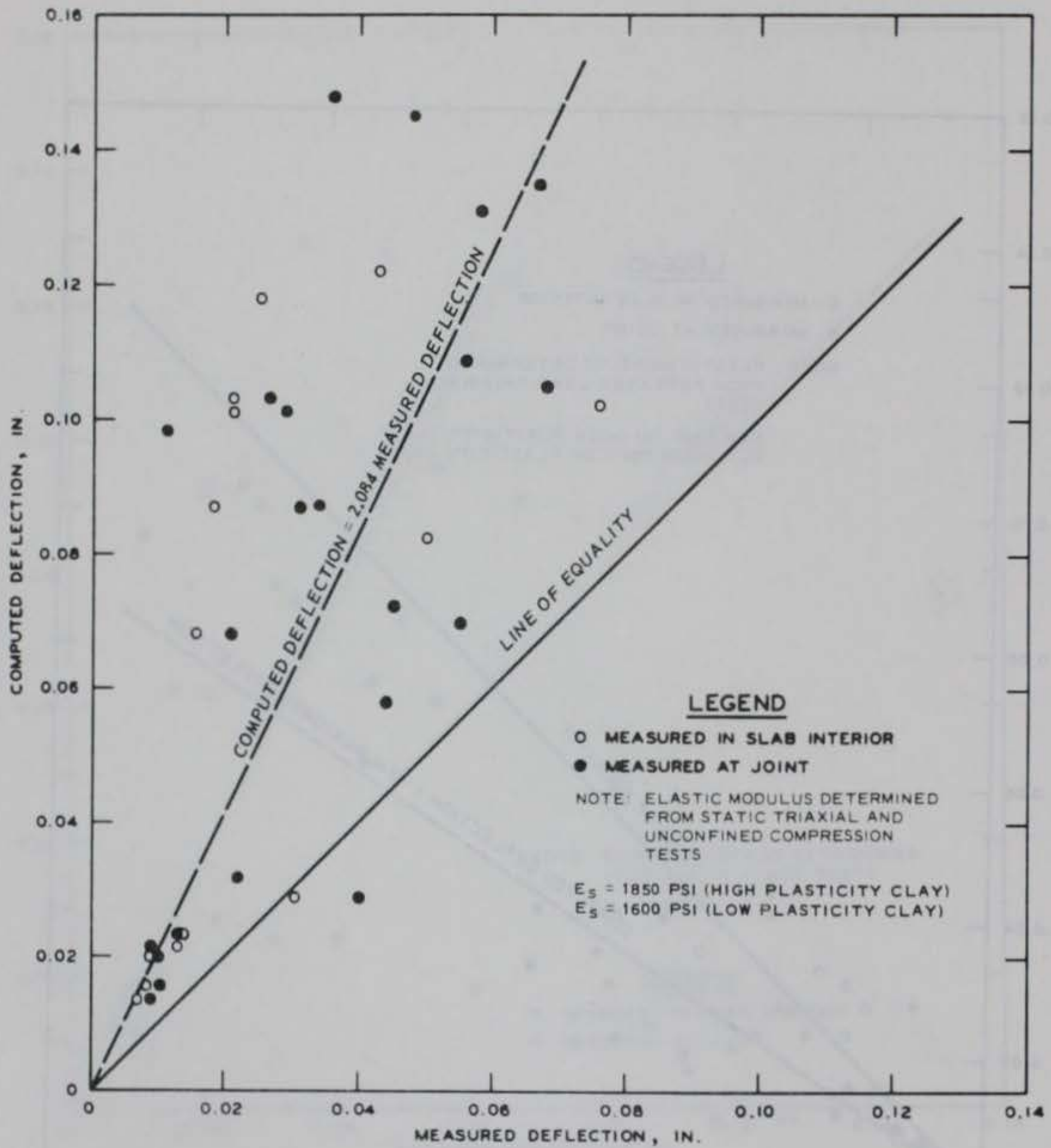


Figure A7. Comparison of measured slab deflection and deflections computed with the subgrade characterized with static triaxial and unconfined compression tests



closest to the line of equality. The coefficient from the linear regression was 0.950 for this case.

In the plots of measured versus computed slab bending strains (Figures A8-A11), the comparisons indicate that the use of repeated load test characterizations results in regression relationships closer to the line of equality than the use of static load tests. The use of static load tests results in overprediction of the strains. Once again, the use of the characterization with a repeated plate bearing test resulted in the correlation closest to the line of equality. The coefficient from the linear regression was 1.023 for this case.

The position of the regression lines relative to the lines of equality is interpreted to mean that the repeated load tests yield more representative characterizations than the static tests. In addition, it appears that the cyclic plate load test is the most accurate for the particular cases compared. Although accuracy of prediction of pavement response was a major factor, other factors entered into the final selection of the repeated load triaxial tests for characterizing subgrade soils.

## CONSIDERATION OF STATE OF STRESS

### EFFECTS OF STATE OF STRESS

The load deformation and strength characteristics of paving materials and subgrade soils are dependent on the state of stress at which they exist. For this discussion, consider that the materials are linearly elastic and that the magnitude of the modulus of elasticity and Poisson's ratio will depend on the state of stress.

Certain materials are more sensitive to the state of stress at which they exist in the pavements than are others. The modulus of granular materials has been related to confining pressure and overall state of stress. Two such relationships are illustrated in Figures A12 and A13 for two granular base course materials. In terms of strength, the effect of confinement may be explained by the influence of the angle of internal friction, as defined in the Mohr-Coulomb failure theory. The fact that granular materials have a relatively large angle

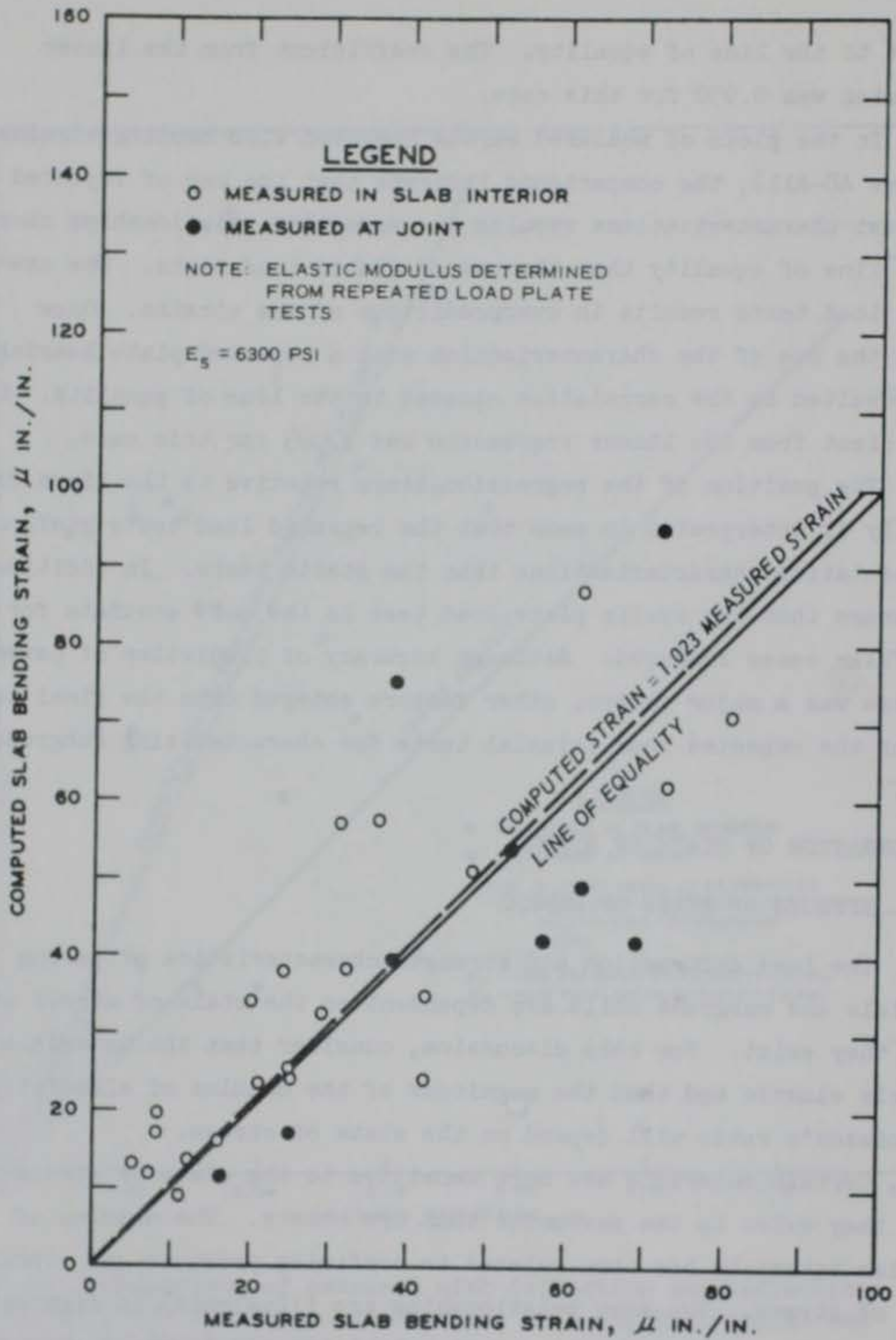


Figure A8. Comparison of measured slab bending strain and strains computed with the subgrade characterized with cyclic plate bearing tests



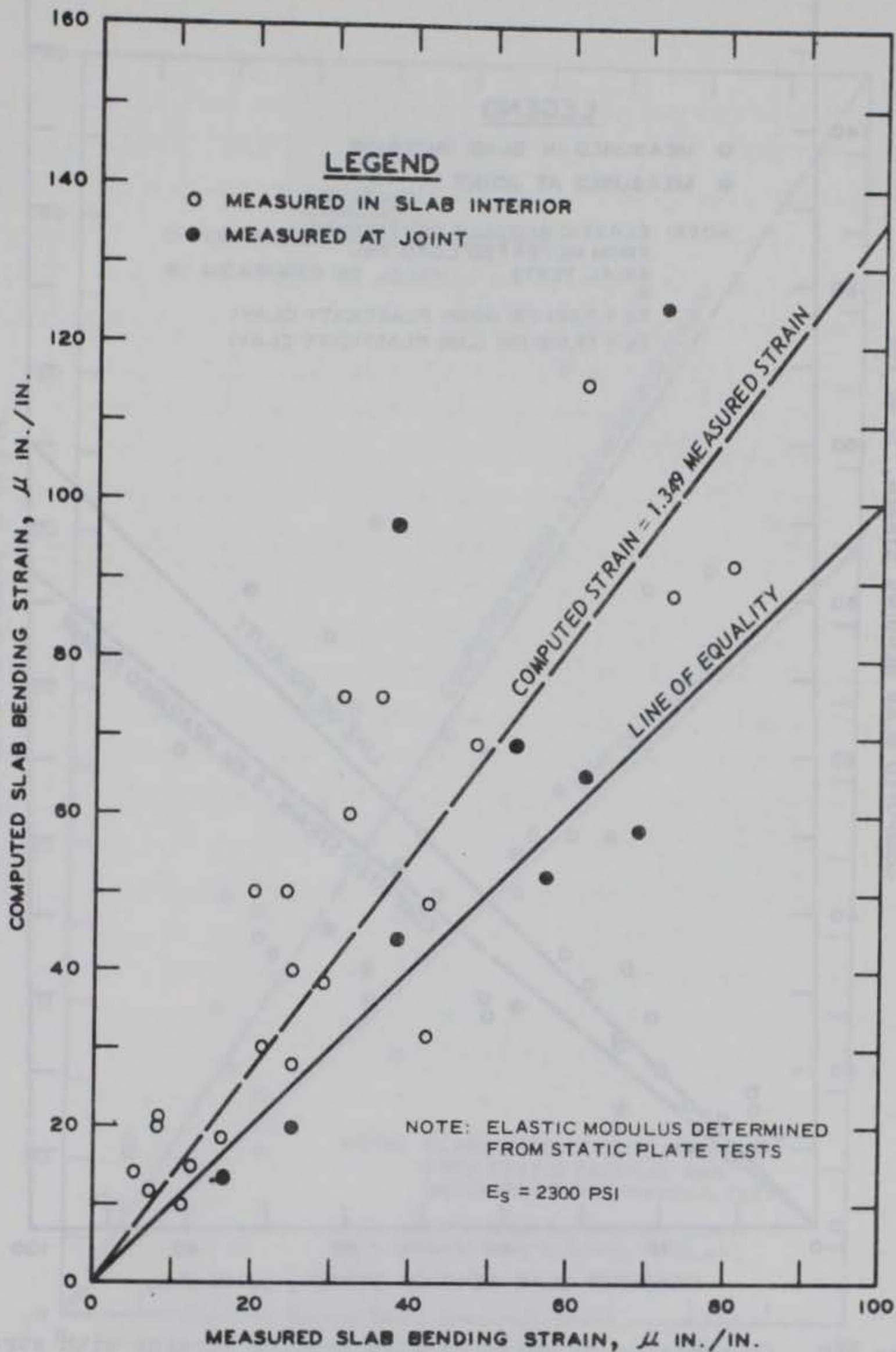


Figure A9. Comparison of measured slab bending strain and strains computed with the subgrade characterized with static plate bearing tests

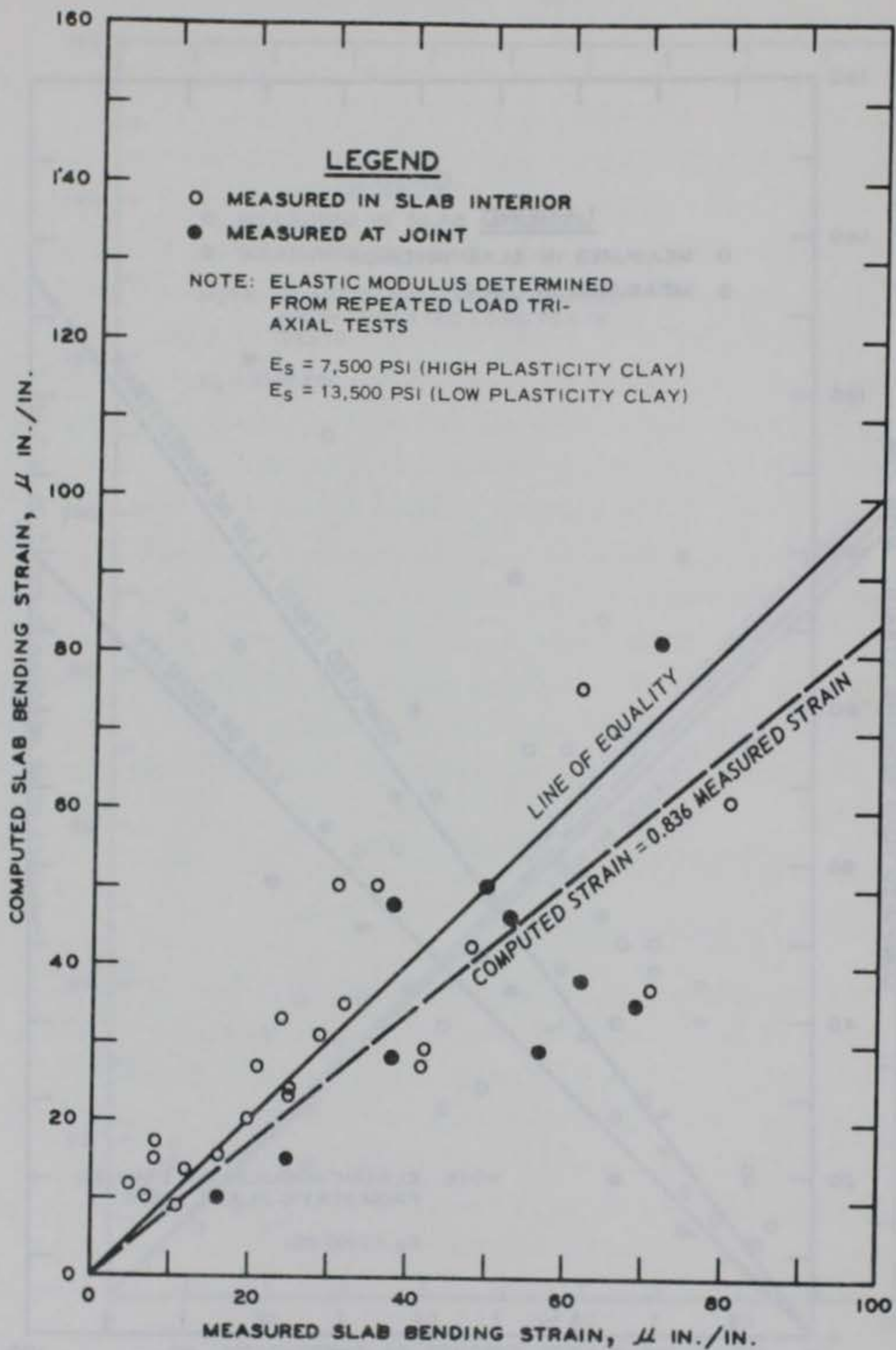


Figure A10. Comparisons of measured slab bending strains with strains computed with the subgrade characterized with repeated load triaxial tests



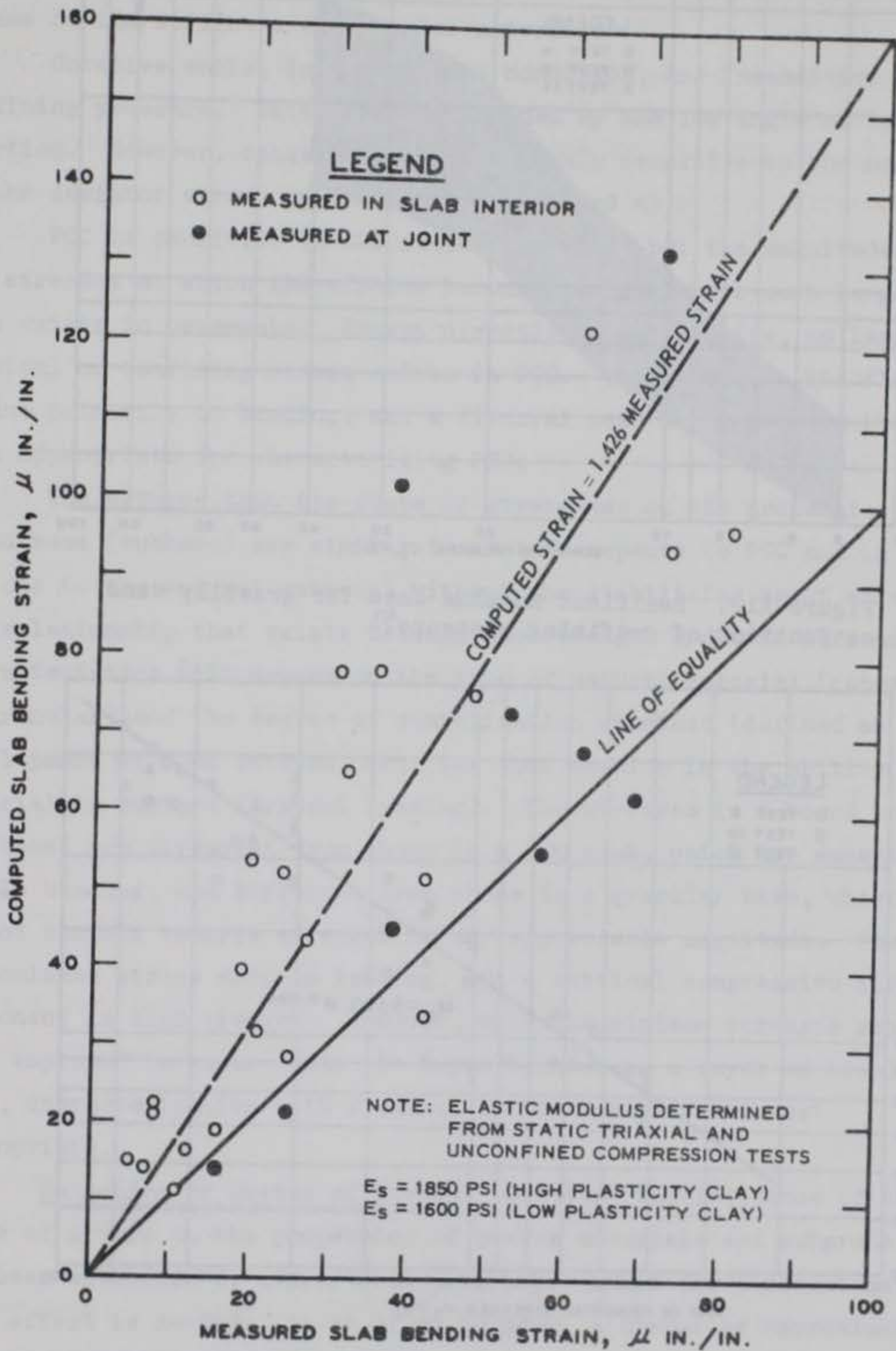


Figure A11. Comparison of measured slab bending strains with strains computed with the subgrade characterized with static triaxial tests

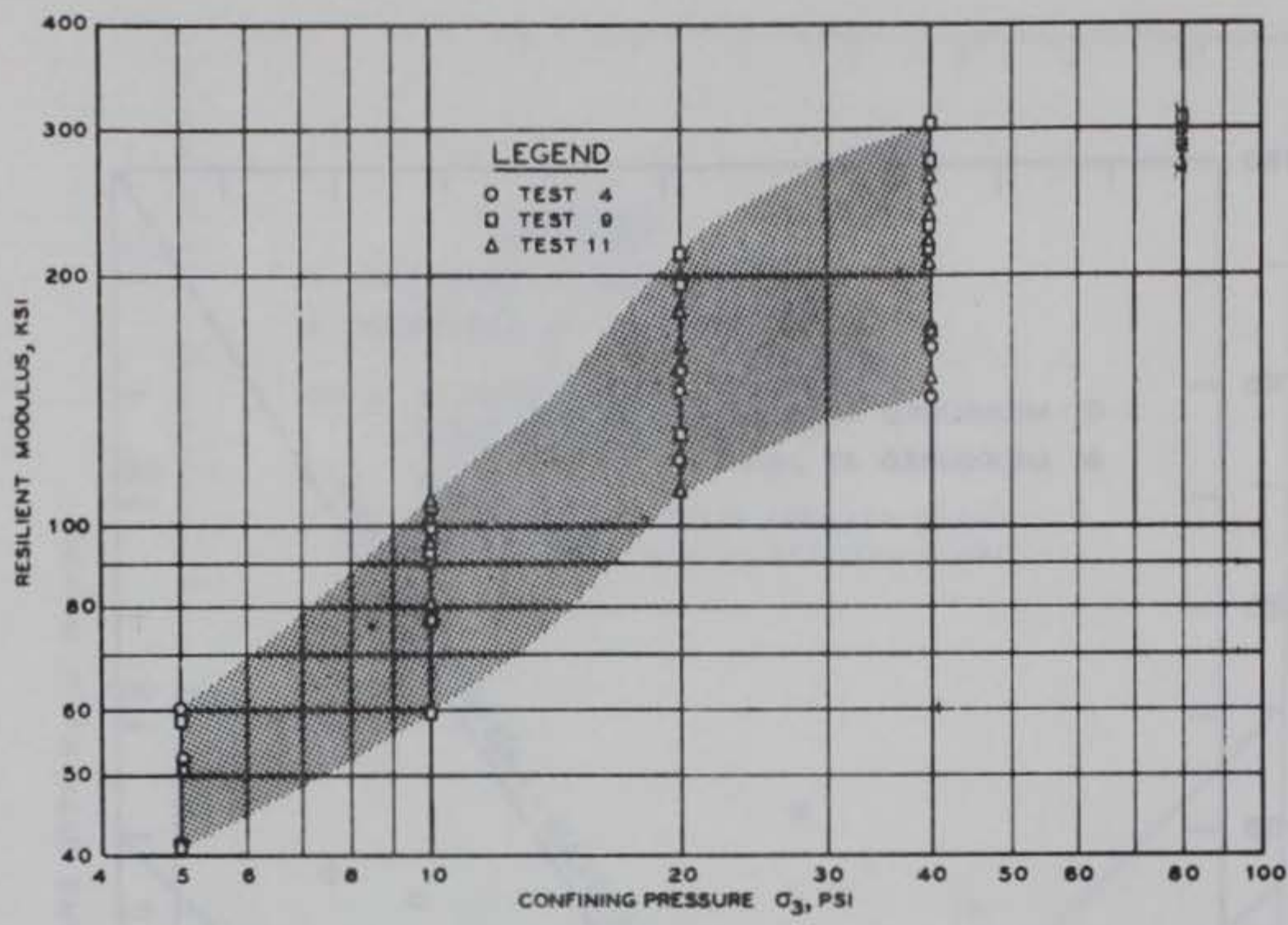


Figure A12. Resilient modulus data for gravelly sand as function of confining pressure<sup>51</sup>

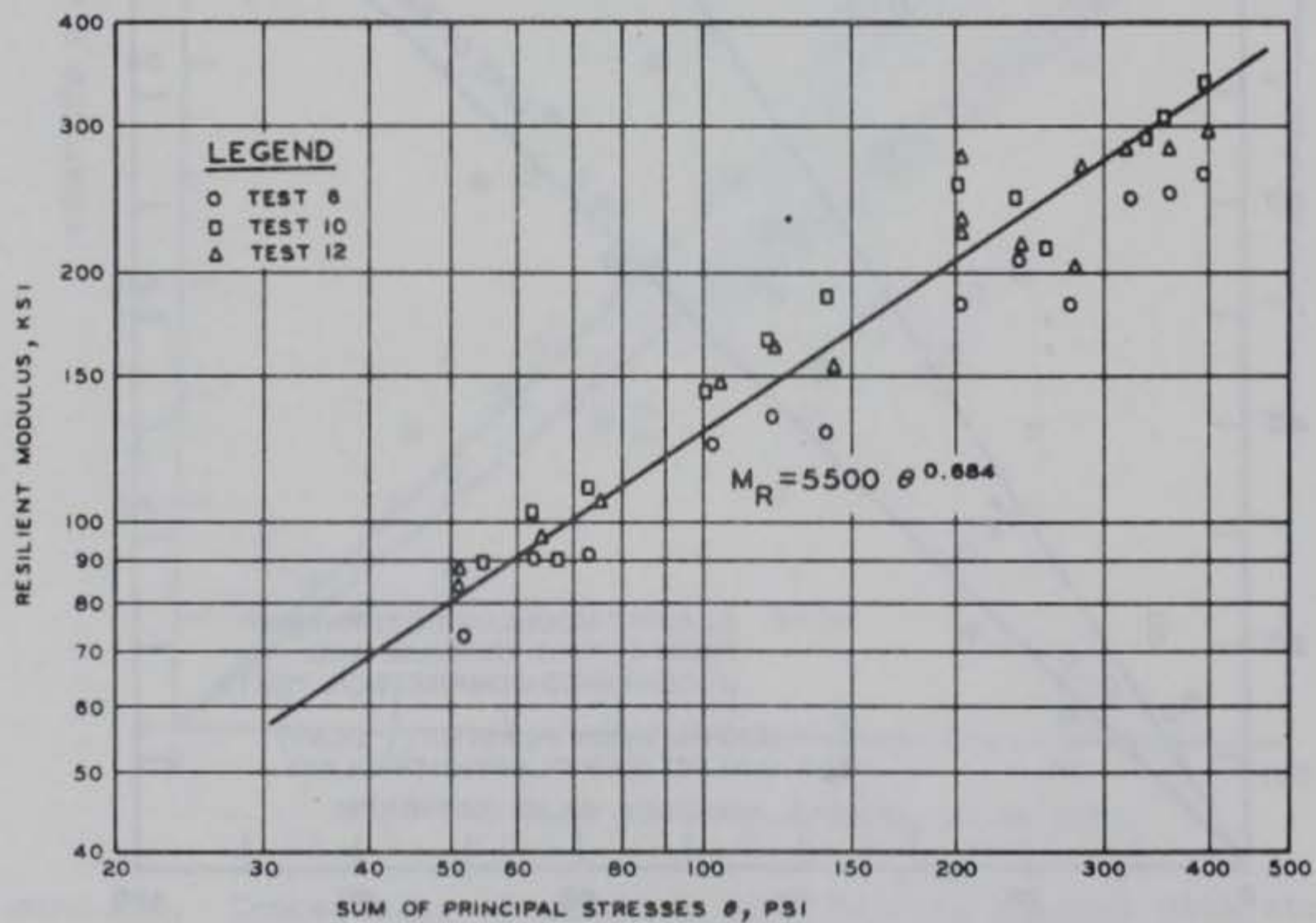


Figure A13. Resilient modulus data for dense crushed limestone<sup>51</sup>



of internal friction also accounts for the large influence of confining stress on the stiffness of granular materials.

Cohesive soils, in a saturated condition, are insensitive to confining pressure. This may be explained by the low angle of internal friction. However, cohesive soils are highly sensitive to the magnitude of the deviator stress applied (Figures A2 and A3).

PCC is sensitive to the state of stress, but the magnitude of the stresses at which the effects become significant is much larger than exists in pavements. Except directly beneath a tire, no large vertical or confining stress exists in PCC. The stress in the slabs is due primarily to bending, and a flexural test is considered the most appropriate for characterizing PCC.

The effects that the state of stress has on the properties of a bound base (subbase) are similar in certain aspects to PCC and in other aspects to the natural material without the stabilizing agent added. The relationship that exists between the strength and load deformation characteristics will depend on the type of natural material (cohesive or granular) and the degree of stabilization attained (defined as the development of bond between particles that results in the ability of the material to sustain flexural loading). The stresses in a bound base (subbase) are different from those in a PCC slab, which are essentially simple bending, and different from those in a granular base, which cannot sustain tensile stresses of any appreciable magnitude. The predominate stress mode is bending, but a vertical compressive stress component is also present. However, with the minimum strength requirement employed to ensure that the layer behaves as a layer of bound material, characterization with flexural tests is considered most appropriate.

Selection of States of Stress. Now that the influence of the state of stress on the properties of paving materials and subgrade soils has been established, a practical usable procedure for accounting for this effect is needed. As so often happens, a number of approximations of actual conditions are necessary.

The state of stress in a pavement layer or subgrade varies with



depth and with horizontal location. The exact distribution of stresses within a pavement structure will depend on the composition of the structure and the loading. Figures A14-A19 show examples of the variability that may be expected. Pavement structures are infinite in variety, and loading conditions may vary widely; however, Figures A14-A19 represent real pavement structures and loads. The general trends illustrated in these examples are representative of pavements for aircraft operation.

Interpretation of Figures A14-A19 and subsequent figures requires a definition of terms and the establishment of a sign convention for stresses. The sign convention used herein will be that compressive stresses are positive and tensile stresses are negative. The following terminology and relationships are established:

$\sigma_1$  = major principal stress

= principal stress with the largest numerical value

$\sigma_3$  = minor principal stress

= principal stress with the smallest numerical value

$\sigma_2$  = intermediate principal stress

= principal stress with a numerical value between the major and minor principal stress

$\sigma_d = \sigma_1 - \sigma_3$

= deviator stress

$\theta = \sigma_1 + \sigma_2 + \sigma_3$

= first stress invariant

The definition of deviator stress is consistent with the definition previously given for conditions in a triaxial test.

The stresses plotted in Figures A14-A19 were computed with the elastic layered model. The material properties used were obtained from a rather extensive testing program. However, the material characterization would not reflect precisely the influence of the state of stress. Only two constants are used for each material, but the stresses vary throughout each material. The validity of the computed stresses then is questionable and should be considered only as an approximation. One quickly gets into a "vicious cycle," and the futility of precise material characterization becomes apparent. To be precise, the material



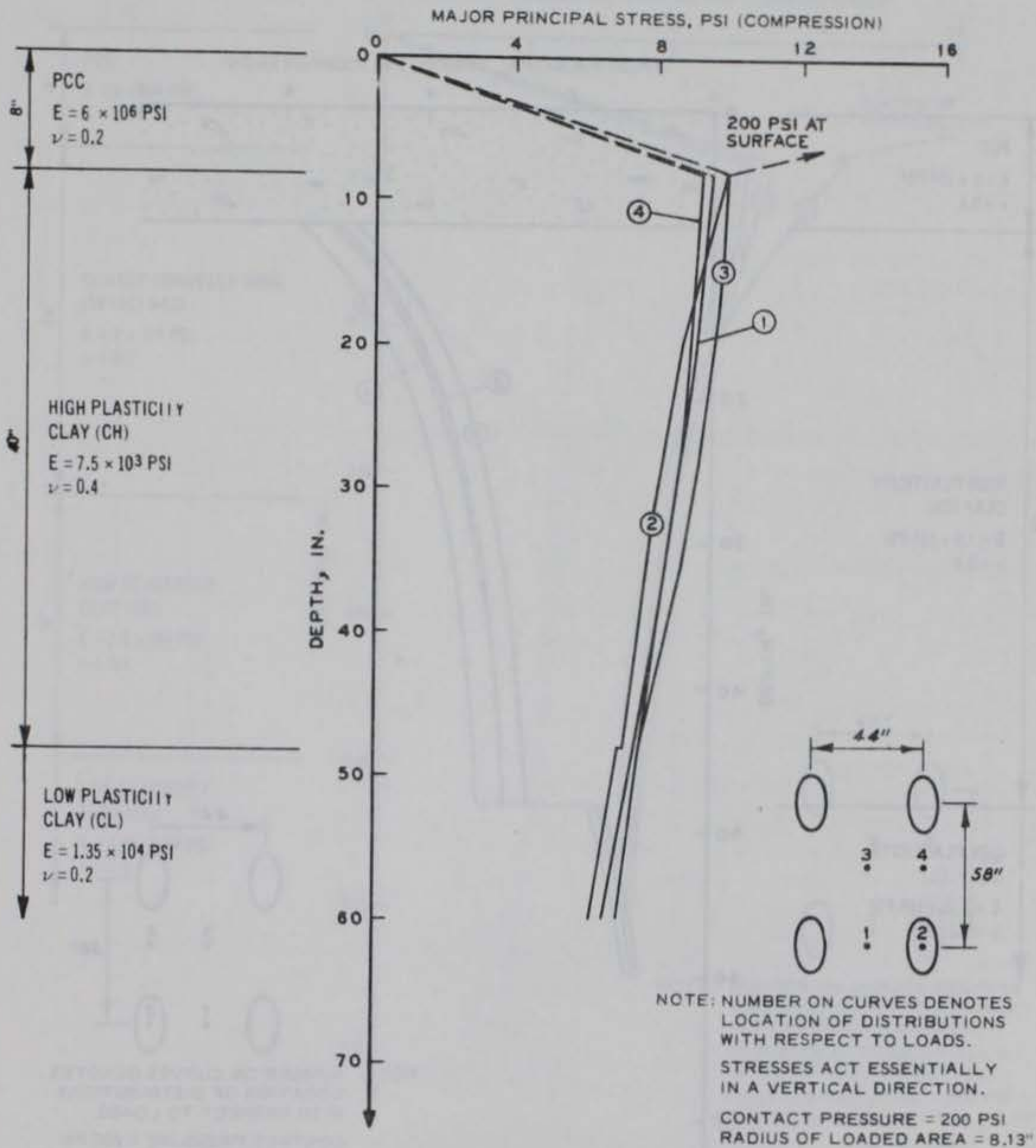


Figure A14. Distribution of major principal stress in a rigid pavement with no base loaded with a dual-tandem gear

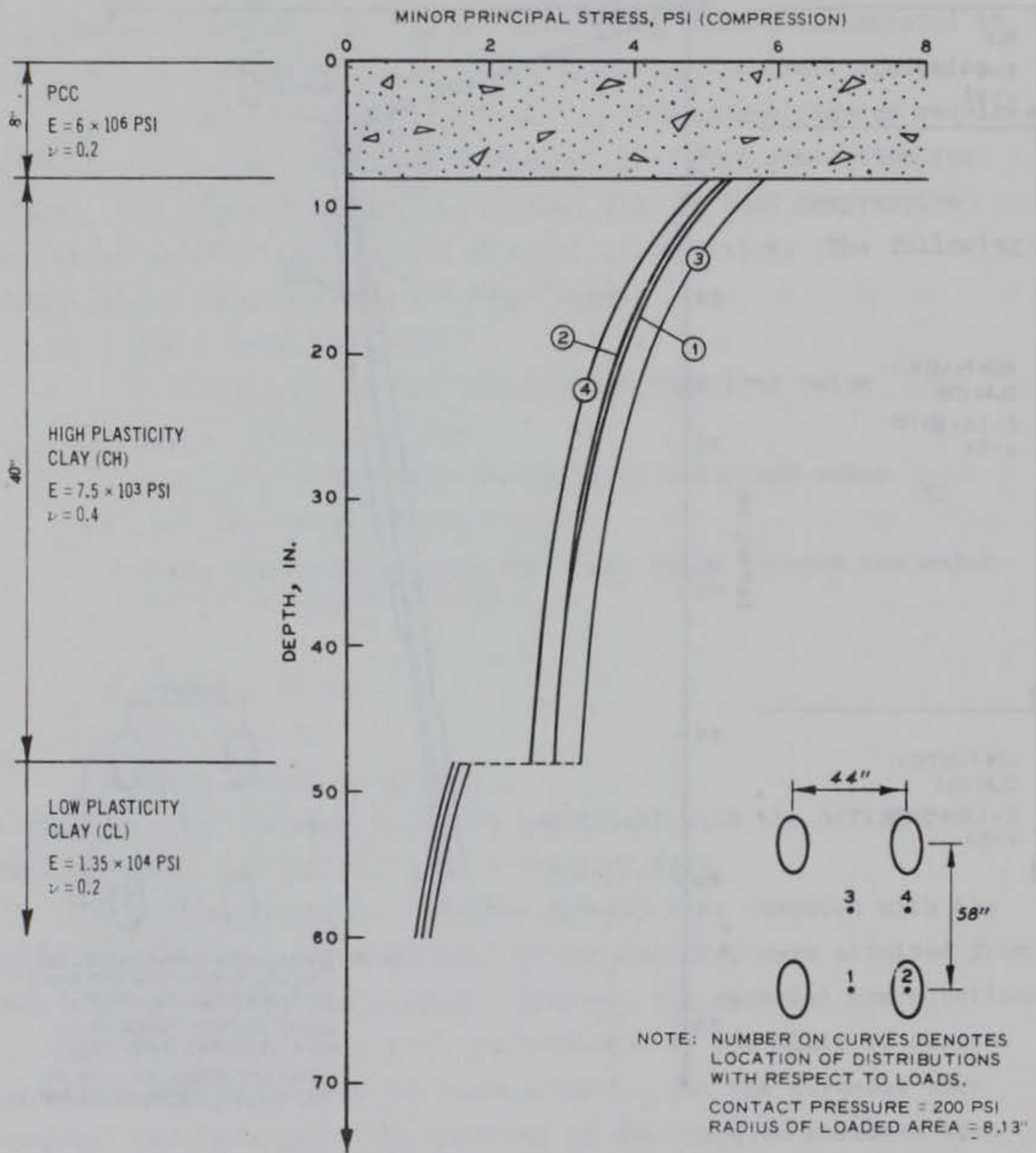


Figure A15. Distribution of minor principal stress in a rigid pavement with no base loaded with a dual-tandem gear



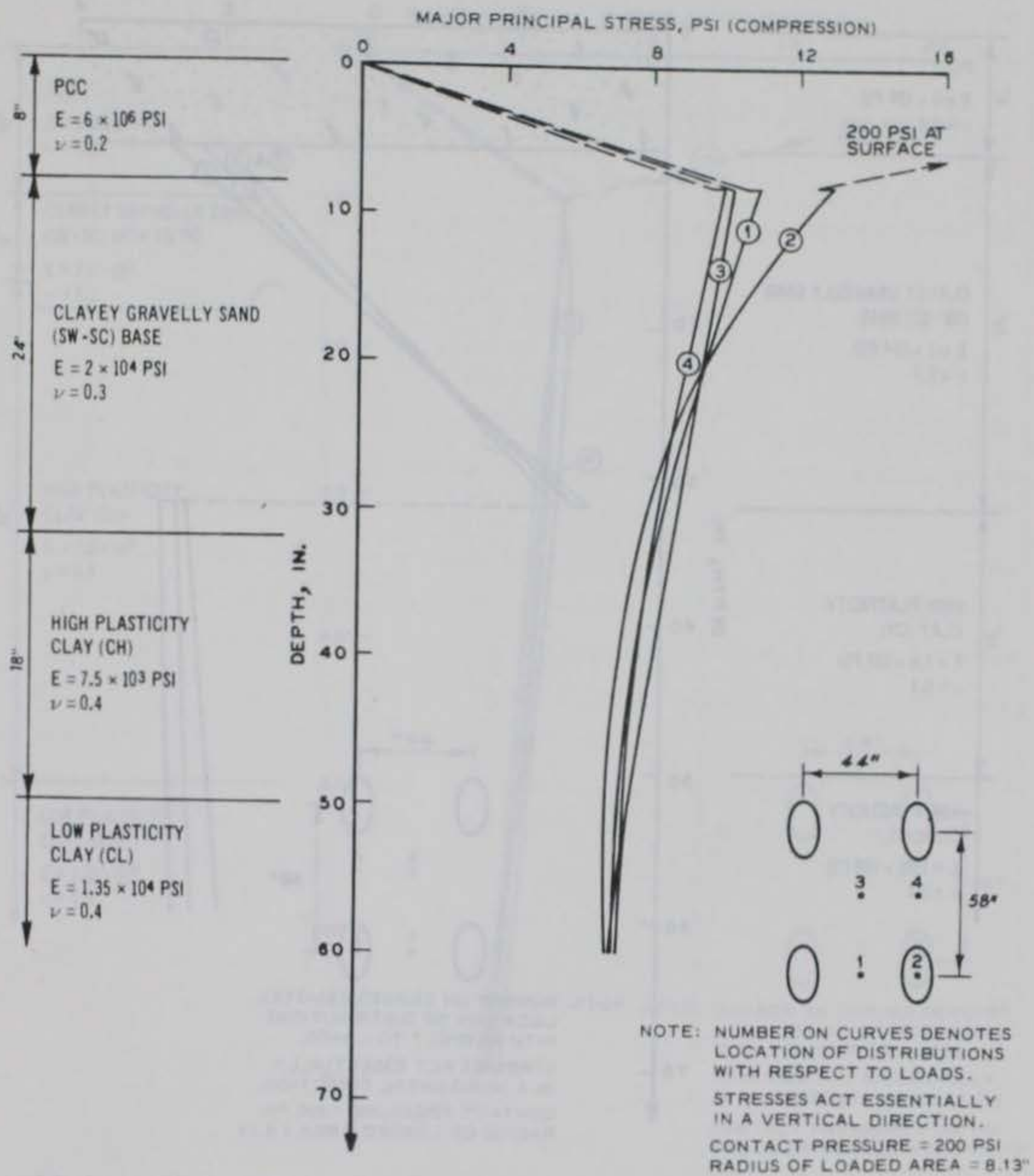


Figure A16. Distribution of major principal stress in a rigid pavement with a granular base loaded with a dual-tandem gear

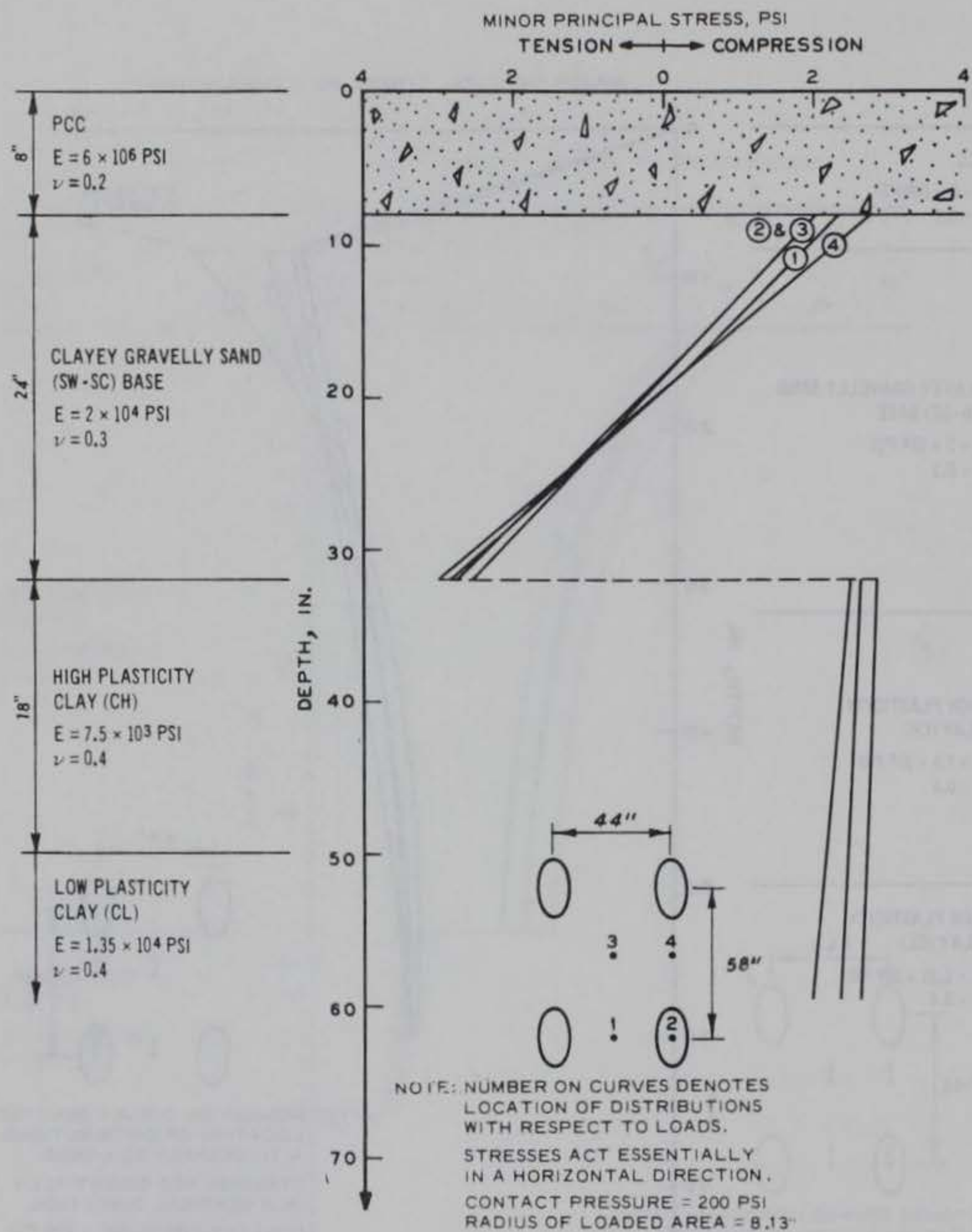


Figure A17. Distribution of minor principal stress in a rigid pavement with a granular base loaded with a dual-tandem gear



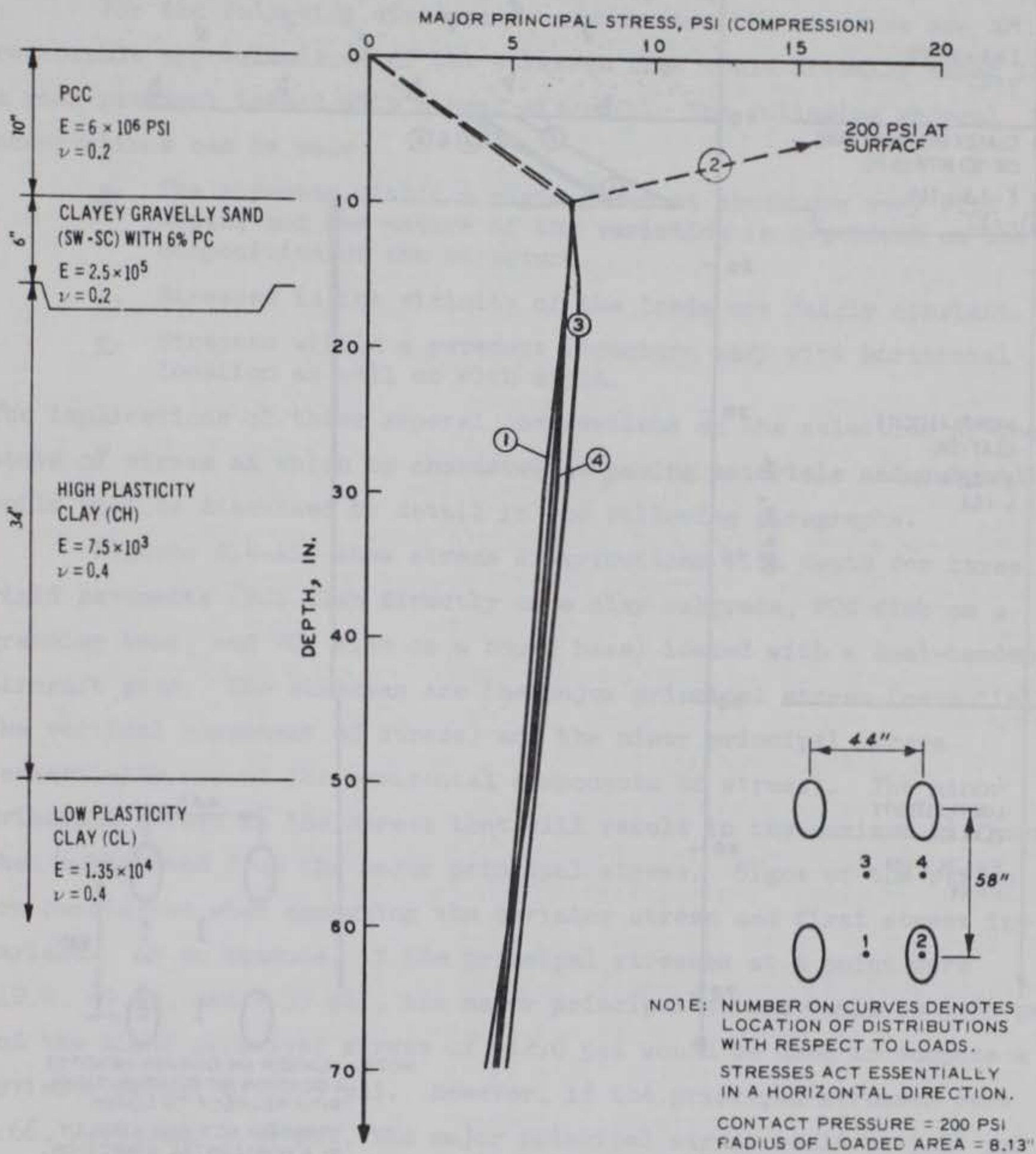


Figure A18. Distribution of major principal stress in a rigid pavement with a bound base loaded with a dual-tandem loading

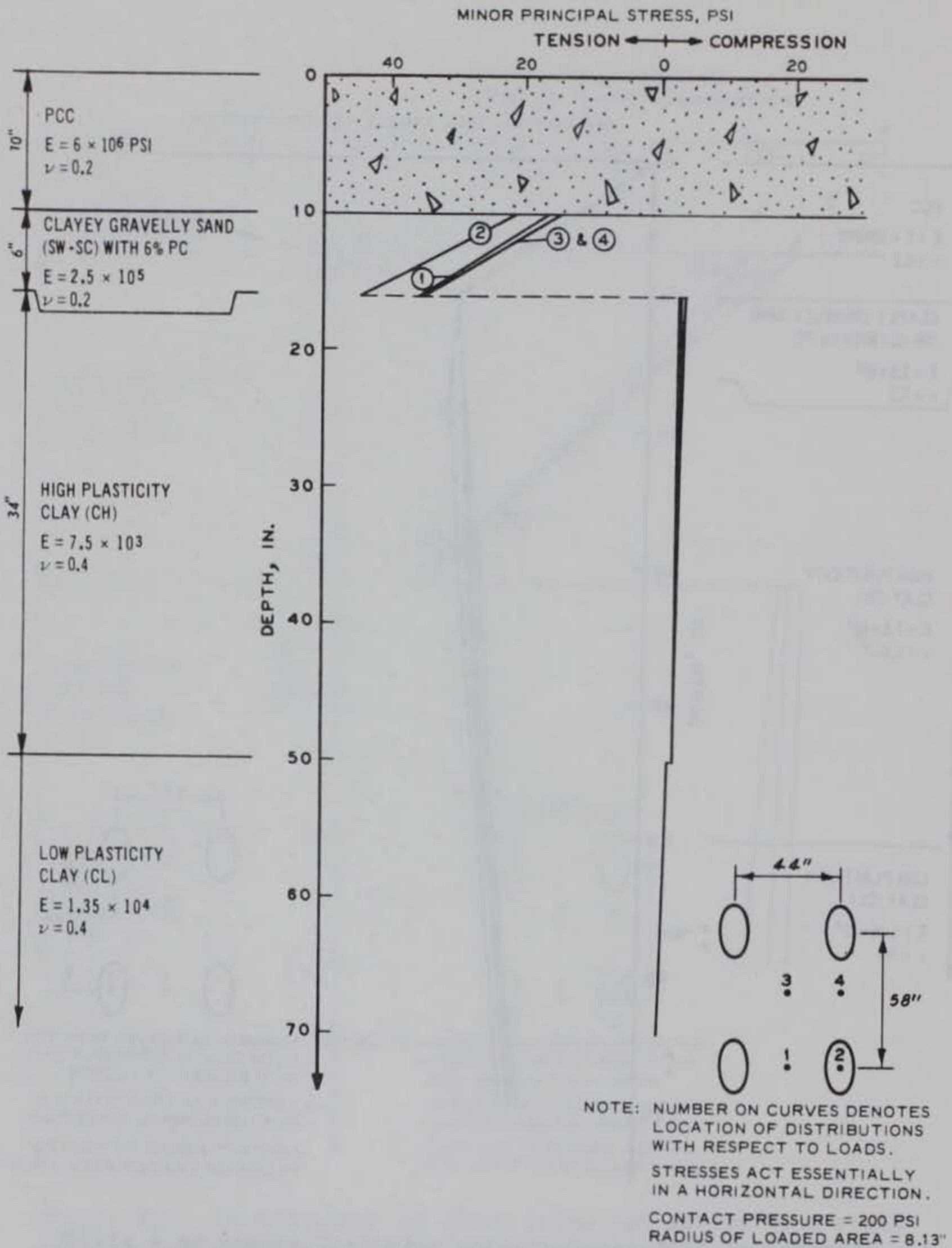


Figure A19. Distribution of minor principal stress for a rigid pavement with a bound base loaded with a dual-tandem gear



properties would have to be a continuous function of location within the pavement structure.

For the following discussion, assume that the stresses are reasonable approximations of the stresses that would actually exist in a real pavement loaded with a real aircraft. The following general observations can be made:

- a. The stresses within a rigid pavement structure vary with depth, and the nature of the variation is dependent on the composition of the structure.
- b. Stresses in the vicinity of the loads are fairly constant.
- c. Stresses within a pavement structure vary with horizontal location as well as with depth.

The implications of these general observations on the selection of the state of stress at which to characterize paving materials and subgrade soils will be discussed in detail in the following paragraphs.

Figures A14-A19 show stress distributions with depth for three rigid pavements (PCC slab directly on a clay subgrade, PCC slab on a granular base, and PCC slab on a bound base) loaded with a dual-tandem aircraft gear. The stresses are the major principal stress (essentially the vertical component of stress) and the minor principal stress (essentially one of the horizontal components of stress). The minor principal stress is the stress that will result in the maximum difference when subtracted from the major principal stress. Signs of the stress are considered when computing the deviator stress and first stress invariant. As an example, if the principal stresses at a point were -12.0, -9.82, and 5.55 psi, the major principal stress would be 5.55 psi and the minor principal stress of -12.0 psi would be used to compute a deviator stress of 17.5 psi. However, if the principal stresses were 2.66, 2.79, and 5.58 psi, the major principal stress would be 5.58 psi and the minor principal stress of 2.66 psi would be used to compute a deviator stress of 2.92 psi. The general trends illustrated in Figures A14-A19 are that the major principal (vertical) stress decreases at a rather slow rate with depth and that the variation in the minor principal (horizontal) stress will depend on the composition of the pavement structure.



Figures A14 and A15 show distributions for a pavement composed of a PCC slab directly on a clay subgrade. The stress parameter of primary interest for characterizing cohesive soils is the deviator stress. Combining the distributions in Figures A14 and A15 results in the distribution of deviator stress in Figure A20. Since the modulus of cohesive materials varies with deviator stress, the modulus of the clay subgrade should also vary with depth. However, from a practical point of view, the variability is not really that great and the change is rather gradual. This implies that characterization at a given deviator stress will be applicable for appreciable depths (i.e., 5 psi for at least 5 ft for the example under consideration). The same type patterns were observed in the subgrade beneath the granular and bound bases.

Figures A16 and A17 show distributions for PCC slabs on a 24-in.-thick granular base over the clay subgrade. Of interest in Figure A16 is the fact that the nature of the distribution and magnitude of the stresses are about the same as in Figure A14 for the PCC slabs directly on the clay subgrade. However, the minor principal stresses in the granular base (Figure A17) are quite different from the stresses in the subgrade (Figure A15). There is some small compressive (confining) stress at the top of the granular base layer, but at the bottom, the bending action has resulted in tensile stresses. Although the tensile stresses are small, granular bases are normally considered incapable of sustaining tensile stresses. Part of this effect may be caused by the assumption of complete continuity at the interface between the PCC slab and the granular base. If some slip were permitted at the interface (which is probably what actually occurs), the compressive stress at the top of the layer would be larger and the tensile stress at the bottom of the layer would be smaller. This is illustrated in Figure A21, which shows distributions of horizontal stresses for the case where the PCC layer is free to slip horizontally relative to the granular base layer and the case where there is complete continuity at this interface. These horizontal stresses are principal stresses since they are located along a line through the center of a circular loaded area where the shear stresses are zero. For comparative purposes, these may be considered equivalent to the minor principal stresses previously discussed.



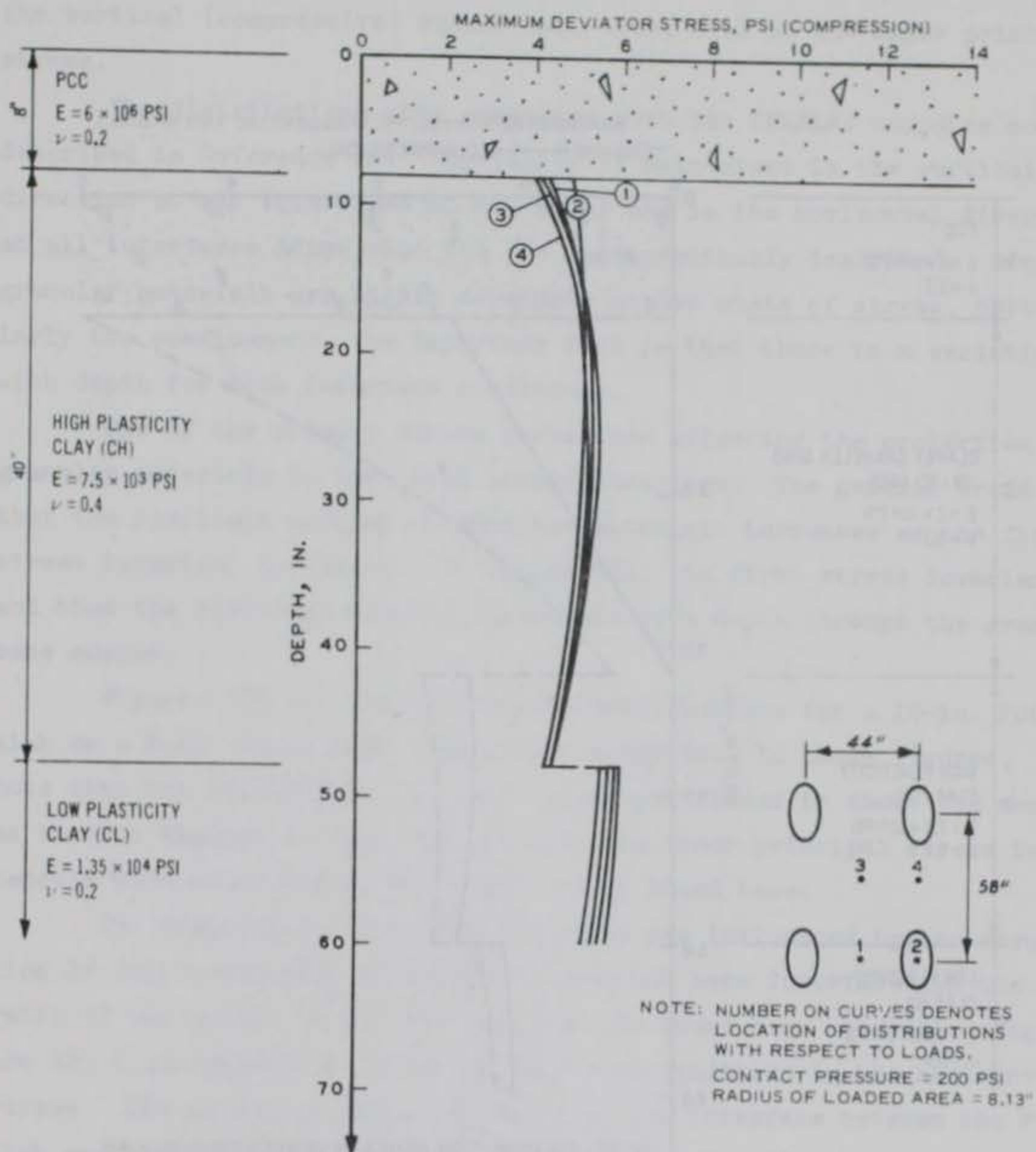


Figure A20. Distribution of maximum deviator stress in a rigid pavement with no base loaded with a dual-tandem loading

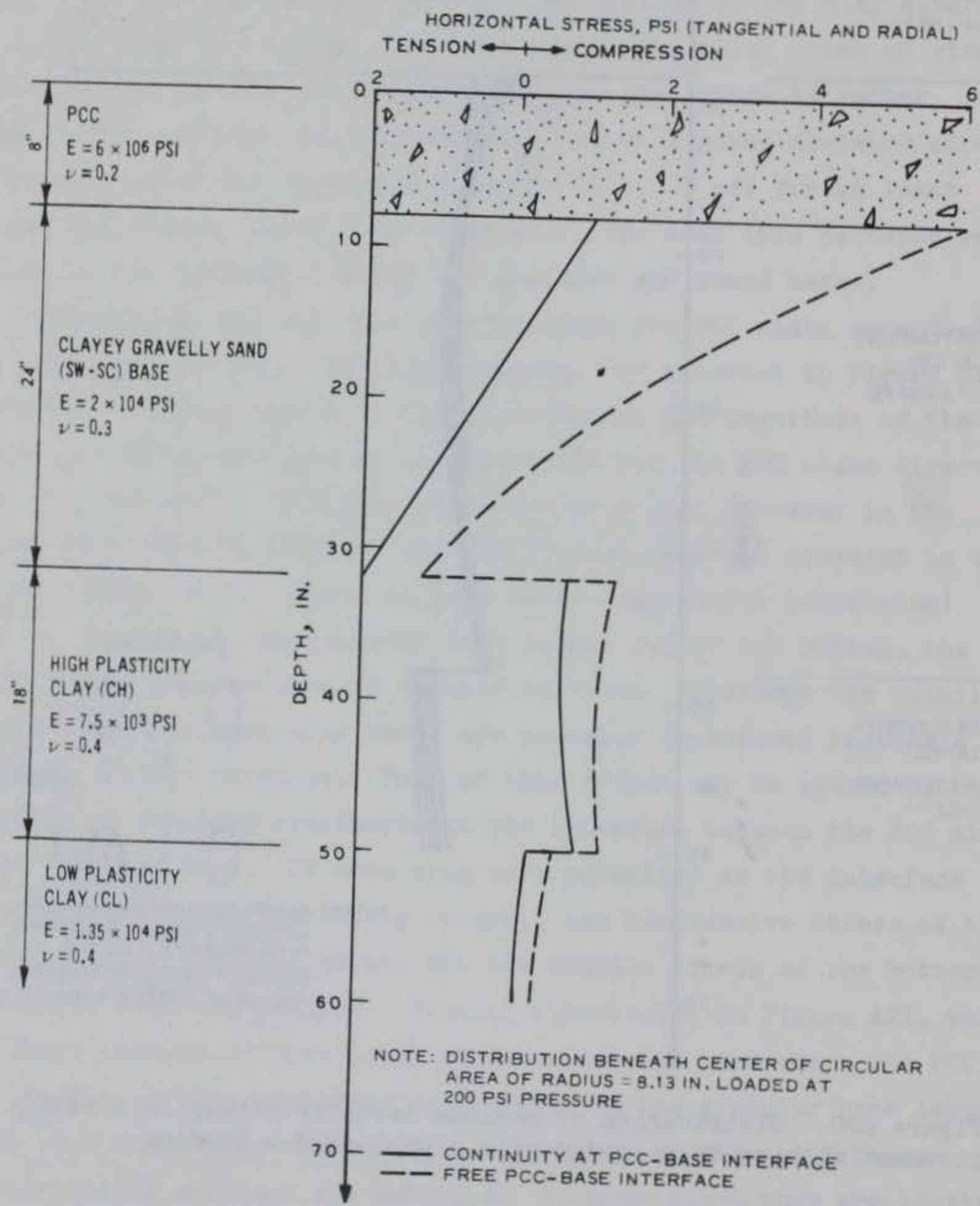


Figure A21. Horizontal stress distribution illustrating effect of interface condition between PCC slab and granular base



However, for the case of a free interface condition, the horizontal (compressive) stress in the top of the base layer may be greater than the vertical (compressive) stress and, thus, will be the major principal stress.

The distributions were generated with the CRANLAY computer code described in Reference 22. Continuity is maintained in the vertical direction at all interfaces at all times and in the horizontal direction at all interfaces other than the one case previously described. Since granular materials are highly dependent on the state of stress, particularly the confinement, the important fact is that there is a variation with depth for both interface conditions.

One of the primary stress parameters affecting the properties of granular materials is the first stress invariant. The general trend is that the resilient modulus of granular materials increases as the first stress invariant increases. In Figure A22, the first stress invariant, and thus the resilient modulus, decreases with depth through the granular base course.

Figures A18 and A19 show stress distributions for a 10-in. PCC slab on a 6-in. bound base over a clay subgrade. In these figures, note that the distribution of major principal stress is about the same as that in Figures A14 and A16 and that the minor principal stress is tensile throughout the entire depth of the bound base.

The magnitude of the stresses shown was influenced by the assumption of full continuity at the PCC slab-bound base interface and the ratio of the moduli of the PCC slab and the bound base material. Figure A23 illustrates the effect of interface condition in the horizontal stress. The effect of horizontal slip at the interface between the PCC slab and the bound base layer is to reduce the tensile stresses in the bound base layer. When horizontal slip is permitted at this interface, the two layers respond as separate slabs. The stresses in the top of the bound base layer are compressive and may be larger than the vertical component. When full continuity is assumed at the interface, the PCC and bound base layers tend to function as a composite beam and the stresses in the top of the bound base layer are tensile.

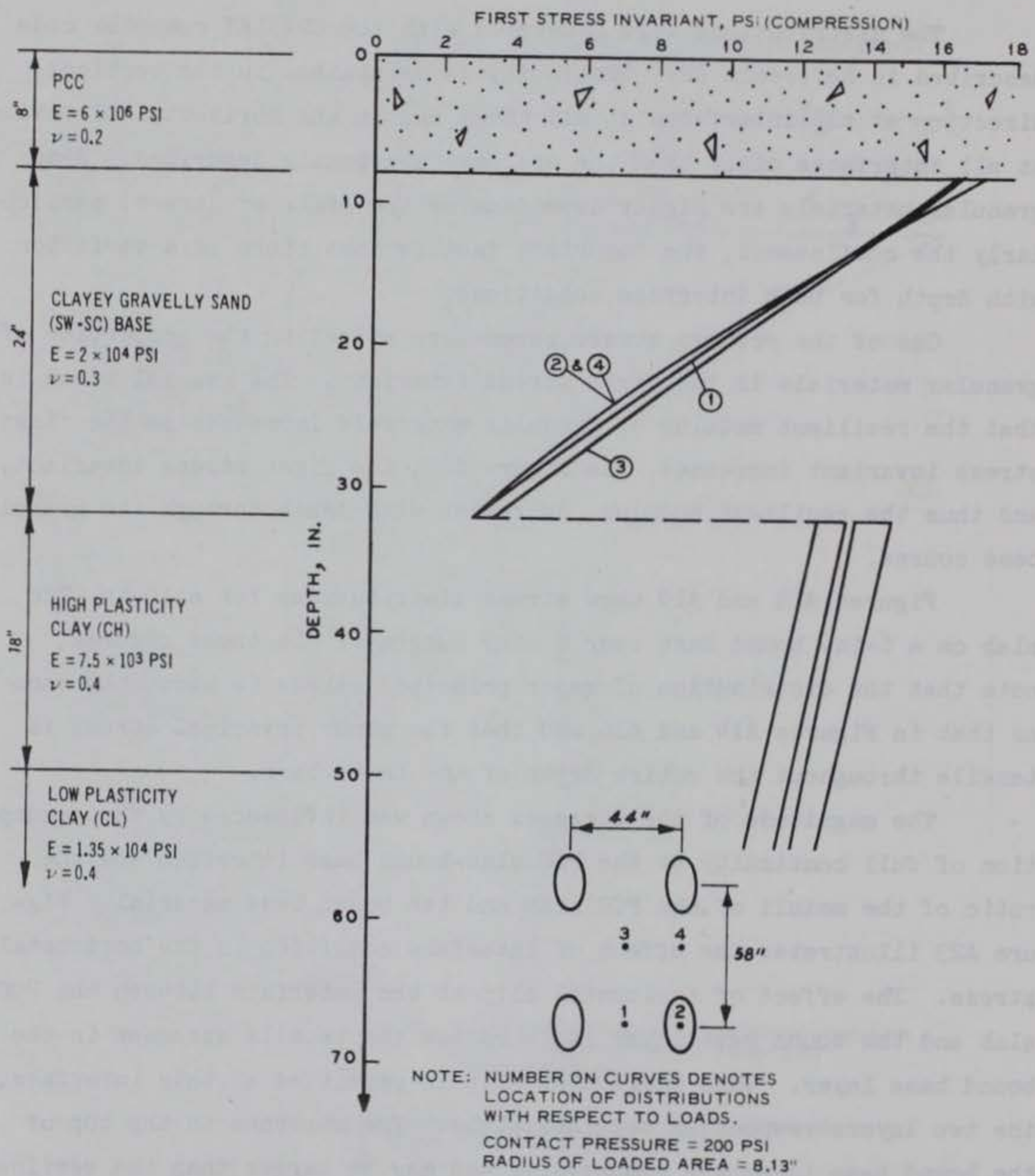


Figure A22. Distribution of the first stress invariant in a rigid pavement with a granular base loaded with a dual-tandem gear



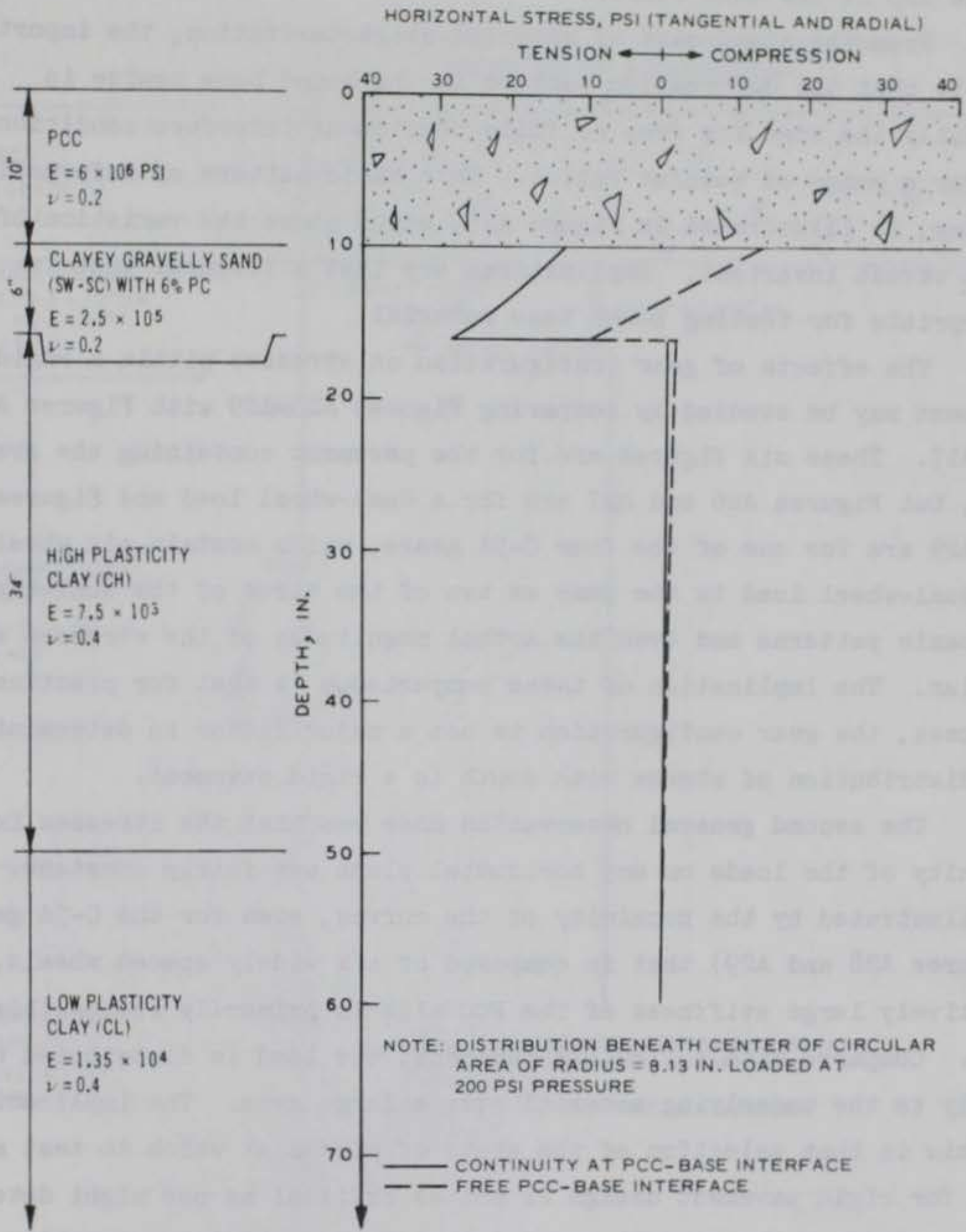


Figure A23. Horizontal stress distribution illustrating effect of interface condition between PCC slab and bound base

Figure A24 shows the effect of the modulus ratio between the PCC slab and the base material. The smaller the ratio the more pronounced the bending. For full continuity, this means larger tensile stresses in the top of the base course.

From the standpoint of material characterization, the important fact is that the deformation pattern in the bound base course is basically the same for free or fully continuous interface conditions and for a range of modulus ratios. This basic pattern of deformation, bending, is illustrated in Figure A25, which shows the variation of the first stress invariant. Implications are that a flexural test is appropriate for testing bound base material.

The effects of gear configuration on stresses within a rigid pavement may be studied by comparing Figures A26-A29 with Figures A16 and A17. These six figures are for the pavement containing the granular base, but Figures A26 and A27 are for a dual-wheel load and Figures A28 and A29 are for one of the four C-5A gears, which contain six wheels. The dual-wheel load is the same as two of the tires of the dual-tandem. The basic patterns and even the actual magnitudes of the stresses are similar. The implication of these comparisons is that for practical purposes, the gear configuration is not a major factor in determining the distribution of stress with depth in a rigid pavement.

The second general observation made was that the stresses in the vicinity of the loads on any horizontal plane are fairly constant. This is illustrated by the proximity of the curves, even for the C-5A gear (Figures A28 and A29) that is composed of six widely spaced wheels. The relatively large stiffness of the PCC slab is primarily responsible for this. Compared with a flexible pavement, the load is distributed uniformly to the underlying material over a large area. The implication of this is that selection of the state of stress at which to test material for rigid pavement design is not as critical as one might determine from a study of the overall sensitivity of the material properties to the state of stress.

The third general observation is related to the second. Although



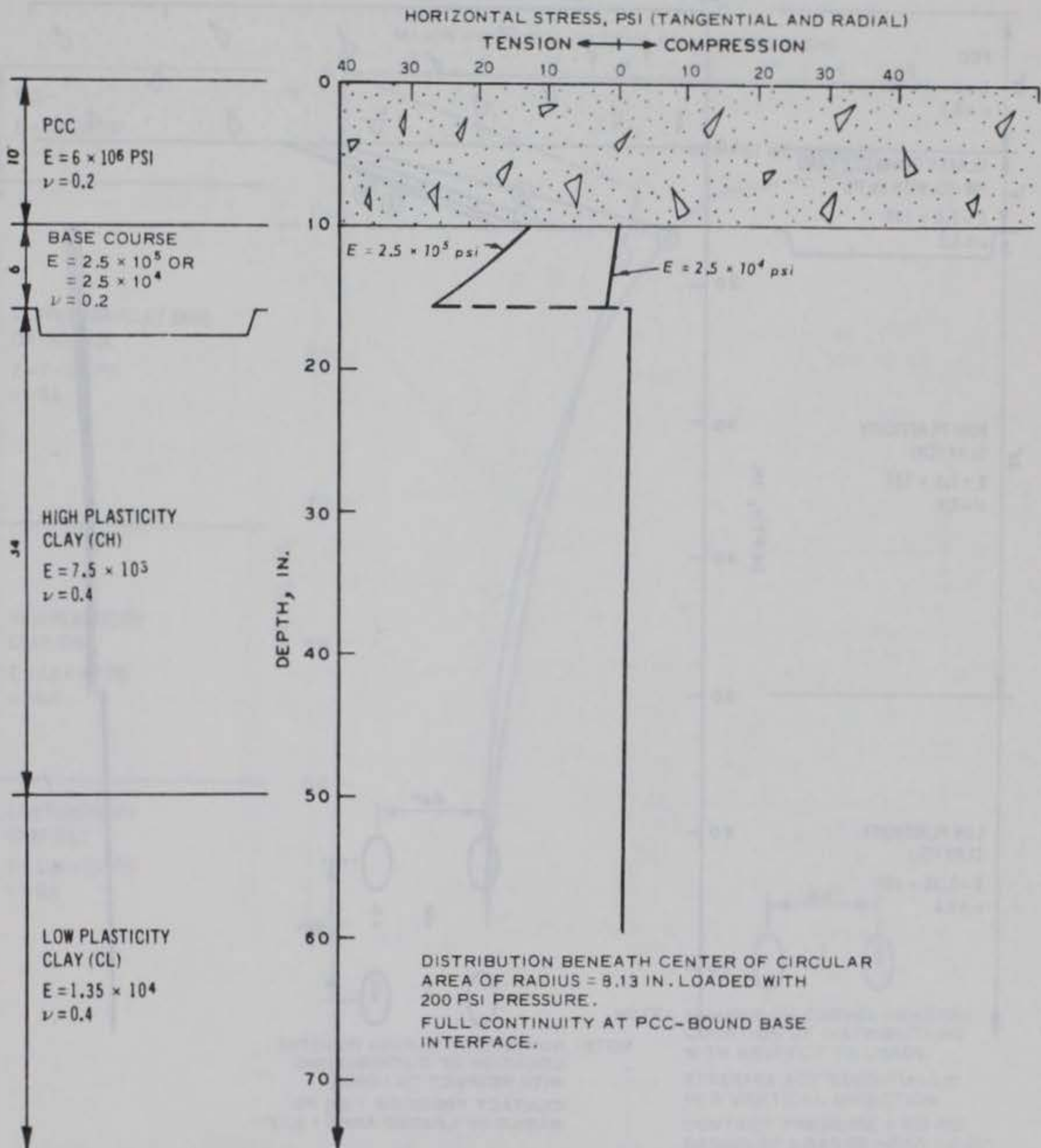


Figure A24. Horizontal stress distribution illustrating effect of ratio of moduli of PCC slab and base layer

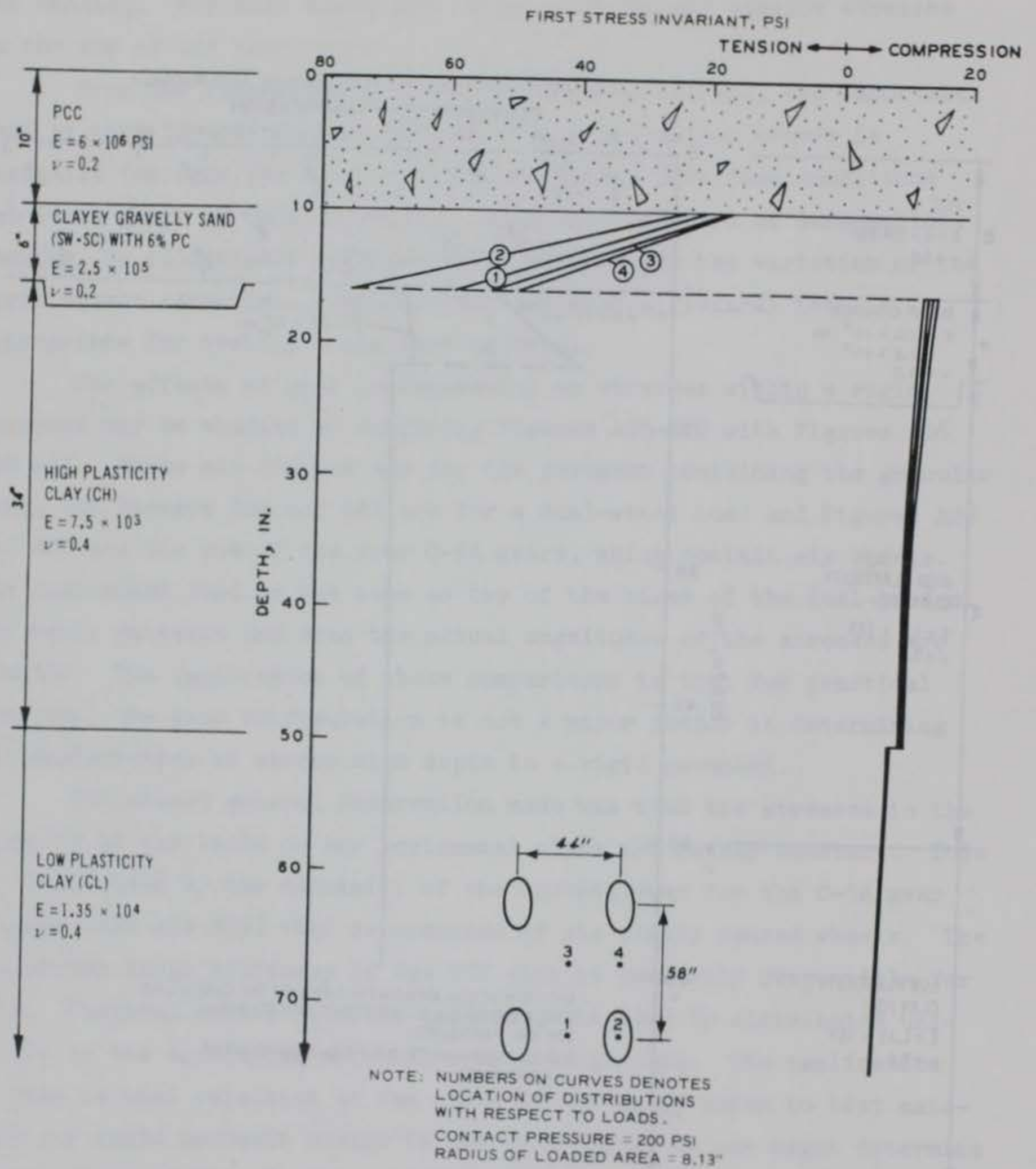


Figure A25. Distribution of the first stress invariant for a rigid pavement with a bound base loaded with a dual-tandem gear



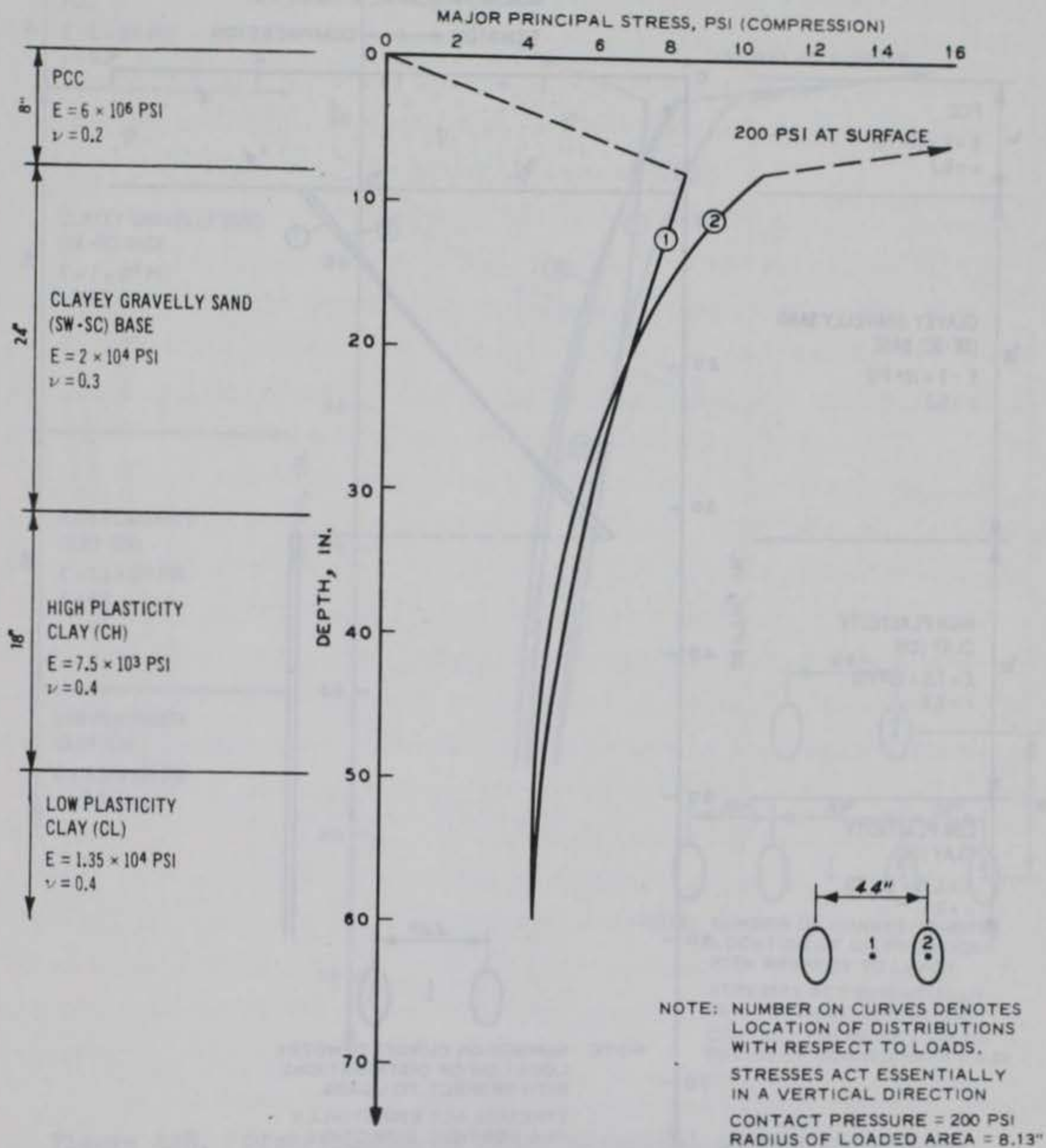


Figure A26. Distribution of major principal stress in a rigid pavement with a granular base loaded with a dual-wheel gear

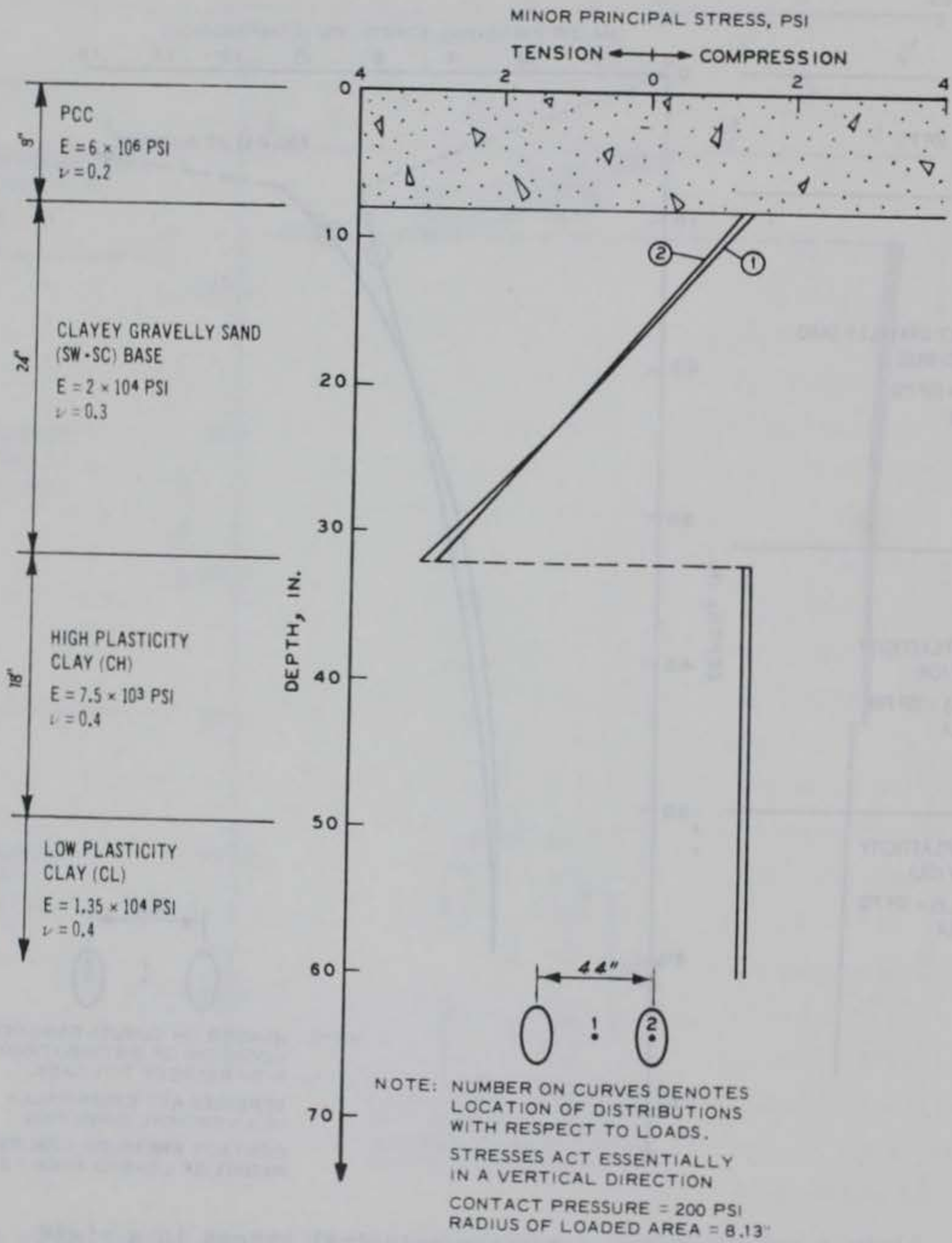


Figure A27. Distribution of minor principal stress in a rigid pavement with a granular layer loaded with a dual-wheel gear



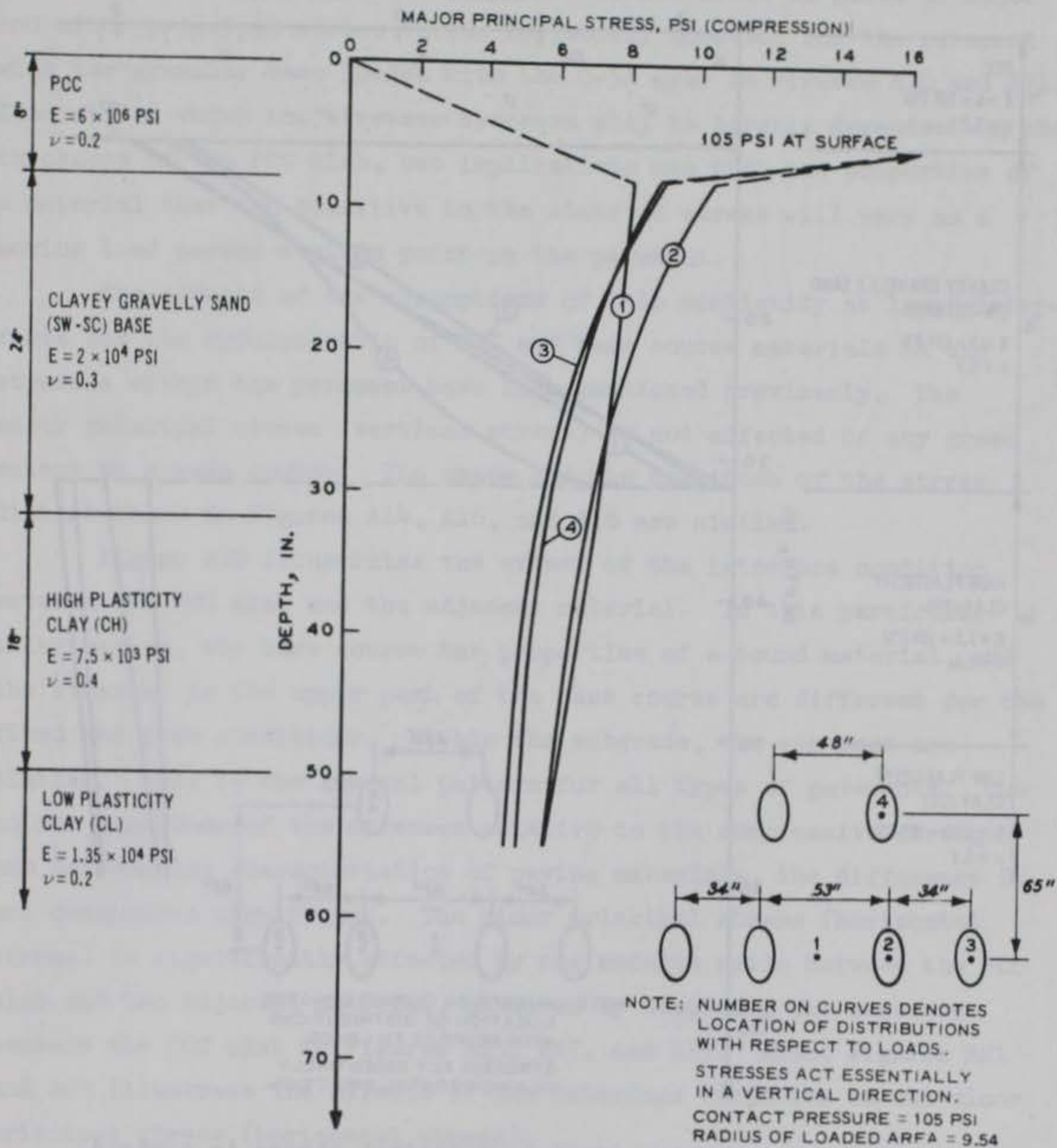


Figure A28. Distribution of major principal stress in a rigid pavement with a granular base loaded with a C-5A gear

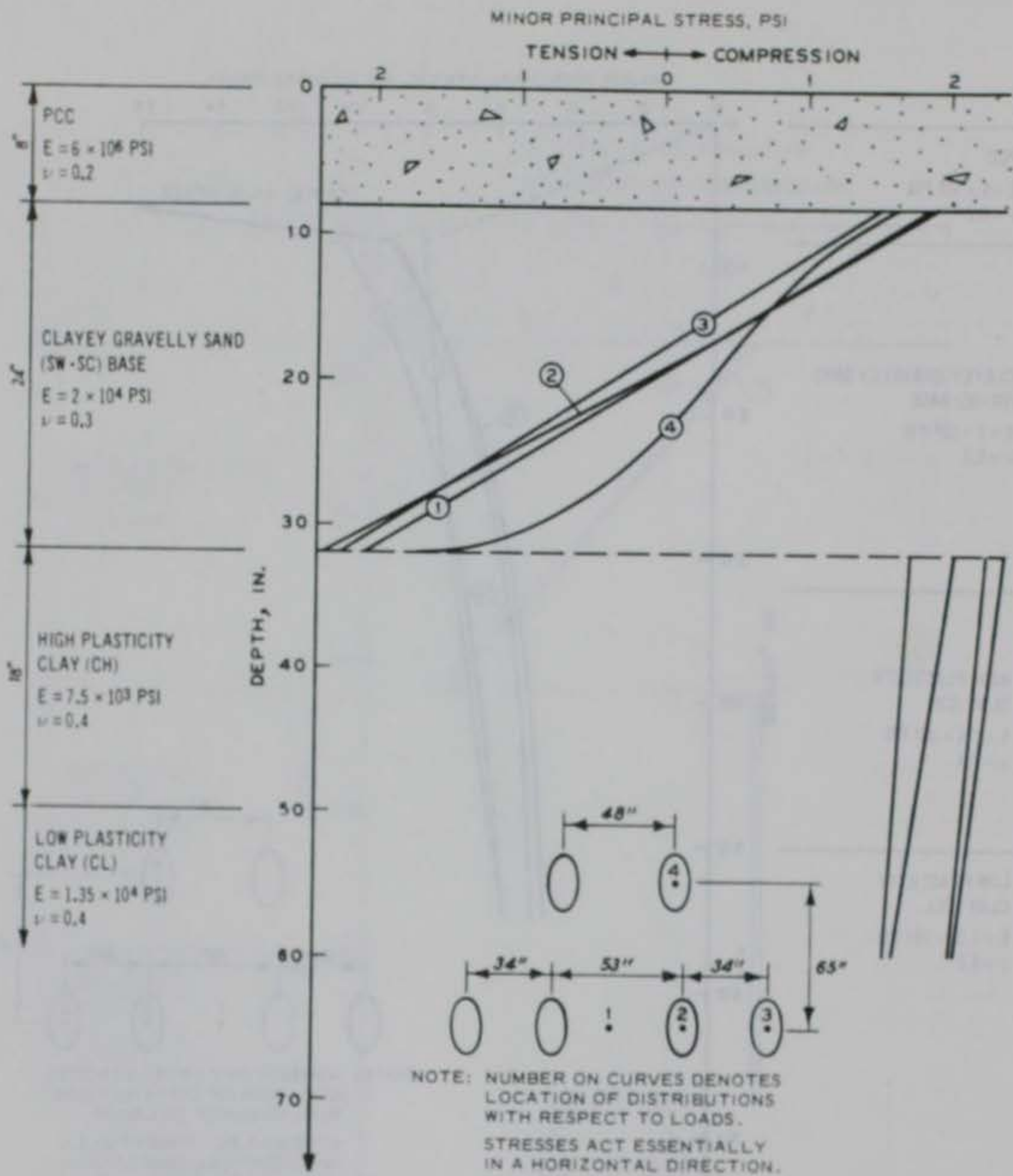


Figure A29. Distribution of minor principal stress in a rigid pavement with a granular base loaded with a C-5A gear



the stresses in a pavement at a particular depth may be relatively constant in the vicinity of the loads, they will decrease as the distance from the load increases. Examples of this are shown as plots of major and minor principal stress versus horizontal location for the pavement with the granular base loaded with the C-5A gear in Figures A30 and A31. The rate at which the stresses decrease will be largely dependent on the thickness of the PCC slab, but implications are that the properties of a material that are sensitive to the state of stress will vary as a moving load passes a given point on the pavement.

The effects of the assumptions of full continuity at layer interfaces and the modulus ratio of PCC and base course materials on the stresses within the pavement have been mentioned previously. The major principal stress (vertical stress) is not affected to any great extent by a base course. The shape and the magnitude of the stress distributions in Figures A14, A16, and A18 are similar.

Figure A32 illustrates the effect of the interface condition between the PCC slab and the adjacent material. In this particular illustration, the base course has properties of a bound material, and the stresses in the upper part of the base course are different for the fixed and free conditions. Within the subgrade, the stresses are similar. This is the general pattern for all types of pavements. Due to the magnitude of the stresses relative to the compressive strength and deformation characteristics of paving materials, the difference is not considered significant. The minor principal stress (horizontal stress) is significantly affected by the modulus ratio between the PCC slab and the adjacent material, as shown by comparing the stresses beneath the PCC slab in Figures A15, A17, and A19. Also, Figures A21 and A23 illustrate the effects of the interface condition on the minor principal stress (horizontal stress).

The ratio of the thicknesses of the PCC slab and the base course will also affect the stresses in the base course. In general, the smaller the thickness ratio, the more pronounced the bending. With full continuity between the PCC slabs and the second layer, the second layer will function in conjunction with the PCC slab as a composite beam

A-48

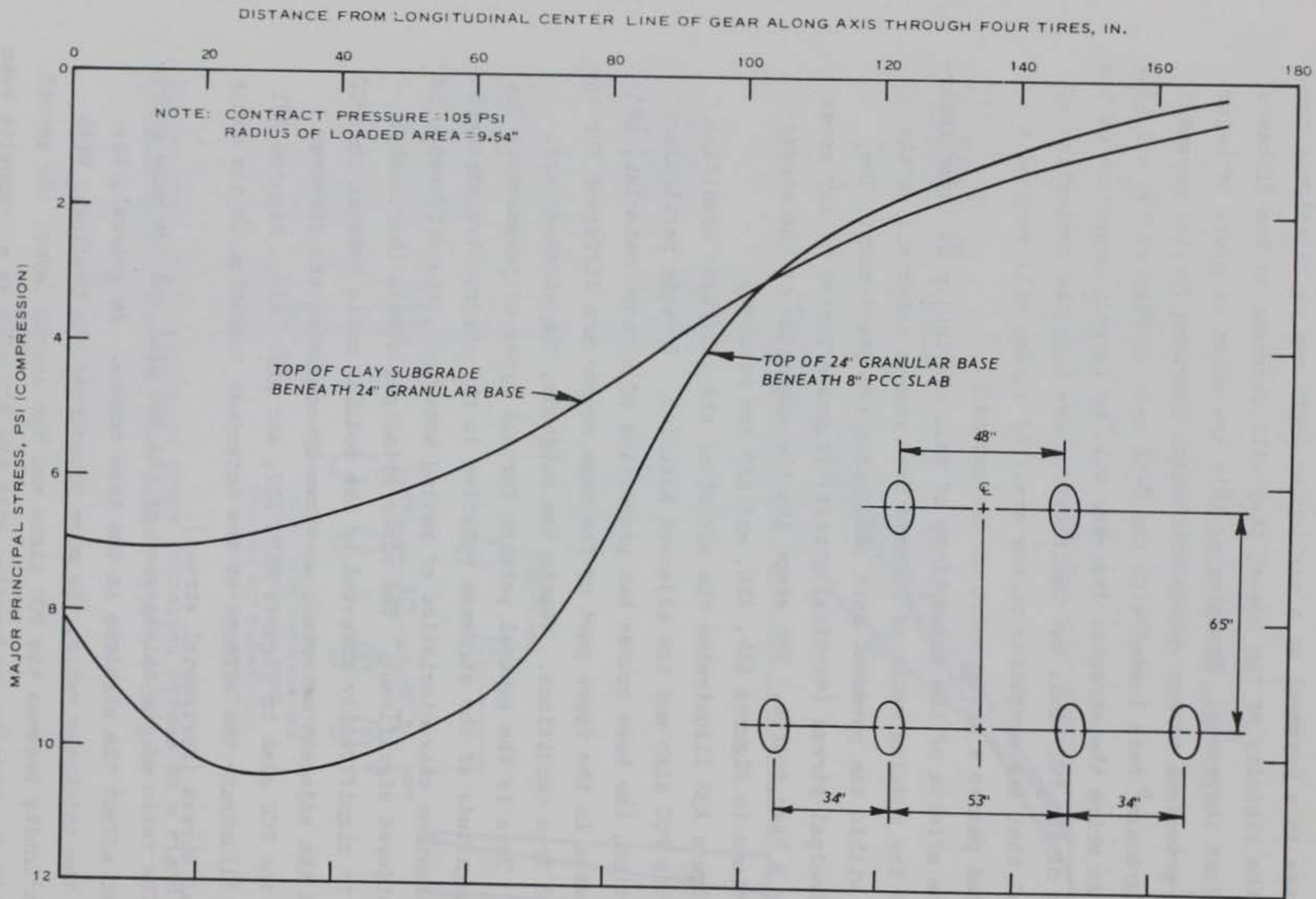


Figure A30. Variation of major principal stress at the top of the granular base and at the top of the subgrade



A-49

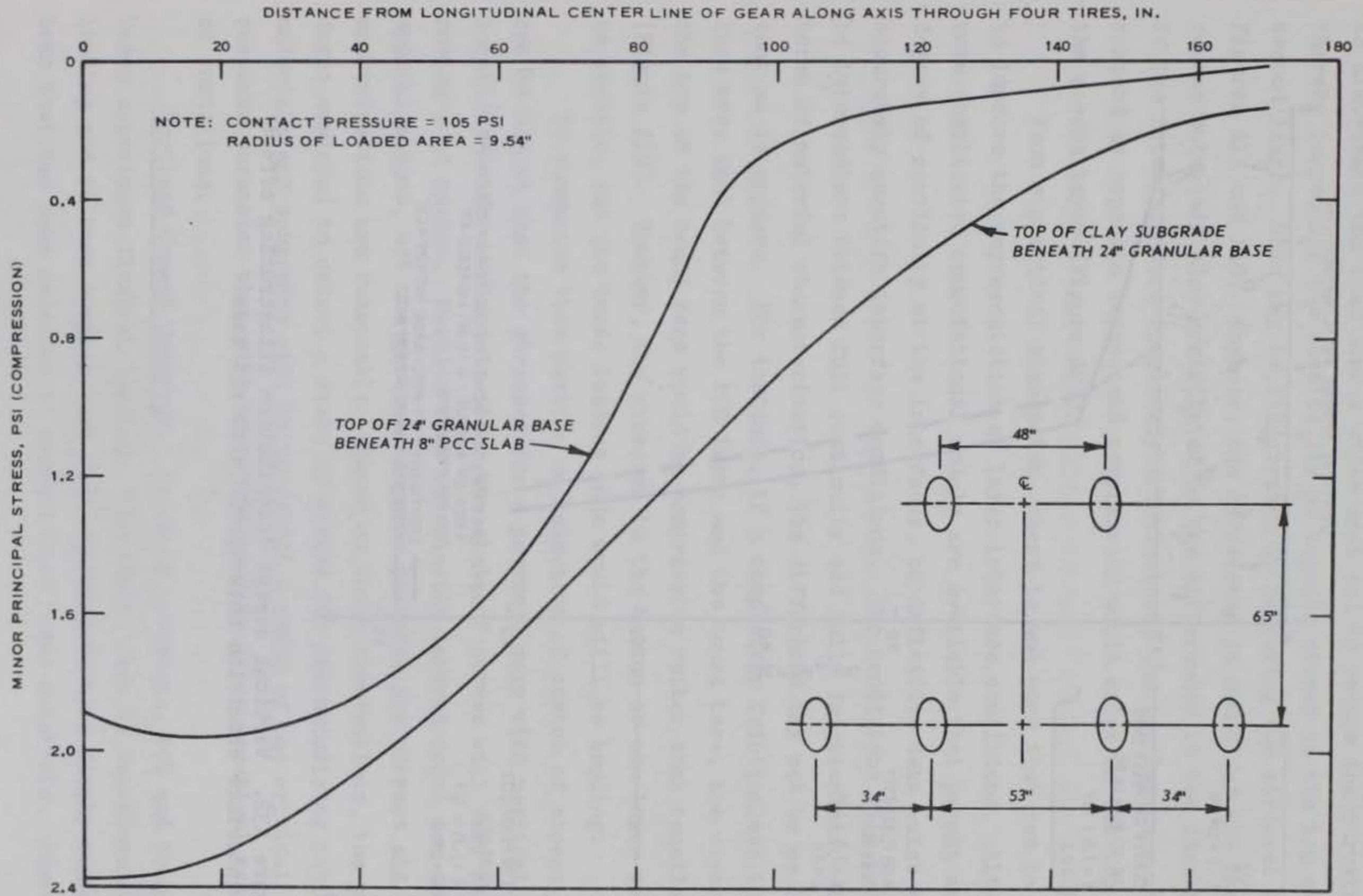


Figure A31. Variation of minor principal stress at the top of the granular base and at the top of the subgrade

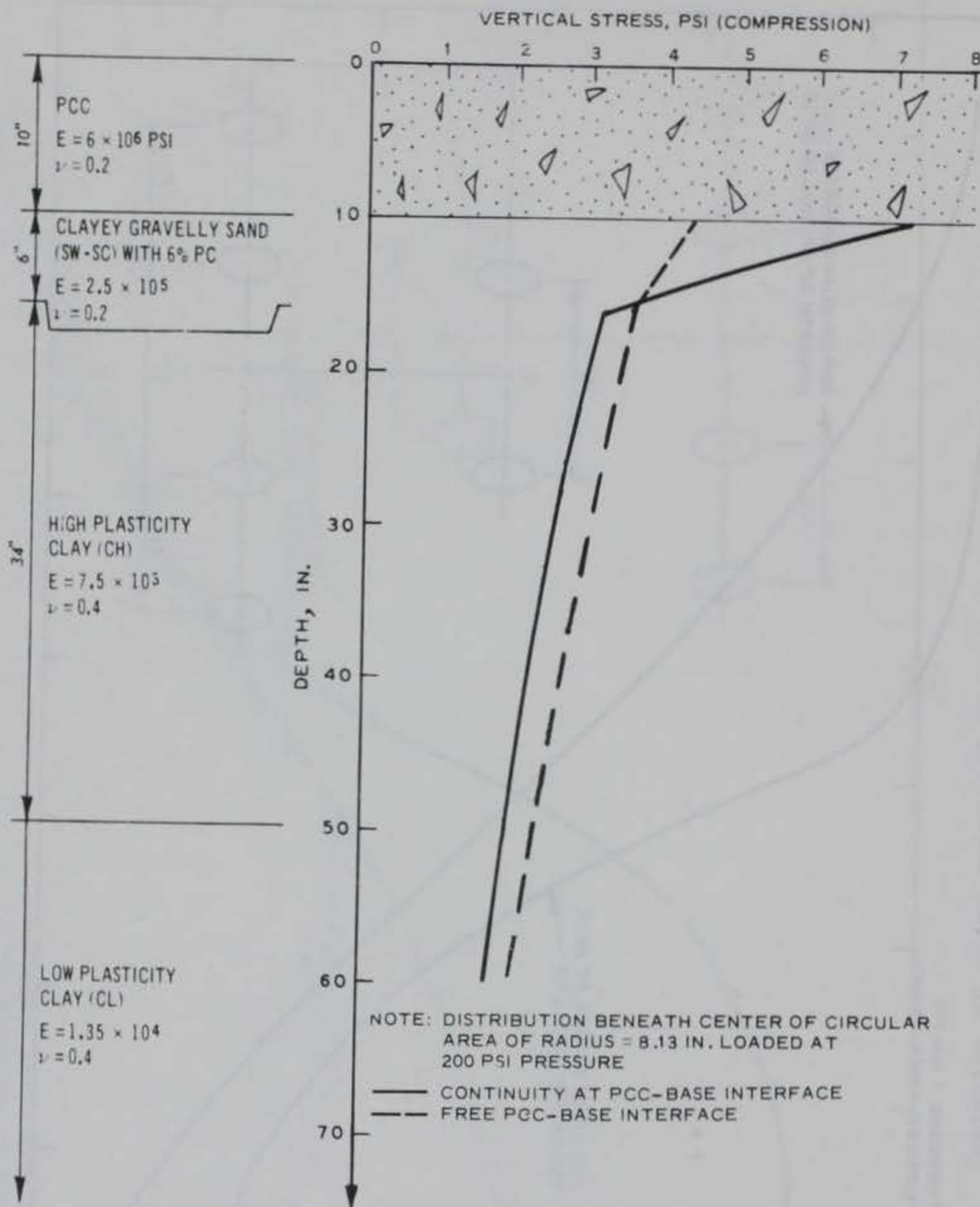


Figure A32. Vertical stress distribution illustrating effect of interface condition between PCC slab and base



to distribute the load over a wider area and to reduce the curvature, thereby increasing the possibility of tensile stress in the top of the second layer. This may be illustrated by comparing the stresses in Figures A17 and A19. However, the difference in moduli of the base course materials also contributed to the differences in the distributions. If the interface were completely frictionless, the two layers would respond as separate layers and compression would exist in the top of the second layer (Figure A23).

From a practical standpoint, there is not much that can be done to improve the representation of layer interface conditions. Although more complicated computational models are available that permit any degree of continuity at the interfaces, no definitive data exist to accurately quantify interface conditions. The conditions will probably be intermediate between full continuity and fully frictionless. In terms of material characterization, the difference may not be as important as it appears. For instance, if a completely frictionless interface were used between the PCC layer and the bound base, the stress in the top of the bound base would be compressive rather than tensile (Figure A19). However, the stresses in the bottom of the layer would be tensile, and the basic loading mode would still be bending.

To summarize this section on selection of states of stress, it can be stated that the stresses for a pavement vary with vertical location, or for a fixed location the state of stress will vary as a moving load passes. Results from the elastic layered model are only approximations, but the general response patterns are correct and the approximations are reasonable. Based on these observations, the procedures employed to select a state of stress for characterizing paving materials and subgrades will be to select a value of the critical response parameter that will be representative for a practical range of conditions.

Portland Cement Concrete. In rigid pavements, PCC and bound bases experience flexural loading. Certainly, this is two-dimensional loading and is more complex than that experienced by a simply supported beam that has been selected to characterize these materials. However,



of the types of tests available, the flexural tests were considered the most practical and usable.

There are several discrepancies between the state of stress in a PCC slab or a bound base layer and a simply supported beam that is tested to characterize the material. In a beam, a plane stress condition exists, whereas in a pavement slab, the stresses are three-dimensional (if the vertical stresses are considered). Certainly, the horizontal components of stress due to the bending are the largest components of stress, but the vertical support provided by the underlying material affects the response of the slabs. Forrest, Katona, and Griffin,<sup>61</sup> recognizing that the conditions in a slab are different from those in a beam, have suggested a series of tests to better define these differences. Because of differences in the deformed shape of slabs, they suggest that strain in the slab rather than stress may be the critical parameter. Nevertheless, the use of a flexural test on a simply supported unconfined beam loaded with essentially point loads was considered adequate for determining the modulus of elasticity and strength of PCC.

Bound Bases (Subbases). The same type test is used to characterize bound bases, although the conditions may be less representative than for PCC slabs. The vertical stresses will be distributed over the top and bottom of the layer, rather than just on the bottom as it is for the PCC surface layer. Certainly, stresses in the bound layer will be different from those in a simply supported beam loaded with essentially point loads. The shape the bound base layer takes may also be much different. In a simply supported beam, there will be compressive bending stresses in the top of the beam, but in the bound base layer, there may be tensile stresses throughout the layer. This results from the composite action of the PCC slab and base (Figures A19 and A25). The magnitude of the stresses will depend on the bond between the PCC and bound base layers and the modulus ratios between the two layers. However, the general trend is that the loaded and support conditions result in stress conditions different from those for a simply supported beam.



For the test pavements (described in Appendix B) that have contained bound base layers, there is no apparent relationship between the state of stress and the traffic that the pavement will sustain. Figure A33 shows a plot of minor principal stress directly below the PCC slabs versus the traffic level at failure, and Figure A34 shows the minimum first stress invariant plotted versus the traffic level at failure in the layer directly beneath the PCC slab for the test pavements described in Appendix B. In the pavements with no base, the stress would be in the top of the subgrade, and in the pavements with bases (bound or granular), the stress would be in the top of the base layer. The open circles are for pavements with bound bases, and no relationship with traffic is apparent in either figure.

Another interesting aspect of Figures A33 and A34 is the difference between the pavements with bound bases and those with granular or no bases. The stresses were computed with layered elastic theory that assumes full continuity between layers. The moduli for the bound base materials were larger than those for the granular base materials, which were in turn larger than the subgrade. The three distinct groupings of data are thought to be a result of the effects of the assumption of full continuity and modulus ratio between the PCC and the second material. Nevertheless, the general trend, indicating that the basic loading mode in the bound base layer was flexural, is valid. This is indicated by the fact that the minor principal stresses (horizontal stress essentially) and the first stress invariants are both tensile, whereas for the pavements with no base or granular bases, the values are compressive. This condition is representative for a large area in the base layer since the average values for the several computational points (as illustrated on the sketches in Figures A14-A29) are approximately equal to the minimum, or maximum, as the case may be, value. As an example, consider the six pavements with bound bases. If the minimum first stress invariant is selected from the stresses computed at the locations shown in Figures A14-A29, then the average of these values is -17.71 psi; whereas, if values from all computational points are used, the average is -16.12 psi. For the minor





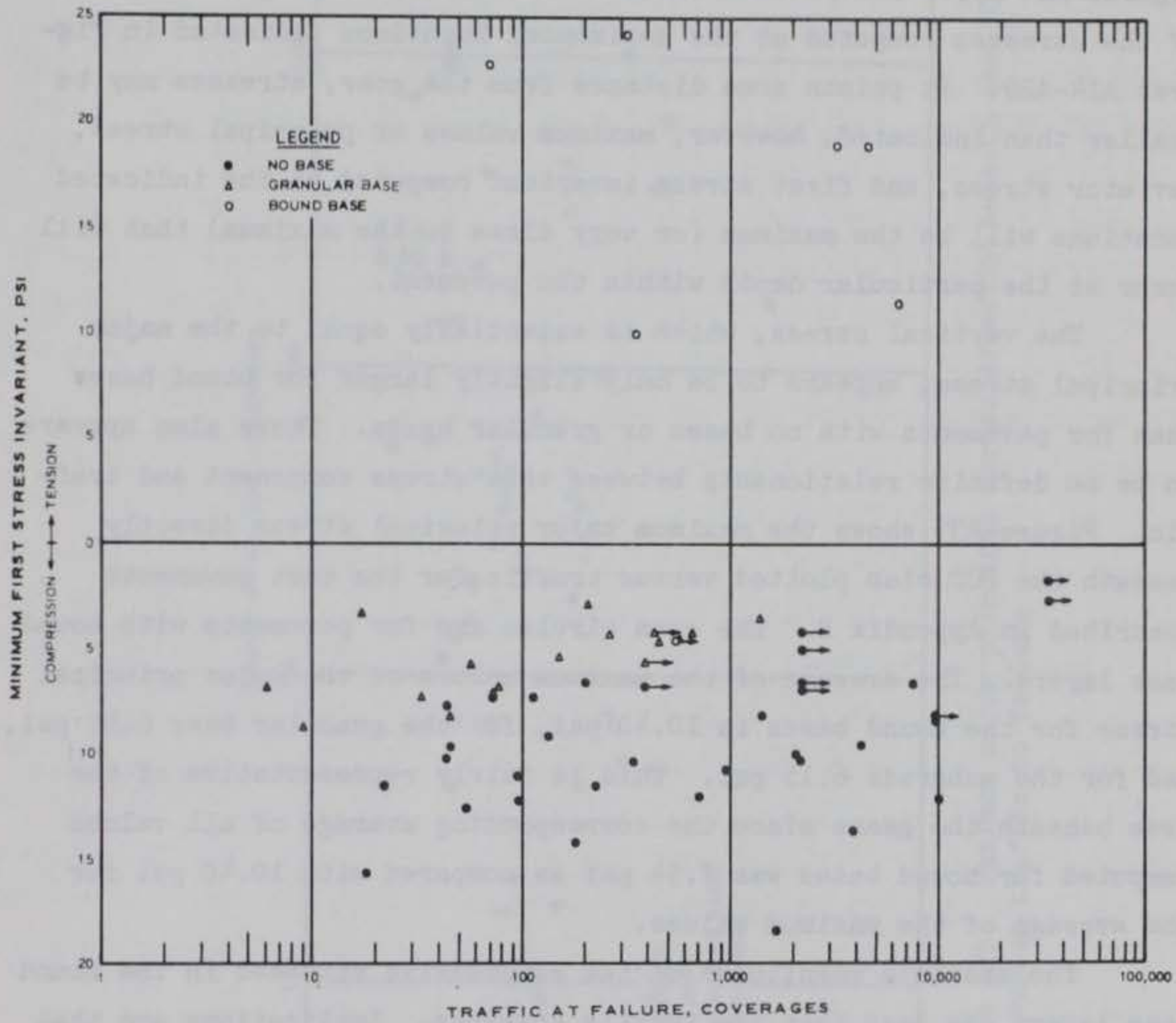


Figure A34. Minimum first stress invariant directly beneath the PCC slab versus traffic to failure

principal stress, the average of the minimum values is -15.81 psi, and the average of all values is -13.32 psi.

The references to minimum values of minor principal stress and first stress invariant are not actually correct. These stresses should be referred to as the minimum values within the area bounded by the wheel loads of a gear. Stresses were computed at the locations shown in Figures A14-A29. The minimum values referred to herein are the minimum of the stresses computed at the horizontal locations indicated in Figures A14-A29. At points some distance from the gear, stresses may be smaller than indicated; however, maximum values of principal stress, deviator stress, and first stress invariant computed at the indicated locations will be the maximum (or very close to the maximum) that will occur at the particular depth within the pavement.

The vertical stress, which is essentially equal to the major principal stress, appears to be only slightly larger for bound bases than for pavements with no bases or granular bases. There also appears to be no definite relationship between this stress component and traffic. Figure A35 shows the maximum major principal stress directly beneath the PCC slab plotted versus traffic for the test pavements described in Appendix B. The open circles are for pavements with bound base layers. The average of the maximum values of the major principal stress for the bound bases is 10.40 psi, for the granular base 6.87 psi, and for the subgrade 6.15 psi. This is fairly representative of the area beneath the gears since the corresponding average of all values computed for bound bases was 7.54 psi as compared with 10.40 psi for the average of the maximum values.

The absolute magnitudes of the compressive stresses in the bound base layers are less than the tensile stresses. Implications are that the flexural tests are more appropriate for bound bases than a compression test.

A simply supported unconfined beam loaded at the third point with essentially point loads is recommended for PCC and bound bases (sub-bases). For PCC, the beam is loaded to failure to determine the flexural strength, and the modulus of elasticity is computed from the



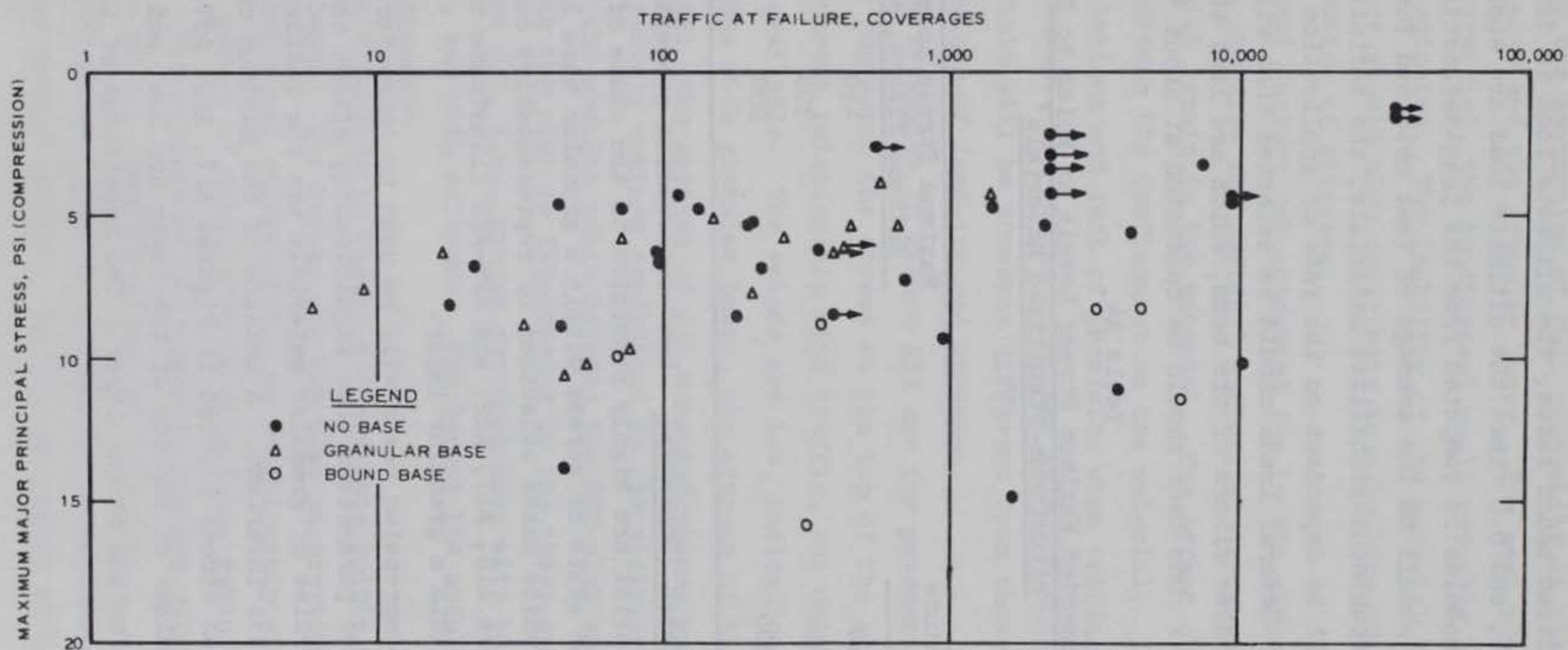


Figure A35. Maximum major principal stress directly beneath the PCC slab versus traffic to failure

slope of the straight-line portion of the load-deflection curve. For chemically stabilized bound bases, the ultimate load is determined, loads of 0.4, 0.6, and 0.8 times the ultimate load are applied repetitively, and the modulus is computed from the load-deflection curves. The modulus used should be the average of that obtained for the three loadings. For bituminous-stabilized materials, the definition of an ultimate load will be dependent on the rate of application of load and the temperature. Several loads should be selected that will result in stresses in the outer fibers of the beam, which are less than the values shown in Table A4. One test should be conducted at about 50 psi.

Table A4

Recommended Maximum Stress Levels at Which to Test  
Bituminous-Stabilized Materials

<u>Temperature</u> <u>Range, °F</u>	<u>Maximum Stress Level in</u> <u>Extreme Fibers, psi</u>
40-60	450
60-80	300
80-100	200

Granular Bases (Subbases). Load-deformation properties of granular base material are highly sensitive to the state of stress. Unfortunately, the state of stress within a granular base layer is also highly variable, which makes selection of representative conditions difficult. Figures A16, A17, A22, and A26-A29 illustrate the distribution of stress within a granular layer.

Triaxial compression tests will be used to characterize granular materials. The two parameters that significantly affect the load-deformation properties of granular materials are the confining pressure and the first stress invariant. A measure of the minimum confinement is the minor principal stress plotted in Figures A17, A22, A27, and A29. The compressive values at the top of the layer are low, and the tensile values are at the bottom of the layer. The magnitudes of these stresses



are affected by the assumption of full continuity at the interface between the PCC slab and the granular layer. For real conditions where some slip is permitted, the confinement would probably be somewhat greater than indicated. The inability of the material to sustain tensile stresses should also contribute to a buildup of confinement by a redistribution of stresses.

Additional factors not accounted for in the stress computations are overburden stresses and residual horizontal stresses, induced during compaction, which remain in the material. The effect of these stresses would be to increase the confinement on the material. There are also equipment limitations and lack of precision when testing at low stress levels. As a result, the states of stress selected for characterizing granular materials will be somewhat different from those indicated by the computed values of load-induced stresses.

The open triangles in Figure A33 are for pavements with granular bases and thus represent the stress at the top of the granular layer. There is no apparent relationship with traffic, but only a limited range of traffic is available. The values are low, indicating low confinement. For the pavements with granular bases, the average of the minimum values was only 0.38 psi (the average of all computed values was 0.50 psi, indicating relatively uniform conditions in the vicinity of the load). The effects of the modulus ratio between the PCC slab and the material directly beneath the slab is illustrated by the three groupings of the points in Figure A33, i.e., groups for pavements with bound bases, with granular bases, and with no bases. The larger the modulus ratio, the larger the confinement.

The open triangles in Figure A34 are data points for pavements with granular bases. The trends are the same as previously discussed for the minor principal stress, i.e., no relationship with traffic, three distinct groups of data, effects of modulus ratio, and uniformity beneath loads. The average of the computed minimum values is 5.96 psi, and the average of all computed values is 7.33 psi.

Figure A35 shows a plot of maximum major principal (essentially vertical) stress versus traffic. For the pavements with granular bases,



there is no apparent relationship with traffic. In addition, there is not much difference between the three types of sections, although the points for bound bases, denoted by the open circles, are higher than for the other two conditions. The average of the maximum values of major principal stress for the pavements with no base was 6.15 psi, for pavements with granular base 6.87 psi, and for pavements with bound bases 10.40 psi.

For characterizing granular bases, triaxial compression tests should be conducted at confining pressures of 2, 4, 6, and 10 psi. Axial stresses should be applied that result in ratios with confining stresses ( $\sigma_1/\sigma_3$ ) of 2, 3, 4, and 5. Plots of resilient modulus versus first stress invariant, similar to the plot shown in Figure A28, should be prepared and an average relationship established. From this relationship, a value of resilient modulus at a first stress invariant of 10 psi should be selected.

No well-defined relationships exist for Poisson's ratio. However, plots of Poisson's ratio versus ratio of axial to confining stress ( $\sigma_1/\sigma_3$ ) should be made, and representative values selected.

#### SUBGRADE SOILS

Subgrade soils beneath rigid pavements are subjected primarily to compressive stresses. Figures A14-A19 illustrate the distribution of major and minor principal stresses in the subgrade of rigid pavements with no base, with a granular base layer, and with a bound base layer. The stresses within the subgrade are always compressive.

Cohesive soils, which will be the predominate type encountered, are sensitive to the deviator stress, i.e., the difference between the major and minor principal stress. Figure A20 contains distributions of deviator stress with depth for a PCC slab directly on a subgrade loaded with a dual-tandem gear. Differences between the major (Figures A16 and A18) and the minor principal stresses (Figures A17 and A19) in the subgrade for pavements with granular and bound bases are similar to those shown in Figure A20.

Cohesionless subgrade soils are similar to granular base material



in that they will be sensitive to the confining stress and the total state of stress as represented by the first stress invariant. Figures A15, A17, A19, A27, and A29 show distributions of the minor principal stress in the subgrade for the three types of pavements considered. Considering that the loads are applied vertically and that the major principal stresses act essentially in the vertical direction, the minor principal stresses that act essentially in the horizontal direction are confining stresses. Within the subgrade, the values are always compressive but are small in magnitude. Distribution of the first stress invariant is shown in Figures A22 and A25, respectively, for the pavements with granular and bound bases. Within the subgrade, the values of the first stress invariant indicate that the loading is essentially compressive.

The distributions shown were computed with material properties of the subgrade obtained from tests on the cohesive subgrade soils. The modulus of elasticity would probably be higher for cohesionless soils than for cohesive soils, and the Poisson's ratio would be lower. However, the general trends illustrated by the computations, i.e., low compressive confining stresses and compressive first stress invariants, should be applicable to cohesionless subgrade soils.

Triaxial compression tests will be used to characterize subgrade soils. The deviator stress in the triaxial tests will be the difference between axial stress applied to the specimen and the confining pressure in the triaxial chamber. For cohesive soils, this should approximate as closely as possible conditions in the subgrade. The maximum deviator stress is considered appropriate for characterizing cohesive materials, since the general trends indicated in Figures A2 and A3 have been found to hold for a wide range of materials, i.e., the resilient modulus decreases as deviator stress increases.

The maximum deviator stress at the top of the subgrade versus the traffic to failure in Figure A36 applies to the test pavements described in Appendix B. There are no apparent relationships with traffic and no easily discernible differences between pavements without bases, with granular bases, or with bound bases. The average value for pavements

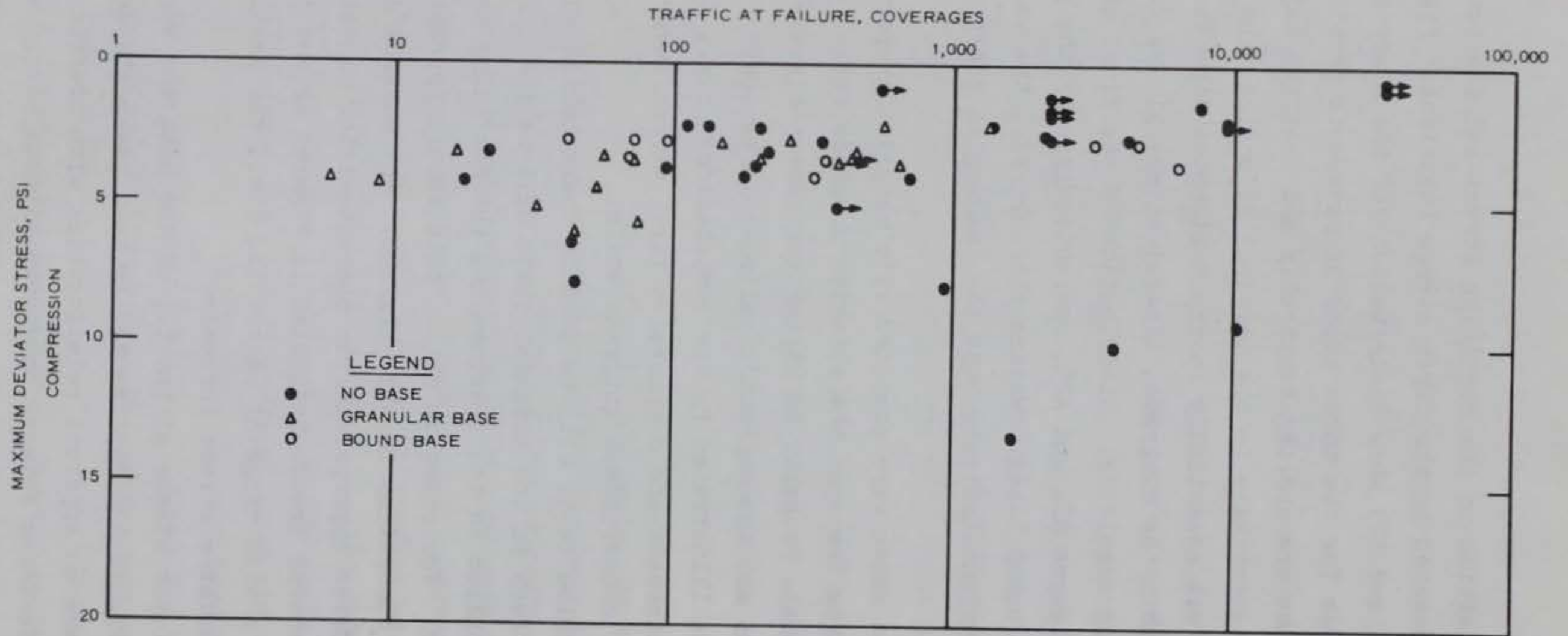


Figure A36. Maximum deviator stress at the top of the subgrade versus traffic to failure



without bases is 3.69 psi, with granular bases, 3.79 psi, and with bound bases, 3.46 psi; the overall average is 3.70 psi. Stresses due to the overburden and residual stresses remaining after compaction were not considered in the computation of these stresses.

For characterizing cohesive materials, the triaxial tests should be conducted at a range of stress conditions and a composite curve established in Figures A2 and A3. Tests should be conducted at confining stresses of 2, 4, and 6 psi, and at axial stresses applied that will result in a range of deviator stress from about 2 to 16 psi. From the composite curve, the resilient modulus used to represent the material should be selected at a deviator stress of 5 psi. No well-defined relationships exist for Poisson's ratio, but similar plots should be made and a representative value selected.

For cohesionless soils, the confining stress in the triaxial tests should approximate conditions in the subgrade. The minor principal stress in the subgrade is a measure of the confinement. For cohesionless subgrade soils, it is considered appropriate to select properties at minimum values of the first stress invariant and confining stress, since the general trends illustrated in Figures A12 and A13 are applicable for cohesionless subgrade soils, i.e., as the confining stress and the first stress invariant decreases, the resilient modulus decreases.

The minor principal stress and minimum first stress invariant at the top of the subgrade versus the traffic to failure in Figures A37 and A38, respectively, apply to the test pavements described in Appendix B. As previously noted, these are the minimum values in the vicinity of the load or loads, and smaller values (in fact, zero) will exist at locations far removed from the loads. There are no obvious relationships with traffic for either of the parameters. There are some apparent differences in the stresses for the different type pavements. The average of the minor principal stress at the top of the subgrade is 1.99 psi for pavements with no base, 1.25 psi for pavements with granular bases, and 2.54 psi for pavements with bound bases. The overall average is 1.82 psi. The average of the minimum first stress

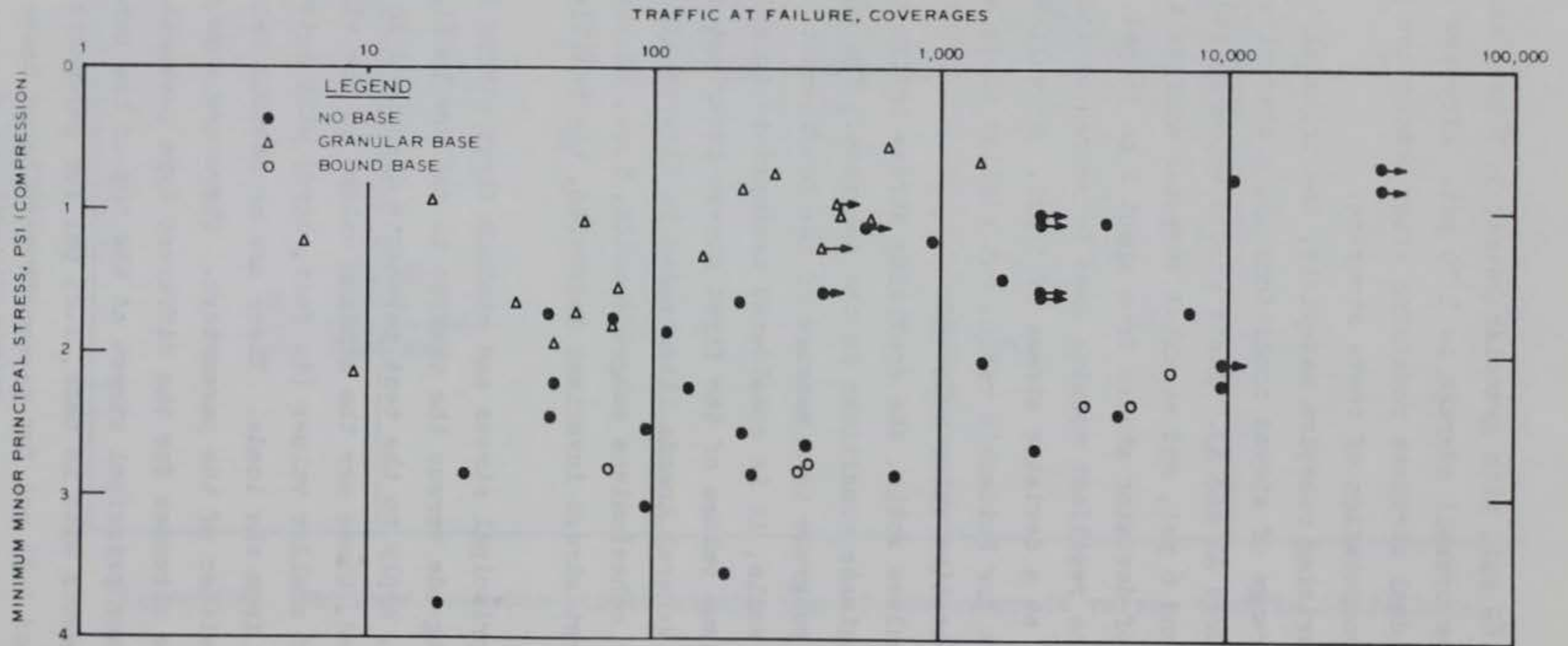


Figure A37. Minimum minor principal stress at the top of the subgrade versus traffic at failure



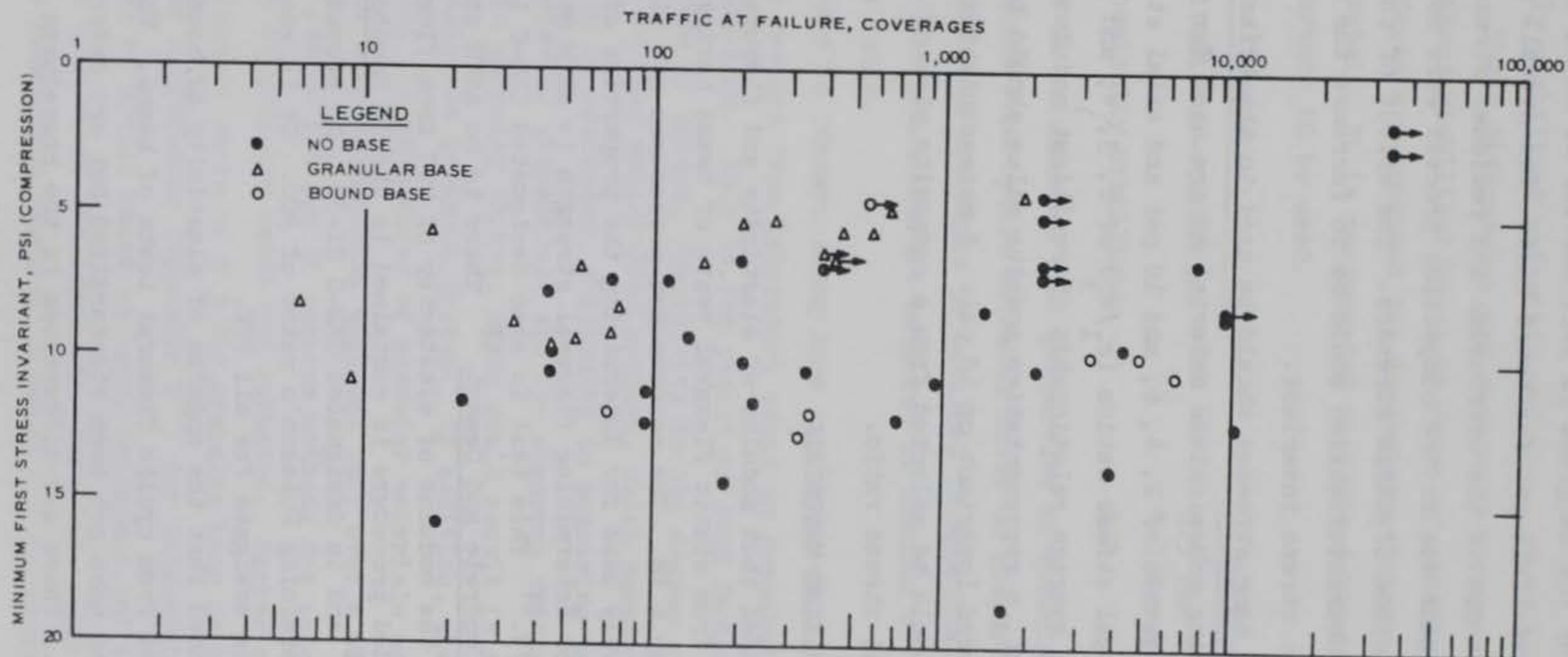


Figure A38. Minimum first stress invariant at the top of the subgrade versus traffic at failure

invariant at the top of the subgrade is 9.27 psi for no base, 6.59 psi for granular bases, and 11.15 psi for bound base. The overall average is 8.63 psi. Stresses due to the overburden and residual stresses that may exist in the subgrade due to the compaction process were not considered in the computation of these stresses. The effect of these stresses on material characterization would be to increase the confinement and the first stress invariant.

Basically, the same stresses should be used in the triaxial tests for characterizing cohesionless material as are used for granular bases. Confining pressures of 2, 4, 6, and 10 psi and axial stresses that result in principal stress ratios ( $\sigma_1/\sigma_3$ ) of 2, 3, 4, and 5 should be applied. From the average relationship of resilient modulus versus first stress invariant, a representative modulus value should be selected at a first stress invariant of 10 psi. A representative value of Poisson's ratio should be selected from a composite plot of Poisson's ratio versus principal stress ratio.

#### SUMMARY FOR CHARACTERIZING MATERIALS

It is recommended that modulus of elasticity and flexural strength of PCC be determined from static flexural tests of beams having a cross-sectional area of 6 by 6 in. The recommended procedures are widely accepted and extensively used for determining the properties of PCC. The test procedure for determining flexural strength is ASTM Standard Method of Test C 78-75.<sup>57</sup> This test is also designated CRD-C 16-66 in the CE Handbook for Concrete and Cement.<sup>56</sup> There is no ASTM standard test for determining the modulus of elasticity of PCC from flexural tests. The recommended procedure is contained in the CE Handbook for Concrete and Cement<sup>56</sup> and is designated CRD-C 21-58. No procedures are provided for determining Poisson's ratio of PCC. It is recommended that a value of 0.2 be assigned for all PCC.

It is recommended that the modulus of elasticity of bound base material be determined from cyclic flexural tests of beams. The recommended test procedures have not been standardized but are described in detail in Appendix C. There are differences in the procedures for



chemically stabilized materials and those stabilized with bituminous binders. These differences are necessary because of the sensitivity of bituminous-stabilized bases to rates of loading and temperature. No procedures are provided for determining Poisson's ratio of bound base material. It is recommended that the following values extracted from Reference 10 be used.

<u>Material</u>	<u>Poisson's Ratio</u>
Bituminous-stabilized	0.5 for E < 500,000 psi 0.3 for E > 500,000 psi
Chemically stabilized	0.2

It is recommended that properties of granular bases (subbases) be determined from cyclic triaxial tests on prepared samples. The recommended test procedure is outlined in Appendix D. The outputs from the test procedure are measures of modulus of elasticity and Poisson's ratio.

There is concern among some engineers as to the accuracy with which the results from laboratory tests on granular materials represent field conditions. This is the result of such factors as the sensitivity to the state of stress, sensitivity to the degree of compaction, inability to take undisturbed samples, which necessitates laboratory preparation of specimens, difficulty in measuring parameters needed to compute material properties, and the apparent existence of tensile stresses in granular layers, which would result in redistributions of stress within the pavement system. In addition, there is also the feeling that the properties of granular materials meeting requirements for base or subbase material will not vary over a wide range. These factors have led to the use of various methods for selecting representative properties of granular bases and subbases. Barker and Brabston recommend a Poisson's ratio of 0.3 for granular base or subbase materials and provide a procedure (Appendix G<sup>10</sup>) for determining representative values of moduli based on layer thickness and the modulus of the foundation upon which the layer was compacted. This procedure appears to produce reasonable results. However, it is recommended that it be



used in conjunction with test results to determine a representative modulus rather than as the sole method. The use of a value for Poisson's ratio of 0.3 is acceptable unless there is reason to believe that it is significantly different for the material in question.

It is recommended that the modulus of elasticity and Poisson's ratio of subgrade soils be determined from cyclic triaxial tests on undisturbed samples when possible or on samples prepared as close as possible to field conditions when fill is involved. The recommended test procedures are outlined in Appendix E. The procedures are similar to those used for granular base (subbase) materials. There are differences in details of the test procedures and presentation of results for cohesive and cohesionless materials. These differences are necessary because of the sensitivity of cohesive soils to moisture and the differences in the behavior as a function of the state of stress. As with other materials, determination of a representative Poisson's ratio is difficult, and the values of 0.4 for cohesive and 0.3 for cohesionless materials suggested by Barker and Brabston<sup>10</sup> may be used if test results prove unreliable.



## APPENDIX B: DESCRIPTION OF TEST PAVEMENTS

The pavements described herein were part of eight test tracks. These test tracks will be referred to as Lockbourne No. 1, Lockbourne No. 2, Lockbourne No. 3, Sharonville Channelized Traffic, Sharonville Heavy Load, Multiple-Wheel Heavy Gear Load (MWHGL), Keyed Longitudinal Joint Study (KLJS), and Soil Stabilization Pavement Study (SSPS). The pavements were constructed and tested by the U. S. Army Corps of Engineers during the period from 1943 to 1973. The pavements were constructed under controlled conditions, and simulated aircraft traffic was applied in an accelerated manner.

### LOCKBOURNE NO. 1

The Lockbourne No. 1 Test Track was constructed between August and November 1943 at the Lockbourne Army Air Base near Columbus, Ohio. The construction, testing, and analyses of the data from this test track are discussed in References 40-42. This test track had two continuous traffic lanes 20 ft wide, composed of adjacent 20- by 20-ft slabs. The concrete test slabs varied in thicknesses from 5 to 10 in. and were placed with and without base courses. The type base material varied and the thickness ranged from 6 to 12 in. Transition slabs between the traffic slabs and turnaround sections at each end combined to form a continuous track, which was subjected to single-wheel loadings of 20, 37, and 60 kips. Between 5 June and 10 July 1944 some sections of the test track were reconstructed due to early failure caused by the traffic loading tests.

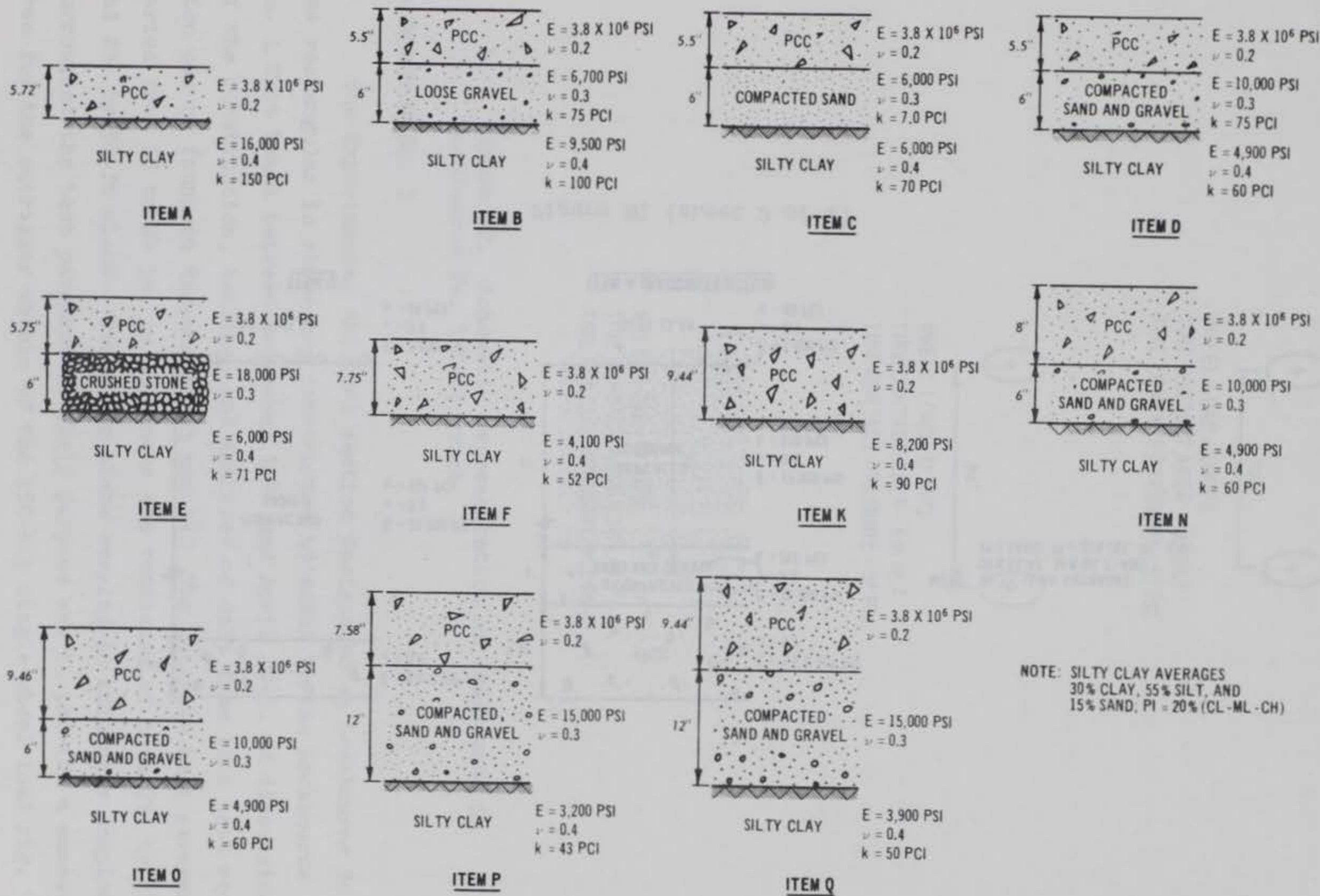
Table B1 summarizes the flexural strength of the PCC concrete and the traffic applied to each pavement. Figure B1 illustrates the properties of the pavements used in this study; Figure B2, the loads used to traffic the test pavements. The two tires in Figure B2 were on one axle of the load cart but were far enough apart so that the overlap in zones of influence was small.

Table B1

Summary of Load, PCC Flexural Strength, and  
Traffic--Lockbourne No. 1 Test Track

<u>Item</u>	<u>Load, kips</u>	<u>Flexural Strength psi</u>	<u>Traffic Coverages</u>	<u>Remarks</u>
A	20	740	390+	First crack
A	37	780	45	First crack
B	20	740	187	First crack
B	37	780	35	First crack
C	20	740	200	First crack
C	37	780	44	First crack
D	20	740	450	First crack
D	37	780	33	First crack
E	20	740	430+	First crack
E	37	780	77	First crack
F	20	740	550+	No failures
F	37	780	111	First crack
K	37	780	700	First crack
K	60	735	72	First crack
N	37	780	150	First crack
N	60	735	9	First crack
O	37	780	573	First crack
O	60	735	72	First crack
P	37	780	262	First crack
P	60	735	6	First crack
Q	37	780	1390	First crack
Q	60	735	57	First crack
U	37	780	88	First crack
U	60	735	1.5	First crack
A (Reonstr)	37	725	658	First crack





B-3

Figure B1. Description of test pavements in Lockbourne No. 1 Test Track (sheet 1 of 2)

B-4

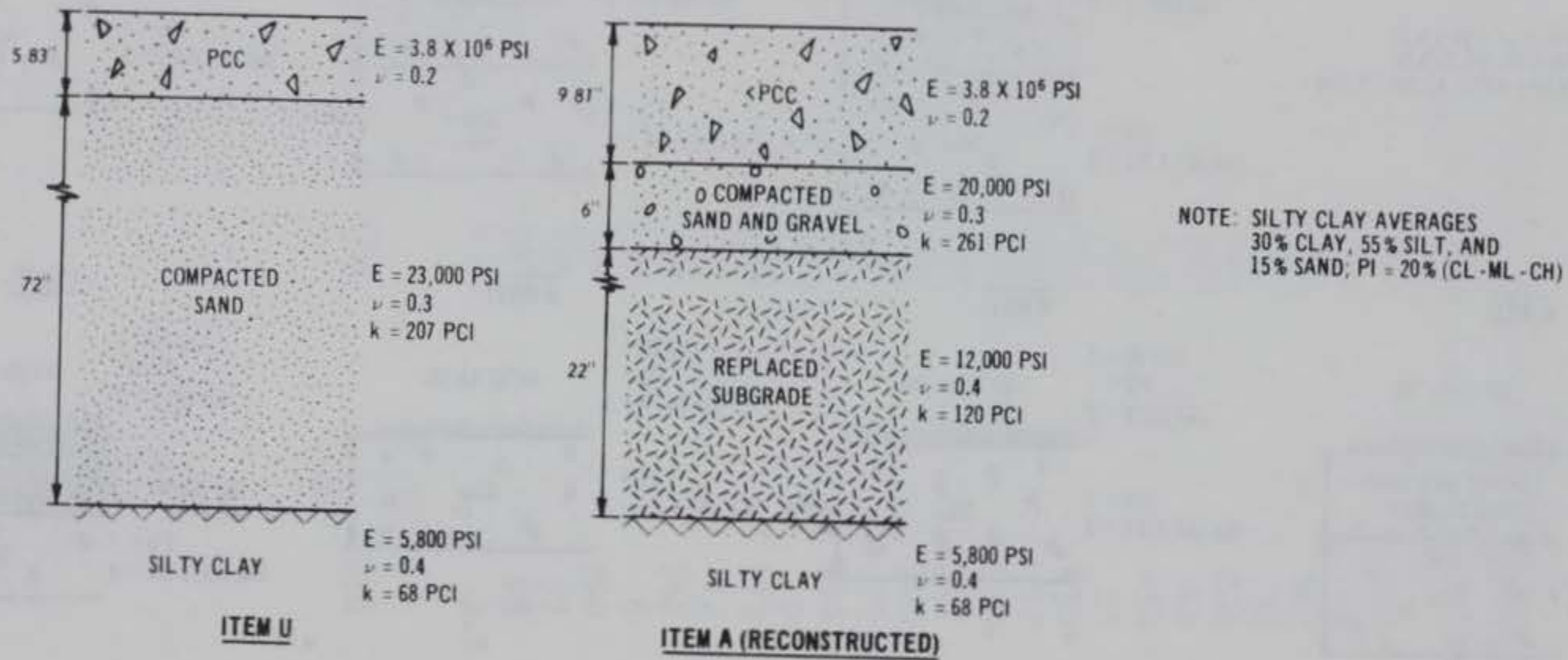


Figure B1 (sheet 2 of 2)



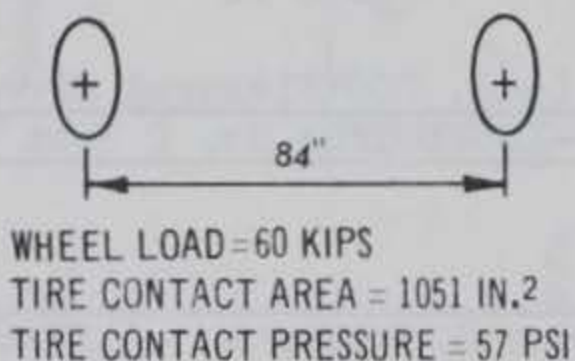
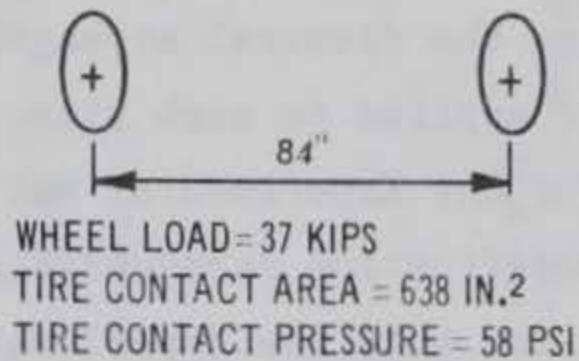
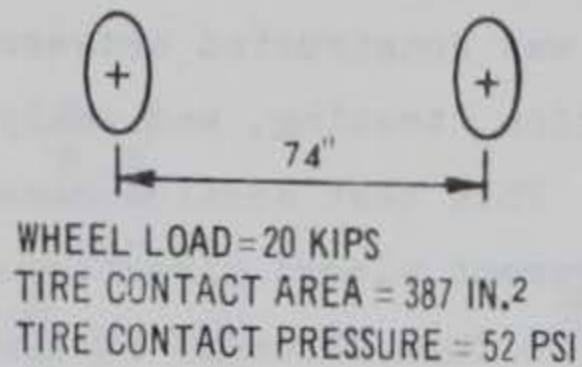


Figure B2. Schematic representation of loads used in Lockbourne No. 1 Test Track

#### LOCKBOURNE NO. 2

The Experimental Mat test section designated as Lockbourne No. 2 was rectangular in shape and constructed adjacent to the Lockbourne No. 1 Test Track between September 1944 and April 1945. A discussion of the construction, testing, and analyses of data from this test section can be found in References 43 and 44. The concrete test pavements varied from 15 to 24 in. in thickness and consisted of both 25- by 25- and 25- by 50-ft slabs. Perimeter slabs varying in thickness completely surrounded the test pavements. Their purpose was to provide a maneuver area for the outrigger wheels of the 150-kip single-wheel load rig.

The Lockbourne No. 2 Modification test section was an extension of the Experimental Mat and was constructed between August and October 1946. A discussion of construction, testing, and analyses of data can be found in References 45 and 46. This test section consisted of 12-, 15-, and 20-in. plain concrete pavement placed directly on the subgrade. The test slabs were arranged to form three 25-ft lanes with transition slabs separating the three design thicknesses. Traffic was applied with a special loading device that produced a 150-kip load on four wheels.

Table B2 summarizes the flexural strengths of the concrete test pavements and the traffic applied to each item. The pavement properties used in this study are for the Experimental Mat section (Figure B3) and for the Multiple-Wheel Modification section (Figure B4). The load assembly in Figure B5 is for both the Experimental Mat and the Modification sections.

Table B2

Summary of Load, PCC Flexural Strength, and  
Traffic--Lockbourne No. 2 Test Track

<u>Item</u>	<u>Load, kips</u>	<u>Flexural Strength</u> <u>psi</u>	<u>Traffic</u> <u>Coverages</u>	<u>Remarks</u>
E1	150	725	97	First crack
E2	150	680	942	First crack
E3	150	710	17	First crack
E4	150	680	203	First crack
E5	150	695	43	First crack
E6	150	700	2204+	No failure
E7	150	760	2204+	No failure
M1	150	725	134	First crack
M2	150	725	2204+	No failure
M3	150	725	2204+	No failure

Note: Items E1-E7 (Experimental Mat) loaded with single wheel.  
Items M1-M3 (Modification) loaded with dual-tandem gear.



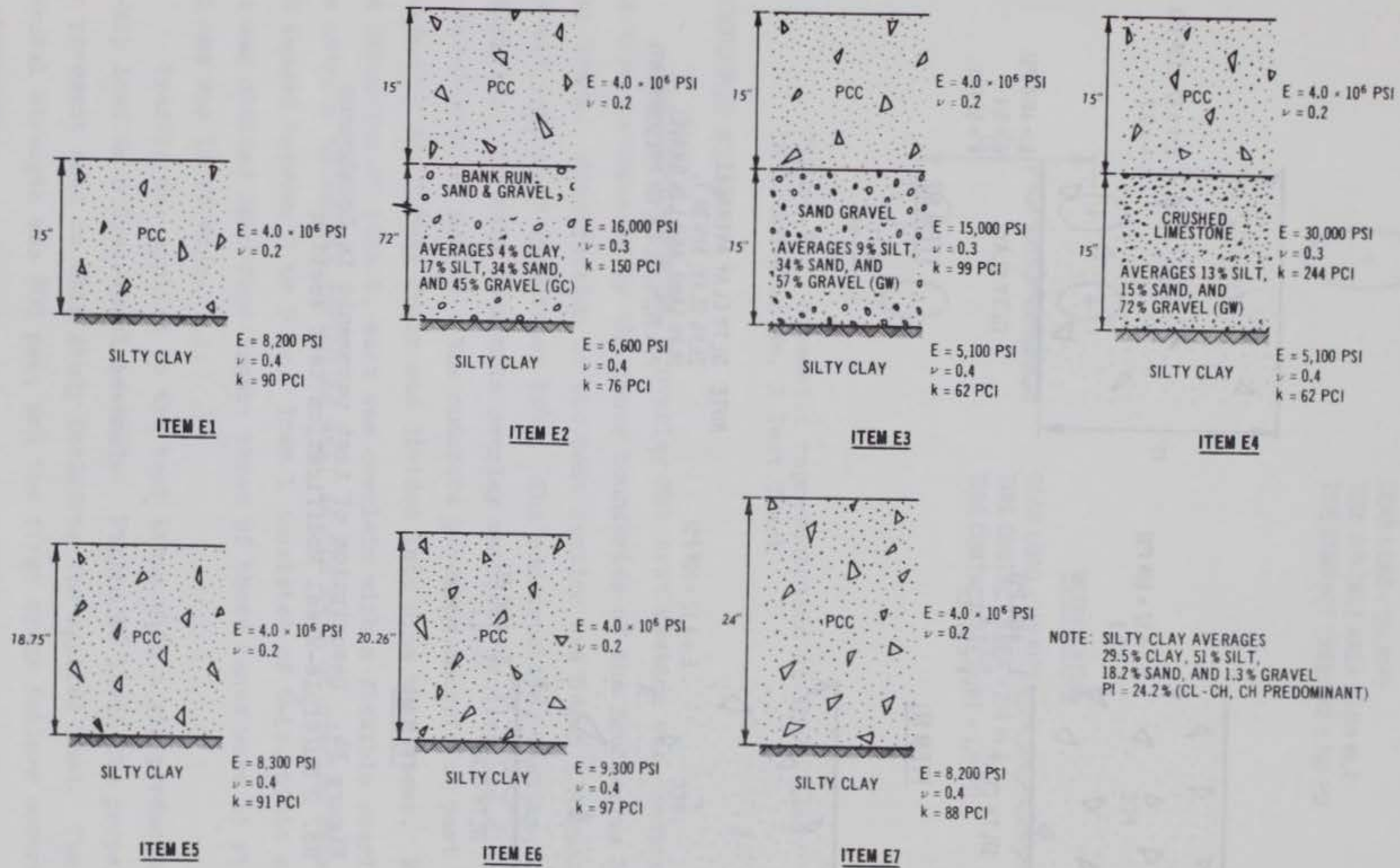
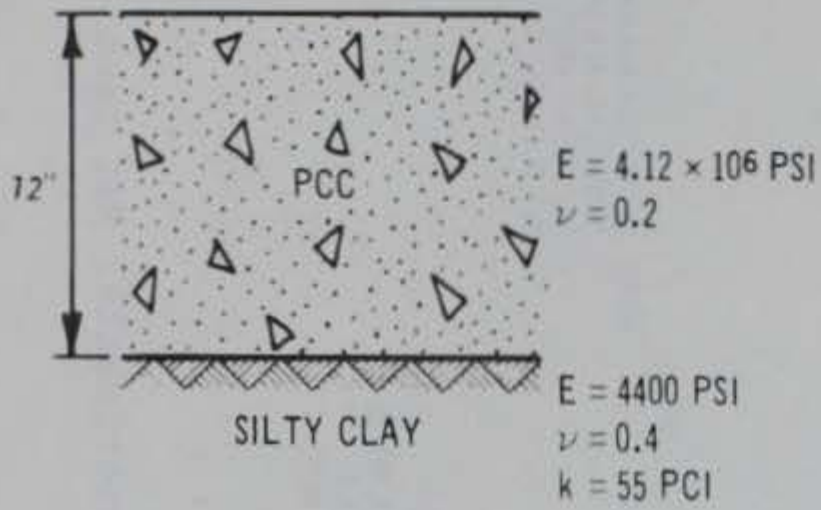
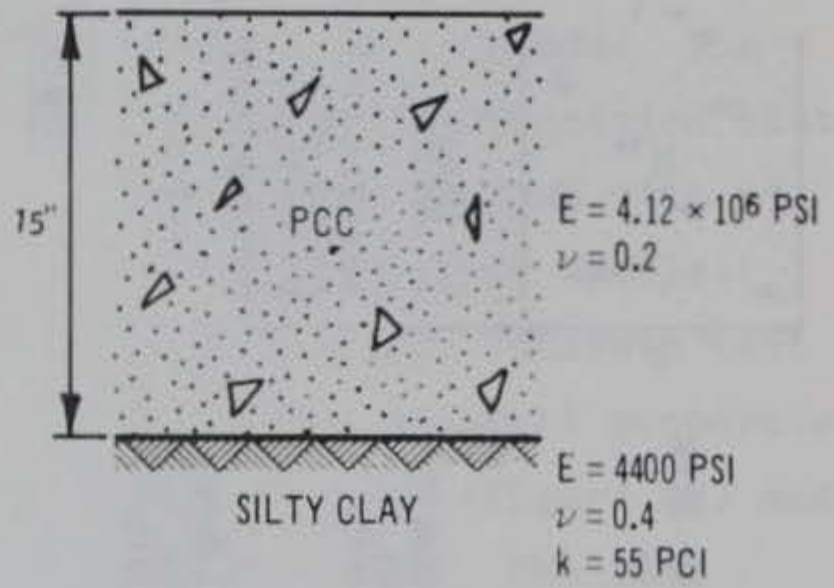


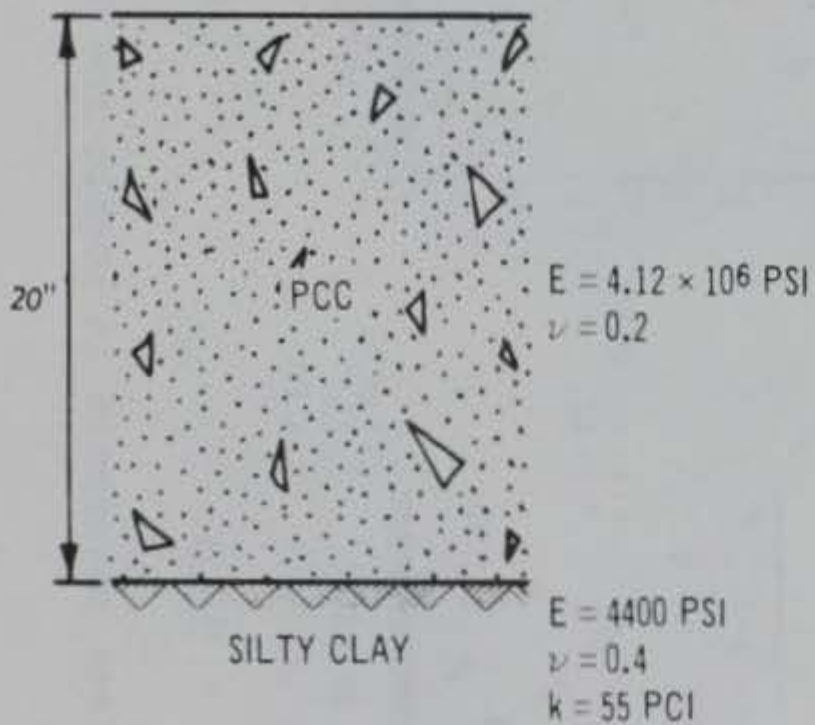
Figure B3. Description of test pavements in Lockbourne No. 2 Experimental Mat test section



ITEM M1



ITEM M2

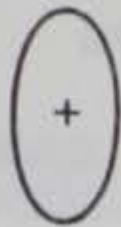


ITEM M3

NOTE: SILTY CLAY AVERAGES  
29.5% CLAY, 51% SILT,  
18.2% SAND, AND 1.3% GRAVEL  
PI = 29.2% (CL-CH, CH PREDOMINANT)

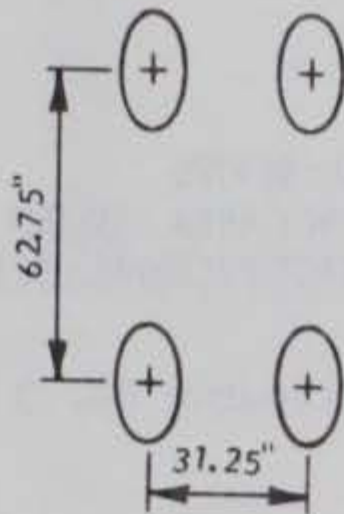
Figure B4. Description of test pavements in Lockbourne No. 2 Multiple-Wheel Modification test section





#### EXPERIMENTAL MAT

GEAR LOAD = 150 KIPS  
TIRE CONTACT AREA = 1459 IN.<sup>2</sup>  
TIRE CONTACT PRESSURE = 103 PSI



#### MODIFICATION

GEAR LOAD = 150 KIPS  
TIRE CONTACT AREA = 270 IN.<sup>2</sup>  
TIRE CONTACT PRESSURE = 139 PSI

Figure B5. Schematic representation of loads used in Lockbourne No. 2 Test Track

#### LOCKBOURNE NO. 3

The Lockbourne No. 3 Overlay Mat test section was constructed in the area encompassed by the inner boundaries of the Lockbourne No. 1 Test Track. Construction of the test section was begun 1 August 1946 and was completed 26 October 1946. The construction, testing, and analyses of the data from this overlay mat test section are discussed in References 45 and 46. The concrete pavement comprising part of the Lockbourne No. 3 Test Track was divided into nine test items. With the exception of item 1, each was overlain with a flexible overlay. The overlay thickness varied as well as the type of overlay material and ranged between 3 to 9 in. Item 1 consisted of 6-in. plain concrete and was divided into four lanes; three of these lanes were 25 ft wide and one was 10 ft wide.

Traffic was applied to the test items with a rig producing a 60-kip load on a dual-wheel assembly. Figure B6 lists the properties of the pavement used in this study including the applied load. The PCC flexural strength was 800 psi, and the first crack failure occurred at 18 coverages.

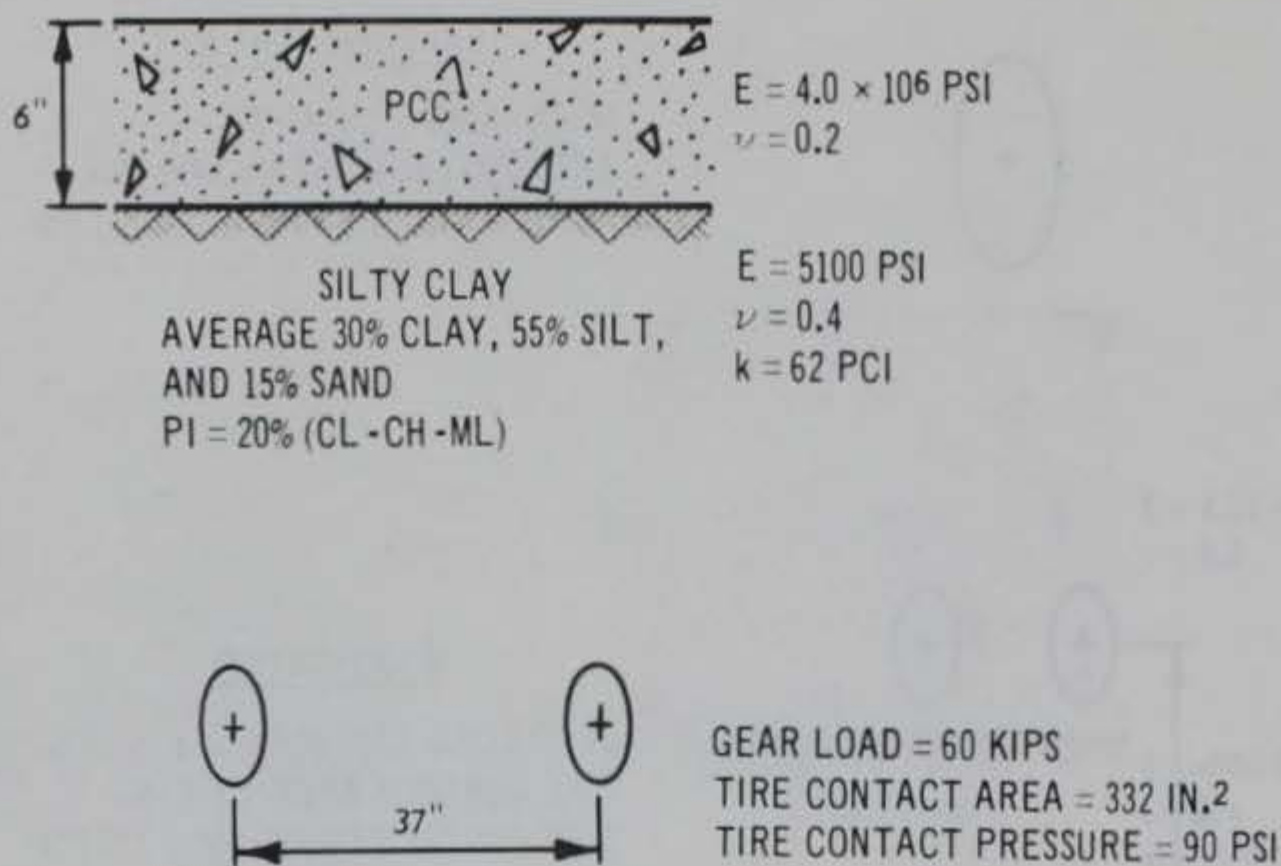


Figure B6. Summary of data from Lockbourne No. 3 Test Track

#### SHARONVILLE CHANNELIZED TRAFFIC

Two channelized traffic test sections, one on a high bearing-capacity foundation and the other on a low bearing-capacity foundation, were constructed at Sharonville, Ohio, between November 1955 and February 1956. The construction, testing, and analyses of data from this test track are discussed in References 34 and 47. The two channelized traffic test sections, designated as Parts 1 and 2, were 25 ft wide and about 600 ft long, and contained no longitudinal joints. The test items in each section varied from 50 to 65 ft in length. Each item was separated by a heavily reinforced concrete transition slab 10 ft long. Traffic was applied to both sections by using a load rig which produced a 100-kip load on a dual gear.

Table B3 summarizes the flexural strength of the test items and the amount of traffic applied to each. Figure B7 shows the pavement properties used in this study; Figure B8, the load used to traffic the Sharonville Channelized test pavement.



Table B3

Summary of Load, PCC Flexural Strength, and Traffic--Sharonville Channelized Test Track

Item	Load, kips	Flexural Strength		Traffic Coverages	Remarks
		psi			
57	100	740		34,650+	No failure
58	100	740		34,650+	No failure
59	100	730		7,600	First crack
60	100	730		1,674	First crack
61	100	730		3,867	First crack
62	100	730		10,082	First crack

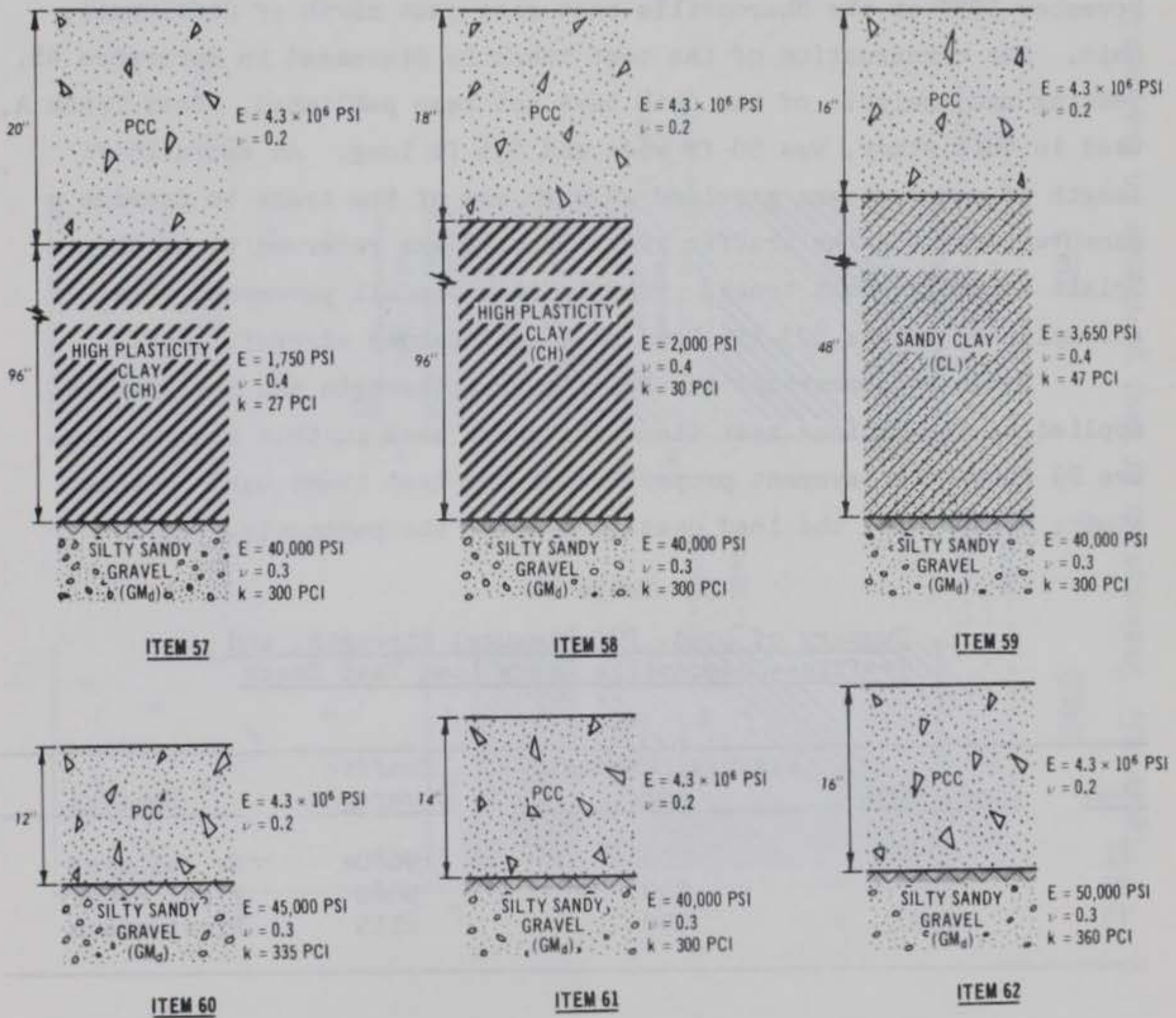


Figure B7. Description of test pavements in Sharonville Channelized Traffic Test Track

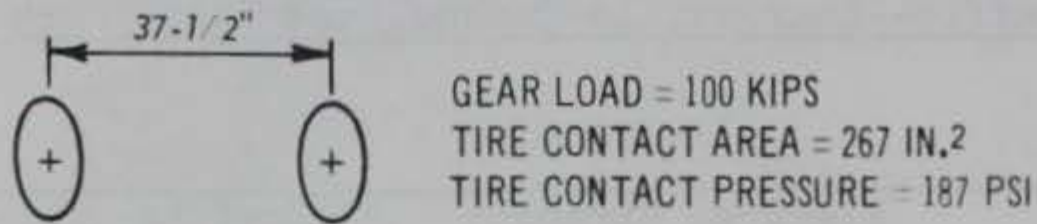


Figure B8. Schematic representation of loads used in Sharonville Channelized Traffic Test Track

#### SHARONVILLE HEAVY LOAD

The Heavy Load Test Track was constructed between July and November 1957 at the Sharonville test site just north of Cincinnati, Ohio. The construction of the test track is discussed in Reference 48. Testing and analysis of the data have not been published. Test Track A, used in this study, was 50 ft wide and 525 ft long. An extra 25-ft length of pavement was provided at each end of the track to provide a maneuver area for the traffic rig. Track A was referred to as the "plain concrete" test track. Traffic tests on all pavements were accomplished with a 325-kip load on a dual-tandem aircraft gear.

Table B4 summarizes the PCC flexural strength and the traffic applied to the various test items that were used in this study. Figure B9 shows the pavement properties of the test items used in this study; Figure B10, the load used to traffic the pavements.

Table B4

Summary of Load, PCC Flexural Strength, and Traffic--Sharonville Heavy Load Test Track

<u>Item</u>	<u>Load, kips</u>	<u>Flexural Strength psi</u>	<u>Traffic Coverages</u>	<u>Remarks</u>
71	325	800	9680+	No failure
72	325	800	9680	First crack
73	325	800	2115	First crack



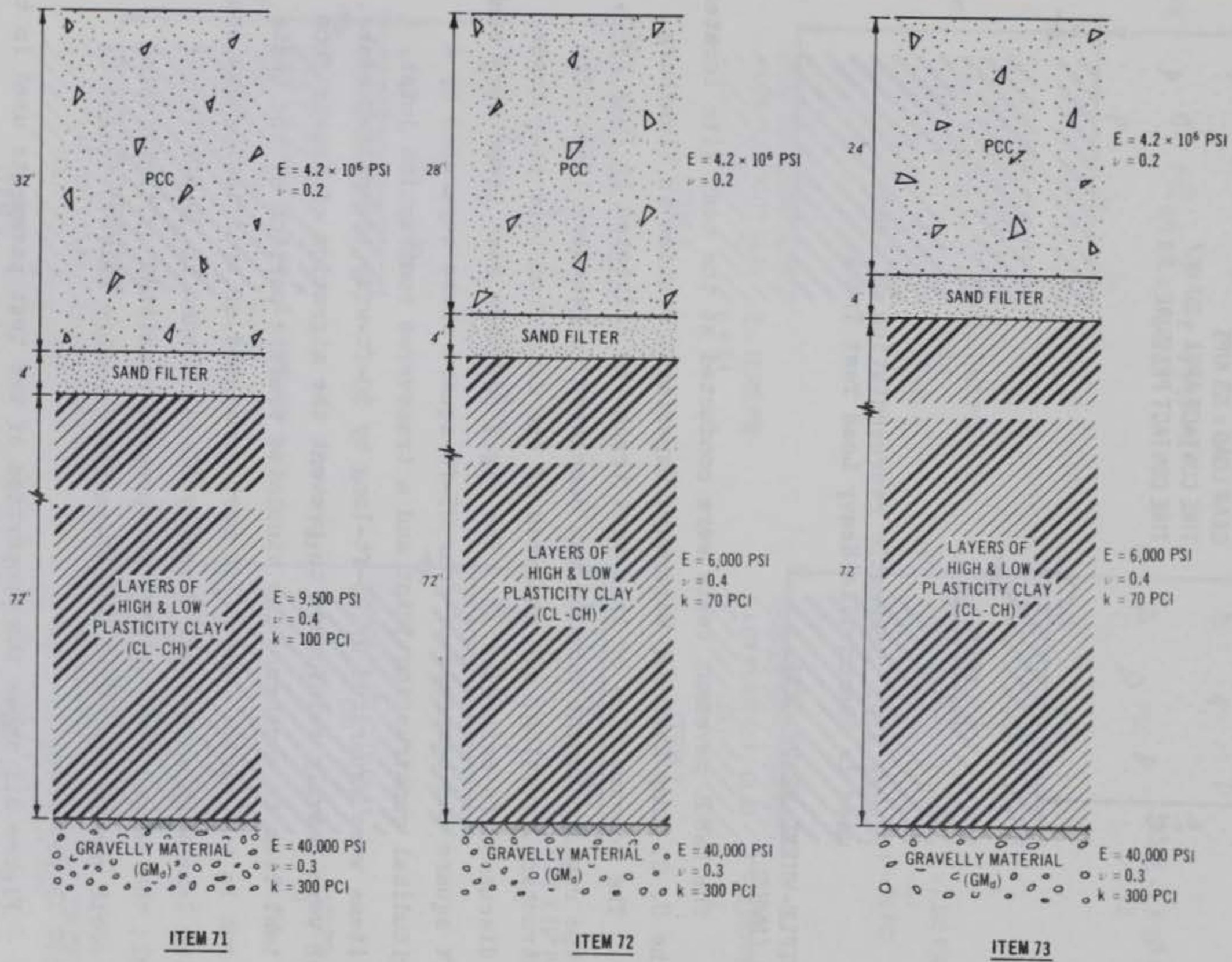


Figure B9. Description of test pavements in Sharonville Heavy Load Test Track



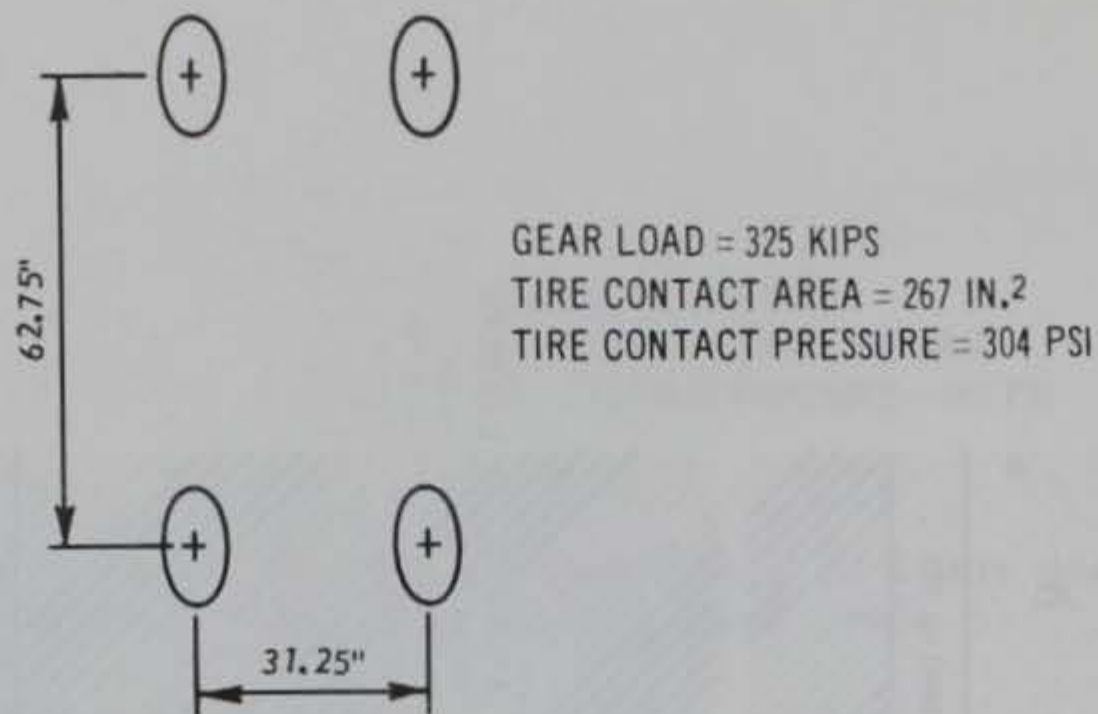


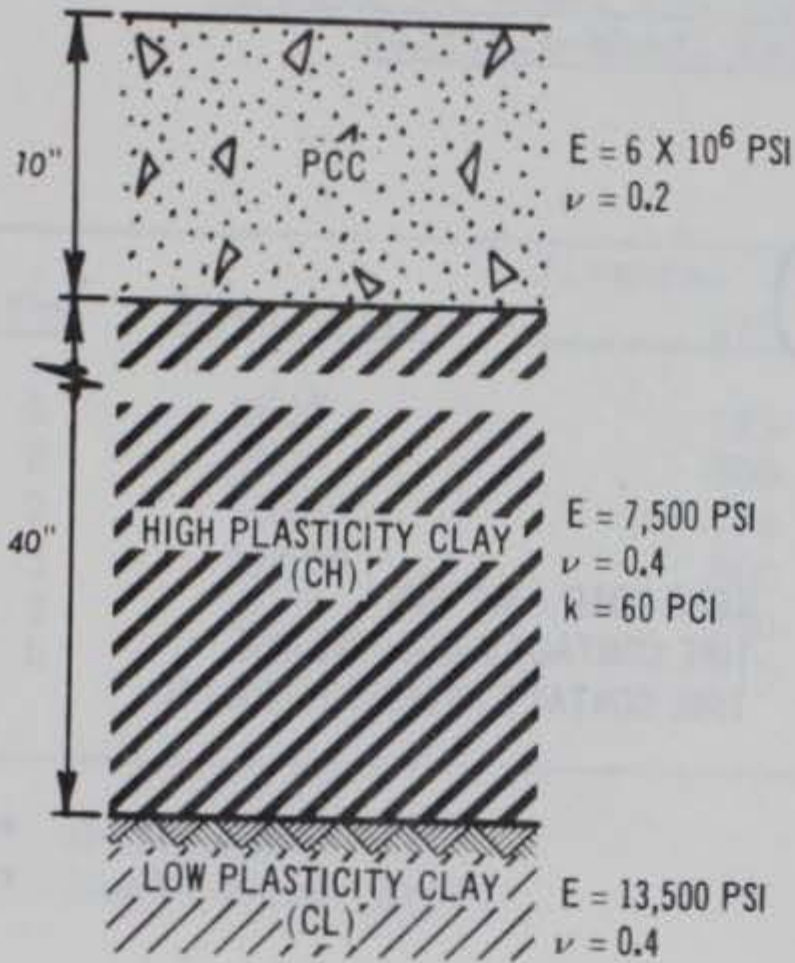
Figure B10. Schematic representation of loads used in Sharonville Heavy Load Test Track

MULTIPLE-WHEEL HEAVY GEAR  
 LOAD (MWHGL)

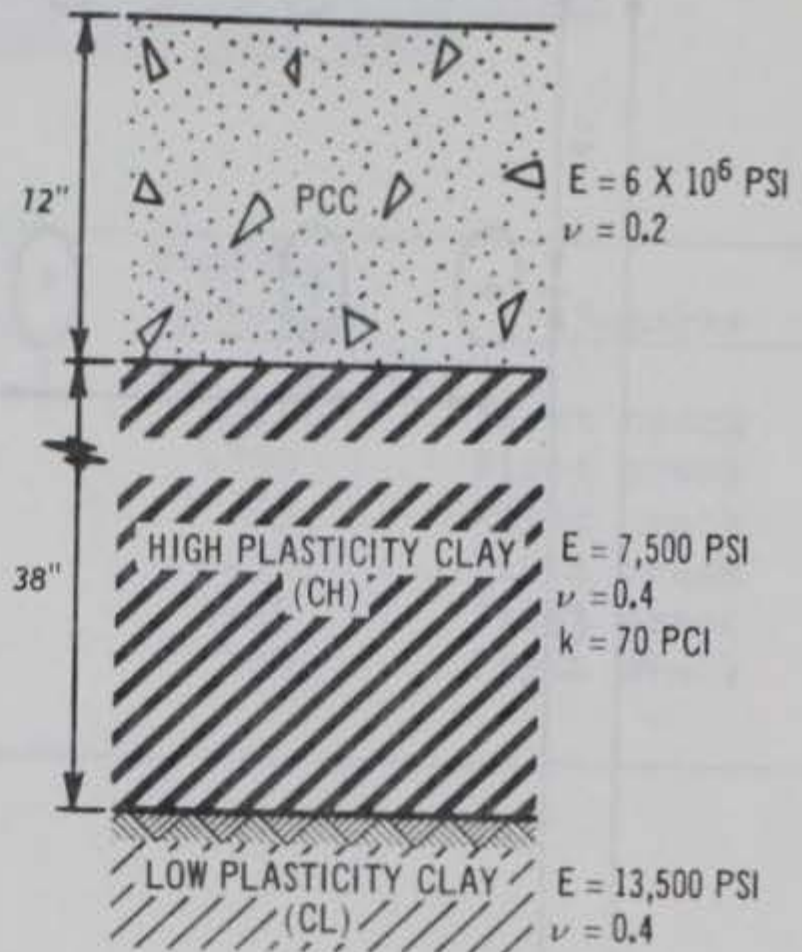
The MWHGL pavement tests were conducted at the test site located at the U. S. Army Engineer Waterways Experiment Station in Vicksburg, Miss. The construction of this test track was initiated in July 1968, and the rigid pavement portion was completed in December 1968. The construction, testing, and analyses of the data from this test track are discussed in Reference 35. The rigid pavement test items were each 50 ft square and composed of four 25-ft-square slabs separated by a longitudinal construction joint and a transverse contraction joint. The items were separated by 25-ft-long by 50-ft-wide transition slabs, which were heavily reinforced to prevent the migration of cracks from one test item to another. The simulated traffic portion of the tests was run in two parts: the first part consisted of trafficking the south paving lane with a 12-wheel assembly (C-5A) loaded to 30,000 lb per wheel; the second part of the test program consisted of trafficking the north paving lane with a dual-tandem assembly (B-747) loaded to 41,500 lb per wheel.

Figure B11 shows the properties of the test pavements used in this study; Figure B12, the load assemblies used to traffic the test items. Table B5 summarizes the wheel loads, PCC flexural strengths, and the traffic applied to the test pavements.

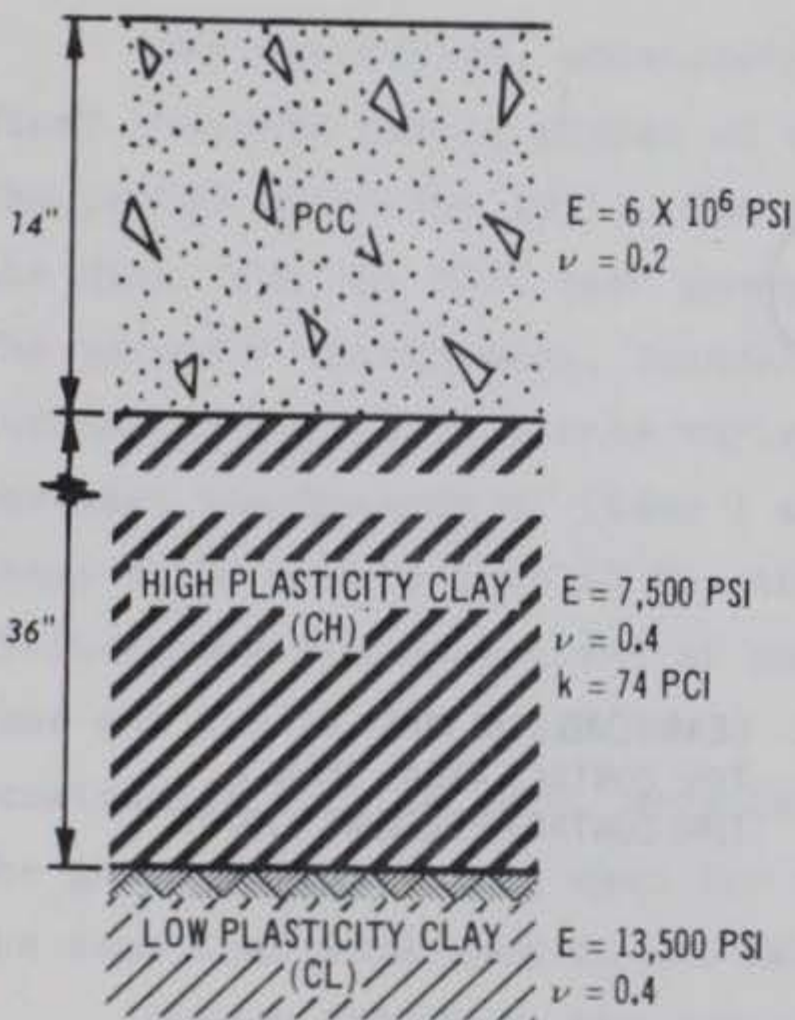




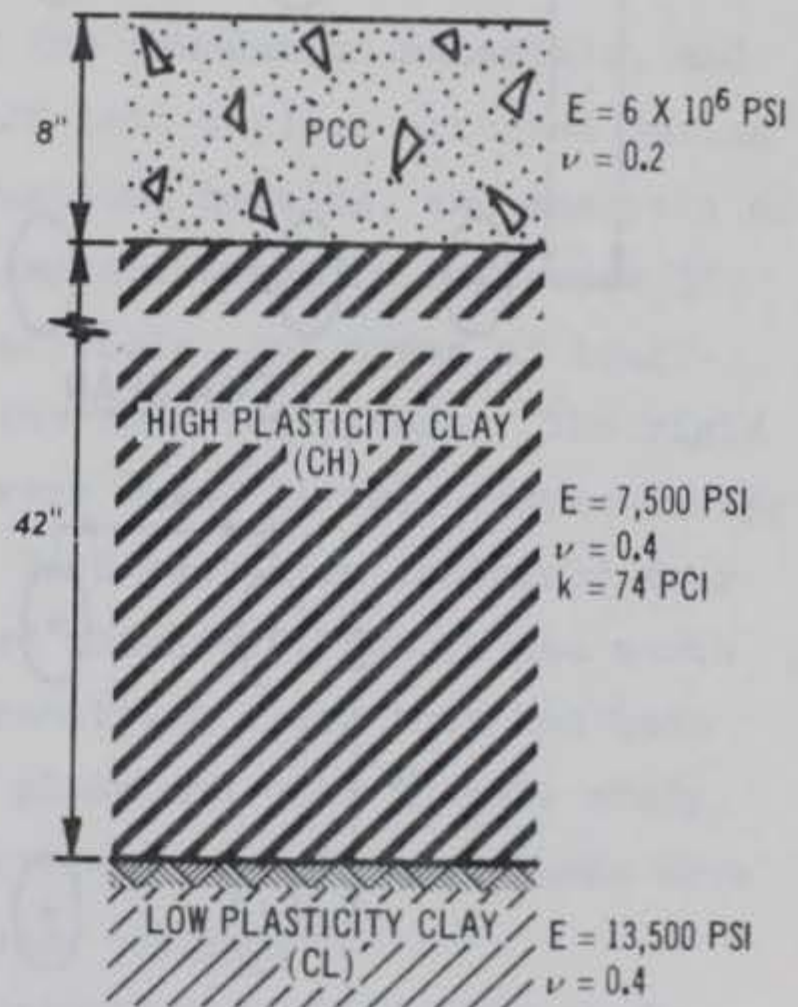
ITEM 1



ITEM 2

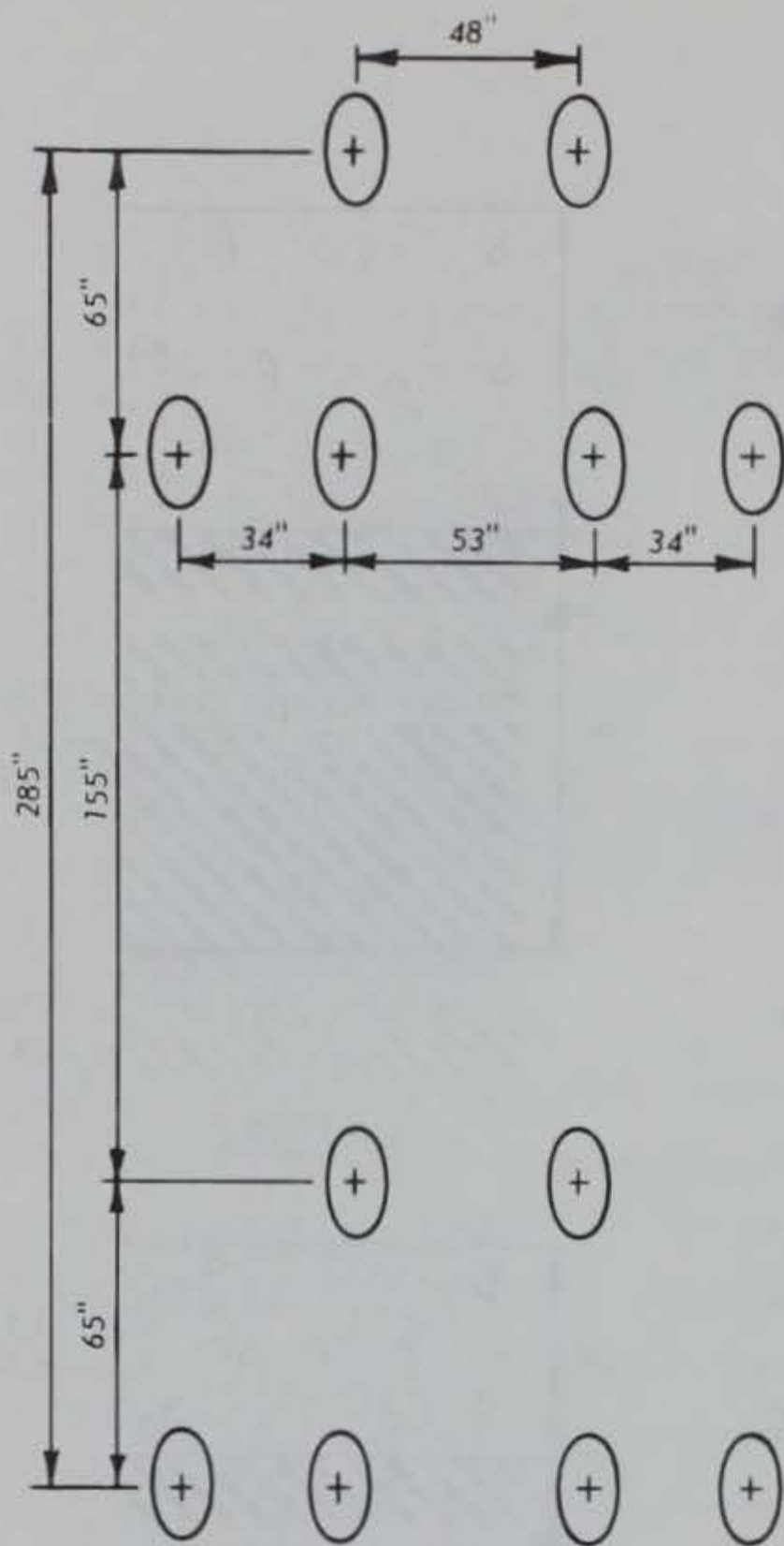


ITEM 3



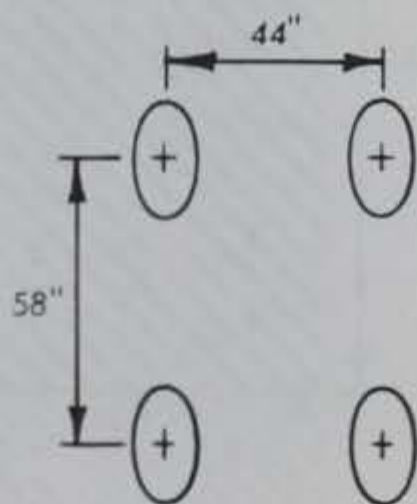
ITEM 4

Figure B11. Description of test pavements in Multiple-Wheel Heavy Gear Load Test Track



GEAR LOAD = 360 KIPS  
 TIRE CONTACT AREA = 285 IN.<sup>2</sup>  
 TIRE CONTACT PRESSURE = 106 PSI

C-5A GEAR



GEAR LOAD = 166 KIPS  
 TIRE CONTACT AREA = 207 IN.<sup>2</sup>  
 TIRE CONTACT PRESSURE = 200 PSI

DUAL TANDEM GEAR

Figure B12. Schematic representation of loads used in Multiple-Wheel Heavy Gear Load Test Track



Table B5

Summary of Load, PCC Flexural Strength, and Traffic--  
Multiple-Wheel Heavy Gear Load Test Track

<u>Item</u>	<u>Load, kips</u>	<u>Flexural Strength psi</u>	<u>Traffic Coverages</u>	<u>Remarks</u>
1	360*	725	221	First crack
2	360*	800	4230	First crack
2	166**	700	95	First crack
3	166**	660	205	First crack
3	360*	700	1400	First crack
4	360*	775	180	First crack

\* C-5A gear.

\*\* Dual-tandem gear.

KEYED LONGITUDINAL  
JOINT STUDY (KLJS)

The excavation, construction of the foundation materials, and final concrete paving phases of the KLJS test section occurred during the period April-May 1971. The construction, testing, and analysis of the data from the KLJS test pavements are discussed in Reference 38. The pavement thicknesses, foundation materials, and types of longitudinal construction joints varied in the four test items. The rigid pavement thicknesses of items 1 and 2 were 8 and 11 in., respectively; items 3 and 4 were both 10 in. thick. Each test item contained four 25-ft-square concrete slabs at uniformed thickness, two in the north lane and two in the south lane. The transition slabs that had been constructed for the MWHGL were left in place and used in this study. The gear configurations used for trafficking the KLJS test items were the same that were used in the MWHGL study (Figure B12).

Figure B13 shows the pavement properties used in this study. Table B6 summarizes the wheel loads, concrete flexural strengths, and traffic coverages applied to the test items.



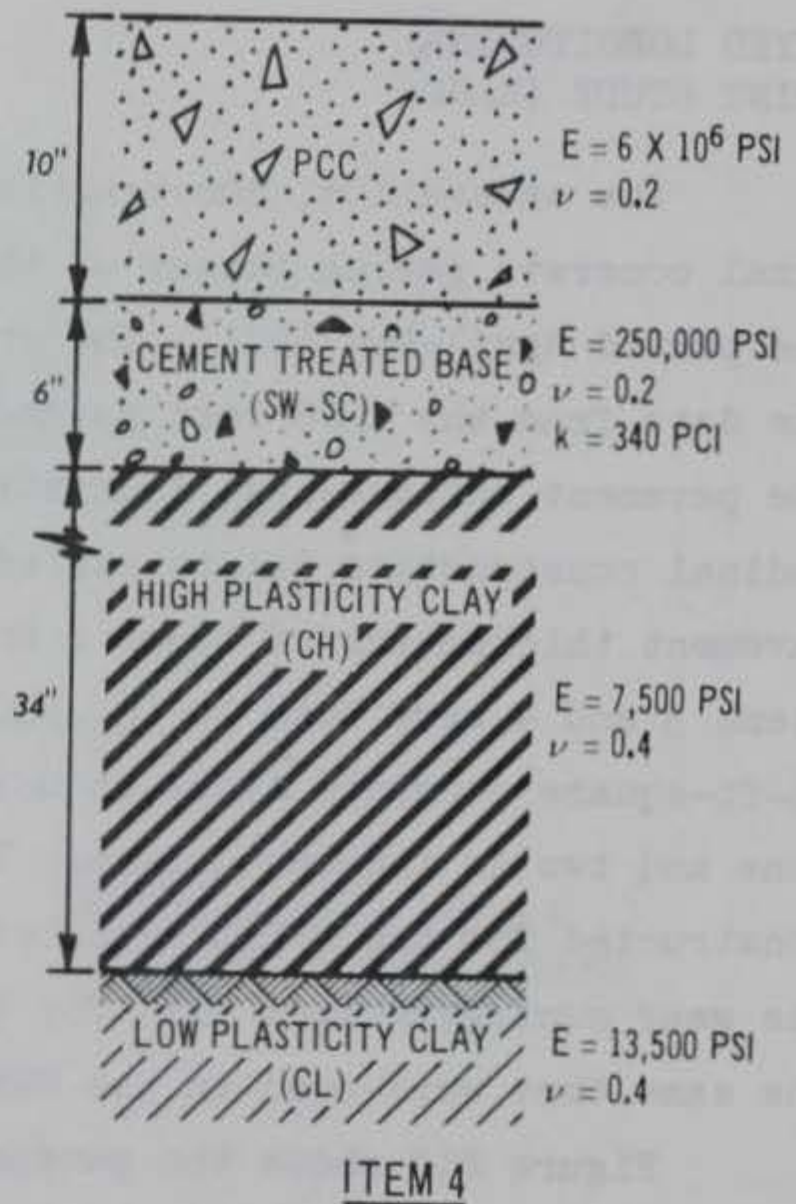
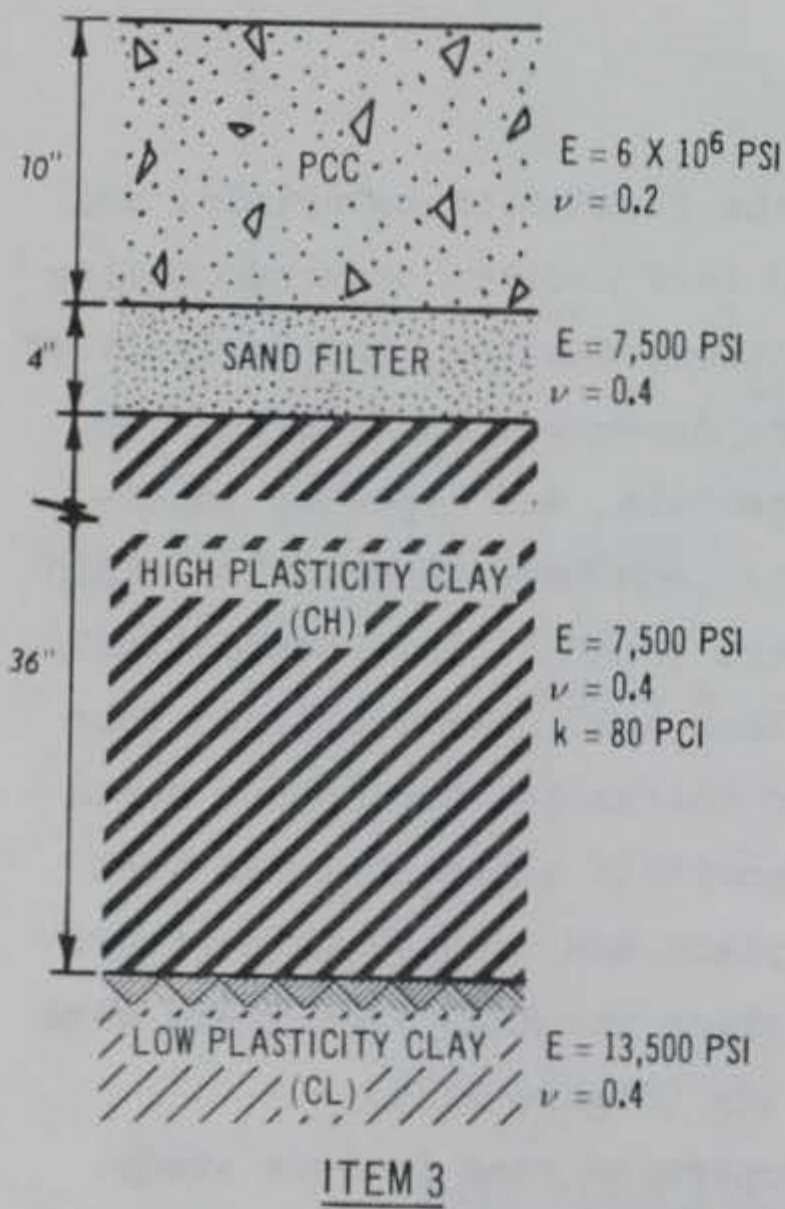
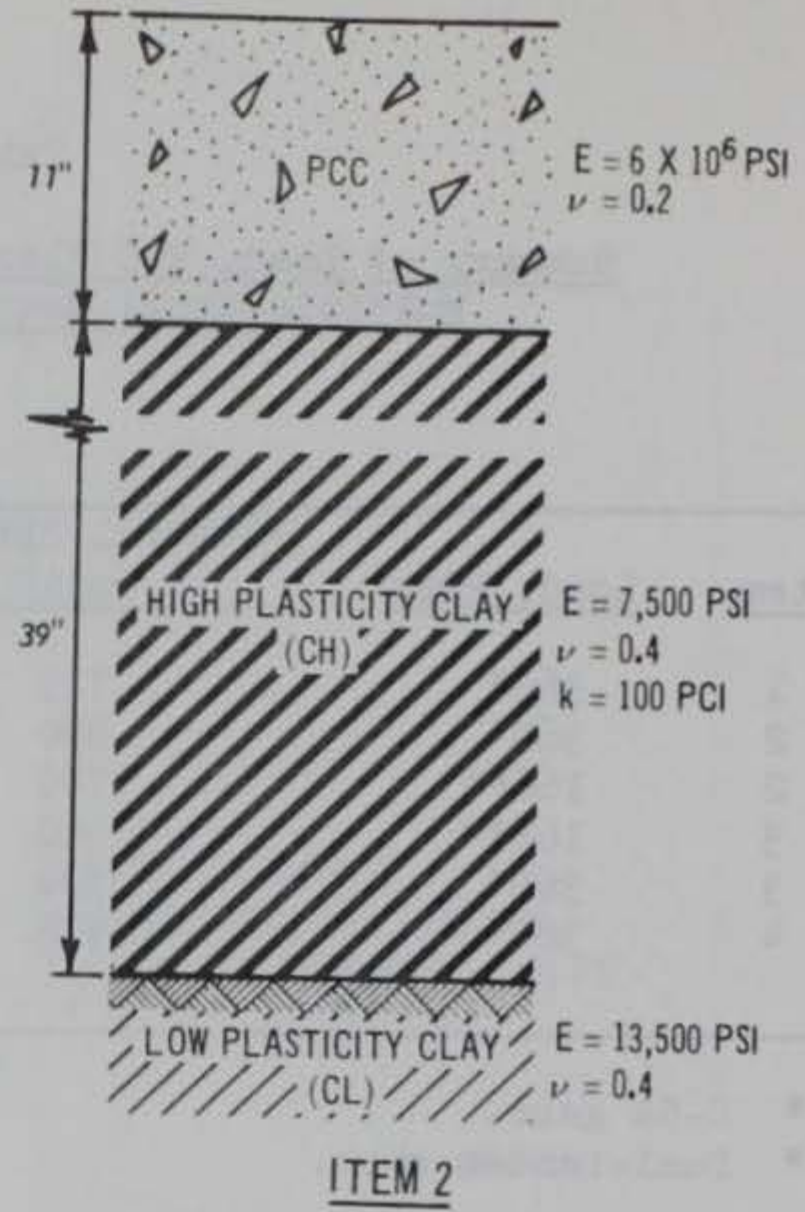
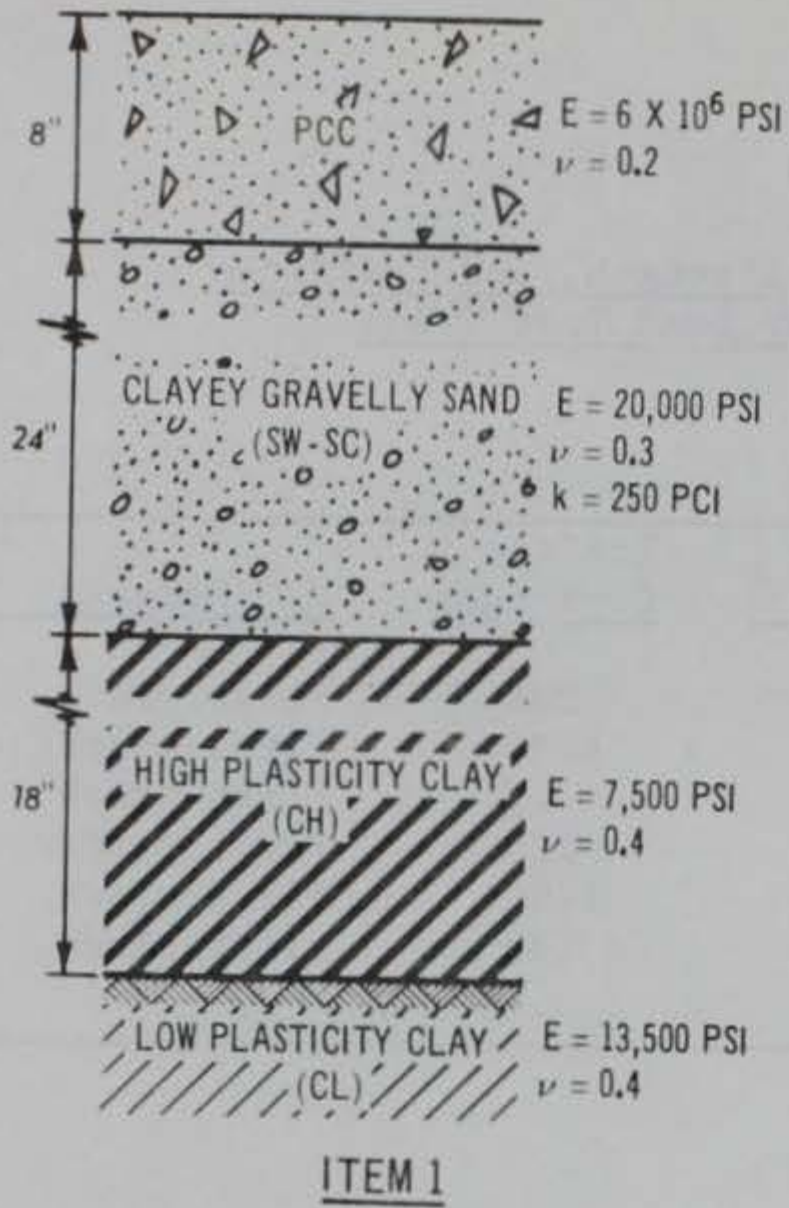


Figure B13. Description of test pavements in Keyed Longitudinal Joint Study



Table B6

Summary of Load, PCC Flexural Strengths, and Traffic--  
Keyed Longitudinal Joint Study

<u>Item</u>	<u>Load, kips</u>	<u>Flexural Strength</u> <u>psi</u>	<u>Traffic</u> <u>Coverages</u>	<u>Remarks</u>
1	360*	905	54	First crack
2	360*	730	344	First crack
3	360*	810	22	First crack
4	360*	860	6336	First crack
4	166**	860	320	First crack

\* C-5A gear.

\*\* Dual-tandem gear.

SOIL STABILIZATION  
PAVEMENT STUDY (SSPS)

This final test section, designated the SSPS, was constructed during the period March-August 1972. This area had been used previously for the MWHGL and KLJS tests. The construction, testing, and analyses of the data from this test section are discussed in Reference 39. The test section was 290 ft long and 50 ft wide and consisted of five test items, each 50 ft square and separated by 10-ft-wide transition slabs. The concrete in each item was first placed in the north paving lane (25- by 50-ft sections) between the transition slabs. Only two items from this test track were used in this study. These were 15-in.-thick slabs on 6-in.-thick bound base course layers. Simulated aircraft traffic was applied to the test items using a dual-tandem assembly. A net weight of 200 kips (50 kips/wheel) was used for trafficking lane 1 and 240 kips (60 kips/wheel) for trafficking lane 2. The contact area for both loads was maintained at 267 sq in. by using inflation pressures of 190 and 250 psi for the 200- and 240-kip loads, respectively.

Figure B14 shows the pavement properties used in this study; Figure B15, the loads used to traffic the test pavements. Table B7 summarizes the concrete flexural strengths and the traffic applied to each test item.



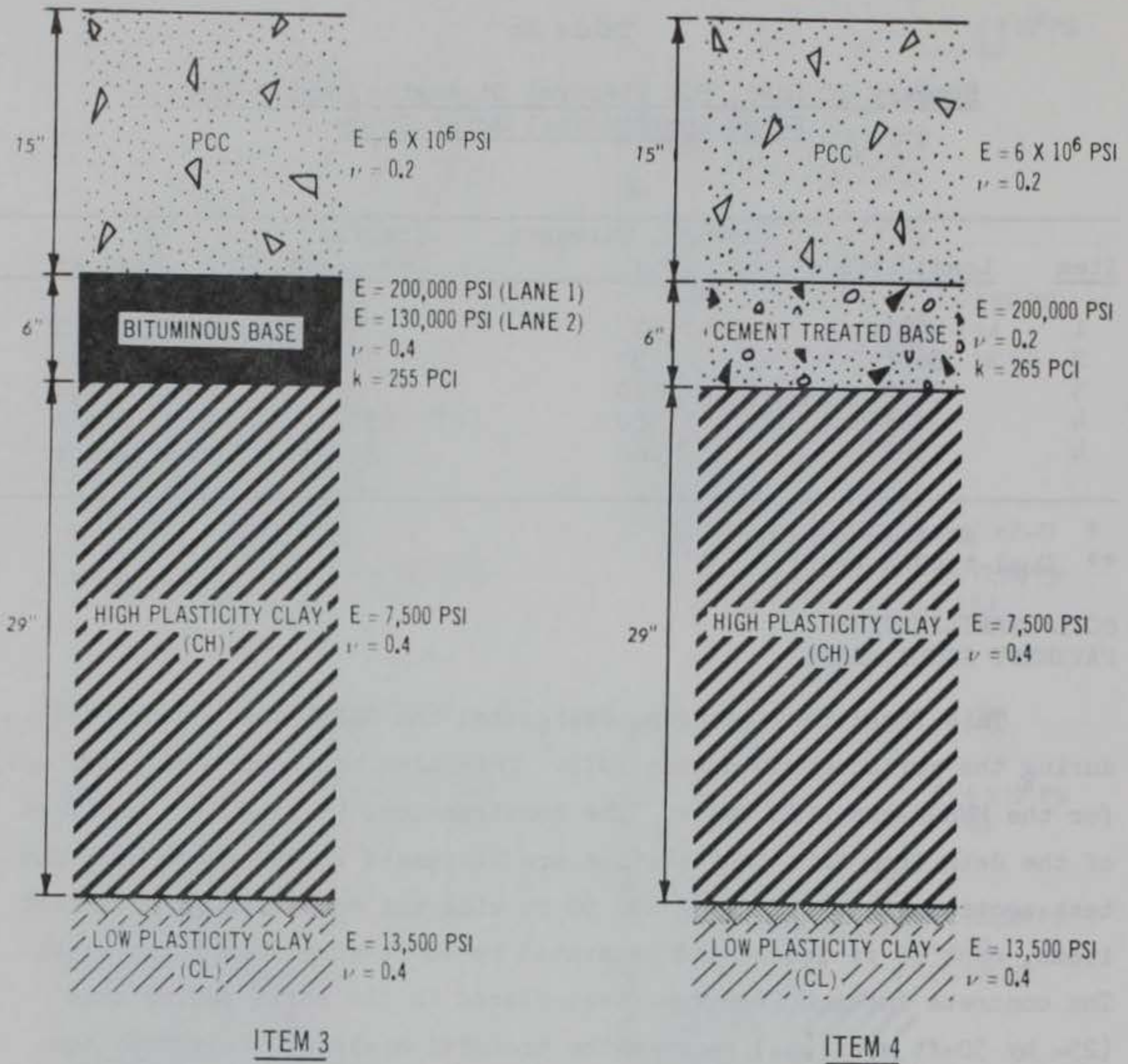
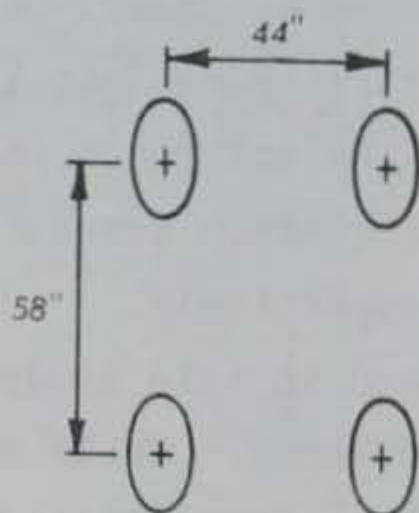


Figure B14. Description of test pavements in Soil Stabilization Pavement Study



	200-KIP GEAR LOAD	240-KIP GEAR LOAD
TIRE CONTACT AREA, IN. <sup>2</sup>	267	267
TIRE CONTACT PRESSURE, PSI	187	225

Figure B15. Schematic representation of loads used in Soil Stabilization Pavement Study



Table B7

Summary of Load, PCC Flexural Strength, and Traffic--  
Soil Stabilization Pavement Study

<u>Item</u>	<u>Load, kips</u>	<u>Flexural Strength psi</u>	<u>Traffic Coverages</u>	<u>Remarks</u>
3	200	900	3215	First crack
3	240	900	350	First crack
4	200	870	4660	First crack
4	240	870	70	First crack

## APPENDIX C: LABORATORY PROCEDURE FOR DETERMINING THE FLEXURAL MODULUS OF BOUND BASES

The procedure contained herein involves application of a repetitive loading to a beam specimen under controlled stress conditions. Applied load and deflection along the neutral axis and at the lower surface are monitored, and the results are used to determine the flexural modulus. Because of the sensitivity of bituminous-stabilized materials to temperature, rate of loading, and repeated loading, some differences are noted with the procedure for chemically stabilized materials.

### SPECIMEN PREPARATION

#### CHEMICALLY STABILIZED MATERIAL

Beam specimens should be prepared following the general procedures outlined in ASTM Standard Procedure Designation: D 1632-63.<sup>65</sup> This method describes procedures for molding 3- by 3- by 11-1/4-in. specimens; however, any size mold may be used for the test. For soils containing aggregate particles larger than 3/4 in., it is recommended that molds on the order of 4 by 4 to 6 by 6 in. be used. In general, specimens should have an approximately square cross-sectional configuration and a length adequate to accommodate an effective test span equal to three times the height or width. Specimens should be molded to the stabilizer treatment level, moisture content, and density expected in the field structures. Specimens should be moist-cured for 28 days.

#### BITUMINOUS-STABILIZED MATERIAL

Beam specimens should be prepared following the general procedures outlined in ASTM Standard Procedure Designation: D 3202-73.<sup>66</sup> If there is undue movement of the mixture under the compactor foot during beam compaction, the temperature, foot pressure, and number of tamping blows should be reduced. Similar modifications to compaction procedures should be made if specimens with less density are desired.



A diamond-blade masonry saw is used to cut 3-in.- (or slightly less) deep by 3-in.- (or slightly less) wide test specimens from the 15-ft-long beams. Specimens with suitable dimensions can also be cut from pavement samples. The widths and depths of the specimens are measured to the nearest 0.01 in. at the center and at 2 in. from both sides of the center. Mean values are determined and used for subsequent calculations.

#### EQUIPMENT

The following equipment is required:

- a. Loading frame capable of receiving specimen for third-point loading test.
- b. A 3000-lb capacity electrohydraulic testing machine capable of applying static and repeated tension-compression loads in the form of haversine waves.
- c. Load cell (approximately 3000-lb capacity).
- d. Two linear variable differential transformers (LVDT's).
- e. Recording equipment for monitoring deflection, strain, and load.
- f. Miscellaneous pins and yokes, as described in the equipment setup below, for mounting the LVDT's.
- g. Controlled-temperature cabinet capable of controlling temperature within  $\pm 1^{\circ}\text{F}$ .

#### EQUIPMENT SETUP

##### CHEMICALLY STABILIZED MATERIALS

Figures C1-C3 present the details of the equipment. The beam should be positioned so that the molding laminations are horizontal. The three yokes are positioned over the top of the beam and held in place by threaded pins positioned along the neutral axis. The end pins, A and C, are positioned directly over the end reaction points, and the middle pin B is positioned at the center of the beam. A metal bar rests on top of the pins. At the A position, the bar is equipped with a lower vertical tab having a hold that slips loosely over the pin. A nut is placed on the end of the pin to prevent the bar from slipping. At the center or B position, the bar is equipped with a vertical tab onto which

C-3

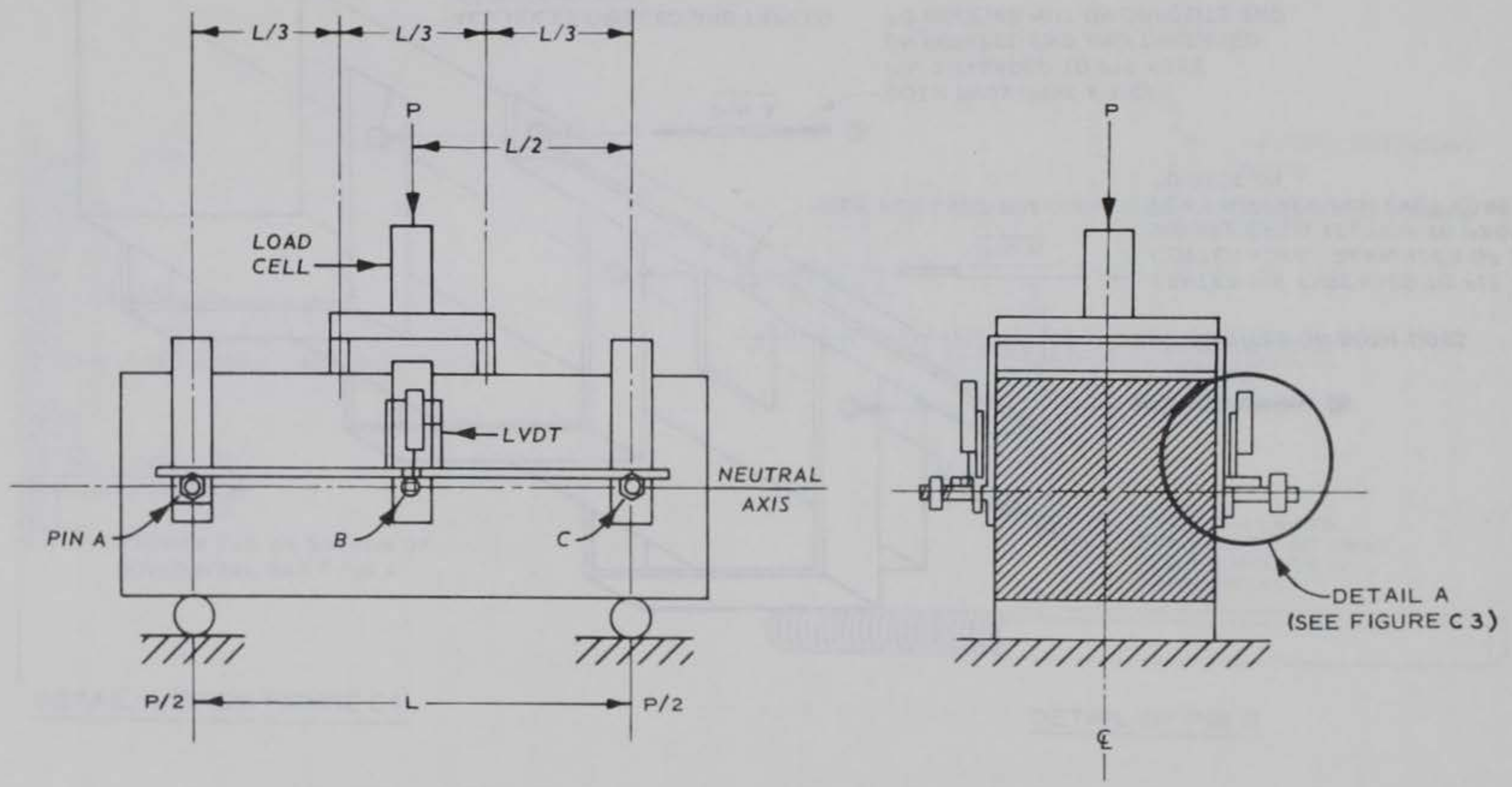


Figure C1. General view of equipment setup for one-way loading



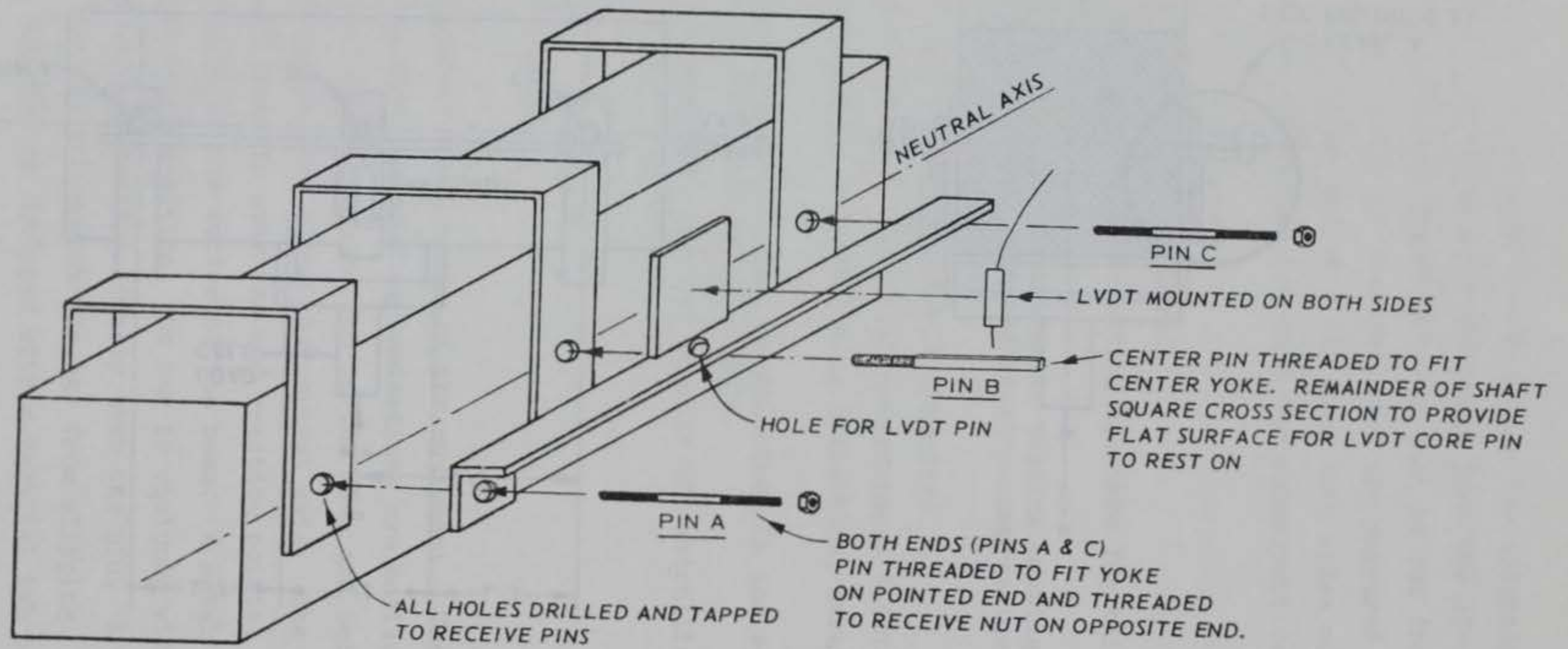
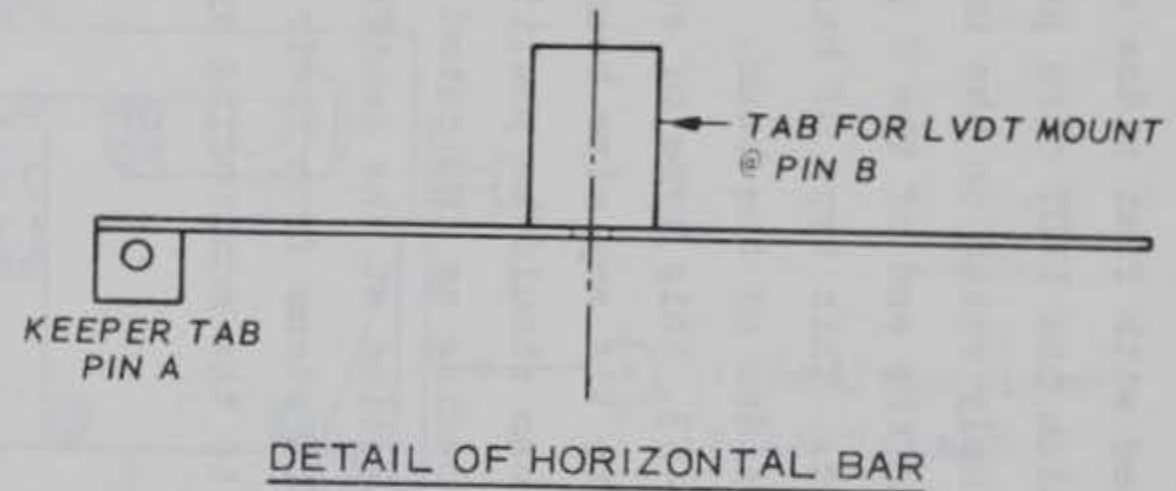
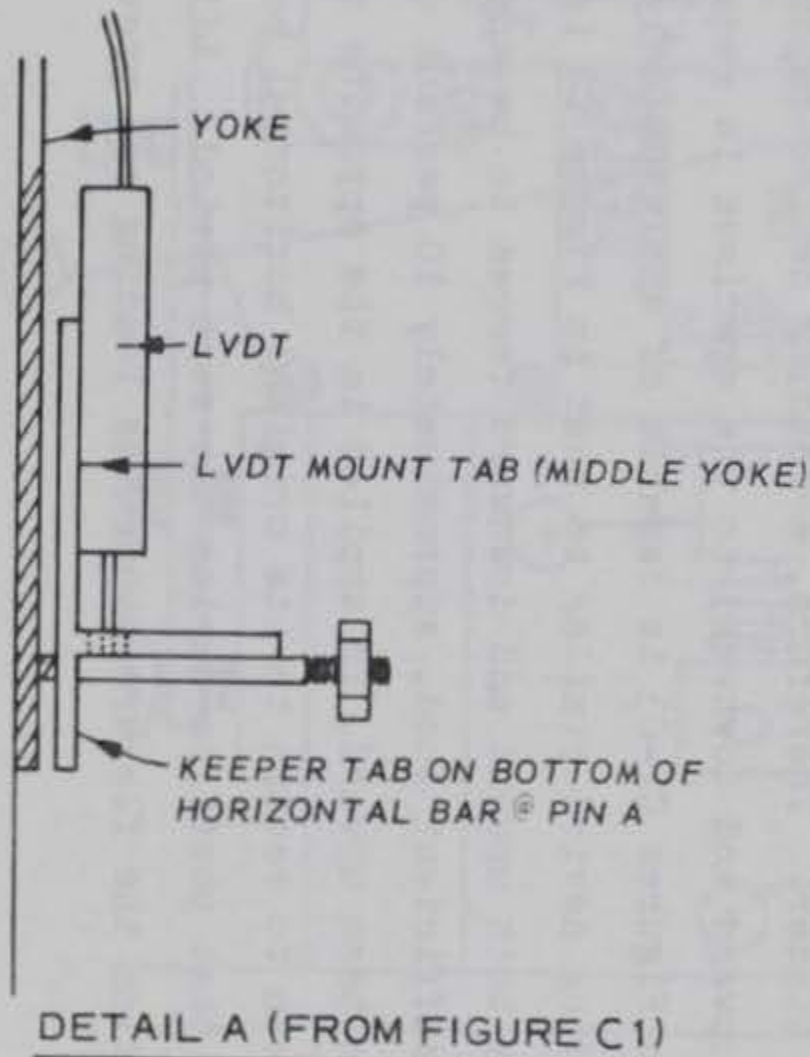


Figure C2. Details of equipment setup

C-5



NOTE: PIN B IS ALWAYS POSITIONED SO THAT FLAT SURFACE IS HORIZONTAL

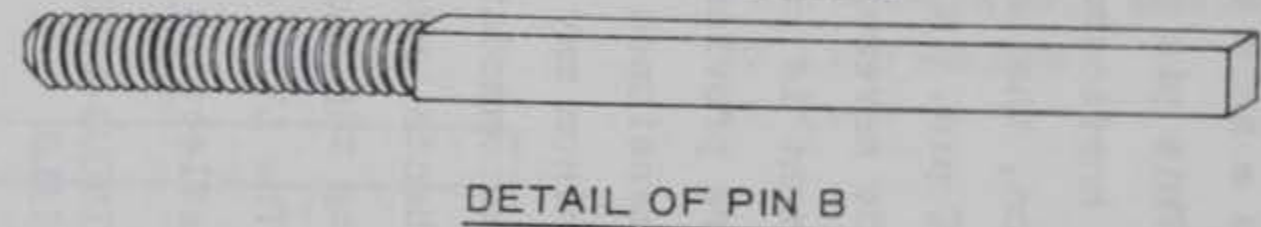


Figure C3. Details of pins A and B and horizontal bar



an LVDT is cemented in a vertical position. At this position on the bar, there is a hole through which the LVDT core pin falls to rest on the B pin. This pin must be fabricated with flat sides on the shaft to provide a horizontal surface on which the LVDT core pin rests. At the C position, the end of the bar simply rests on the unthreaded portion of the C pin. A nut is placed on the end of the C pin to prevent excessive side movement of the bar end. This type of bar, pin, and LVDT arrangement is provided on both sides of the beam. Although no dimensions are provided in Figures C1-C3, this type of equipment can easily be dimensioned and fabricated to fit any size beam. Either steel or aluminum may be used. The beam should be positioned and arranged to accommodate third-point loading as indicated in Figure C2. As the beam bends under loading, deflection at the center is measured by determining the movement of the LVDT stems from their original positions. The LVDT's are connected to the monitoring system to give an average deflection reading.

#### BITUMINOUS-STABILIZED MATERIALS

Bituminous-stabilized materials are affected by temperature, rate of loading, and repeated load applications. The tests should be conducted in a controlled-temperature cabinet capable of controlling temperature within  $\pm 1^{\circ}\text{F}$ . The beam will tend to deform permanently under repeated load applications or its own weight due to the viscous nature of the binder. Therefore, a loading device capable of transmitting both upward and downward to the specimen is required. The arrangement in Figures C1-C3 is capable of applying only a downward force. A loading device similar to that in Figure C4 is needed. This device permits both upward and downward forces to be applied to the specimen. A sufficient load, approximately 10 percent of the load deflecting the beam upward, is applied in the opposite direction forcing the beam to return to its original horizontal position and holding it at that position during the rest period. Adjustable stop nuts installed on the flexure apparatus loading rod prevent the beam

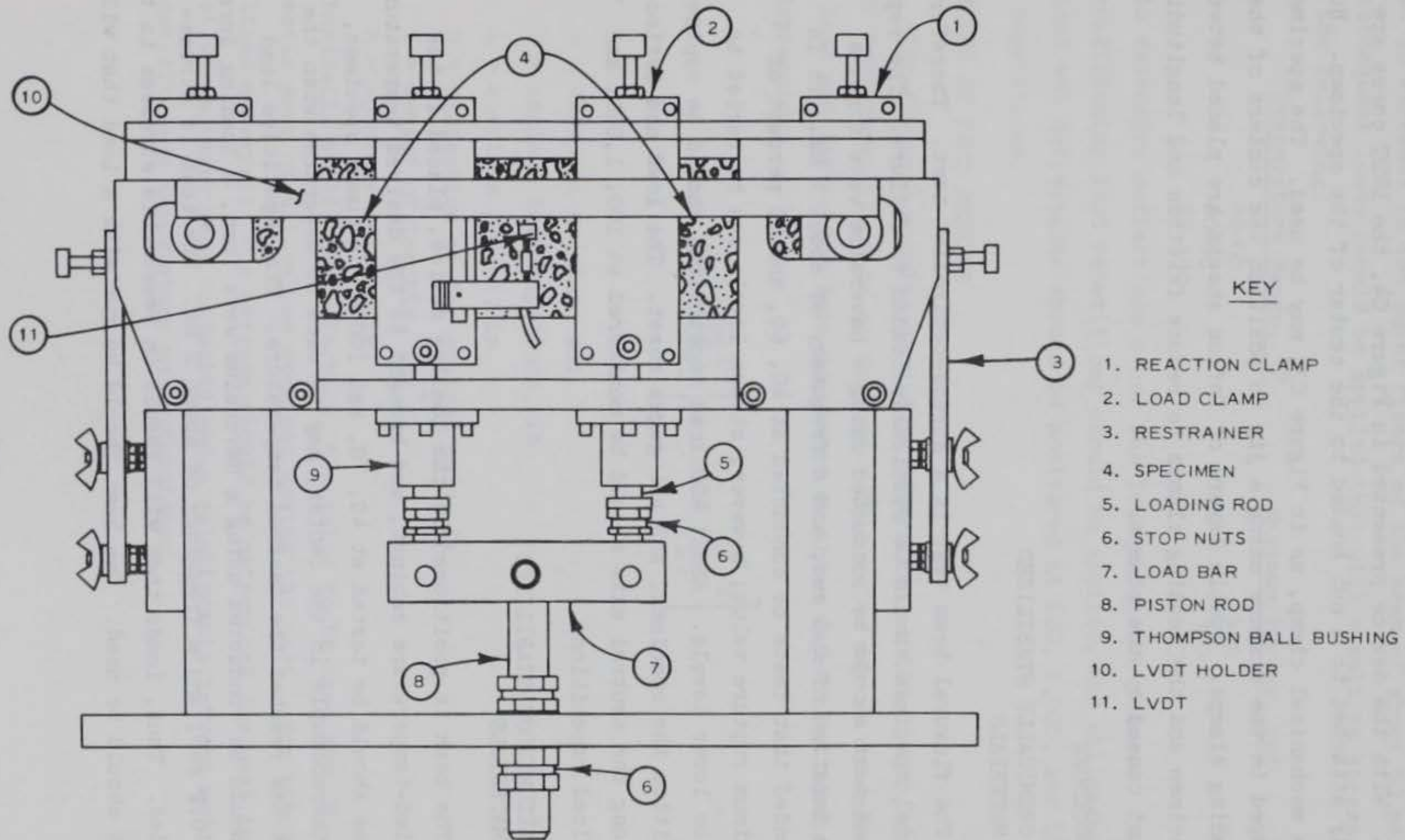


Figure C4. General view of equipment setup for two-way loading



from bending below the initial horizontal position during the rest period. With the device presented in Figure C4, the LVDT cores are normally attached to a nut bonded to the center of the specimen. However, a mechanical clamp, as in Figure C3, may be used. The specimen is clamped in the fixture using a jig to position the centers of the two loading clamps. Double layers of Teflon sheets are placed between the specimen and the loading clamps to reduce friction and longitudinal restraint caused by the clamps.

#### TEST PROCEDURE

##### CHEMICALLY STABILIZED MATERIALS

The flexural beam test is a stress-controlled test. Therefore, an initial specimen should be statically loaded to failure. The repetitive load test should be conducted using a haversine wave form, a loading duration of 0.5 sec, and a frequency of about 1 Hz. It is recommended that tests be conducted at 40, 60, and 80 percent of the maximum rupture value; however, stress levels can be varied to higher or lower levels. About 400 load repetitions should be applied to condition the specimen, and all gages reset. The load and deflection along the neutral axis should be monitored at 100, 1,000, and 10,000 load repetitions.

##### BITUMINOUS-STABILIZED MATERIALS

The beam is positioned in the loading device, placed in the controlled-temperature cabinet, and brought to the desired temperature. Specimens should be tested at 40, 70, and 100°F. A dummy specimen, with a thermocouple in the center, may be used to determine when the specimen has reached the desired temperature. The repetitive load tests should be conducted using a haversine wave form, a loading duration of 0.2 sec, and a frequency of about 2 Hz. The test is stress-controlled. Thus, loads that will result in reasonable stresses in the specimen should be used. One test should be run with a load that will

result in stresses in the outer fibers of the beam of about 50 psi, and subsequent loads should be applied that will result in stress less than the following:

<u>Temperature Range, °F</u>	<u>Maximum Stress, psi</u>
40-60	450
60-80	300
80-100	200

Should excessive deflections occur the load should be reduced. About 500 conditioning load repetitions should be applied, and all gages reset. The load and deflections should be monitored at 100, 1,000, and 10,000 load repetitions.

#### REPORTING OF TEST RESULTS

The flexural modulus should be determined at 100, 1,000, and 10,000 load repetitions or at failure. This value may be determined from load and deflection data monitored at these repetition levels using the expression

$$E = \frac{23PL^3}{1296dI} \left[ 1 + 2.11 \left( \frac{h}{L} \right)^2 \right] \quad (C1)$$

where

E = flexural modulus, psi

P = maximum load amplitude, lb

L = specimen length, in.

d = deflection at the neutral axis, in.

I = moment of inertia, in.<sup>4</sup>

h = specimen height, in.

For chemically stabilized materials, the value to be used for E is the arithmetic mean of all values obtained during the test. For bituminous-stabilized materials, the average should be determined for each temperature at which tests were conducted and a relationship between modulus of elasticity and temperature was established.



## APPENDIX D: LABORATORY PROCEDURE FOR DETERMINING THE RESILIENT MODULUS OF GRANULAR BASE MATERIALS

This procedure is designed to determine resilient properties of granular base (subbase) materials. The test is similar to a standard triaxial compression test, the primary exception being that the deviator stress is applied repetitively at several stress levels. The procedure allows testing under a repetitive stress state similar to that encountered in a base (subbase) course layer in a pavement under a moving wheel load.

### DEFINITIONS

The following symbols and terms are used in the description of this procedure:

- a.  $\sigma_1$  = total axial stress.
- b.  $\sigma_3$  = total radial stress, i.e., confining pressure in the triaxial test.
- c.  $\sigma_d$  = deviator stress ( $\sigma_1 - \sigma_3$ ), i.e., the repeated axial stress in this procedure.
- d.  $\epsilon_1$  = total axial strain due to  $\sigma_d$ .
- e.  $\epsilon_R$  = resilient axial strain due to  $\sigma_d$ .
- f.  $\epsilon_\ell$  = resilient lateral strain due to  $\sigma_d$ .
- g.  $M_R$  = the resilient modulus =  $\sigma_d / \epsilon_R$ .
- h.  $\nu_R$  = the resilient Poisson's ratio =  $\epsilon_\ell / \epsilon_R$ .
- i.  $\theta$  = sum of the principal stresses in the triaxial state of stress ( $\sigma_1 + 2\sigma_3 = \sigma_d + 3\sigma_3$ ).
- j.  $\sigma_1 / \sigma_3$  = principal stress ratio.
- k. Load duration = time interval during which the sample is subjected to a stress deviator.
- l. Cycle duration = time interval between successive applications of the deviator stress.

### SPECIMENS

For base course materials, 6-in.-diam specimens are generally required with the maximum particle size being limited to 1 in. The specimen height should be at least twice the diameter. Methods for



preparation of specimens are set forth in Engineer Manual EM 1110-2-1906.<sup>67</sup>

## EQUIPMENT

### TRIAXIAL TEST CELL

The triaxial cell shown schematically in Figure D1 is suitable for use in resilient testing of soils. The equipment is similar to most standard cells. However, there are a few specialized criteria that must be met to provide acceptable test results. Generally, the equipment is slightly larger than most standard cells to accommodate the 6-in.-diam specimens and the internally mounted load and deformation measuring equipment. Additional outlets for the electrical leads from these measuring devices are required.

Cell pressures of 80 psi are generally sufficient to duplicate the maximum confining pressures under aircraft loadings. Compressed air is generally used as the confining fluid to avoid detrimental effects of water on the internally mounted electronic measuring equipment.

### END PLATENS

End platens should be "frictionless," as "barrelling" caused by end restraint jeopardizes resilient Poisson's ratio values by causing lateral deformations to be concentrated in the middle of the specimen. Furthermore, nonuniform displacements can create problems with axial strain measurements due to realignment of the LVDT clamps. Whereas "frictionless" platens (Figure D2) may not be entirely frictionless under short-term repetitive loadings, they constitute an improvement over conventional end platens. The essential features of "frictionless" end platens are (a) hard polished end plates, (b) coated by high-vacuum silicone grease, (c) covered by a thin rubber sheet. If externally mounted axial deformation measuring devices, such as an LVDT or potentiometer mounted on the loading piston, or devices measuring the total specimen displacements are used, the use of frictionless caps and bases with grease invalidates any measurements. In this case, the deformation due to the grease and rubber sheet or Teflon probably exceeds the actual



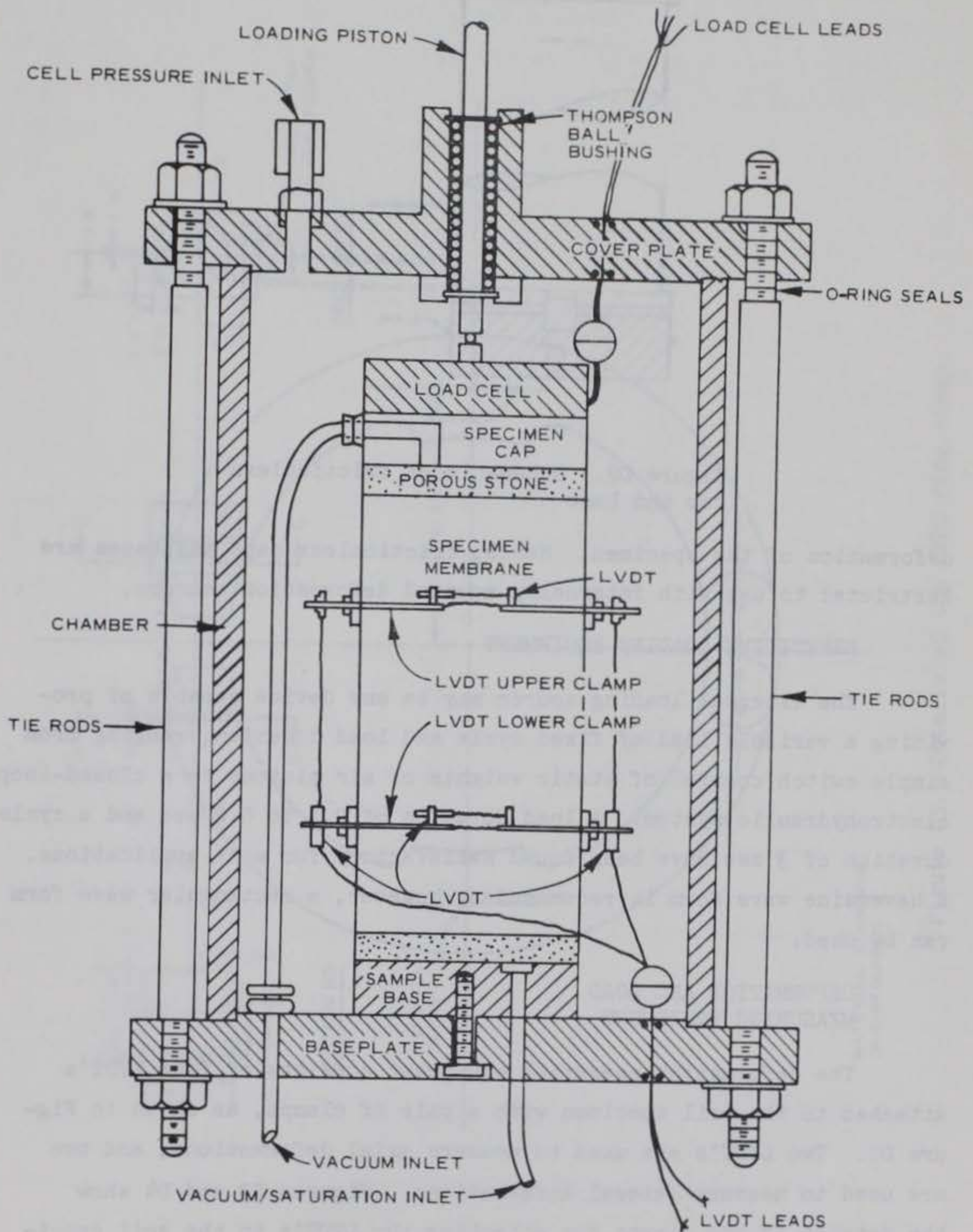


Figure D1. Triaxial cell used in resilience testing of granular base material

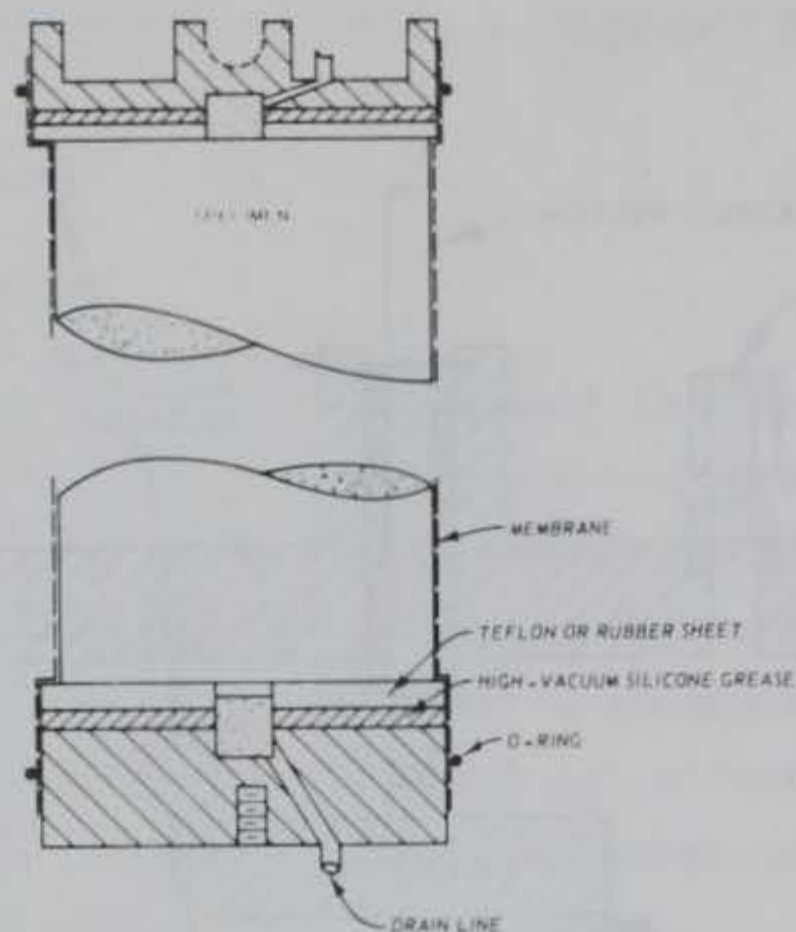


Figure D2. Schematic of frictionless cap and base

deformation of the specimen. Hence, frictionless caps and bases are restricted to use with internally mounted deformation sensors.

#### REPETITIVE LOADING EQUIPMENT

The external loading source may be any device capable of providing a variable load of fixed cycle and load duration, ranging from simple switch control of static weights or air pistons to a closed-loop electrohydraulic system. A load duration of 0.1 to 0.2 sec and a cycle duration of 3 sec have been found satisfactory for most applications. A haversine wave form is recommended; however, a rectangular wave form can be used.

#### DEFORMATION AND LOAD MEASURING EQUIPMENT

The deformation measuring equipment consists of four LVDT's attached to the soil specimen with a pair of clamps, as shown in Figure D1. Two LVDT's are used to measure axial deformations, and two are used to measure lateral deformations. Figures D3 and D4 show the details of the clamps for attaching the LVDT's to the soil specimens. Only a-c transducers that have a minimum sensitivity of



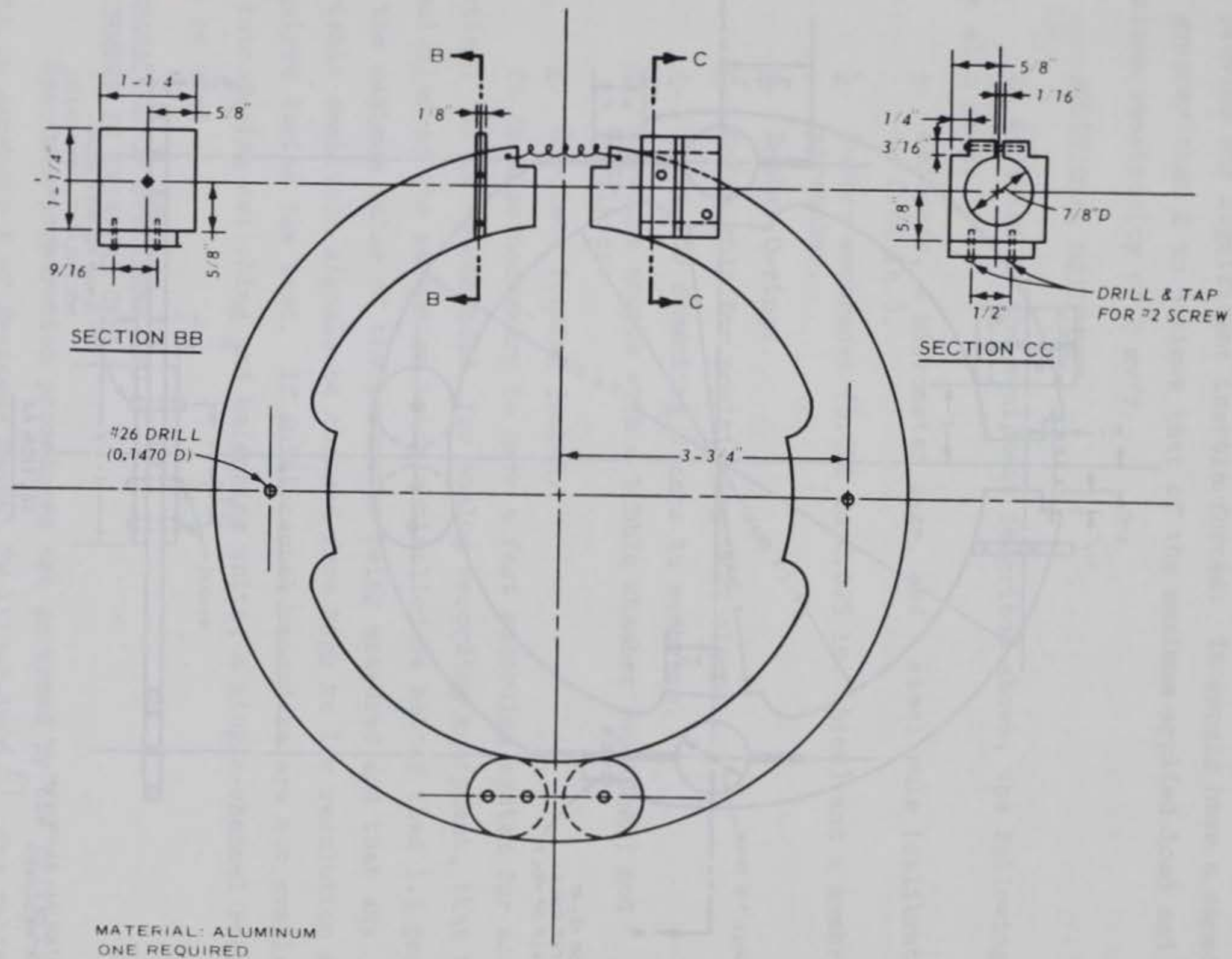


Figure D3. Details of top LVDT ring clamp

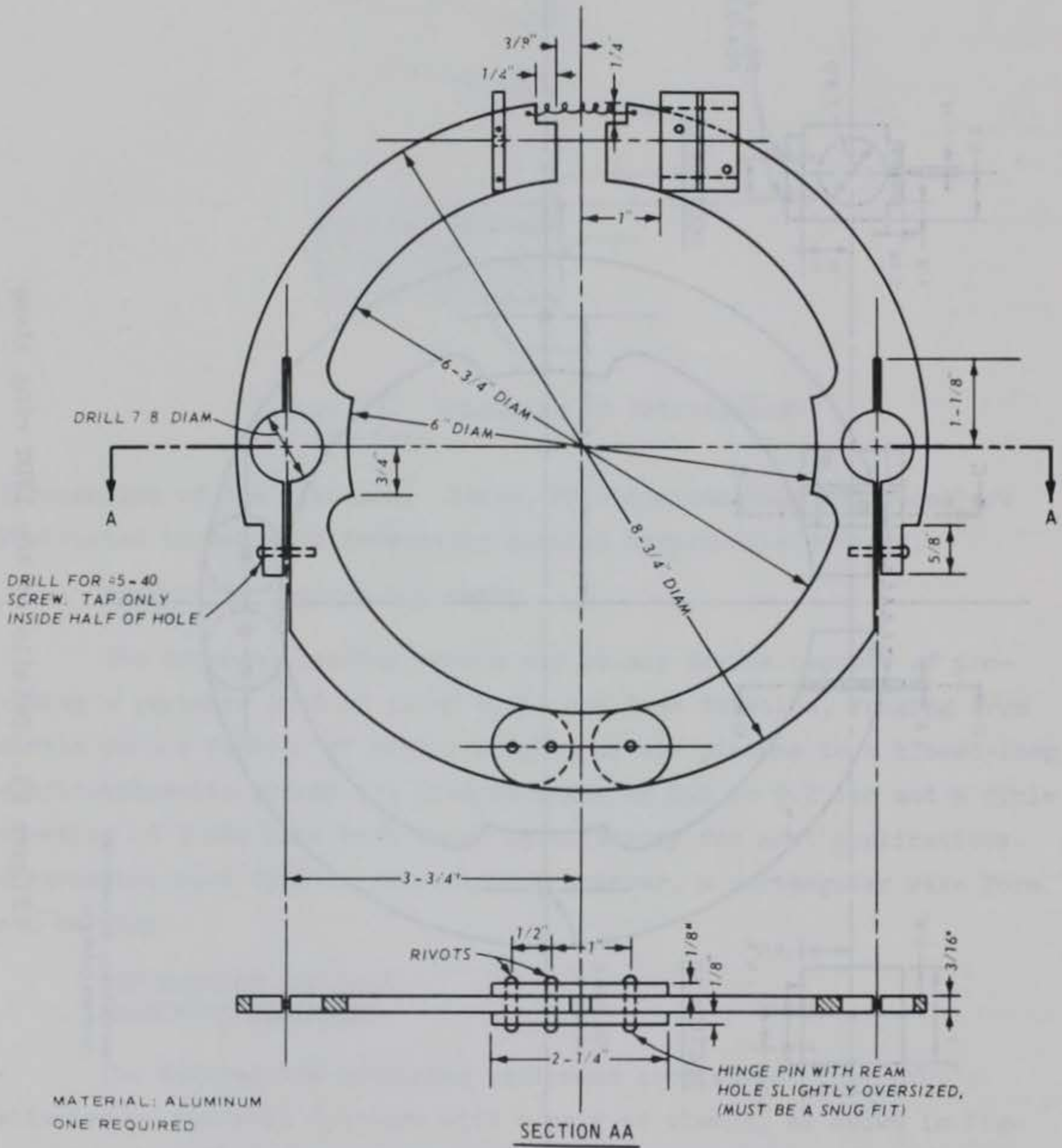


Figure D4. Details of bottom LVDT ring clamp



0.2 mv/0.001 in./v should be used. Load is measured with an internally mounted load cell that is sufficiently lightweight so as not to provide any significant inertia forces. It should have a capacity no greater than 2 to 3 times that of the maximum applied load and a minimum sensitivity of 2 mv/v.

#### ADDITIONAL EQUIPMENT

In addition to the equipment described above, the following items are also used:

- a. Calipers, a micrometer gage, and a steel rule (calibrated to 0.01 in.).
- b. Rubber membranes (0.012 to 0.025 in. thick) and a membrane stretcher.
- c. Rubber O-rings.
- d. Guide rods for positioning LVDT clamps.
- e. Epoxy for cementing clamps to membrane.
- f. A vacuum source with a bubble chamber (optional) and regulator.
- g. Specimen forming jacket.

It is also necessary to have a fast recording system for accurate testing. It is recommended, for analog recording equipment, that the resolution of the parameter being controlled be better than 1.5 percent of the maximum value of the parameter being measured and that any variable amplitude signals be changed from high to low resolution as required during the test. If multichannel recorders are not available, by introducing switching and balancing units, a single-channel recorder can be used.

#### PREPARATION OF SPECIMENS AND PLACEMENT IN TRIAXIAL CELL

Specimen preparation procedures are governed by the criteria set forth in Appendix X of Engineer Manual EM 1110-2-1906.<sup>67</sup> The following procedures describe a step-by-step account for preparing remolded specimens. Generally, for base course materials, 6-in.-diam specimens are required with the maximum particle size being limited to 1 in. in diameter.



## MATERIAL PREPARATION

The material should be air-dried and subsequently sufficient water added to bring the material to the desired compaction water content (usually field condition). Sealing the material in a container for 24 hr prior to compaction will allow the moisture to equilibrate. For well-graded materials, it may be necessary to break the material down into several sieve sizes and recombine for each layer to prevent serious segregation of material in the specimen. If the compaction effort required to duplicate the desired testing water content and density is known, sufficient material for several specimens may have to be prepared. The compaction effort required will then be established on a trial-and-error basis.

## SPECIMEN COMPACTION

Generally, base course materials are compacted on the triaxial cell baseplate using a split mold. If the particles are angular, two membranes may be required: one used during compaction and the second placed after compaction to seal any holes punctured in the membrane. A successful procedure has been to use a Teflon-lined mold and a thin sheet of wrapping paper instead of a membrane. Often the density is sufficiently high and the water content such that effective cohesion will permit a free-standing specimen to be prepared. In this case, the wrapping paper is carefully removed and a membrane substituted. In most cases, impact or kneading compaction is used. Although EM 1110-2-1906<sup>67</sup> mentions vibratory compaction, vibratory compaction is only permitted on uniform materials where segregation is not a problem. The specimens should be compacted in layers, the height of which exceeds the maximum particle size.

It may be necessary to place a thin layer of fine sand in the bottom layer to provide a smooth bearing surface. Likewise, after compacting and trimming the topmost layer (it may be necessary to remove large particles from this layer), fine sand can be sieved on the surface to fill in the voids and provide a smooth bearing surface for the top cap.



Center the top cap and lightly tap the cap to level and ensure a good smooth contact of the cap on the specimen. A level placed on top of the cap is used to check leveling. The forming mold is then removed, the membrane placed using a membrane stretcher and sealed with O-rings or a hose clamp, and a vacuum applied. Check for leakage by using a bubble chamber or closing the vacuum line and observing if a vacuum is maintained in the specimen. Specimen dimensions should be measured to determine density conditions. A  $\pi$ -tape has been found most useful for diametrical measurements.

#### PLACEMENT OF LVDT MEASUREMENT CLAMPS

Measure the diameter as accurately as possible at the location of the LVDT clamps for calculation of radial strains. Place the lower LVDT clamp in the specimen at approximately the lower third point of the specimen. A "jig" or gage rods have been used successfully to assist in placing the clamps. The lower LVDT clamp generally holds the LVDT body. Repeat the procedure for the upper clamp, being careful to align the clamps so the LVDT core matches the LVDT body. It is essential that the clamps lie in a horizontal plane and their spacing be precisely known for calculating the axial strain. Again, gage rods or a "jig" in conjunction with a small level have been used successfully for this operation. With the clamps in position and secured by the springs, a small amount of epoxy (a "5-min" epoxy has been used; rubber cement was found unacceptable) is placed on top of the four contact points and allowed to dry.

Install the LVDT's and connect the recording unit. Generally,  $\pm 0.040$ -in. LVDT's are used for radial deformations, while  $\pm 0.100$ -in. LVDT's are used for axial deformations. Balance the vertical spacing between LVDT clamps or check gage rods for secure contact, and record LVDT readings and spacing. Remove gage rods and assemble triaxial chamber. Any shifting of LVDT clamps during chamber assembly will be noted by LVDT reading changes and can be accounted for.



## RESILIENT TESTING

The resilient properties of granular materials are dependent primarily upon confining pressure and to a lesser extent upon cyclic deviator stress. Therefore, it is necessary to conduct the tests for a range of confining pressures and deviator stress values. Generally, chamber pressure values of 2, 4, 6, and 10 psi are suitable. Ratios of  $\sigma_1/\sigma_3$  of 2, 3, 4, and 5 are typically used for the cyclic deviator stress. Tests should be conducted in an undrained condition with excess pressures relieved after application of each stress state. The testing procedure is as follows:

- a. Balance the recorders and recording bridges and record calibration steps.
- b. Apply about 2-psi axial load  $\sigma_d$  as a seating load simulating the weight of the pavement and ensuring contact is maintained between the loading piston and top cap during testing.
- c. Condition the specimen by applying 500 to 1000 load repetitions with drainage lines open. This conditioning stress should be the maximum stress expected to be applied to the specimen in the field by traffic. If this is unknown, a chamber pressure of 5 or 10 psi and a deviator stress ( $\sigma_1 - \sigma_3$ ) twice the chamber pressure can be used.
- d. Decrease the chamber pressure to the lowest value to be used. Apply 200 load repetitions of the smallest deviator stress under undrained conditions, recording the resilient deformations and load at or near the 200th repetition. After 200 load repetitions, relieve any pore pressures, increase the deviator stress to the next highest value, and repeat procedure over the range of deviator stresses to be used.
- e. After completing the stress states for the initial confining pressure, repeat for each succeeding higher chamber pressure.
- f. After completion of the loading, remove the axial load, apply a vacuum to the specimen, release the confining pressure, and disassemble the triaxial chamber.
- g. Check the calibration of the LVDT's and load cell.
- h. Dry the entire specimen for determination of the water content.



## COMPUTATIONS AND PRESENTATION OF RESULTS

### COMPUTATIONS

The computations consist of the following:

- a. From the measured dimensions and weights, compute and record the initial dry density, degree of saturation, and water content using the equations in Appendix II, EM 1110-2-1906.<sup>67</sup>
- b. The resilient modulus is computed and recorded for each stress state using the following formulas:
  - (1) Resilient axial strain  $\epsilon_R = \Delta H_r / H_i$ .
  - (2) Resilient lateral strain  $\epsilon_l = \Delta D_r / D_i$ .
  - (3) Deviator stress  $\sigma_d = \Delta P / A_o$ .
  - (4) Resilient modulus  $M_R = \sigma_d / \epsilon_R$ .
  - (5) Resilient Poisson's ratio  $\nu_R = \epsilon_l / \epsilon_R$ .

where

$\Delta H_r$  = resilient change in gage height (distance between LVDT clamps) after specified number of load repetitions

$H_i$  = instantaneous gage height after specified number of load repetitions. Can be calculated from  $H_o - \Delta H$ . If  $\Delta H$  is small,  $H_o$  can be used.

$H_o$  = initial gage height or distance between LVDT's less adjustments occurring during triaxial chamber assembly

$\Delta H$  = permanent change in gage height

$\Delta P$  = change in axial load, maximum axial load minus surcharge load

$A_o$  = original cross-sectional area of specimen

$\Delta D_r$  = resilient change in diameter after specified number of load repetitions

$D_i$  = instantaneous diameter after specified number of load repetitions. Can be calculated from  $D_o + \Delta D$ .

$D_o$  = initial specimen diameter

$\Delta D$  = permanent change in specimen diameter

### PRESENTATION OF RESULTS

Test results should be presented in the form of plots of  $\log M_R$  versus  $\log$  of the sum of the principal stresses and  $\nu_R$  versus the

principal stress ratio (Figure D5). The equation of the line for resilient modulus is  $M_R = K_1(\theta)^{K_2}$  where  $K_1$  is the intercept when  $\theta = 1$  psi and  $K_2$  is the slope of the line.

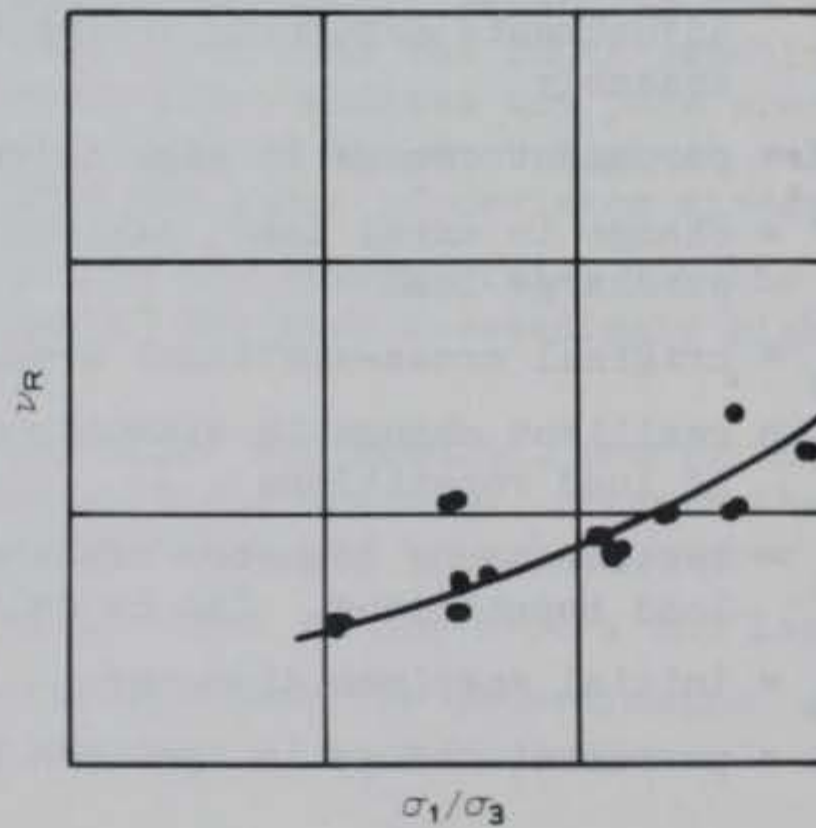
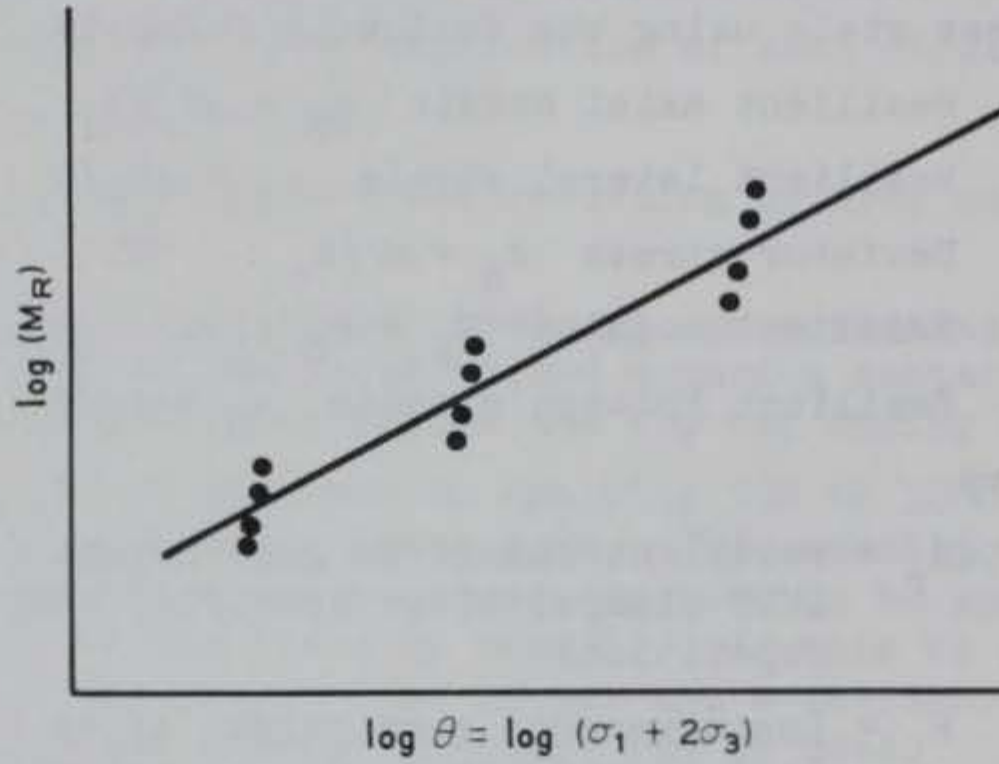


Figure D5. Representation of results of resilience test on cohesionless soils



## APPENDIX E: LABORATORY PROCEDURE FOR DETERMINING THE RESILIENT MODULUS OF SUBGRADE SOILS

The objective of this test procedure is to determine a modulus value for subgrade soils by means of resilient triaxial techniques. The test is similar to a standard triaxial compression test, the primary exception being that the deviator stress is applied repetitively and at several stress levels. This procedure allows testing of soil specimens in a repetitive stress state similar to that encountered by a soil in a pavement under a moving wheel load.

### DEFINITIONS

The following symbols and terms are used in the description of this procedure:

- a.  $\sigma_1$  = total axial stress.
- b.  $\sigma_3$  = total radial stress; i.e., confining pressure in the triaxial test chamber.
- c.  $\sigma_d = \sigma_1 - \sigma_3$  = deviator stress; i.e., the repeated axial stress in this procedure.
- d.  $\epsilon_1$  = total axial strain due to  $\sigma_d$ .
- e.  $\epsilon_R$  = resilient or recoverable axial strain due to  $\sigma_d$ .
- f.  $\epsilon_\ell$  = resilient or recoverable axial strain due to  $\sigma_d$ .
- g.  $M_R = \sigma_d / \epsilon_R$  = resilient modulus.
- h.  $\nu_R = \epsilon_R / \epsilon_\ell$  = resilient Poisson's ratio.
- i.  $\theta = \sigma_1 + 2\sigma_3 = \sigma_d + 3\sigma_3$  = sum of the principal stresses in the triaxial state of stress.
- j.  $\sigma_1 / \sigma_3$  = principal stress ratio.
- k. Load duration = time interval over which the specimen is subjected to a deviator stress.
- l. Cycle duration = time interval between successive applications of a deviator stress.

### SPECIMENS

Various diameter soil specimens may be used in this test, but the recommended specimen diameter is 2.5 to 3.0 in., or at least four times maximum particle size for granular materials. The specimen height should



be at least twice the diameter. Undisturbed or laboratory molded specimens can be used. Procedures for obtaining undisturbed soil specimens are given in Engineer Manual EM 1110-2-1907, "Soil Sampling."<sup>68</sup> Methods for laboratory preparation of molded specimens and for back-pressure saturation of specimens, if required, are presented in EM 1110-2-1906, "Laboratory Soils Testing."<sup>67</sup>

## EQUIPMENT

### TRIAxIAL TEST CELL

The triaxial cell in Figure E1 is suitable for use in resilience testing of soils. This equipment is similar to most standard cells, with the exceptions of being somewhat larger to facilitate the internally mounted load and deformation measuring equipment and having additional outlets for the electrical leads from the measuring devices. For the type of equipment shown, air or nitrogen is used as the cell fluid.

### REPETITIVE LOADING EQUIPMENT

The external loading source may be any device capable of providing a variable load of fixed cycle and load duration, ranging from simple cam-and-switch control of static weights of air pistons to a closed-loop electrohydraulic system. A load duration of 0.2 sec and a cycle duration of 3 sec have been found to be satisfactory for most applications. A haversine wave form is recommended; however, a rectangular wave form can be used.

### DEFORMATION AND LOAD MEASURING EQUIPMENT

The deformation measuring equipment consists of linear variable differential transducers (LVDT's) attached to the soil specimen by a pair of clamps. The transducers should have a high resolution and a small range to measure the extremely small resilient deformations. Two LVDT's are used for the measurement of axial deformation, and two for the measurement of lateral deformation. The clamps and LVDT's are shown in position on a soil specimen in Figure E1, and the details of the



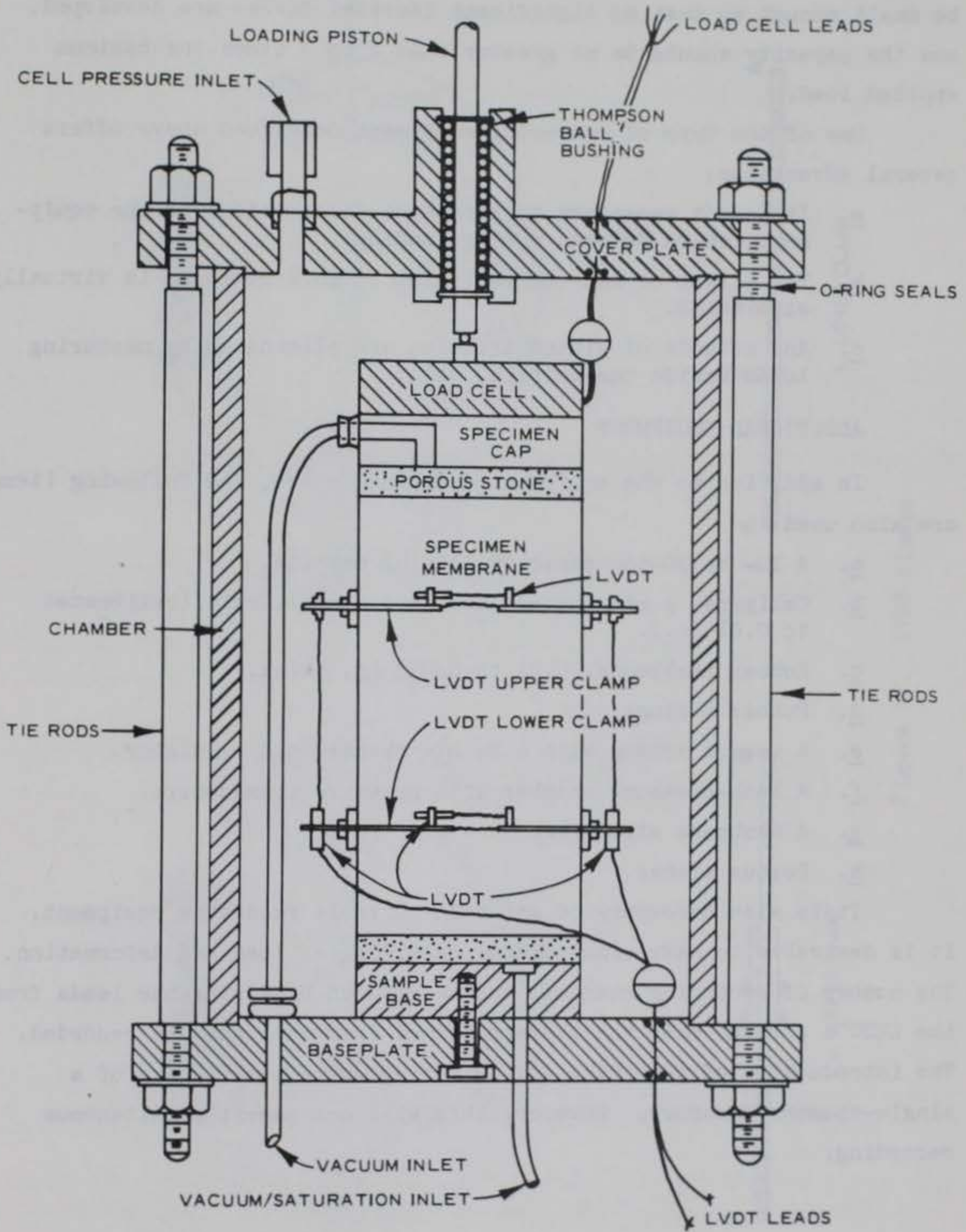


Figure E1. Triaxial cell

clamps in Figure E2. Load is measured by placing a load cell between the specimen cap and the loading piston (Figure E1). The load cell must be small enough so that no significant inertial forces are developed, and the capacity should be no greater than 2 to 3 times the maximum applied load.

Use of the type of measuring equipment described above offers several advantages:

- a. It is not necessary to reference deformations to the equipment, which deforms during loading.
- b. The effect of end-cap restraint on soil response is virtually eliminated.
- c. Any effects of piston friction are eliminated by measuring loads inside the triaxial cell.

#### ADDITIONAL EQUIPMENT

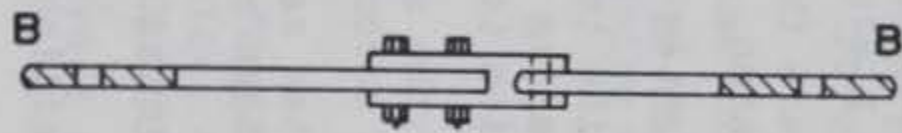
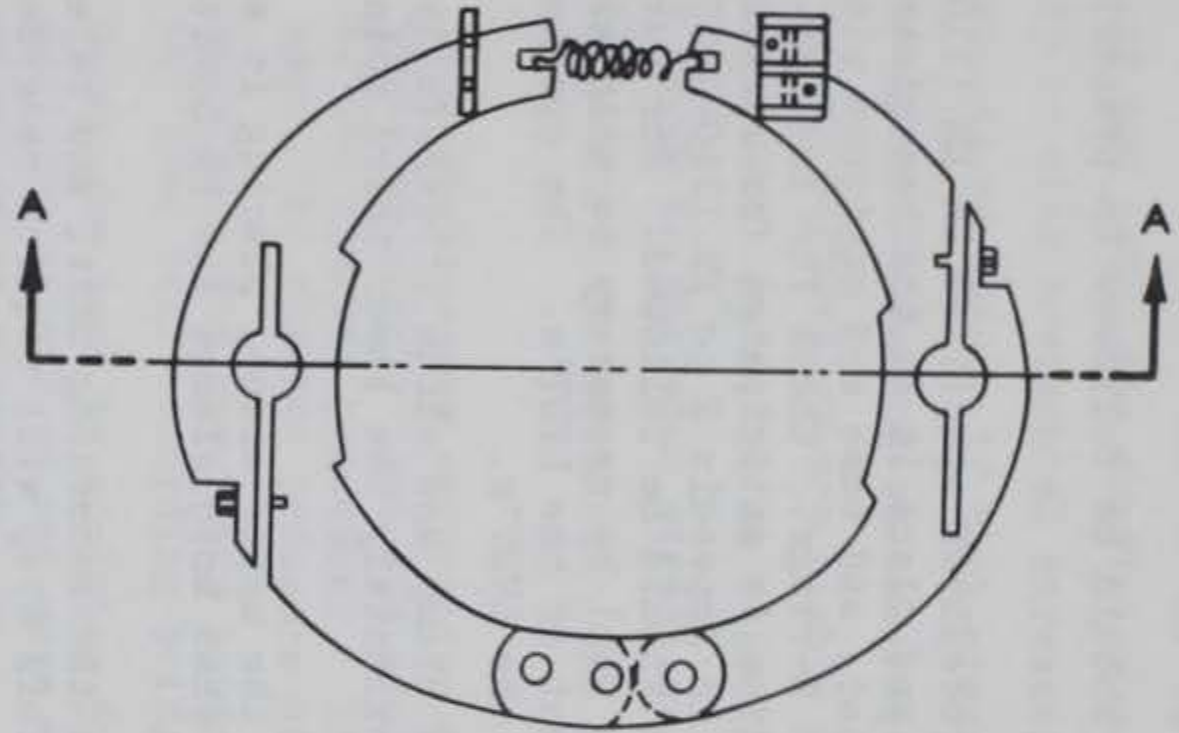
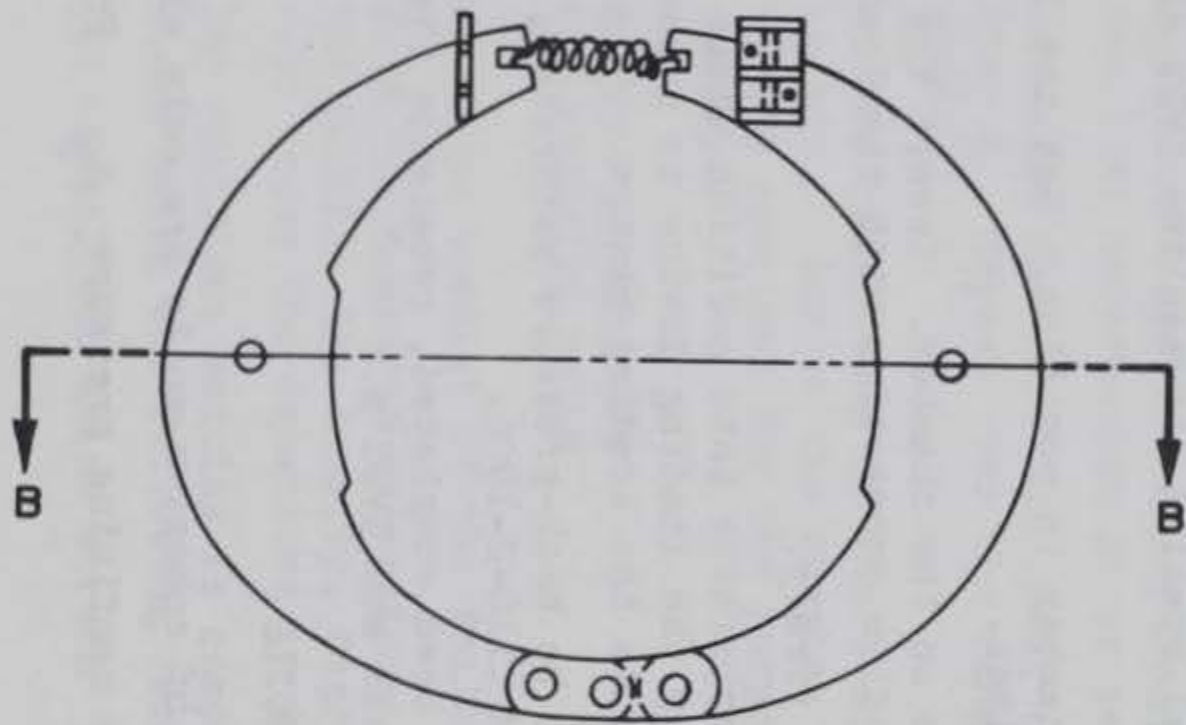
In addition to the equipment described above, the following items are also used:

- a. A 10- to 30-ton-capacity loading machine.
- b. Calipers, a micrometer gage, and a steel rule (calibrated to 0.01 in.).
- c. Rubber membranes, 0.01 to 0.025 in. thick.
- d. Rubber O-rings.
- e. A vacuum source with a bubble chamber and regulator.
- f. A back-pressure chamber with pressure transducers.
- g. A membrane stretcher.
- h. Porous stones.

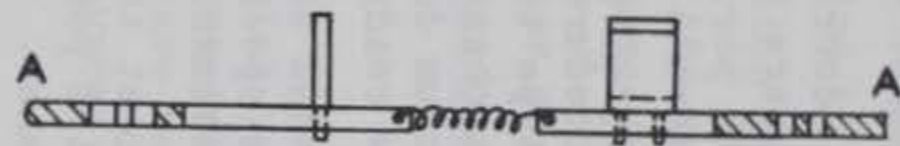
It is also necessary to maintain suitable recording equipment. It is desirable to have simultaneous recording of load and deformation. The number of recording channels can be reduced by wiring the leads from the LVDT's so that only the average signal from each pair is recorded. The introduction of switching and balancing units permits use of a single-chamber recorder. However, this will not permit simultaneous recording.



E-5



a. UPPER CLAMP



b. LOWER CLAMP

Figure E2. LVDT clamps

## PREPARATION OF SPECIMENS AND PLACEMENT IN TRIAXIAL CELL

The following procedures should be followed in preparing and placing specimens:

- a. In accordance with procedures specified in EM 1110-2-1906,<sup>67</sup> prepare the specimen and place it on the baseplate complete with porous stones, cap, and base and equipped with a rubber membrane secured with O-rings. Check for leakage. If back-pressure saturation is anticipated for cohesive soils, procedures indicated in Appendix X to EM 1110-2-1906 for the Q-type triaxial tests should be followed. For purely noncohesive soils, it will be necessary to maintain the vacuum during placement of the LVDT's. The specimen is now ready to receive the LVDT's.
- b. Extend the lower LVDT clamp and slide it carefully down over the specimen to approximately the lower third point of the specimen.
- c. Repeat this step for the upper clamp, placing it at the upper third point. Ensure that both clamps lie in horizontal planes.
- d. Connect the LVDT's to the recording unit, and balance the recording bridges. This step will require recorder adjustments and adjustment of the LVDT stems. When a recording bridge balance has been obtained, determine (to the nearest 0.01 in.) the vertical spacing between the LVDT clamps and record this value.
- e. Place the triaxial chamber in position. Set the load cell in place on the specimen.
- f. Place the cover plate on the chamber. Insert the loading piston, and obtain a firm connection with the load cell.
- g. Tighten the tie rods firmly.
- h. Slide the assembled apparatus into position under the axial loading device. Bring the loading device to a position in which it nearly contacts the loading piston.
- i. If the specimen is to be back-pressure saturated, proceed in accordance with EM 1110-2-1906.
- j. After saturation has been completed, rebalance the recorder bridge to the load cell and LVDT's.

## RESILIENCE TESTING OF COHESIVE SOILS

The resilient properties of cohesive soils are only slightly affected by the magnitude of the confining pressure  $\sigma_3$ . For most



applications, this effect can be disregarded. When back-pressure saturation is not used, the confining pressures used should approximate the expected in situ horizontal stresses. Chamber pressures of 2, 4, and 6 psi should be used. If back-pressure saturation is used, the chamber pressure will depend on the required saturation pressure.

Resilient properties are highly dependent on the magnitude of the deviator stress  $\sigma_d$ . It is therefore necessary to conduct the tests for a range in deviator stress values. Deviator stresses ranging from 2 to 16 psi are recommended. The following procedure should be followed:

- a. If back-pressure saturation is not used, connect the chamber pressure supply line and apply the confining pressure (equal to the chamber pressure). If back-pressure saturation is used, the chamber pressure will already have been established.
- b. Rebalance the recording bridges for the LVDT's, and balance the load cell recording bridge.
- c. Begin the test by applying 500 to 1000 repetitions of a deviator stress of not more than one-half the unconfined compressive strength.
- d. Decrease the deviator load to the lowest value to be used. Apply 200 repetitions of load, recording the recovered vertical deformation at or near the last repetition.
- e. Increase the deviator load, recording deformations as in Step d. Repeat over the range of deviator stresses to be used.
- f. At the completion of the loading, reduce the chamber pressure to zero. Remove the chamber LVDT's and load cell. Use the entire specimen for the purpose of determining the moisture content.

#### COMPUTATIONS AND PRESENTATION OF RESULTS FOR COHESIVE SOILS

Computations consist of the following:

- a. From the measured dimensions and weights, compute and record the initial dry density, degree of saturation, and water content using the equations in Appendix II, EM 1110-2-1906.<sup>67</sup>
- b. The resilient modulus is computed and recorded for each stress state using the following formulas:

(1) Resilient axial strain  $\epsilon_R = \Delta H_r / H_i$ .



- (2) Resilient lateral strain  $\epsilon_l = \Delta D_r / D_i$  .
- (3) Deviator stress  $\sigma_d = \Delta P / A_o$  .
- (4) Resilient modulus  $M_R = \sigma_d / \epsilon_r$  .

where

$\Delta H_r$  = resilient change in gage height (distance between LVDT clamps) after specified number of load repetitions.

$H_i$  = instantaneous gage height after specified number of load repetitions. Can be calculated from  $H_o - \Delta H$  . If  $\Delta H$  is small,  $H_o$  can be used.

$H_o$  = initial gage height or distance between LVDT's less adjustments occurring during triaxial chamber assembly

$\Delta H$  = permanent change in gage height

$\Delta P$  = change in axial load, maximum axial load minus surcharge load

$A_o$  = original cross-sectional area of specimen

$\Delta D_r$  = resilient change in diameter after specified number of load repetitions

$D_i$  = instantaneous diameter after specified number of load repetitions. Can be calculated from  $D_o + \Delta D$  .

$D_o$  = initial specimen diameter

$\Delta D$  = permanent change in specimen diameter

The results of the resilience tests can be presented in the form of a summary table, such as Table E1, and graphically as shown in Figure E3 for the resilient modulus.

#### RESILIENCE TESTING OF COHESIONLESS SOILS

The resilient modulus of cohesionless soils  $M_R$  is dependent upon the magnitude of the confining pressure  $\sigma_3$  and is nearly independent of the magnitude of the repeated axial stress. Therefore, it is necessary to test cohesionless materials over a range of confining and axial stresses. (The confining pressure is equal to the chamber pressure less the back pressure for saturated specimens.) The following procedures should be used for this type of test:

- a. Use confining pressures of 2, 4, 6, and 10 psi. At each confining pressure, test at four values of the principal





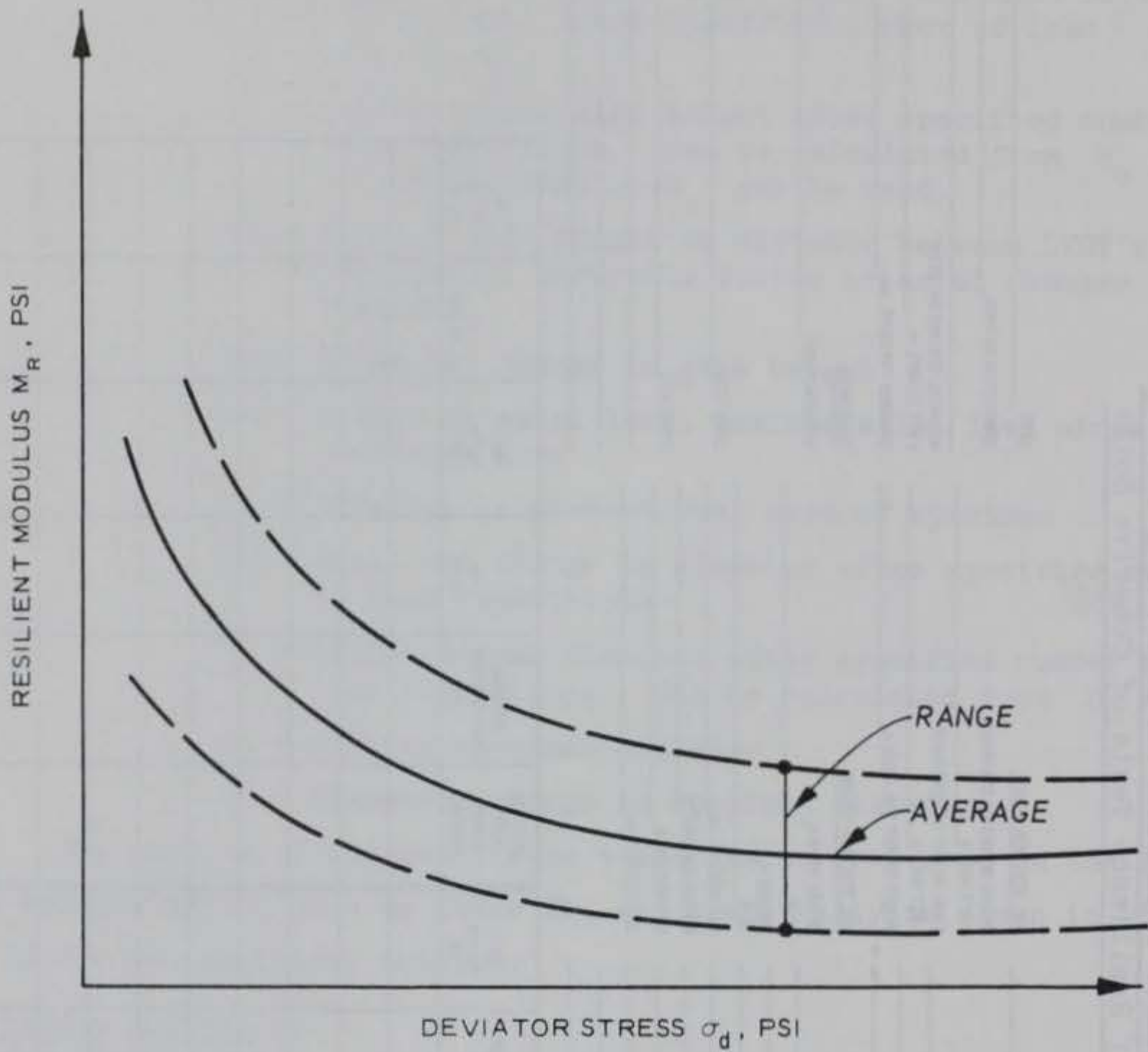


Figure E3. Presentation of results of resilience tests on cohesive soils



stress difference corresponding to multiples (2, 3, 4, 15) of the cell pressure.

- b. Before beginning to record deformations, apply a series of conditioning stresses to the material to eliminate initial loading effects. The greatest amount of volume change occurs during the application of the conditioning stresses. Simulation of field conditions suggests that drainage of saturated specimens should be permitted during the application of these loads but that the test loading (beginning in Step f below) should be conducted in an undrained state.
- c. Set the axial load generator to apply a deviator stress of 10 psi (i.e., a stress ratio equal to 3). Activate the load generator and apply 200 repetitions of this load. Stop the loading.
- d. Set the axial load generator to apply a deviator stress of 200 psi (i.e., a stress ratio equal to 5). Activate the load generator and apply 200 repetitions of this load. Stop the loading.
- e. Repeat as in Step d above maintaining a stress ratio equal to 6 and using the following order and magnitude of confining pressures: 10, 20, 10, 5, 3, and 1 psi.
- f. Begin the record test using a confining pressure of 2 psi and an equal value of deviator stress. Record the resilient deformation after 200 repetitions. Increase the deviator stress to twice the confining pressure and record the resilient deformation after 200 repetitions. Repeat until a deviator stress of 4 times the confining pressure is reached (stress ratio of 5).
- g. Repeat as in Step f above for each value of confining pressure.
- h. When the test is completed, decrease the back pressure to zero, reduce the chamber pressure to zero, and dismantle the cell. Remove the LVDT clamps, etc. Remove the soil specimen, and use the entire amount of soil to determine the moisture content.

#### COMPUTATIONS AND PRESENTATION OF RESULTS FOR COHESIONLESS SOILS

Computations are similar to those for cohesive soils. The ratio of axial and confining stress and the first stress invariant are added. Tests results can be presented in the form of a summary table, such as Table E2, or a plot of  $\log M_R$  versus log of the sum of the principal stresses (Figure E4).

Table E2

Example Data Form for Recording Results of Resilience Tests of Cohesive Soils

SOIL SAMPLE _____ _____ LOCATION _____ SAMPLE NO. _____ SPECIFIC GRAVITY $G_s$ _____ SOIL SPECIMEN MEASUREMENTS DIAMETER (in.) $\left\{ \begin{array}{l} \text{TOP} \text{ _____} \\ \text{MIDDLE} \text{ _____} \\ \text{BOTTOM} \text{ _____} \\ \text{AVERAGE} \text{ _____} \end{array} \right.$ MEMBRANE THICKNESS, in. _____ NET DIAMETER, in. _____ SPECIMEN + CAP + BASE HEIGHT, in. _____ CAP + BASE HEIGHT, in. _____ INITIAL LENGTH $L_0$ , in. _____	SOIL SPECIMEN WEIGHT INITIAL WEIGHT OF CONTAINER + WET SOIL, g _____ FINAL WEIGHT OF CONTAINER + WET SOIL, g _____ WEIGHT OF WET SOIL USED, g _____ SOIL SPECIMEN VOLUME INITIAL AREA $A_0$ (in. <sup>2</sup> ) _____ VOLUME $A_0 L_0$ (in. <sup>3</sup> ) _____ WET DENSITY, pcf _____ WATER CONTENT, % _____ SATURATION, % _____ DRY DENSITY, pcf _____ VOID RATIO $e$ _____	DATE _____ COMPACTION METHOD _____ VERTICAL SPACING BETWEEN LVDT CLAMPS, in. _____ CONSTANTS VERTICAL LVDT _____ LOAD CELL _____ COMMENTS _____ _____ _____
---	---	---

CONFINING PRESSURE $\sigma_3$ psi	LOAD CELL CHART READING	DEVIATOR LOAD lb	$\sigma_d = \sigma_1 - \sigma_3$ psi	$\sigma_1/\sigma_3$ psi	$\sigma_1$ psi	VERTICAL LVDT CHART READING	VERTICAL DEFORMATION in.	$\epsilon_R$ in./in.	$M_R = \sigma_d / \epsilon_R$ psi	$\epsilon_f$ in./in.	$\epsilon_{Rf}$ in./in.

E-12



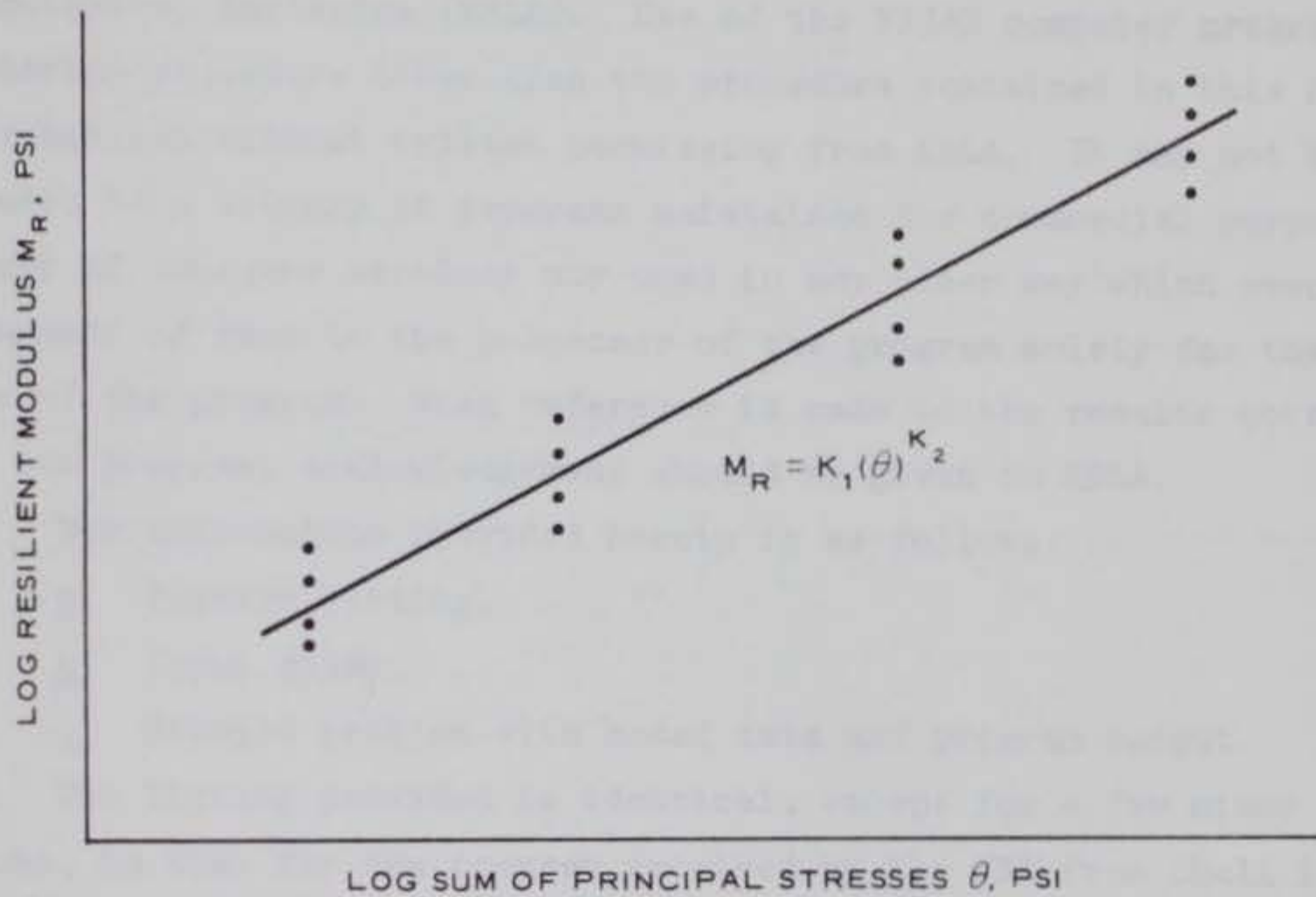


Figure E4. Presentation of results of resilience tests on cohesionless soils

APPENDIX F: USER INFORMATION FOR THE  
BISAR COMPUTER PROGRAM

INTRODUCTION

The copyright of much of the information provided herein is vested in Shell Research N.V. The information is published with the expressed permission of the Shell Oil Company and Koninklijke/Shell Laboratorium, Amsterdam (KSLA). Use of the BISAR computer program in any design procedure other than the procedure contained in this document is prohibited without written permission from KSLA. It may not be included in a library of programs maintained for commercial purposes by sellers of computer services nor used in any other way which results in payment of fees to the possessor of the program solely for the usage of the program. When reference is made to the results obtained with the program, acknowledgement should be given to KSLA.

The information provided herein is as follows:

- a. Program listing.
- b. Input guide.
- c. Example problem with coded data and program output.

The listing provided is identical, except for a few minor modifications, to that for the program received by the WES from Shell in 1974. The modifications made at the WES are primarily changes in input format and changes necessary for the program to run on a Honeywell 6000 series computer. The information provided with the input guide was extracted from the User's Manual<sup>23</sup> for the BISAR computer program. The data for the example problem were developed at the WES, and the output given is from a Honeywell 6000 computer located there.

PROGRAM LISTING

A complete listing of the computer program is presented on the following pages.







```

C                                     =THE MIDPOINTS OF THE THREE ACCOMPANYING MAIN0620
C                                     MOHR'S CIRCLES, MAIN0630
C                                     =THE TOTAL STRAIN ENERGY AND STRAIN MAIN0640
C                                     ENERGY OF DISTORTION, MAIN0650
C-----MAIN0660
LOGICAL STRESS, EPS, RLOW, AID(27), N, L, N2, L2, NZEP, NZEQ MAIN0670
INTEGER REQUEST(27), IQ(3), DATE(3), ISTRSS(27), INTV(10), IVER1(7), MAIN0680
+ IVER2(10) MAIN0690
REAL NU, K5, MU, LDSTHS(10), HUSTH(10), LOAD, INT(17), V(15), X(10), Y(10), MAIN0700
+ A(3,3), HM(3,3), W(3), C(39), B(3,3), TEXT(20), ACCUR(3), PSI(10), AK(9), MAIN0710
+ ALK(9) MAIN0711
DOUBLE PRECISION CZ, ELLE, ELLK MAIN0720
COMMON/ASCT/LAYER, NLAYS, M, R, Z, NU(10), ACCUR, LOAD, HUSTRS, NZEHOS, H(9) MAIN0730
+, K5(10), E(10), AL(9), THICK(9), RADIUS(10) MAIN0740
COMMON/STADTA/STRESS(27), EPS(17), RLOW, ST, CT, L, ACC MAIN0750
COMMON/CJ-ST/CZ, ELLE, ELLK, ALMBDA MAIN0760
COMMON/CNTING/F10M1, F100, F101, F11M2, F11M1, F110, F111 MAIN0770
COMMON/TAPE/NOUT MAIN0780
DATA NBLANK, ISTRSS, IREF1, IREF2/ MAIN0790
+ " ", "UH ", "UT ", "UZ ", "SRH", "STT", "SZZ", "SRT", "SRZ", "STZ", "ERR" MAIN0800
+, "ETT", "EZZ", "ERT", "ERZ", "ETZ", "UX ", "UY ", "SXX", "SXY", "SXZ", "SYY" MAIN0810
+, "SYZ", "EXX", "EXY", "EXZ", "EYY", "EY ", "LOAD", "STHS"/ MAIN0820
DATA REQUEST/"UH ", "UT ", "UZ ", "SRH", "STT", "SZZ", "SRT", "SRZ", "STZ",
1"ERR",
2"ETT", "EZZ", "ERT", "ERZ", "ETZ", "UX ", "UY ", "SXX", "SXY", "SXZ", "SYY",
3"SYZ", "EXX", "EXY", "EXZ", "EYY", "EY "/
DATA IVER1, IVER2/1,2,3,6,7,13,14,4,5,8,9,10,11,12,15,16,17/ MAIN0830
DATA IDENT/"LOAD"/
C-----MAIN0840
C                                     THESE ARE THREE ACCURACIES MAIN0850
C                                     ACCUR(1) IS USED FOR TESTING SEVERAL MAIN0860
C                                     VARIABLES AGAINST EACH OTHER, MAIN0870
C                                     ACCUR(2) IS USED FOR ABSOLUTE ACCURACY MAIN0880
C                                     OF THE INTEGRATION PROCEDURE MAIN0890
C                                     ACCUR(3) IS USED FOR RELATIVE ACCURACY MAIN0900
C                                     OF THE INTEGRATION PROCEDURE MAIN0910
C                                     NIN , MAIN0920
C                                     NOUT ARE SYMBOLIC NAMES FOR INPUT AND MAIN0930
C                                     OUTPUT MEDIA RESP. MAIN0940
C-----MAIN0950
ACCUR(1)=1.0E-04 MAIN0960
ACCUR(2)=1.0E-4 MAIN0970
ACCUR(3)=1.0E-3 MAIN0980
ACC=ACCUR(1) MAIN0990
NIN=5 MAIN1000
NOUT=6 MAIN1010
V2=1.414214 MAIN1020
WRITE(NOUT,9000) MAIN1030
C-----MAIN1040
C                                     READ TEXT AND DATE CARD MAIN1050
C-----MAIN1060
READ(NIN,9010)TEXT
WRITE(NOUT,9020)TEXT
C-----MAIN1090
C                                     READ NUMBER OF SYSTEMS AND SET LOOP MAIN1100
C-----MAIN1110
READ(NIN,9030)NSYS
800 FORMAT(V)
DO 460 ISYS=1,NSYS MAIN1130
C-----MAIN1140
C                                     READ NUMBER OF LAYERS AND THEIR PARAMETERS MAIN1150

```



```

C-----MAIN1160
  READ(NIN,9030)NLAYS,ISMO,IRED
  IF(NLAYS.EQ.1) GO TO 10
  M=NLAYS-1
  DO 315 I=1,M
315 READ(NIN,9050)E(I),NU(I),THICK(I),AK(I)
10 READ(NIN,9050)E(NLAYS),NU(NLAYS)
C-----MAIN1220
C          READ NUMBER OF LOADS AND THEIR PARAMETERS MAIN1230
C-----MAIN1240
  READ(NIN,9030)NLOAD
  NZEP = .FALSE.
  NZEQ = .FALSE.
  DO 30 I=1,NLOAD
  READ(NIN,9050)LDSTRS(I),RADIUS(I),X(I),Y(I),HOSTR(I),PSI(I)
  PSI(I)=.0174533*PSI(I)
  IF(LDSTRS(I).GT.ACCUR(1)) NZEP = .TRUE.
  IF(HOSTR(I).GT.ACCUR(1)) NZEQ = .TRUE.
  IF(IDENT.EQ.IHEF1) GO TO 20
  IF(IDENT.NE.IHEF2) WRITE(NOUT,9040) LDSTRS(I),HOSTR(I)
  GO TO 30
20 LDSTRS(I) = LDSTRS(I)/(3.14159*RADIUS(I)*RADIUS(I))
  HOSTR(I) = HOSTR(I)/(3.14159*RADIUS(I)*RADIUS(I))
30 CONTINUE
C-----MAIN1410
C          TEST ON OBVIOUS MISTAKES IN SYSTEM'S DATA-MAIN1411
C          CARDS.
C          WHEN IRED % 0 THE REDUCED SPRINGCOMPLIAN- MAIN1412
C          CE WAS READ.
C          A NON-VANISHING SLIPRESISTANCE IS SUBSTI- MAIN1413
C          TUTED TO PREVENT RIGID-BODY MOTION OF THE MAIN1414
C          TOPLAYERS
C-----MAIN1450
  DO 50 J = 1,NLAYS
  IF((1.0-NU(J)).LT.ACCUR(1)) GO TO 410
  IF(E(J).LT.ACCUR(1)) GO TO 420
  IF(J.EQ.NLAYS) GO TO 50
  IF(IRED.EQ.0) GO TO 40
  ALK(J) = AK(J)
  IF(ALK(J).LT.1000.0.OR..NOT.NZEQ) GO TO 50
  ALK(J) = 1000.0
  AK(J) = 1000.0
  GO TO 50
40 ALK(J) = AK(J)*E(J)/(1.0+NU(J))
  IF(ALK(J).LT.1000.0.OR..NOT.NZEQ) GO TO 50
  ALK(J) = 1000.0
  AK(J) = ALK(J)*(1.0+NU(J))/E(J)
50 CONTINUE
C-----MAIN1490
C          OUTPUT OF ALL PHYSICAL DATA OF SYSTEM MAIN1500
C          AND LOADS BY CALLING IN SYSTEM. MAIN1510
C-----MAIN1520
  CALL SYSTEM(ISYS,E,NU,THICK,AK,NLAYS,M,NLOAD,LDSTRS,HOSTR,ALK,
+ RADIUS,X,Y,PSI,ISMO,IRED)
  IF(.NOT.NZEP.AND..NOT.NZEQ) GO TO 430
C-----MAIN1560
C          CALCULATION OF CONSTANTS USED IN SUHROU- MAIN1570
C          TIME MATRIX TO BUILT UP VARIOUS MATRICES MAIN1580
C          BY CALLING IN MACONI. MAIN1590
C-----MAIN1600
  CALL MACONI(ISMO,ALK,NEWSYS)
  MAIN1610

```



```

60 IF(NEWSYS.EQ.0) GO TO 70 MAIN1630
   CALL SYSTEM(ISYS,E,NU,THICK,AK,NLAYS,M,NLOAD,LDSTHS,H0STH,ALK, MAIN1640
   +   RADIUS,X,Y,PSI,ISHU,IRED) MAIN1650
C-----MAIN1660
C           READ STRESSES,STRAINS AND DISPLACEMENTS MAIN1670
C           TO BE CALCULATED. MAIN1680
C-----MAIN1690
70 CONTINUE
   DO 90 I=1,27 MAIN1710
     IF(REQUEST(I).EQ.NBLANK) GO TO 80 MAIN1720
     IF(REQUEST(I).NE.1STHSS(I)) WRITE(NOUT,9070) 1STHSS(I) MAIN1730
     AID(I)=.TRUE. MAIN1740
     GO TO 90 MAIN1750
80   AID(I)=.FALSE. MAIN1760
90 CONTINUE MAIN1770
C-----MAIN1780
C           CONSYS DETERMINES FOR EACH SYSTEM WHICH MAIN1790
C           STRESSES,STRAINS AND DISPLACEMENTS WILL MAIN1800
C           BE CALCULATED. MAIN1810
C-----MAIN1820
   CALL CONSYS(AID,NZEP,NZEG,N,L) MAIN1830
C-----MAIN1840
C           READ NUMBER OF POSITIONS AND SET LOOP MAIN1850
C-----MAIN1860
100 READ(NIN,9030)NPOS
    DO 400 IPOS=1,NPOS MAIN1880
      N2 = N MAIN1890
      L2 = L MAIN1900
      DO 110 I=1,3 MAIN1910
        DO 110 J=1,3 MAIN1920
          A(I,J)=0.0 MAIN1930
110
C-----MAIN1940
C           READ POINT COORDINATES AND LAYERNUMBER. MAIN1950
C-----MAIN1960
   READ(NIN,9060)LAYER,AX,AY,DEPTH,ETA
     ETA=.0174533*ETA MAIN1980
     IF(NLAYS.EQ.1) LAYER=1 MAIN1990
     WRITE(NOUT,9090) IPOS,LAYER,AX,AY,DEPTH MAIN2000
     TMIN=1.0E+10 MAIN2010
     IF(NLAYS.EQ.1) GO TO 130 MAIN2020
     J=LAYER+1 MAIN2030
     J=MIN0(J,M) MAIN2040
     DO 120 I=1,J MAIN2050
       IF(THICK(I).LT.TMIN) TMIN=THICK(I) MAIN2060
120 CONTINUE MAIN2070
130 UX=0.0 MAIN2080
    UY=0.0 MAIN2090
    UZ=0.0 MAIN2100
    MU=NU(LAYER) MAIN2110
    FT=(1.0+MU)/E(LAYER) MAIN2120
C-----MAIN2130
C           SET LOOP FOR NUMBER OF LOADS. MAIN2140
C-----MAIN2150
    DO 330 I=1,NLOAD MAIN2160
      DO 140 J=1,17 MAIN2170
        INT(J)=0.0 MAIN2180
140       DO 150 J=1,27 MAIN2190
          STRESS(J)=AID(J) MAIN2200
150       IF(NLAYS.EQ.1) GO TO 160 MAIN2210
C-----MAIN2220
C           CALCULATION OF CONSTANTS NEEDED FOR THE MAIN2230

```



```

C          EVALUATION OF THE CHARACTERISTIC FUNCTI= MAIN2240
C          ONS IN MATRIX BY CALLING IN MA2CON,    MAIN2250
C          MA2CON,                                MAIN2260
C-----MAIN2270
C          CALL MA2CON(TMIN,I,ISMU,ALK)           MAIN2280
C-----MAIN2290
C          DETERMINATION OF POINT COORDINATES IN THE MAIN2300
C          CYLINDRICAL COORDINATE SYSTEM WITH LOAD= MAIN2310
C          AXIS AS AXIS OF SYMMETRY.            MAIN2320
C-----MAIN2330
160      IF(X(I).EQ.AX.AND.Y(I).EQ.AY) GO TO 170    MAIN2340
          THETA=ATAN2((AY-Y(I)),(AX-X(I)))-PSI(I)  MAIN2350
          GO TO 180                                MAIN2360
170      THETA=ETA-PSI(I)                          MAIN2370
180      RADDIS=SQRT((AX-X(I))**2+(AY-Y(I))**2)    MAIN2380
          WRITE(NOUT,9100) I,RADDIS,THETA         MAIN2390
          H=RADDIS/RADIUS(I)                      MAIN2400
          Z=DEPTH/RADIUS(I)                      MAIN2410
          IF(NLAYS.EQ.1) GO TO 230                MAIN2420
190      IF(LAYER.GT.1) GO TO 210                 MAIN2430
          IF(Z.GT.-ACCUR(1).AND.Z.LT.(H(1)+ACCUR(1))) GO TO 230 MAIN2440
200      WRITE(NOUT,9110)                         MAIN2450
          GO TO 400                                MAIN2460
210      IF(LAYER.LT.NLAYS) GO TO 220            MAIN2470
          IF(Z.GT.(H(H)-ACCUR(1))) GO TO 230     MAIN2480
          GO TO 200                                MAIN2490
220      IF(Z.GT.(H(LAYER-1)-ACCUR(1)).AND.Z.LT.(H(LAYER)+ACCUR(1)
+      )) GO TO 230                               MAIN2500
          GO TO 200                                MAIN2510
230      HADI=RADIUS(I)                           MAIN2520
          LOAD=LDSTKS(I)                          MAIN2530
          H0STKS=H0STR(I)                         MAIN2540
          HLOW=R.LT.ACCUR(1)                      MAIN2550
          ST=SIN(THETA)                          MAIN2560
          CT=COS(THETA)                          MAIN2570
          MAIN2580
C-----MAIN2590
C          COMPNT DETERMINES FOR EACH POINT=LOAD  MAIN2600
C          CONFIGURATION WHICH INTEGRALS HAVE TO BE MAIN2610
C          CALCULATED.                            MAIN2620
C-----MAIN2630
          CALL COMPNT(R,H0STRS,LOAD,Z,N2,L2)      MAIN2640
          IF(LAYER.NE.1) GO TO 250                MAIN2650
          CZ = DBLE(Z)                            MAIN2660
          IF(Z.LT.ACCUR(1).AND.ABS(R-1,0).LT.ACCUR(1)) GO TO 240 MAIN2670
          MAIN2680
C-----MAIN2690
C          ASYMPT DETERMINES THE LIPSCHITZ-MANKEL MAIN2700
C          INTEGRALS NEEDED FOR THE ASYMPTOTIC PART MAIN2710
C          OF THE INTEGRALS, FOR POINTS IN THE TOP= MAIN2720
C          LAYER ONLY.                            MAIN2730
C-----MAIN2740
          CALL ASYMPT(R,ACCUR(1))                 MAIN2750
          GO TO 250                                MAIN2760
C-----MAIN2770
C          FOR POINTS AT THE RIM OF THE LOAD THE  MAIN2780
C          LIPSCHITZ-MANKEL INTEGRALS CAN BE GIVEN MAIN2790
C          DIRECTLY.                              MAIN2800
C-----MAIN2810
240      F10M1 = 0.63662                          MAIN2820
          F100 = 0.5                              MAIN2830
          F11M1 = 0.5                             MAIN2840
          F11M2 = 0.424413                       MAIN2850

```



```

      F101 = 0.0
      F110 = 0.0
      F111 = 0.0
C-----
C                                     COMPUTATION OF THE REQUIRED INTEGRALS BY
C                                     CALLING IN GENDAT AND INGRAL
C-----
250      INTT = 0
      DO 260 J = 1,17
          INT(J) = 0.0
260      CONTINUE
      DO 270 J = 1,10
          INTV(J) = 0
          K = IVER2(J)
          IF(.NOT.EPS(K)) GO TO 270
          INTV(J) = K
          INTT = INTT+1
270      CONTINUE
          IF(INTT.EQ.0) GO TO 280
          IF(NLAYS.NE.1) CALL GENDAT(1,NZEROS,R,ACC)
          CALL INGRAL(2,INTV,INTT,INT)
280      INTT = 0
      DO 290 J = 1,7
          INTV(J) = 0
          K = IVER1(J)
          IF(.NOT.EPS(K)) GO TO 290
          INTV(J) = K
          INTT = INTT+1
290      CONTINUE
          IF(INTT.EQ.0) GO TO 300
          IF(NLAYS.NE.1) CALL GENDAT(0,NZEROS,R,ACC)
          CALL INGRAL(1,INTV,INTT,INT)
300      PS10 = PS1(I)
C-----
C                                     CALC COMPUTES AND OUTPUTS THE STRESSES,
C                                     STRAINS AND DISPLACEMENTS, INDUCED BY EACH
C                                     LOAD SEPARATELY.
C-----
      CALL CALC(INT,V,R,MU,RADI,FT,LOAD,HOSIRS,PS10,Z)
      IF(.NOT.N2) GO TO 330
C-----
C                                     COMPUTATION AND SUMMATION OF CARTESIAN
C                                     COORDINATES, THE USED COORDINATE SYSTEM IS
C                                     THE ONE WHEREIN POINTCOORDINATES WERE
C                                     STATED.
C-----
      UZ = UZ+V(3)
      IF(ABS(RADDIS).LT.ACCUR(1)) GO TO 310
      CT = (AX-X(I))/RADDIS
      ST = (AY-Y(I))/RADDIS
      GO TO 320
310      CT = COS(ETA)
      ST = SIN(ETA)
320      CT2 = CT*CT
      ST2 = ST*ST
      STCT = ST*CT
      A(1,1) = A(1,1)+V(4)*CT2+V(5)*ST2-2.0*V(7)*STCT
      A(1,2) = A(1,2)+V(7)*(CT2-ST2)+(V(4)-V(5))*STCT
      A(1,3) = A(1,3)+V(8)*CT-V(9)*ST
      A(2,1) = A(1,2)
      A(2,2) = A(2,2)+V(4)*ST2+V(5)*CT2+2.0*V(7)*STCT

```



```

      A(2,3)=A(2,3)+V(8)*ST+V(9)*CT      MAIN3460
      A(3,1)=A(1,3)                      MAIN3470
      A(3,2)=A(2,3)                      MAIN3480
      A(3,3)=A(3,3)+V(6)                 MAIN3490
      UX   =UX+V(1)*CT-V(2)*ST          MAIN3500
      UY   =UY+V(1)*ST+V(2)*CT          MAIN3510
330    CONTINUE                          MAIN3520
      TRACE=A(1,1)+A(2,2)+A(3,3)         MAIN3530
      AH   =(1.0+MU)/E(LAYER)            MAIN3540
      AC   =MU*TRACE/E(LAYER)            MAIN3550
      DO 350 I=1,3                        MAIN3560
        DO 340 J=1,3                      MAIN3570
          B(I,J)=AH*A(I,J)                MAIN3580
          IF(I.NE.J) GO TO 340            MAIN3590
          B(I,J)=H(I,J)=AC                MAIN3600
340    CONTINUE                          MAIN3610
350    CONTINUE                          MAIN3620
-----
C                                     MAIN3630
C                                     MAIN3640
C                                     MAIN3650
C                                     MAIN3660
C                                     MAIN3670
      WRITE(NOUT,9120)                    MAIN3680
      EPS(1)=STRESS(18)                   MAIN3690
      EPS(2)=STRESS(21)                   MAIN3700
      EPS(3)=STRESS( 6)                   MAIN3710
      EPS(4)=STRESS(22)                   MAIN3720
      EPS(5)=STRESS(20)                   MAIN3730
      EPS(6)=STRESS(19)                   MAIN3740
      C(1)=A(1,1)                          MAIN3750
      C(2)=A(2,2)                          MAIN3760
      C(3)=A(3,3)                          MAIN3770
      C(4)=A(2,3)                          MAIN3780
      C(5)=A(1,3)                          MAIN3790
      C(6)=A(1,2)                          MAIN3800
      CALL OUTPUT(EPS,C,6,1)                MAIN3810
      EPS(1)=STRESS(23)                   MAIN3820
      EPS(2)=STRESS(26)                   MAIN3830
      EPS(3)=STRESS(12)                   MAIN3840
      EPS(4)=STRESS(27)                   MAIN3850
      EPS(5)=STRESS(25)                   MAIN3860
      EPS(6)=STRESS(24)                   MAIN3870
      C(1)=H(1,1)                          MAIN3880
      C(2)=H(2,2)                          MAIN3890
      C(3)=H(3,3)                          MAIN3900
      C(4)=H(2,3)                          MAIN3910
      C(5)=H(1,3)                          MAIN3920
      C(6)=H(1,2)                          MAIN3930
      CALL OUTPUT(EPS,C,6,2)                MAIN3940
      EPS(1)=STRESS(16)                   MAIN3950
      EPS(2)=STRESS(17)                   MAIN3960
      EPS(3)=STRESS( 3)                   MAIN3970
      C(1)=UX                               MAIN3980
      C(2)=UY                               MAIN3990
      C(3)=UZ                               MAIN4000
      CALL OUTPUT(EPS,C,3,3)                MAIN4010
360    IF(.NOT.L2) GO TO 400              MAIN4020
-----
C                                     MAIN4030
C                                     MAIN4040
C                                     MAIN4050
C                                     MAIN4060
      JACOBI COMPUTES PRINCIPAL VALUES AND
      DIRECTIONS OF TOTAL STRESSES AND STRAINS.
      THE PRINCIPAL VALUES ARE SORTED ACCORDING

```



```

C                                     TO MAGNITUDE BY CALLING IN ESORT,          MAIN4070
C-----
C      CALL JACOBI(A,HH,3,3,1,W,IQ)          MAIN4080
C      CALL ESORT(A,HH,3,3,1,W,IQ)          MAIN4090
C-----
C                                     DETERMINATION OF MAX. SHEAR STRESSES AND    MAIN4120
C                                     STRAINS WITH THEIR DIRECTIONS AND DETERMI-  MAIN4130
C                                     NATION OF MIDPOINTS OF THE MOHR'S CIRCLE.    MAIN4140
C-----
C      DO 370 J=1,3                      MAIN4150
C      C(J )=AH*A(J,J)-AC                 MAIN4160
C      C(J+ 5)=(HH(J,1)-HH(J,3))/V2       MAIN4170
C      C(J+ 9)=(HH(J,1)+HH(J,3))/V2       MAIN4180
C      C(J+14)=(HH(J,1)-HH(J,2))/V2       MAIN4190
C      C(J+18)=(HH(J,1)+HH(J,2))/V2       MAIN4200
C      C(J+23)=(HH(J,2)-HH(J,3))/V2       MAIN4210
C      C(J+27)=(HH(J,2)+HH(J,3))/V2       MAIN4220
370  CONTINUE                             MAIN4230
C      C( 4)=0.5*(A(1,1)-A(3,3))          MAIN4240
C      C( 9)=0.5*(A(1,1)+A(3,3))          MAIN4250
C      C(13)=0.5*(A(1,1)-A(2,2))          MAIN4260
C      C(18)=0.5*(A(1,1)+A(2,2))          MAIN4270
C      C(22)=0.5*(A(2,2)-A(3,3))          MAIN4280
C      C(27)=0.5*(A(2,2)+A(3,3))          MAIN4290
C      C( 5)=0.5*(C(1)-C(3))              MAIN4300
C      C(14)=0.5*(C(1)-C(2))              MAIN4310
C      C(23)=0.5*(C(2)-C(3))              MAIN4320
C      IF(C(13).GT.C(22)) GO TO 390       MAIN4330
C      DO 380 I=1,9                       MAIN4340
C      C(I+30)=C(I+12)                    MAIN4350
C      C(I+12)=C(I+21)                    MAIN4360
C      C(I+21)=C(I+30)                    MAIN4370
380  CONTINUE                             MAIN4380
C-----
C                                     OUTPUT FOR PRINCIPAL STRESSES, ETC, MAXIMUM  MAIN4400
C                                     SHEAR STRESSES, ETC AND STRAIN ENERGIES.    MAIN4410
C-----
C      390  WRITE(NOUT,9130)A(1,1),C(1),HH(1,1),HH(2,1),HH(3,1),          MAIN4420
C      +      A(2,2),C(2),HH(1,2),HH(2,2),HH(3,2),          MAIN4430
C      +      A(3,3),C(3),HH(1,3),HH(2,3),HH(3,3),          MAIN4440
C      +      (C(I),I=4,30)          MAIN4450
C      HX = (A(1,1)*C(1)+A(2,2)*C(2)+A(3,3)*C(3))*0.5          MAIN4460
C      BY = 0.0000007*AH*(C(4)*C(4)+C(13)*C(13)+C(22)*C(22))  MAIN4470
C      WRITE(NOUT,9200) BX,BY          MAIN4480
400  CONTINUE                             MAIN4490
C      GO TO 460          MAIN4500
410  WRITE(NOUT,9140) J          MAIN4510
C      GO TO 440          MAIN4520
420  WRITE(NOUT,9180) J          MAIN4530
C      GO TO 440          MAIN4540
430  WRITE (NOUT,9190)          MAIN4550
C-----
C                                     FOR SYSTEMS FOR WHICH IT IS CLEAR THAT    MAIN4580
C                                     MISTAKES OCCUR IN THE INPUTCARDS, THE      MAIN4590
C                                     REQUEST AND POINT INPUT CARDS ARE SKIPPED.  MAIN4600
C                                     PROGRAM PROCEEDS BY TAKING NEXT SYSTEM.    MAIN4610
C-----
C      440  READ (NIN,9150)          MAIN4620
C      READ(NIN,9030) NPOS          MAIN4630
C      DO 450 I=1,NPOS              MAIN4640
450  READ (NIN ,9150)              MAIN4650

```



```

460 CONTINUE
WRITE(NOUT,9160)
STOP
9000 FORMAT(1H1,17X,11("B"),5X,"III",5X,11("S"),6X,9("A"),5X,11("R")/
+
18X,12("B"),4X,"III",4X,12("S"),5X,11("A"),4X,12("R")/
+18X,"BH",8X,"HHH III SSS",14X,"AAA",7X,"AAA RH",8X,"RRH"/
+18X,"BB",9X,"BB III SS",15X,"AA",9X,"AA RR",9X,"RH"/
+18X,"BB",7X,"BBH III SSS",14X,"AA",9X,"AA RR",8X,"RR"/
+18X,11("B"),5X,"III",4X,11("S"),5X,13("A"),3X,12("R")/
+18X,11("B"),5X,"III",5X,11("S"),4X,13("A"),5X,11("R")/
+18X,"BH",7X,"BBH III",14X,"SSS AA",9X,"AA RH",5X,"RH"/
+18X,"BB",8X,"BB III",15X,"SS AA",9X,"AA RH",6X,"RR"/
+18X,"BH",7X,"BBH III",14X,"SSS AA",9X,"AA RH",7X,"RH"/
+18X,12("B"),4X,"III",3X,13("S"),4X,"AA",9X,"AA RR",8X,"RR"/
+18X,11("B"),5X,"III",3X,12("S"),5X,"AA",9X,"AA RH",9X,"RR"////
+75X,"THIS "BISAM" PROGRAM HAS BEEN OBTAINED FROM"/89X,"SHELL RES
+EARCH B.V."/89X,"FOR THE SOLE USE OF"/76X,
+"SHELL OIL COMPANY"/76X,"HOUSTON, TEXAS"
+
//76X,"ALL RIGHTS ARE RESERVED,
+ USE OF THIS PROGRAM"/76X,"BY UNAUTHORIZED PERSONS IS PROHIBITED")
9010 FURHAT(20A4)
9020 FORMAT(1H1,25(/),15X,20A4)
9030 FORMAT(I2,I3,I1)
9040 FORMAT(" NOTE THAT ",E12.6," AND ",E12.6," WILL BE CONSIDERED TO B
+E LOADS IN STRESS UNITS")
9050 FORMAT(6F10.0)
9060 FORMAT(I2,8X,4F10.0)
9070 FORMAT(" NOTE THAT INCORRECT SPELLING HAS NOT STOPPED THE EVALUATI
+ON OF STRESS",4X,A3)
9080 FORMAT(I2,4E12.6)
9090 FORMAT(1H1,///52X,"POSITION NUMBER ",I2//54X,"LAYER NUMBER ",I2//
+55X,"COORDINATES"/46X,"X",11X,"Y",11X,"Z"/40X,3E12.4)
9100 FORMAT(/21X,"DISTANCE TO LOAD-AXIS(",I2,")",34X,"THETA"/25X,E12.4,
+41X,E12.4/)
9110 FORMAT(/,30X,"THIS POSITION HAS BEEN OMITTED SINCE THE LAYER NUMH
+ER IS INCORRECT")
9120 FORMAT(/30X,"XX",10X,"YY",10X,"ZZ",10X,"YZ",10X,"XZ",10X,"XY",10X,
+"UX",10X,"UY",10X,"UZ")
9130 FORMAT(/" P R I N C I P A L V A L U E S A N D D I R E C T I O N H
+S O F T U T A L S T R E S S E S A N D S T R A I N S"/15X,"NOM
+HMAL",9X,"NORMAL",9X,"SHEAR",10X,"SHEAR",13X,"X",14X,"Y",14X,"Z"/1
+5X,"STRESS",9X,"STRAIN",9X,"STRESS",9X,"STRAIN",9X,"COMPONENT",6X,
+"COMPONENT",6X,"COMPONENT"/" MAXIMUM",2E15.3,30X,3F15.3/" MINIMAX"
+,2E15.3,30X,3F15.3/" MINIMUM",2E15.3,30X,3F15.3/" MAXIMUM",30X,2E1
+5.3,3F15.3/8X,E15.3,45X,3F15.3/" MINIMAX",30X,2E15.3,3F15.3/8X,
+E15.3,45X,3F15.3/" MINIMUM",30X,2E15.3,3F15.3/8X,E15.3,45X,3F15.3)
9140 FORMAT(" THE PROBLEM CANNOT BE SOLVED,NU(",I2,") EQUALS ONE")
9150 FORMAT(/)
9160 FORMAT(1H1)
9170 FORMAT(A4,6X,6F10.0)
9180 FORMAT(" THE PROBLEM CANNOT BE SOLVED,E(",I2,") EQUALS ZERO")
9190 FURHAT(" SYSTEM SKIPPED NO LOADS")
9200 FURHAT(1H0,13X," STRAIN ENERGY",E11.4/" STRAIN ENERGY OF DISTORTIO
+N",E11.4)
END
SUBROUTINE SYSTEM(ISYS,E,NU,THICK,AK,NLAYS,M,NLOAD,LDSTRS,HUSTR,
1ALK,RADIUS,X,Y,PSI,ISMD,IHEU)
C-----
C THIS SUBROUTINE OUTPUTS ALL PHYSICAL DATA
C OF THE MULTI-LAYERED SYSTEM AND ALL DATA
C ON CONFIGURATION AND MAGNITUDE OF THE

```



```

C                                LOADS.                                SYST0070
C-----SYST0080
  INTEGER ROUGH(2),SMOOTH(2),ISMTH(2)                                SYST0090
  REAL E(10),NU(10),THICK(9),AK(9),ALK(4),LDSTHS(10),HUSTH(10),    SYST0100
  1RADIUS(10),X(10),Y(10),PSI(10)                                SYST0110
  COMMON/TAPE/NOUT                                SYST0120
  DATA ROUGH,SMOOTH/"ROU","GH","SMU","OTH"/                                SYST0130
  WRITE(NOUT,1001) ISYS                                SYST0140
  IF(IRED.EQ.0) WRITE(NOUT,1002)                                SYST0150
  IF(IRED.NE.0) WRITE(NOUT,1007)                                SYST0151
  IF(NLAYS.EQ.1) GO TO 40                                SYST0160
  DO 30 I=1,M                                SYST0170
    IF(ISMO.EQ.1) GO TO 10                                SYST0180
    ISMTH(1) = ROUGH(1)                                SYST0190
    ISMTH(2) = ROUGH(2)                                SYST0200
    IF(ALK(I).LT.100.0) GO TO 20                                SYST0210
  10  ISMTH(1) = SMOOTH(1)                                SYST0220
    ISMTH(2) = SMOOTH(2)                                SYST0230
  20  WRITE(NOUT,1003) I,ISMTH(1),ISMTH(2),E(I),NU(I),THICK(I),AK(I) SYST0240
  30  CONTINUE                                SYST0250
  40  WRITE(NOUT,1004) NLAYS,E(NLAYS),NU(NLAYS)                                SYST0260
    WRITE(NOUT,1005)                                SYST0270
    DO 50 I = 1,NLOAD                                SYST0280
  50  WRITE(NOUT,1006) I,LDSTHS(I),HOSTR(I),RADIUS(I),X(I),Y(I),PSI(I) SYST0290
  1001 FORMAT(1H1,10(/),52X,"SYSTEM NUMBER",3X,12)                                SYST0300
  1002 FORMAT(5(/),8X,"LAYER",4X,"CALCULATION",2X,"YOUNG""S",4X,"POISSON"SYST0310
  1"S",3X,"THICKNESS",3X,"INTERFACE"/8X,"NUMBER",3X,"METHOD",7X,"MODUSYST0320
  2LUS",4X,"RATIO",18X,"SPRINGCOMPL"/)                                SYST0330
  1003 FORMAT(10X,12,5X,2A3,3X,4E12,4)                                SYST0340
  1004 FURMAT(10X,12,14X,2E12,4)                                SYST0350
  1005 FORMAT(/7/8X,"LOAD",5X,"NORMAL",7X,"SHEAR",5X,"RADIUS OF",7X,"LOADSYST0360
  1 = POSITION",6X,"SHEAR"/8X,"NUMBER",3X,"STRESS",7X,"STRESS",4X,    SYST0370
  2"LOADED AREA",6X,"X",11X,"Y",7X,"DIRECTION"/)                                SYST0380
  1006 FORMAT(10X,12,2X,6E12,4)                                SYST0390
  1007 FORMAT(5(/),8X,"LAYER",4X,"CALCULATION",2X,"YOUNG""S",4X,"POISSON"SYST0400
  1"S",3X,"THICKNESS",3X," REDUCED" /8X,"NUMBER",3X,"METHOD",7X,"MODUSYST0410
  2LUS",4X,"RATIO",18X,"SPRINGCOMPL"/)                                SYST0420
  RETURN                                SYST0430
  END                                SYST0440
  SUBROUTINE MACON1(ISMO,ALK,NSYS)                                MAC00010
C-----MAC00020
C      THIS SUBROUTINE CALCULATES CONSTANTS USED MAC00030
C      IN SUBROUTINE MATRIX TO BUILD UP VARIOUS MAC00040
C      MATRICES.                                MAC00050
C      THE CONSTANTS ARE STORED IN                                MAC00060
C      COMMON/INDATA/.                                MAC00070
C      NUMERICAL STABILITY OF SOLUTIONPROCEDURE MAC00080
C      FOR THE SYSTEM IS TESTED BY CALLING IN" MAC00090
C      MACON,                                MAC00100
C      MATRIX                                MAC00110
C      WHEN INSTABILITY HAS TO BE EXPECTED THE MAC00120
C      SMOOTH CALCULATION PROCEDURE IS CHOSEN BY MAC00130
C      TAKING ISMU = 1 AND NSYS IS SET EQUAL 1 . MAC00140
C-----MAC00150
  REAL K1,K2,K3(10),K4(10),K5,K6,NU,II,LOAD,ACCUH(3),ALK(4)                                MAC00160
  COMMON/ASDT/LAYER,NLAYS,M,R,Z,NU(10),ACCUH,LOAD,HOSTRS,NZEROS,H(9)MAC00170
  1,K5(10),E(10),AL(4),THICK(9),RADIUS(10)                                MAC00180
  COMMON/INDATA/XMAX, A1(9),B1(9),C1(9),D(9),EE(9),F(9),G(9),H1(9),MAC00190
  1I1(9),K1(9),K2(9),K6(10),BE(9),BU(9),HUU(4),BMU(9),B2U(9),B2UU(9),MAC00200
  2J2(9),J1,T2(10),SS(2,10),G012(9),G021(9),G022(9),G122(9),    MAC00210
  3H012(9),H022(9),H122(9),D012(9),DU22(4),C011(9),C012(9),E012(9),    MAC00220

```



```

4F012(9),F112(9),F022(9),CC(4,2,9),DU(2,2,4),FF(2,2,9),GG(2,2,10), MACU023U
5HH(2,2,10),HR(4,2,10),DD2(9),G20(9),G21(9),H20(9),H021(9),GG2(10), MACU024U
6HH2(10),G011(9),G111(9),G012(9),G112(9),G212(9),G022(9),G122(9), MACU025U
7UF0(9),UF1(9),Z011,Z111,Z211,Z012,Z112,Z212,Z312,Z021,Z121,Z022, MACU026U
8Z122,Z222,K4 MACU027U
COMMON/TAPE/NOUT MACU028U
NSYS = 0 MACU029U
IF(NLAYS,EQ,1) GO TO 10 MACU030U
GG(1,1,1) = -1.0 MACU031U
GG(2,1,1) = 1.0 MACU032U
GG(1,2,1) = 1.0-2.0*NU(1) MACU033U
GG(2,2,1) = 2.0*NU(1) MACU034U
HH(1,1,1) = 1.0 MACU035U
HH(1,2,1) = GG(1,2,1) MACU036U
HH(2,1,1) = 1.0 MACU037U
HH(2,2,1) = -GG(2,2,1) MACU038U
HR(1,1,NLAYS) = 0.0 MACU039U
HR(1,2,NLAYS) = 0.0 MACU040U
RR(2,1,NLAYS) = 0.0 MACU041U
RR(2,2,NLAYS) = 0.0 MACU042U
RR(3,1,NLAYS) = 1.0 MACU043U
RR(3,2,NLAYS) = 0.0 MACU044U
RR(4,1,NLAYS) = 0.0 MACU045U
RR(4,2,NLAYS) = 1.0 MACU046U
SS(1,NLAYS) = 0.0 MACU047U
SS(2,NLAYS) = 1.0 MACU048U
GG2(1) = 1.0 MACU049U
HH2(1) = -1.0 MACU050U
10 K5(1)=1.0-2.0*NU(1) MACU051U
IF(NLAYS,EQ,1) GO TO 70 MACU052U
K = 0 MACU053U
K6(1) = 4.0*(1.0-NU(1)) MACU054U
DO 30 J=1,M MACU055U
  K1(J)=(1.0+NU(J+1))*E(J)/((1.0+NU(J))*E(J+1)) MACU056U
  K2(J)=1.0-K1(J) MACU057U
  K3(J)=NU(J+1)-NU(J)*K1(J) MACU058U
  K4(J)=8.0*NU(J)*NU(J+1) MACU059U
  K5(J)=1.0-2.0*NU(J) MACU060U
  K6(J+1) = 4.0*(1.0-NU(J+1)) MACU061U
  A1(J)= K6(J)-K2(J) MACU062U
  B1(J)= K2(J)+K1(J)*K6(J+1) MACU063U
  C1(J)=2.0*K2(J) MACU064U
  D(J)= K2(J)*(1.0-4.0*NU(J)) MACU065U
  EE(J)= K2(J)*(1.0+K4(J))-0.0*K3(J) MACU066U
  F(J)= A1(J)-B1(J) MACU067U
  G(J)= K2(J)*(1.0-K4(J))+2.0*K3(J) MACU068U
  H1(J)=4.0*K2(J)*(NU(J+1)-NU(J)) MACU069U
  II(J)= D(J)-H1(J) MACU070U
30 CONTINUE MACU071U
  K5(M+1)=1.0-2.0*NU(M+1) MACU072U
  IF(ISHO,LT,1) GO TO 70 MACU073U
  DO 40 I = 1,M MACU074U
    IF(ALK(I),LT,100.0) GO TO 50 MACU075U
40 CONTINUE MACU076U
  GO TO 70 MACU077U
C-----MACU078U
C CALCULATION OF CONSTANTS ONLY NEEDED IN MACU079U
C MATRIX FOR STABILITY TEST. MACU080U
C-----MACU081U
50 THIN = 1.0E+10 MACU082U
  NTELL = 2 MACU083U

```



```

IF(AID(10),AND,,NOT,NZEU) AID(4)=,TRUE,
IF(AID(6),AND,,NOT,NZEP) AID(12)=,TRUE,
IF(AID(4)) CALL LOGSET(JARG(1,6),AID)
IF(AID(10)) AID(11)=,TRUE,
IF(AID(5)) AID(11)=,TRUE,
IF(AID(12)) AID(6)=,TRUE,
IF(AID(8)) AID(14)=,TRUE,
IF(AID(14)) AID(8)=,TRUE,
IF(AID(5),AND,AID(6)) CALL LOGSET(JARG(1,7),AID)
IF(AID(11),AND,AID(12)) CALL LOGSET(JARG(1,8),AID)
IF(,NOT,NZEU) GO TO 20
IF(AID(7)) AID(13)=,TRUE,
IF(AID(13)) AID(7)=,TRUE,
IF(AID(9)) AID(15)=,TRUE,
IF(AID(15)) AID(9)=,TRUE,
IF(AID(5),AND,AID(10)) CALL LOGSET(JARG(1,9),AID)
IF(AID(6),AND,AID(10)) CALL LOGSET(JARG(1,10),AID)
IF(AID(1),AND,AID(2)) CALL LOGSET(JARG(1,11),AID)
IF(AID(4),AND,AID(7)) CALL LOGSET(JARG(1,12),AID)
IF(AID(7),AND,AID(10)) CALL LOGSET(JARG(1,13),AID)
IF(AID(8),AND,AID(9)) CALL LOGSET(JARG(1,14),AID)
GO TO 30
20 IF(AID(1)) CALL LOGSET(JARG(1,11),AID)
IF(AID(4)) CALL LOGSET(JARG(1,12),AID)
IF(AID(8)) CALL LOGSET(JARG(1,14),AID)
30 N = ,FALSE,
L = ,TRUE,
IF(AID(3),OR,AID(6),OR,AID(12),OR,AID(16),OR,AID(17)) N=,TRUE,
DO 50 I = 18,27
IF(AID(I)) GO TO 40
L = ,FALSE,
GO TO 50
40 N = ,TRUE,
50 CONTINUE
RETURN
END
SUBROUTINE LOGSET(I,LOG)
C-----
C THIS SUBROUTINE,CALLED IN BY CONSYS AND LOGS0020
C CONPNT,SETS THE LOGICAL VARIABLES LOG(K) LOGS0030
C TRUE FOR THE K=VALUES,STORED IN THE ARGU- LOGS0040
C MENT I. LOGS0050
C-----
LOGICAL LOG(I) LOGS0060
INTEGER I(1) LOGS0070
DO 10 L=1,6 LOGS0080
IF(I(L),EQ,0) GO TO 20 LOGS0090
K=I(L) LOGS0100
LOG(K)=,TRUE, LOGS0110
10 CONTINUE LOGS0120
20 RETURN LOGS0130
END LOGS0140
SUBROUTINE MA2CON(TMIN,I,ISMO,ALK) LOGS0150
C-----
C THIS SUBROUTINE CALCULATES CONSTANTS USED MA2C0010
C IN SUBROUTINE MATRIX TO BUILD UP VARIOUS MA2C0020
C MATRICES. THESE CONSTANTS ALL DEPENDENT MA2C0030
C ON ALK(J) AND / OR RADIUS(I), ARE STORED MA2C0040
C IN COMMUN/INDATA/. MA2C0050
C-----
REAL K1,K2,K4(10),K5,K6,K11,K12,NU,II,LOAD,ACCUK(3),ALK(9) MA2C0060
MA2C0070
MA2C0080
MA2C0090

```



```

DUMMY = 0.0 MAC00840
LAYER = NLAYS MAC00850
T2(NLAYS) = 0.0 MAC00860
DO 60 K = 1,M MAC00870
  IF (THICK(K),LT,TMIN) TMIN = THICK(K) MAC00880
  DUMMY = DUMMY+THICK(K) MAC00890
  T2(K) = 2.0*THICK(K)/RADIUS(1) MAC00900
  H(K) = DUMMY/RADIUS(1) MAC00910
60 CONTINUE MAC00920
CALL MA2CUN(TMIN,1,ISMU,ALK) MAC00930
TX = 6.6*RADIUS(1)/TMIN MAC00940
XMAX = TX+1.0 MAC00950
-----MAC00960
C TEST ON NUMERICAL STABILITY OF THE SOLU- MAC00970
C TION-PROCEDURE TO BE FOLLOWED FOR THIS MAC00980
C SYSTEM BY CALLING IN THE MATRIX SUBROUTI- MAC00990
C NE WITH NTELL = 2 . MAC01000
C AFTER TEST THE SMOOTH OR ROUGH CALCULATI- MAC01010
C ON PROCEDURE IS CHOSEN. MAC01020
C TEST IS ONLY NECESSARY IF NOT DIRECTLY MAC01030
C THE SMOOTH CALCULATION PROCEDURE HAS BEEN MAC01040
C CHOSEN BY ISMU=1. MAC01050
-----MAC01060
CALL MATRIX(TX,1,NTELL) MAC01070
IF(NTELL.EQ.2) GO TO 70 MAC01080
ISMU = 1 MAC01090
NSYS = 1 MAC01100
WRITE(NOUT,1001) MAC01110
70 RETURN MAC01120
1001 FORMAT(" THE MORE STABLE SMOOTH CALCULATION PROCEDURE HAS BEEN CHO- MAC01130
1SEN.") MAC01140
END MAC01150
SUBROUTINE CONSYS(AID,NZEP,NZEU,N,L) CONS0010
-----CONS0020
C THIS SUBROUTINE DETERMINES FOR EACH SYS- CONS0030
C TEM THE CYLINDRICAL COMPONENTS NEEDED FOR CONS0040
C COMPUTATION OF THE REQUIRED CARTESIAN CONS0050
C COMPONENTS OF STRESSES,STRAINS AND DISPLA- CONS0060
C CEMENT. GIVEN THIS SET OF COMPONENTS A CONS0070
C FURTHER SELECTION IS PERFORMED ON THE CONS0080
C COMPONENTS THAT CAN BE COMPUTED WITH THE CONS0090
C INTEGRALS. CONS0100
C CONSYS CALLS IN SUBROUTINE LOGSET CONS0110
-----CONS0120
LOGICAL AID(27),NZEP,NZEU,EPS(5),N,L CONS0130
INTEGER JARG(6,14) CONS0140
DATA JARG/ CONS0150
1 4, 5, 7,18,19,21, 8, 9,20,22, 0, 0, 10,11,13,23,24,26, CONS0160
214,15,25,27, 0, 0, 1, 2,16,17, 0, 0, 5,10,12, 0, 0, 0, CONS0170
3 4,10,12, 0, 0, 0, 4, 5,10, 0, 0, 0, 4, 6,12, 0, 0, 0, CONS0180
4 4, 5,12, 0, 0, 0, 16,17, 0, 0, 0, 0, 18,19,21,23,24,26, CONS0190
523,24,26, 0, 0, 0, 20,22,25,27, 0, 0/ CONS0200
EPS(1) = AID(18).OR.AID(19).OR.AID(21) CONS0210
EPS(2) = AID(20).OR.AID(22) CONS0220
EPS(3) = AID(23).OR.AID(24).OR.AID(26) CONS0230
EPS(4) = AID(25).OR.AID(27) CONS0240
EPS(5) = AID(16).OR.AID(17) CONS0250
DO 10 I = 1,5 CONS0260
  IF(.NOT.EPS(I)) GO TO 10 CONS0270
  CALL LOGSET(JARG(I,I),AID) CONS0280
10 CONTINUE CONS0290

```



```

COMMON/ASDT/LAYER,NLAYS,M,H,Z,NU(10),ACCUR,LOAD,HOSTHS,NZEROS,H(9)MA2C010U
1,K5(10),E(10),AL(9),THICK(9),RADIUS(10)MA2C011U
COMMON/INDATA/XMAX,A1(9),B1(9),C1(9),D(9),EE(9),F(9),G(9),H1(9),MA2C012U
1I1(9),K1(9),K2(9),K6(10),HE(9),HU(9),BUU(9),BMU(9),H2U(9),B2UU(9),MA2C013U
2J2(9),J1,I2(10),SS(2,10),G012(9),G021(9),G022(9),G122(9),MA2C014U
3H012(9),H022(9),H122(9),D012(9),D022(9),C011(9),C012(9),E012(9),MA2C015U
4F012(9),F112(9),F022(9),CC(4,2,9),DD(2,2,9),FF(2,2,9),GG(2,2,10),MA2C016U
5HM(2,2,10),HR(4,2,10),D02(9),G2U(9),G21(9),H20(9),H021(9),GG2(10),MA2C017U
6HM2(10),Q011(9),Q111(9),Q012(9),Q112(9),Q212(9),Q022(9),Q122(9),MA2C018U
7QF0(9),QF1(9),Z011,Z111,Z211,Z012,Z112,Z212,Z312,Z021,Z121,Z022,MA2C019U
8Z122,Z222,K4MA2C020U
XMAX = 6.5*RADIUS(1)/TMINMA2C021U
K = 0MA2C022U
DO 30 J = 1,MMA2C023U
AL(J) = ALK(J)/(RADIUS(I)+ALK(J))MA2C024U
K12 = 1.0-AL(J)MA2C025U
Q011(J) = K12*B1(J)MA2C026U
Q111(J) = 2.0*AL(J)*NU(J+1)MA2C027U
Q012(J) = -K12*EE(J)MA2C028U
Q022(J) = K12*A1(J)MA2C029U
Q122(J) = AL(J)*M5(J)MA2C030U
QF0(J) = K12*A1(J)*B1(J)MA2C031U
QF1(J) = 2.0*AL(J)*(1.0-NU(J)+(1.0-NU(J+1))*K1(J))MA2C032U
IF (ISMU.EQ.1) GO TO 20MA2C033U
IF (ALK(J).GE.100.0) GO TO 20MA2C034U
HE(J) = -AL(J)/(1.0-AL(J))MA2C035U
BU(J) = HE(J)*2.0*NU(J+1)MA2C036U
BUU(J) = BU(J)*K5(J)MA2C037U
BMU(J) = BE(J)*K5(J)MA2C038U
B2U(J) = BE(J)*(K5(J)-2.0*NU(J+1))MA2C039U
B2UU(J) = BE(J)*(K5(J)+2.0*NU(J+1))MA2C040U
GO TO 30MA2C041U
20 K11 = 2.0*(NU(J)-NU(J+1))MA2C042U
K = K+1MA2C043U
J2(K) = JMA2C044U
GG(1,1,K+1) = K2(J)MA2C045U
G012(K) = K11-K2(J)*(2.0-4.0*NU(J+1))MA2C046U
G021(K) = -K12*K2(J)MA2C047U
G022(K) = (K11-K2(J))*K12MA2C048U
G122(K) = -2.0*NU(J+1)*AL(J)MA2C049U
HM(1,1,K+1) = -3.0+4.0*NU(J)-K1(J)MA2C050U
H012(K) = -2.0+2.0*NU(J)+6.0*NU(J+1)-K4(J)-(2.0-4.0*NU(J+1))*MA2C051U
1 K1(J)MA2C052U
H021(K) = HM(1,1,K+1)*K12MA2C053U
H022(K) = -K12*(1.0-2.0*NU(J)-6.0*NU(J+1)+K4(J)-K1(J))MA2C054U
H122(K) = 2.0*AL(J)*NU(J+1)MA2C055U
DD(1,1,K) = -K6(J)MA2C056U
D012(K) = -K6(J)*K5(J)MA2C057U
DD(2,1,K) = -K12*K6(J)MA2C058U
D022(K) = -NU(J)*2.0*DD(2,1,K)MA2C059U
C011(K) = -1.0+4.0*NU(J)MA2C060U
C012(K) = 4.0*NU(J)*K5(J)MA2C061U
CC(2,1,K) = -2.0MA2C062U
E012(K) = -K11MA2C063U
F012(K) = K4(J)-2.0*(NU(J)+NU(J+1))MA2C064U
F112(K) = 2.0*E012(K)MA2C065U
F022(K) = 1.0-4.0*NU(J+1)MA2C066U
FF(2,1,K) = 2.0MA2C067U
DD2(K) = 2.0*K12/K1(J)MA2C068U
G20(K) = K12*(1.0-1.0/K1(J))MA2C069U
G21(K) = AL(J)*0.5/K1(J)MA2C070U

```



```

      H20(K) = K12*(1.0+1.0/K1(J))
30 CONTINUE
      J1 = K
      DUMMY=0.0
      T2(NLAYS) = 0.0
      DO 40 K = 1,M
        DUMMY=DUMMY+THICK(K)
        T2(K)=2.0*THICK(K)/RADIUS(I)
        H(K)=DUMMY/RADIUS(I)
        K12 = 1.0-AL(K)
        Q112(K) = -K12*F(K)*H(K)+Q111(K)*K5(K)
        Q212(K) = AL(K)*H(K)*(2.0*NU(K+1)-K5(K))
40 CONTINUE
      IF(LAYER.EQ.NLAYS) GO TO 50
C-----
C          THESE CONSTANTS ARE USED FOR THE ASYMPTOTIC
C          EVALUATION OF THE CHARACTERISTIC
C          FUNCTIONS IN MATHIX.
C-----
      J = LAYER
      RK1 = 2.0*NU(J+1)*C1(J)
      RK2 = 2.0*NU(J+1)*A1(J)
      RK3 = 2.0*NU(J+1)*D(J)
      Z021 = Q011(J)*C1(J)
      RK4 = Z021*H(J)
      K12 = 1.0-AL(J)
      Z011 = Q011(J)*D(J)
      Z111 = AL(J)*(RK3-G(J)-K5(J)*B1(J))-RK4
      Z211 = AL(J)*H(J)*(B1(J)-II(J)-RK1)
      Z012 = -K12*(D(J)*EE(J)+A1(J)*G(J))
      Z112 = Q122(J)*(RK2-G(J)+RK3+EE(J))+K12*H(J)*(A1(J)*
1      H1(J)+C1(J)*EE(J)-D(J)*F(J))
      Z212 = -AL(J)*H(J)*(K5(J)*(RK1+H1(J)+II(J))-RK3+EE(J)+
1      RK2+G(J))-RK4*H(J)
      Z312 = AL(J)*H(J)*H(J)*(H1(J)-RK1-II(J))
      Z121 = AL(J)*(RK1-H1(J)+II(J))
      Z022 = K12*(A1(J)*II(J)-EE(J)*C1(J))
      Z122 = AL(J)*(RK2+EE(J)+K5(J)*(RK1+II(J)))+RK4
      Z222 = Z121*H(J)
50 RETURN
      END
      SUBROUTINE CONPNT(R,HUSTRS,LUAD,Z,N2,L2)
C-----
C          THIS SUBROUTINE DETERMINES FOR EACH POINT
C          LOAD CONFIGURATION SEPARATELY THE
C          INTEGRALS NEEDED FOR COMPUTATION OF THE
C          DESIRED COMPONENTS OF STRESS,ETC.
C          FOR POINTS AT THE RIM OF THE LOAD SOME
C          COMPONENTS CANNOT BE CALCULATED BECAUSE
C          OF SINGULAR BEHAVIOUR, A MESSAGE IS
C          PRINTED.
C-----
      LOGICAL STRESS,EPS,RLOW,N2,L2
      REAL LOAD
      INTEGER IARG(6,12),KARG(6,4),JJ(12,15)
      COMMON/STWDTA/STRESS(27),EPS(17),RLOW,ST,CT,L,ACC
      COMMON/TAPE/NOU
      DATA IARG/
1 7,12,17, 0, 0, 0,      12,14,17, 0, 0, 0,      10,11, 0, 0, 0, 0,
2 7, 8, 9,12,14,17,      7, 9,12,14,17, 0,      8, 9, 0, 0, 0, 0,
3 7,12,14,15,17, 0,      6,10,16, 0, 0, 0,      10,13,16, 0, 0, 0,

```



```

4 7, 8,12,14,17, 0,      7,12,14,17, 0, 0,      8, 9, 0, 0, 0, 0/CUNP021U
  DATA KAHG/
1 1, 2, 4, 0, 0, 0,      2, 4, 0, 0, 0, 0,      1, 2, 0, 0, 0, 0,CUNP022U
2 4, 5,10,11,12, 0/
  DATA JJ/
1 1, 0, 0, 0, 0, 0, 0, 0, 0, 0, 0, 0, 0, 0, 0, 0, 0, 0, 0, 0,CUNP023U
2 0, 1, 0, 0, 0, 0, 0, 0, 0, 0, 0, 0, 0, 0, 0, 0, 0, 0, 0, 0,CUNP024U
3 1, 1, 0, 0, 0, 0, 0, 0, 0, 0, 0, 0, 0, 0, 0, 0, 0, 0, 0, 0,CUNP025U
4 1, 0, 0, 0, 0, 0, 0, 0, 1, 0, 0, 0, 0, 0, 0, 0, 0, 0, 0, 0,CUNP026U
5 0, 1, 0, 0, 0, 0, 0, 0, 0, 1, 0, 0, 0, 0, 0, 0, 0, 0, 0, 0,CUNP027U
6 1, 1, 0, 0, 0, 0, 0, 0, 1, 1, 0, 0, 0, 0, 0, 0, 0, 0, 0, 0,CUNP028U
7 1, 0, 1, -1, -1, 0, 0, 0, 0, 0, -1, 1, -1, 0, 0, 0, 0, 0, 0, 0, 0,CUNP029U
8 0, 1, 0, 0, 0, 0, 0, -1, 0, 0, 0, 0, 0, 0, 0, 0, 0, 0, 0, 0,CUNP030U
9 1, 1, 1, -1, -1, 0, -1, 0, 0, -1, 1, -1, 0, 0, 0, 0, 0, 0, 0, 0,CUNP031U
1 1, 0, 1, 1, 1, 0, 0, 0, 0, 0, 1, 1, 1, 0, 0, 0, 0, 0, 0, 0,CUNP032U
1 0, 1, 0, 0, 0, 0, 0, 1, 0, 0, 0, 0, 0, 0, 0, 0, 0, 0, 0, 0,CUNP033U
2 1, 1, 1, 1, 1, 0, 1, 0, 0, 0, 1, 1, 1, 0, 0, 0, 0, 0, 0, 0,CUNP034U
3 1, 0, 1, 1, 1, 1, 0, 1, 0, 1, 1, 1, 1, 0, 0, 0, 0, 0, 0, 0,CUNP035U
4 0, 1, 0, 0, 0, 0, 0, 1, 0, 1, 0, 0, 0, 0, 0, 0, 0, 0, 0, 0,CUNP036U
5 1, 1, 1, 1, 1, 1, 1, 1, 1, 1, 1, 1, 1, 1, 1, 1, 1, 1, 1, 1/CUNP037U
  NERR = 0
  DO 10 I = 1,17
    EPS(I) = .FALSE.
10 CONTINUE
  J=3
  IF (ABS(ST).LT.ACC)      J=1
  IF (ABS(CT).LT.ACC)     J=2
  IF (MUSTPS.LT.ACC)     GO TO 20
  IF (RLU=)              GO TO 30
  IF (Z.LT.ACC)          GO TO 40
  I=J+14
  GO TO 50
20 I=2
  IF (RLU=)              I=1
  GO TO 50
30 I=J+5
  IF (Z.LT.ACC)          I=I-3
  GO TO 50
40 I=J+11
  IF (ABS(R-1.0).LT.ACC)  I=I-3
50 IF (STRESS( 4).UR.STRESS(10))CALL LUGSET(KAHG(1,1),EPS)
  IF (STRESS( 5))        CALL LUGSET(KAHG(1,2),EPS)
  IF (STRESS( 3))        EPS( 3)=.TRUE.
  IF (STRESS(11))        EPS( 4)=.TRUE.
  IF (STRESS(12))        CALL LUGSET(KAHG(1,3),EPS)
  IF (STRESS( 6).AND.(Z.GT.ACC)) EPS( 1)=.TRUE.
  IF (.NOT.STRESS( 8))   GO TO 60
  IF (Z.LT.ACC)          GO TO 60
  IF (R.GT.ACC)          EPS(5)=.TRUE.
60 IF (I.LT.3) GO TO 180
  DO 90 J = 1,12
    IF (.NOT.STRESS(J))  GO TO 90
    IF (JJ(J,I-2))      70,90,80
70  NERR = 1
    STRESS(J) = .FALSE.
    L2 = .FALSE.
    GO TO 90
80  CALL LUGSET(IARG(1,J),EPS)
90 CONTINUE
  IF (NERR) 160,160,100
100 IF (I=10) 110,130,120

```



110	WRITE(NOUT,9000)	CONP0820
	GO TO 140	CONP0830
120	WRITE(NOUT,9020)	CONP0840
	STRESS(13) = ,FALSE.	CONP0850
	GO TO 140	CONP0860
130	WRITE(NOUT,9010)	CONP0870
	STRESS(13) = ,FALSE.	CONP0880
	IF(STRESS(12)) GO TO 150	CONP0890
140	IF(STRESS(3),OR,STRESS(6)) GO TO 150	CONP0900
	IF(STRESS(16)) GO TO 150	CONP0910
	IF(STRESS(17)) GO TO 150	CONP0920
	IF(STRESS(20)) GO TO 150	CONP0930
	IF(STRESS(22)) GO TO 150	CONP0940
	IF(STRESS(25)) GO TO 150	CONP0950
	IF(STRESS(27)) GO TO 150	CONP0960
	N2 = ,FALSE.	CONP0970
150	STRESS(18) = ,FALSE.	CONP0980
	STRESS(19) = ,FALSE.	CONP0990
	STRESS(21) = ,FALSE.	CONP1000
	STRESS(23) = ,FALSE.	CONP1010
	STRESS(24) = ,FALSE.	CONP1020
	STRESS(26) = ,FALSE.	CONP1030
160	IF(LOAD,GT,ACC) GO TO 180	CONP1040
	DO 170 J = 1,5	CONP1050
170	EPS(J) = ,FALSE.	CONP1060
180	RETURN	CONP1070
9000	FORMAT(" AT THIS POINT SRH,STT,ERR AND EZZ HAVE A LOGARITHMIC SINGULARITY")	CONP1080
9010	FORMAT(" AT THIS POINT SRT AND ERT HAVE A LOGARITHMIC SINGULARITY")	CONP1090
	1)	CONP1100
9020	FORMAT(" AT THIS POINT SKR,STT,SRT,ERR,EZZ AND ERT HAVE A LOGARITHMIC SINGULARITY")	CONP1110
	1)	CONP1120
	END	CONP1130
	SUBROUTINE GENDAT(N,NZEROS,R,ACC)	CONP1140
	-----	GEND0010
C		GEND0020
C	THIS SUBROUTINE GIVES THE ZEROS OF THE	GEND0030
C	PRODUCTS $J_0(XR)*J_1(X)$ AND $J_1(XR)*J_1(X)$ IN	GEND0040
C	THE RIGHT ORDER. THE SUBSEQUENT ZEROS ARE	GEND0050
C	STORED IN ZEROS FOR USING THEM IN INGRAL.	GEND0060
C	THE ZEROS OF $J_0$ AND $J_1$ ARE STORED AS	GEND0070
C	BZEROS IN THE BLOCK DATA.	GEND0080
C	-----	GEND0090
	COMMON/GEDATA/BZEROS(149,2),ZEROS(298)	GEND0100
	IF(R,LT,ACC,OR,ABS(N-1,0),LT,ACC) GO TO 40	GEND0110
	I=1	GEND0120
	J=1	GEND0130
	DO 20 K=1,298	GEND0140
	IF(I,GT,149) GO TO 30	GEND0150
	IF(J,GT,149) GO TO 30	GEND0160
	IF(BZEROS(I,2),LT,BZEROS(J,N+1)/R) GO TO 10	GEND0170
	ZEROS(K) = BZEROS(J,N+1)/R	GEND0180
	J=J+1	GEND0190
	GO TO 20	GEND0200
10	ZEROS(K)=BZEROS(I,2)	GEND0210
	I=I+1	GEND0220
20	CONTINUE	GEND0230
30	NZEROS = K-1	GEND0240
	RETURN	GEND0250
40	IF(K,GT,ACC) GO TO 70	GEND0260
50	DO 60 I=1,149	GEND0270
	ZEROS(I)=BZEROS(I,2)	GEND0280



```

60 CONTINUE
NZEROS=149
RETURN
70 IF(N.EQ.1) GO TO 50
DO 80 K=1,149
ZEHOS(2*K-1)=@ZEHOS(K,1)
ZEROS(2*K )=@ZEHOS(K,2)
80 CONTINUE
NZEROS=298
RETURN
END
SUBROUTINE ASYMP(T,R,ACC)
C-----
C THIS SUBROUTINE ORGANIZES THE COMPUTATION OF THE ASYMPTOTIC PART OF THE INTEGRALS AS USED FOR THE TOP-LAYER ONLY.
C ASYMP CALLS IN SUBROUTINE ASS
C ASYMP CALLS IN FUNCTIONS FLE
C FLLK
C FLMBDA
C-----
DOUBLE PRECISION DR,KACC2,C,ELLE,ELLK,FLE,FLLK
COMMON/CONST/C,ELLE,ELLK,ALMBDA
IF(R,LT,ACC) GO TO 10
DR=DBLE(R)
KACC2=((1.000-DR)*(1.000-DH)+C*C)/((1.000+DR)*(1.000+DH)+C*C)
ELLK=FLLK(KACC2)
ELLE=FLE(KACC2)
ALMBDA = FLMBDA(DR,C,ELLK,ELLE,KACC2)
10 CALL ASS(ACC,R)
RETURN
END
DOUBLE PRECISION FUNCTION FLLK(KACC2)
C-----
C THIS FUNCTION-SUBROUTINE EVALUATES THE COMPLETE ELLIPTIC INTEGRAL OF THE FIRST KIND FROM A SERIES-EXPANSION ACCORDING TO BYRD AND FRIEDMAN, HANDBOOK OF ELLIPTIC INTEGRALS FOR ENGINEERS AND PHYSICISTS, FORMULA 900.00 FOR KACC2,GE,0.5
C FORMULA 900.06 FOR KACC2,LT,0.5
C-----
DOUBLE PRECISION KACC2,KA,M1,KACC
KA = 1.000-KACC2
IF(KA,GT,0.500) GO TO 10
FLLK=1.000+KA*(0.2500+KA*(0.14062500+KA*(0.0976562500+KA*(0.074768
1066400+KA*(0.060562133800+KA*(0.050889015000+KA*(0.043878793700+KA*FLLK0150
2*(0.038565346500+KA*(0.034399336400+KA*(0.031045401200+KA*(0.028287
37235300+KA*(0.025979074300+KA*(0.024019115200+KA*(0.022334101200+K
4A*(0.020869976800))))))))))
GO TO 30
10 KACC=DSQRT(KACC2)
IF(KACC,LT,1.00-04) GO TO 20
M1=-DLOG(KACC)
FLLK=M1*(1.000+KACC2*(0.2500+KACC2*(0.14062500+KACC2*(0.0976562500
1+KACC2*(0.074768066400+KACC2*(0.060562133800+KACC2*(0.050889015
20+KACC2*(0.0438787937 00+KACC2*(0.0385653465 00+KACC2*(0.034399336
34 00+KACC2*(0.0310454012 00+KACC2*(0.0282872353 00+KACC2*(0.025979
40743 00+KACC2*(0.0240191152 00+KACC2*0.0223341012 00))))))))))FLLK0270
5+1.3862943600+KACC2*(0.096575590300+KACC2*(0.030885144500+KACC2*(0
6.014937600400+KACC2*(0.008766312200+KACC2*(0.005754887700+KACC2*(0

```



```

7,004064658500+KACC2*(0,003022546500+KACC2*(0,002335157200+KACC2*(0,FLLK0300
8,001858070300+KACC2*(0,001513511600+KACC2*(0,001256591100+KACC2*(0,FLLK0310
9,001059929700+KACC2*(0,000906059600+KACC2*(0,000783411800)))))))))FLLK0320
T))) FLLK0330
FLLK = 2,000*FLLK/3,141592653500 FLLK0340
GO TO 30 FLLK0350
20 FLLK = 0,000 FLLK0360
30 RETURN FLLK0370
END FLLK0380
DOUBLE PRECISION FUNCTION FLLE(KACC2) FLLE0010
C-----FLLE0020
C THIS FUNCTIONSUBROUTINE EVALUATES THE FLLE0030
C COMPLETE ELLIPTIC INTEGRAL OF THE SECOND KIND FROM A SERIES-EXPANSION ACCORDING TO FLLE0040
C BYRD AND FRIEDMAN, HANDBOOK OF ELLIPTIC INTEGRALS FOR ENGINEERS AND PHYSICISTS, FLLE0060
C FORMULA 900,07 FOR KACC2,GE,0,5 FLLE0080
C FORMULA 900,10 FOR KACC2,LT,0,5 FLLE0090
C-----FLLE0100
DOUBLE PRECISION KACC2,KACC,KA FLLE0110
KA = 1,000-KACC2 FLLE0120
IF(KA,GT,0,500) GO TO 10 FLLE0130
FLLE=1,000-KA*(0,2500+KA*(0,04687500+KA*(0,0195312500+KA*(0,010681152300+KA*(0,006729126000+KA*(0,004626274100+KA*(0,003375291800+KA*FLLE0150
2*(0,002571023100+KA*(0,002023490400+KA*(0,001633968500+KA*0,0013473011200))))))))) FLLE0170
GO TO 30 FLLE0180
10 KACC=DSQRT(KACC2) FLLE0190
IF(KACC,LT,1,00-04) GO TO 20 FLLE0200
FLLE=1,000-0,5000*KACC2*DLOG(KACC)*(1,000+KACC2*(0,37500+KACC2*(0,1,23437500+KACC2*(0,170898437500+KACC2*(0,134542519600+KACC2*(0,1112030578600+KACC2*(0,094508171100+KACC2*(0,082272738200+KACC2*(0,0723845653600+KACC2*(0,065358739300+KACC2*(0,059268493100+KACC2*(0,0544217201100+KACC2*(0,049959760600+KACC2*(0,046322580200+KACC2*(0,0431579262300))))))))) +0,2500*KACC2*(1,77258872200+KACC2*(0,2272206770700+KACC2*(0,087325481700+KACC2*(0,046178085600+KACC2*(0,028567001200+KACC2*(0,019418973300+KACC2*(0,014058751800+KACC2*(0,0106488943400+KACC2*(0,008345589500+KACC2*(0,006716673700+KACC2*(0,0055229288800+KACC2*(0,004620493600+KACC2*(0,003922930400+KACC2*(0,0033721254900+KACC2*(0,002929929800))))))))) FLLE0310
FLLE = 2,000*FLLE/3,141592653500 FLLE0320
GO TO 30 FLLE0330
20 FLLE = 2,000/3,141592653500 FLLE0340
30 RETURN FLLE0350
END FLLE0360
FUNCTION FLMBDA(DR,C,ELLK,ELLE,KACC2) FLMB0010
C-----FLMB0020
C THIS FUNCTIONSUBROUTINE EVALUATES THE FLMB0030
C HEUMAN'S-LAMBDA FUNCTION FROM A SERIES-EXPANSION ACCORDING TO FLMB0040
C BYRD AND FRIEDMAN, HANDBOOK OF ELLIPTIC INTEGRALS FOR ENGINEERS AND PHYSICISTS, FLMB0060
C FORMULA 904,00 FLMB0080
C USE IS MADE OF THE COMPLETE ELLIPTIC INTEGRALS OF THE FIRST AND SECOND KIND ELLK AND ELLE EVALUATED BY FLLK AND FLLE, FLMB0090
C-----FLMB0120
DOUBLE PRECISION DR,DASIN,SUM,PHI,DS,DC,A,T,AI,KACC2,TWAI,DAR,ELLK,ELLE,E,K,C FLMB0130
DAR = DASIN(1,000-DR) FLMB0140
IF(C,LT,DAR) GO TO 10 FLMB0150

```



DASIN = DAR/C	FLMB0170
PHI = 1.570796326800-DATAN(DASIN)	FLMH0180
GO TO 30	FLMB0190
10 DASIN = C/DAR	FLMB0200
IF(C.LT.(0.10-05*DAR)) GO TO 20	FLMB0210
PHI = DATAN(DASIN)	FLMB0220
GO TO 30	FLMB0230
20 PHI = DASIN	FLMB0240
30 IF(DABS(PHI-1.570796326800),G1,1.00-6) GO TO 40	FLMB0250
FLMHDA=1.0	FLMB0260
GO TO 60	FLMB0270
40 DS=DSIN(PHI)	FLMH0280
DC=DCOS(PHI)	FLMH0290
E = ELLE	FLMB0300
K = ELLK	FLMB0310
FLMHDA=PHI*E	FLMB0320
T=0.500*(PHI-DS*DC)	FLMB0330
A=0.500*KACC2	FLMB0340
SUM=A*T*(2.000*K-E)	FLMH0350
IF(SUM.LT.1.00-07) GO TO 60	FLMB0360
I=1	FLMB0370
50 FLMHDA = FLMHDA-SNGL(SUM)	FLMH0380
I=I+1	FLMB0390
AI=I	FLMB0400
T=AI=2.000*AI-1.000	FLMH0410
T=0.500*T+T=AI/AI-0.500*DC*(DS**T=AI)/AI	FLMH0420
A=0.500*A*(T=AI-2.000)*KACC2/AI	FLMH0430
SUM=A*T*(2.000*AI*K-T=AI*E)	FLMH0440
IF(SUM.GT.1.00-07) GO TO 50	FLMH0450
60 RETURN	FLMH0460
END	FLMH0470
SUBROUTINE ASS(ACC,R)	ASS 0010
C-----	ASS 0020
C THIS SUBROUTINE COMPUTES THE LIPSCHITZ-	ASS 0030
C HANKEL INTEGRALS I(I,J,K) FROM EXPRESSI-	ASS 0040
C ONS IN EARLIER EVALUATED ELLIPTIC FUNCTI-	ASS 0050
C ONS OF THE FIRST AND SECOND KIND, ELLK AND	ASS 0060
C ELLE, AND HEUMAN'S=LAMHDA FUNCTION, ALMHDA,	ASS 0070
C REFERENCE	ASS 0080
C EASON, NOBLE AND SNEDDON, CERTAIN INTEGRALS	ASS 0090
C OF LIPSCHITZ-HANKEL TYPE INVOLVING PRO-	ASS 0100
C DUCTS OF BESSEL FUNCTIONS, PHILOSOPHICAL	ASS 0110
C TRANSACTIONS, VOL 247, SERIES A935, APRIL	ASS 0120
C 1955, PP 529-546.	ASS 0130
C F10M1=I(1,07-1)	ASS 0140
C F100 =I(1,070)	ASS 0150
C F101 =I(1,071)	ASS 0160
C F11M2=I(1,17-2)	ASS 0170
C F11M1=I(1,17-1)	ASS 0180
C F110 =I(1,170)	ASS 0190
C F111 =I(1,171)	ASS 0200
C-----	ASS 0210
C COMMON/CONST/C,ELLE,ELLK,ALMHDA	ASS 0220
C COMMON/CNTING/F10M1,F100,F101,F11M2,F11M1,F110,F111	ASS 0230
C DOUBLE PRECISION DR,C,DEPR,DEMR,DC2,DR12,DRT,DAD,DR2,DRC2,DRWT,	ASS 0240
C IDEMRR,ELLE,ELLK	ASS 0250
C EC = SNGL(C)	ASS 0260
C IF(W.LT,ACC) GO TO 20	ASS 0270
C EMR = 1.0*H	ASS 0280
C EPR = 1.0*R	ASS 0290
C C2 = EC*EC	ASS 0300



```

HT2 = C2+EPH*EPR
RT = SQRT(RT2)
R2 = R*H
EMRH = 1.0-R2
DR = DBLE(H)
DEPR = 1.000+DR
DEMR = 1.000-DR
DC2 = C*C
DRT2 = DC2+DEPR*DEPR
DRT = DSQRT(DRT2)
DAD = DC2+DEMR*DEMR
DR2 = DR*DR
DRC2 = DR2+DC2
DRRT = DR*DRT
DEMHR = 1.000-DR2
F101 = 0.500*(ELLE*(1.000-DRC2)/(DAD*DRT)+ELLK/DRT)
F110 = DRT*(ELLK*(1.000+DRC2)/DRT2-ELLE)/(2.000*DR)
F111 = C*(ELLE*(1.000+DRC2)/DAD-ELLK)/(2.000*DRRT)
F10M1 = 0.500*ELLE*DRT
F100 = -0.500*C*ELLK/DRT
F11M2 = -C*(C*ELLE*DRT/(4.000*DR)-C*ELLK*(1.000+DR2+0.500*DC2)/
1(2.000*DRRT))/3.000+DR*(DRT*ELLE/2.000+DEMHR*ELLK/(2.000*DRT))/
23.000+(ELLE*DRT/(2.000*DR)-DEMHR*ELLK/(2.000*DRRT))/3.000
F11M1 = 0.500*(0.500*ELLE*C*DRT/DR-ELLK*C*(1.000+DR2+0.500*DC2)/
1DRRT)
HLP = R
IF(R.GT.1.0) HLP=1.0/R
IF(ABS(EMR).LT.ACC) GO TO 10
F10M1 = F10M1+0.5*(SNGL(ELLK)*EMRH/RT+SIGN(EC*ALMBDA,EMR))
F100 = F100+0.5*SIGN(ALMBDA,-EMR)
F11M2 = F11M2-EC*ALMBDA*SIGN(1.0,EMR)*EMRH/(4.0*R)
F11M2 = F11M2-EC*(HLP/2.0+HLP)/3.0
F11M1 = F11M1+SIGN(0.25,EMR)*EMRH*ALMBDA/R+0.5*HLP
IF(R.GT.1.0) GO TO 30
F10M1 = F10M1-EC
F100 = F100+1.0
GO TO 30
10 F10M1 = F10M1-0.5*EC
F100 = F100+0.5
F11M2 = F11M2-0.5*EC
F11M1 = F11M1+0.5*HLP
GO TO 30
20 AD = 1.0+EC*EC
RT = SQRT(AD)
ADRT = AD*RT
F101 = 1.0/ADRT
F110 = 0.5/ADRT
F111 = 1.5*EC/(AD*ADRT)
F10M1 = RT-EC
F100 = 1.0-EC/RT
F11M2 = 0.5*(RT-EC)
F11M1 = 0.5*(1.0-EC/RT)
30 RETURN
END
SUBROUTINE INGRAL(IL,INTV,INTT,INT)
-----
C THIS SUBROUTINE CONTROLS THE SIMULTANEOUS INGR0020
C COMPUTATION OF A GROUP OUT OF THE 17 INTE-INGR0030
C GRALS. INGR0050
C IL=1,THE GROUP WITH J0(XR)J1(X) IN INTEGR,INGR0060
C IL=2,THE GROUP WITH J1(XR)J1(X) IN INTEGR,INGR0070

```







```

IF (INTV3(J),EQ,0) GO TO 2090
IF (ABS(COMP(J)),LT,ACCUR(2)) GO TO 2080
IF (ABS((COMP(J)-FIRST(J)-SECOND(J))/COMP(J)),LT,ACCUR(3))
1 GO TO 2080
GO TO 2090
2080 INTT3 = INTT3-1
IF (LOWER,GT,ACCUR(1)) GO TO 2090
INTT2 = INTT2-1
INTV3(J) = 0
2090 CONTINUE
IF (INTT3,EQ,0) GO TO 2110
ALFA = 0
LOWER = MIDPNT
DELTA = 0.5*DELTA
BETA = BETA+1
IF (BETA,GT,30) GO TO 2150
C-----INGR1300
C ARRIVAL HERE MEANS THAT THE INTEGRAND IS TOO INGR1310
C IRREGULAR TO GET INTEGRATED OVER THE REGION FROM INGR1320
C THE ORIGIN TO THE FIRST BESSEL ZERO. INGR1330
C-----INGR1340
C IRES = 1 INGR1350
DO 2100 J = 1,NINT INGR1360
COMP(J) = SECOND(J) INGR1370
RES(J) = FIRST(J) INGR1380
2100 CONTINUE INGR1390
INTT3 = INTT2 INGR1400
GO TO 2070 INGR1410
2110 DO 2120 J = 1,NINT INGR1420
K = INTV2(J) INGR1430
IF (K,EQ,0) GO TO 2120 INGR1440
INT(K) = INT(K)+FIRST(J)+SECOND(J) INGR1450
IF (INTV3(J),NE,0) GO TO 2120 INGR1460
INTV2(J) = 0 INGR1470
2120 CONTINUE INGR1480
UPPER = LOWER INGR1490
INTT3 = INTT2 INGR1500
IF (ALFA) 3000,2140,2130 INGR1510
2130 DELTA = DELTA*2.0 INGR1520
BETA = BETA-1 INGR1530
2140 ALFA = ALFA+1 INGR1540
GO TO 2020 INGR1550
2150 WRITE(NOUT,9040) INGR1560
GO TO 3180 INGR1570
C-----INGR1580
C INTEGRATION OVER THE REMAINING INTERVALS. INGR1590
C-----INGR1600
3000 IF IN = NZEROS-1 INGR1610
DO 3*10 J = 1,NINT INGR1620
INTV2(J) = INTV(J) INGR1630
3010 CONTINUE INGR1640
INTT2 = INTT INGR1650
DO 3130 IBESS = 1,IFIN INGR1660
DO 3020 J = 1,NINT INGR1670
INTV3(J) = INTV2(J) INGR1680
FIRST(J) = 0.0 INGR1690
3020 CONTINUE INGR1700
INTT3 = INTT2 INGR1710
DO 3070 ORDER = 4,15 INGR1720
CALL QUAD(IL,INTV3,ZEROS(IBESS),ZEROS(IBESS+1),ORDER,SECOND, INGR1730
1 NTELL) INGR1740
INGR1750
INGR1760
INGR1770
INGR1780
INGR1790
INGR1800
INGR1810
INGR1820
INGR1830
INGR1840
INGR1850
INGR1860
INGR1870
INGR1880
INGR1890
INGR1900

```



1050	INT(K) = Z*F111 GO TO 1190	INGR0690 INGR0700
1060	INT(K) = F100-Z*F101 GO TO 1190	INGR0710 INGR0720
1070	INT(K) = -2.0*(1.0-NU(1))*F10M1+Z*F100 GO TO 1190	INGR0730 INGR0740
1080	INT(K) = -2.0*(1.0-NU(1))*F110+Z*F111 GO TO 1190	INGR0750 INGR0760
1090	INT(K) = -F110 GO TO 1190	INGR0770 INGR0780
1100	INT(K) = F11M1-Z*F110 GO TO 1180	INGR0790 INGR0800
1110	INT(K) = F11M1 GO TO 1180	INGR0810 INGR0820
1120	INT(K) = -2.0*(1.0-NU(1))*F11M2+Z*F11M1 GO TO 1180	INGR0830 INGR0840
1130	INT(K) = -F100 GO TO 1190	INGR0850 INGR0860
1140	INT(K) = F10M1 GO TO 1190	INGR0870 INGR0880
1150	INT(K) = F110 GO TO 1190	INGR0890 INGR0900
1160	INT(K) = -F11M1 GO TO 1180	INGR0910 INGR0920
1170	INT(K) = F11M2	INGR0930
1180	IF(R,GE,ACCUR(1)) INT(K) = INT(K)/R	INGR0940
1190	CONTINUE IF(NLAYS,EQ,1) GO TO 3140	INGR0950 INGR0960
C	-----	INGR0970
C	INTEGRATION FROM THE ORIGIN TO THE FIRST	INGR0980
C	BESSEL ZERO.	INGR0990
C	-----	INGR1000
2000	INT12 = INT1 INT13 = INT1 DO 2010 J = 1,NINT INTV2(J) = INTV(J) INTV3(J) = INTV(J)	INGR1010 INGR1020 INGR1030 INGR1040 INGR1050
2010	CONTINUE UPPER = ZEROS(1) BETA = 0 ALFA = 0 IRES = 0 DELTA = 0.5*ZEROS(1)	INGR1060 INGR1070 INGR1090 INGR1080 INGR1100 INGR1110
2020	LOWER = UPPER-DELTA IF(LOWER=ACCUR(1)) 2030,2030,2040	INGR1120 INGR1130
2030	ALFA = -1 LOWER = 0.0	INGR1140 INGR1150
2040	IF(IRES,EQ,1) GO TO 2050 CALL QUAD(IL,INTV3,LOWER,UPPER,16,COMP,NTELL) IF(NTELL,NE,0) GO TO 3180 GO TO 2070	INGR1160 INGR1170 INGR1180 INGR1190
2050	DO 2060 J = 1,NINT COMP(J) = RES(J)	INGR1200 INGR1210
2060	CONTINUE IRES = 0	INGR1220 INGR1230
2070	MIDPNT = 0.5*(LOWER+UPPER) CALL QUAD(IL,INTV3,LOWER,MIDPNT,16,FIRST,NTELL) IF(NTELL,NE,0) GO TO 3180 CALL QUAD(IL,INTV3,MIDPNT,UPPER,16,SECOND,NTELL) IF(NTELL,NE,0) GO TO 3180 DO 2090 J = 1,NINT	INGR1240 INGR1250 INGR1260 INGR1270 INGR1280 INGR1290



	IF(NTELL,NE,0) GO TO 3180	INGR1910
	DO 3060 J = 1,NINT	INGR1920
	K = INTV3(J)	INGR1930
	IF(K,EQ,0) GO TO 3060	INGR1940
	IF(ABS(INT(K)),LT,0,01) GO TO 3030	INGR1950
	IF(ABS((FIRST(J)-SECOND(J))/INT(K)),LT,0,1*ACCUR(3))	INGR1960
1	GO TO 3040	INGR1970
	GO TO 3050	INGR1980
3030	IF(ABS(FIRST(J)-SECOND(J)),GE,0,1*ACCUR(2)) GO TO 3050	INGR1990
3040	INTV3(J) = 0	INGR2000
	INTT3 = INTT3-1	INGR2010
	GO TO 3060	INGR2020
3050	FIRST(J) = SECOND(J)	INGR2030
3060	CONTINUE	INGR2040
	IF(INTT3,EQ,0) GO TO 3080	INGR2050
3070	CONTINUE	INGR2060
	WRITE(NOUT,9020)	INGR2070
	WRITE(NOUT,9050) ZERUS(IBESS)	INGR2080
C	-----	INGR2090
C	ARRIVAL HERE MEANS THAT THE DESIRED ACCURACY CANNOT	INGR2100
C	BE MET BY MEANS OF THE AVAILABLE GAUSS-JACOBI	INGR2110
C	POLYNOMIALS.	INGR2120
C	-----	INGR2130
	GO TO 3180	INGR2140
3080	DO 3120 J = 1,NINT	INGR2150
	K = INTV2(J)	INGR2160
	IF(K,EQ,0) GO TO 3120	INGR2170
	INT(K) = INT(K)+SECOND(J)	INGR2180
	IF(ABS(INT(K)),LT,0,01) GO TO 3090	INGR2190
	IF(ABS(SECOND(J)/INT(K)),LT,0,1*ACCUR(3)) GO TO 3110	INGR2200
	GO TO 3100	INGR2210
3090	IF(ABS(SECOND(J)),LT,0,1*ACCUR(2)) GO TO 3110	INGR2220
3100	KK(J) = 0	INGR2230
	GO TO 3120	INGR2240
3110	KK(J) = KK(J)+1	INGR2250
	IF(KK(J),LT,2) GO TO 3120	INGR2260
	INTV2(J) = 0	INGR2270
	INTT2 = INTT2-1	INGR2280
3120	CONTINUE	INGR2290
	IF(INTT2,EQ,0) GO TO 3140	INGR2300
3130	CONTINUE	INGR2310
	WRITE(NOUT,9030)	INGR2320
	WRITE(NOUT,9050) ZEROS(IFIN)	INGR2330
C	-----	INGR2340
C	ARRIVAL HERE MEANS THAT ALL AVAILABLE BESSEL ZEROS	INGR2350
C	HAVE BEEN EXHAUSTED BECAUSE OF ILL CONVERGENCE OF	INGR2360
C	THE INTEGRALS.	INGR2370
C	-----	INGR2380
	GO TO 3180	INGR2390
3140	DO 3170 J = 1,NINT	INGR2400
	K = INTV(J)	INGR2410
	IF(K,EQ,0) GO TO 3170	INGR2420
	IF(K-S) 3150,3150,3160	INGR2430
3150	INT(K) = INT(K)*LOAD	INGR2440
	GO TO 3170	INGR2450
3160	INT(K) = INT(K)*HOSTRS	INGR2460
3170	CONTINUE	INGR2470
	RETURN	INGR2480
3180	WRITE(NOUT,9010) (INTV3(J),J=1,NINT)	INGR2490
	GO TO 3140	INGR2500
9010	FORMAT(" DURING CALCULATION OF INTEGRALS",10I3)	INGR2510



```

9020 FORMAT(" SUSPEND PROGRAM GAUSS POLYS EXHAUSTED")           INGH2520
9030 FORMAT(" SUSPEND PROGRAM BESSEL ZEROS EXHAUSTED")          INGH2530
9040 FORMAT(" SUSPEND PROGRAM STEPSIZE FIRST INTERVAL TOO SMALL") INGH2540
9050 FORMAT(" AT THE VALUE ",E11.4," FOR THE INTEGRATION VARIABLE") INGH2550
      END                                                         INGH2560
      SUBROUTINE QUAD (IL,INTV,ALO,UP,NGAUSS,FSC,NTELL)           QUAD0010
C-----
C      THIS SUBROUTINE CALCULATES FOR THE SET                   QUAD0020
C      INTV THE INTEGRALS OF THE CORRESPONDING                 QUAD0030
C      FUNCTIONS IGRAND BETWEEN THE LIMITS ALO                 QUAD0040
C      AND UP BY USING A GAUSS QUADRATURE OF                   QUAD0050
C      ORDER NGAUSS.                                           QUAD0060
C      =FOR NGAUSS=16 A LEGENDRE=GAUSS QUADRATURE OF ORDER    QUAD0070
C      RE OF ORDER .                                           QUAD0080
C      =FOR NGAUSS.LT.16 A JACOBI=GAUSSQUADRATURE OF ORDER    QUAD0090
C      RE.                                                       QUAD0100
C      THE ABSCISSAE AND WEIGHTS OF BOTH ARE                   QUAD0110
C      STORED AS AGAUSS AND HGAUSS IN THE BLOCK                QUAD0120
C      DATA.                                                    QUAD0130
C      THE SET OF INTEGRANDS IS COMPUTED DURING                QUAD0140
C      SUBSEQUENT CALLING IN OF*                                QUAD0150
C      SUBROUTINES MATRIX                                       QUAD0160
C      FPIGRA                                                    QUAD0170
C      AND FUNCTION IGRAND                                       QUAD0180
C      THE SET OF RESULTING INTEGRALS IS                        QUAD0190
C      DELIVERED IN FSC                                         QUAD0200
C-----
      INTEGER INTV(10)                                           QUAD0210
      REAL IGRAND,FSC(10)                                         QUAD0220
      COMMON/GAUSS/AGAUSS(16,16),HGAUSS(16,16)                  QUAD0230
      NINT = 7                                                    QUAD0240
      IF(IL.EQ.2) NINT = 10                                       QUAD0250
      DO 10 J = 1,NINT                                           QUAD0260
        K = INTV(J)                                               QUAD0270
        IF(K.EQ.0) GO TO 10                                       QUAD0280
        FSC(J) = 0.0                                             QUAD0290
      10 CONTINUE                                               QUAD0300
      LABEL = 0                                                  QUAD0310
      IF(IL.EQ.2) GO TO 20                                       QUAD0320
      IF((INTV(1)+INTV(2)+INTV(3)).GT.0) LABEL = LABEL+1        QUAD0330
      IF((INTV(4)+INTV(5)).GT.0) LABEL = LABEL+2                QUAD0340
      IF((INTV(6)+INTV(7)).GT.0) LABEL = LABEL+4                QUAD0350
      GO TO 30                                                    QUAD0360
      20 IF((INTV(1)+INTV(2)).GT.0) LABEL = LABEL+1             QUAD0370
      IF((INTV(3)+INTV(4)+INTV(5)+INTV(6)+INTV(7)).GT.0) LABEL = LABEL+2 QUAD0380
      IF((INTV(8)+INTV(9)+INTV(10)).GT.0) LABEL = LABEL+4      QUAD0390
      30 F1 = 0.5*(UP-ALO)                                         QUAD0400
      F2 = 0.5*(UP+ALO)                                         QUAD0410
      IGAUSS = NGAUSS                                           QUAD0420
      IF(NGAUSS.EQ.16) IGAUSS=8                                  QUAD0430
      DO 50 I = 1,IGAUSS                                         QUAD0440
        X = F1*AGAUSS(I,NGAUSS)+F2                               QUAD0450
        CALL MATRIX (X,LABEL,NTELL)                              QUAD0460
        IF(NTELL.EQ.1) RETURN                                   QUAD0470
        CALL FPIGRA (IL,X)                                       QUAD0480
        DO 40 J = 1,NINT                                         QUAD0490
          K = INTV(J)                                           QUAD0500
          IF(K.EQ.0) GO TO 40                                   QUAD0510
          FSC(J) = FSC(J)+HGAUSS(I,NGAUSS)*IGRAND(X,K)        QUAD0520
        40 CONTINUE                                           QUAD0530
      50 CONTINUE                                               QUAD0540
      QUAD0550
      QUAD0560

```



```

DO 60 J = 1,NINT                                QUAD0570
  K = INTV(J)                                    QUAD0580
  IF(K.EQ.0) GO TO 60                            QUAD0590
  FSC(J) = FSC(J)*F1                             QUAD0600
60 CONTINUE                                       QUAD0610
70 RETURN                                         QUAD0620
END                                               QUAD0630
SUBROUTINE MATRIX (X,LABL,NTELL)                 MATR0010
C-----MATR0020
C      THIS SUBROUTINE COMPUTES THE SET OF CHARACTERISTIC-FUNCTIONS TO,VO,SO,UO,T1,V1, MATR0030
C      S1,U1,TQ1 AND SQ1 FOR THE VALUE X OF THE INTEGRATION-PARAMETER. USE IS MADE OF MATR0040
C      CONSTANTS CALCULATED IN MACON1 AND MA2CON. THEY WERE STORED IN COMMON/INDATA/, MATR0050
C      CHARACTERISTIC-FUNCTION VALUES ARE DELIVERED IN COMMON/IGRAN/. MATR0060
C      LABL DETERMINES WHICH CHARACTERISTIC-FUNCTIONS ARE NEEDED" MATR0070
C      =LABL=1"TO,VO,SO,UO MATR0080
C      =LABL=2"TI,V1,S1,U1 MATR0090
C      =LABL=3"TO,VO,SO,UO,T1,V1,S1,U1 MATR0100
C      =LABL=4"TO1,SQ1 MATR0110
C      =LABL=5"TO,VO,SO,UO,TQ1,SQ1 MATR0120
C      =LABL=6"TI,V1,S1,U1,TQ1,SQ1 MATR0130
C      =LABL=7"TO,VO,SO,UO,T1,V1,S1,U1,TQ1,SQ1 MATR0140
C      SUBROUTINE IS INTERRUPTED AND RETURNED WITH NTELL=1 WHEN SOLUTION BECOMES TOO MATR0150
C      INACCURATE BECAUSE OF ILL MATRIX-CONDITION DURING INVERSION. MATR0160
C-----MATR0170
REAL LOAD,NU,W(4,4,4),P(4,2),PP(2,2),K1,K2,K5,K6,I1,NJ(2,2,9),KKK, MATR0250
1 ACCUR(3),VP(2,10),NJ2(4),P3(2),NP2(10),K4(10) MATR0260
COMMON/ASD1/LAYER,NLAYS,M,L,Z,NU(10),ACCUR,LOAD,HOSTHS,NZEROS,H(9) MATR0270
1,K5(10),E(10),AL(9),THICK(9),RADIUS(10) MATR0280
COMMON/INDATA/XMAX, A1(9),H1(9),C1(9),D(4),EE(9),F(9),G(9),H1(9), MATR0290
111(9),K1(9),K2(9),K6(10),BE(9),HU(9),BUU(4),BMU(9),B2U(9),B2UU(9), MATR0300
2J2(9),J1,T2(10),SS(2,10),G012(9),G021(4),G022(9),G122(9), MATR0310
3H012(9),H022(9),H122(9),D012(9),D022(9),C011(9),C012(9),E012(9), MATR0320
4F012(9),F112(9),F022(9),CC(4,2,9),DD(2,2,9),FF(2,2,9),GG(2,2,10), MATR0330
5HH(2,2,10),HH(4,2,10),DD2(9),G20(9),G21(9),H20(9),H021(9),GG2(10), MATR0340
6HH2(10),Q011(9),Q111(9),Q012(9),Q112(9),Q212(9),Q022(9),Q122(9), MATR0350
7QF0(9),QF1(9),Z011,Z111,Z211,Z012,Z112,Z212,Z312,Z021,Z121,Z022, MATR0360
8Z122,Z222,K4 MATR0370
COMMON/IGRAN/TO,VO,SO,UO,T1,V1,S1,U1,TQ1,SQ1,FPIGH,EX1,EX2 MATR0380
COMMON/TAPE/NOU MATR0390
LABEL = LABL MATR0400
IF(LABEL.LT.4) GO TO 1000 MATR0410
IF(X.LT.XMAX) GO TO 100 MATR0420
C-----MATR0430
C      ASYMPTOTIC EVALUATION OF TQ1 AND SQ1 MATR0440
C      FOR X,GE,XMAX. MATR0450
C-----MATR0460
TQ1 = 1.0 MATR0470
IF(LAYER.EQ.1) GO TO 30 MATR0480
J = LAYER-1 MATR0490
DO 20 K = 1,J MATR0500
  TQ1=TQ1+2.0*(1.0-AL(K))/((1.0-AL(K))*(1.0+K1(K))+0.5*AL(K)*X) MATR0510
20 CONTINUE MATR0520
30 SQ1=TQ1*(0.5*AL(LAYER)*X-(1.0-AL(LAYER))*K2(LAYER))/((1.0-AL(LAYER) MATR0530
1 ))*(1.0+K1(LAYER))+0.5*AL(LAYER)*X) MATR0540

```



	LABEL = LABEL=4	MATH0550
	GO TO 1000	MATH0560
C	-----	MATH0570
C	CALCULATION OF TQ1 AND SQ1 FOR X,LT,XMAX	MATH0580
C	-----	MATH0590
	100 IF(J1,EQ,0) GO TO 120	MATH0600
	DO 110 J = 1,J1	MATH0610
	GG2(J+1) = G20(J)-G21(J)*X	MATH0620
	HM2(J+1) = H20(J)+G21(J)*X	MATH0630
	110 CONTINUE	MATH0640
	120 DO 150 K = 1,M	MATH0650
	IF(J1,EQ,0) GO TO 140	MATH0660
	DO 130 I = 1,J1	MATH0670
	IF(J2(I),EQ,K) GO TO 150	MATH0680
	130 CONTINUE	MATH0690
	140 W1 = 0.5*(1.0+K1(K))	MATH0700
	W2 = 0.5*K2(K)	MATH0710
	W3 = BE(K)*0.25*X	MATH0720
	NJ(1,1,K) = W1+W3	MATH0730
	NJ(1,2,K) = W2+W3	MATH0740
	NJ(2,1,K) = W2+W3	MATH0750
	NJ(2,2,K) = W1+W3	MATH0760
	150 CONTINUE	MATH0770
	J5 = J1+1	MATH0780
	DO 300 MM = 1,J5	MATH0790
	N = J5+1-MM	MATH0800
	IF(N=1) 160,160,170	MATH0810
	160 J3 = 1	MATH0820
	GO TO 180	MATH0830
	170 J3 = J2(N-1)+1	MATH0840
	180 IF(J5=N) 190,190,200	MATH0850
	190 J4 = N	MATH0860
	GO TO 210	MATH0870
	200 J4 = J2(N)-1	MATH0880
	210 IF(J3,GT,J4) GO TO 240	MATH0890
	DO 230 IJ = J3,J4	MATH0900
	IK = J4+J3-IJ	MATH0910
	IL = IK+1	MATH0920
	EXPO = -X*T2(IL)	MATH0930
	IF(EXPO,LT,-70.0) GO TO 212	MATH0931
	EXP1 = EXP(EXPO)*SS(1,IL)	MATH0932
	GO TO 214	MATH0933
	212 EXP1 = ^,0	MATH0934
	214 DO 220 I=1,2	MATH0940
	220 SS(I,IK) = NJ(I,1,IK)*EXP1+NJ(I,2,IK)*SS(2,IL)	MATH0950
	230 CONTINUE	MATH0960
	240 NN = N-1	MATH0970
	EXPO = -X*T2(J3)	MATH0971
	IF(EXPO,LT,-70.0) GO TO 242	MATH0972
	EXP2 = EXP(EXPO)	MATH0973
	GO TO 244	MATH0974
	242 EXP2 = 0.0	MATH0975
	244 PROD = GG2(N)*SS(1,J3)*EXP2	MATH0980
	P2 = PROD+HM2(N)*SS(2,J3)	MATH0990
C	-----	MATH1000
C	TEST MATRIX=CONDITION BEFORE INVERSION,	MATH1010
C	-----	MATH1020
	IF(ABS(P2),LT,1.0E-7*ABS(PROD)/ACCUH(5)) GO TO 2000	MATH1030
	PP2 = 1.0/P2	MATH1040
	IF(N,EQ,1) GO TO 310	MATH1050
	NJ2(NN) = PP2*DD2(NN)	MATH1060



DO 270 I = 1,2	MATH1070
270 P3(I) = SS(1,J3)*NJ2(NN)	MATH1080
PP2=P3(1)*EXP2-P3(2)	MATH1090
SS(1,J3-1) = PP2+1.0	MATH1100
SS(2,J3-1) = 1.0	MATH1110
300 CONTINUE	MATH1120
310 IF(NTELL.EQ.2) RETURN	MATH1130
NP2(1) = -PP2	MATH1131
IF(J1.EQ.0) GO TO 390	MATH1140
DO 350 I = 1,J1	MATH1150
J = J1+1-I	MATH1160
IF(LAYER.GT.J2(J)) GO TO 360	MATH1170
350 CONTINUE	MATH1180
J5 = 1	MATH1190
GO TO 390	MATH1200
360 DO 380 I = 1,J	MATH1210
NP2(I+1) = NJ2(I)*NP2(I)	MATH1220
380 CONTINUE	MATH1230
J5 = J+1	MATH1240
390 J = LAYER	MATH1250
S01 = SS(1,J)*NP2(J5)	MATH1260
T01 = SS(2,J)*NP2(J5)	MATH1270
LABEL = LABEL-4	MATH1280
C-----	MATH1290
C	ASYMPTOTIC EVALUATION OF T0,V0,S0,U0,T1,
C	V1,S1 AND U1 FOR X.GE.XMAX,
C-----	MATH1310
1000 IF(LABEL.EQ.0) RETURN	MATH1320
IF(x.LT.XMAX) GO TO 1100	MATH1330
L = LAYER	MATH1340
X2 = x*x	MATH1350
X3 = x2*x	MATH1360
IF(L.EQ.NLAYS) GO TO 1010	MATH1370
Z11 = Z011+x*Z111+x2*Z211	MATH1380
Z12 = Z012+x*Z112+x2*Z212+x3*Z312	MATH1390
Z21 = Z021+x*Z121	MATH1400
Z22 = Z022+x*Z122+x2*Z222	MATH1410
1010 IF(LABEL.GT.1) GO TO 1030	MATH1420
1020 IF(LABEL.EQ.0) RETURN	MATH1430
NP(1,1) = 2.0*NU(1)	MATH1440
NP(2,1) = 1.0	MATH1450
GO TO 1040	MATH1460
1030 NP(1,1) = 1.0-2.0*NU(1)	MATH1470
NP(2,1) = -1.0	MATH1480
1040 PQF = 1.0	MATH1490
IF(L.EQ.1) GO TO 1060	MATH1500
DO 1050 K = 2,L	MATH1510
J = K-1	MATH1520
PQF = PQF*K6(J)/(QF0(J)+QF1(J)*X)	MATH1530
W1 = -AL(J)*X	MATH1540
W9 = H(J)*X	MATH1550
NP(1,K) = NP(1,J)*(Q011(J)+Q111(J)*X+W1*W9)+NP(2,J)*(Q012(J)	MATH1560
1 +Q112(J)*X+Q212(J)*X2+W1*W9*W9)	MATH1570
1050 NP(2,K) = -W1*NP(1,J)+NP(2,J)*(Q022(J)+Q122(J)*X-W1*W9)	MATH1580
IF(L.NE.NLAYS) GO TO 1060	MATH1590
S = 0.0	MATH1600
U = 0.0	MATH1610
GO TO 1070	MATH1620
1060 S = (NP(1,L)*Z11+NP(2,L)*Z12)*PQF/(QF0(L)+QF1(L)*X)	MATH1630
U = (NP(1,L)*Z21+NP(2,L)*Z22)*PQF/(QF0(L)+QF1(L)*X)	MATH1640
1070 T = NP(1,L)*PQF	MATH1650
	MATH1660



V = NP(2,L)*PUF	MATH1670
IF(LABEL,GT,1) GO TO 1080	MATH1680
S0 = S	MATH1690
U0 = U	MATH1700
T0 = T	MATH1710
V0 = V	MATH1720
RETURN	MATH1730
1080 S1 = S	MATH1740
U1 = U	MATH1750
T1 = T	MATH1760
V1 = V	MATH1770
LABEL = LABEL-2	MATH1780
GO TO 1020	MATH1790
-----	
C	MATH1800
C	MATH1810
C	MATH1820
C	MATH1830
1100 IF(J1,EQ,0) GO TO 1120	MATH1840
DO 1110 J = 1,J1	MATH1850
K = J2(J)	MATH1860
W1 = -AL(K)*X	MATH1870
W9 = H(K)*X	MATH1880
CC(1,1,J) = C011(J)+2.0*W9	MATH1890
CC(1,2,J) = C012(J)+2.0*W9*W9	MATH1900
CC(2,2,J) = C011(J)-2.0*W9	MATH1910
DD(1,2,J) = D012(J)+DD(1,1,J)*W9	MATH1920
DD(2,2,J) = D022(J)+DD(2,1,J)*W9	MATH1930
FF(1,1,J) = -C011(J)-2.0*W9	MATH1940
FF(1,2,J) = F012(J)+F112(J)*W9-2.0*W9*W9	MATH1950
FF(2,2,J) = F022(J)+2.0*W9	MATH1960
GG(1,2,J+1) = G012(J)+GG(1,1,J+1)*W9	MATH1970
GG(2,1,J+1) = G021(J)+W1	MATH1980
GG(2,2,J+1) = G022(J)+(G021(J)*H(K)+G122(J))*X+W1*W9	MATH1990
HH(1,2,J+1) = H012(J)+HH(1,1,J+1)*W9	MATH2000
HH(2,1,J+1) = H021(J)+W1	MATH2010
HH(2,2,J+1) = H022(J)+H021(J)*W9+H122(J)*X+W1*W9	MATH2020
1110 CONTINUE	MATH2030
1120 DO 1150 K=1,M	MATH2040
IF(J1,EQ,0) GO TO 1140	MATH2050
DO 1130 I = 1,J1	MATH2060
IF(J2(I),EQ,K) GO TO 1150	MATH2070
1130 CONTINUE	MATH2080
1140 W1 = BMU(K)*X	MATH2090
W9 = H(K)*X	MATH2100
W10 = W9*X	MATH2110
W2 = W10*BF(K)	MATH2120
W11 = W2*W9	MATH2130
W3 = W9*C1(K)	MATH2140
W4 = BE(K)*X	MATH2150
W5 = BU(K)*X	MATH2160
W8 = BUU(K)*X	MATH2170
W7 = C1(K)*W9*W9	MATH2180
W(1,1,K) = A1(K)+W1-W2	MATH2190
W(1,2,K) = -EE(K)+F(K)*W9+W8+B2U(K)*W10-W11	MATH2200
W(1,3,K) = D(K)-W3+W1-W2	MATH2210
W(1,4,K) = -G(K)+H1(K)*W9-BUU(K)*X-W7+B2UU(K)*W10-W11	MATH2220
W(2,1,K) = W4	MATH2230
W(2,2,K) = B1(K)+W5+W2	MATH2240
W(2,3,K) = C1(K)+W4	MATH2250
W(2,4,K) = I1(K)+W3-W5+W2	MATH2260
W(3,1,K) = D(K)+W3-W1-W2	MATH2270



```

w(3,2,K) = G(K)+H1(K)*w9-w8+w7-B2UU(K)*w10-w11
w(3,3,K) = A1(K)-w1-w2
w(3,4,K) = E1(K)+F(K)*w9+w8-B2U(K)*w10-w11
w(4,1,K) = -C1(K)+w4
w(4,2,K) = II(K)-w3+w5+w2
w(4,3,K) = w4
w(4,4,K) = B1(K)-w5+w2
1150 CONTINUE
J5 = J1+1
PKK6 = 1,0
DO 1300 MM = 1,J5
  KK6 = 1,0
  N = J5+1-MM
  IF(N=1) 1160,1160,1170
1160 J3 = 1
  GO TO 1180
1170 J3 = J2(N-1)+1
1180 IF(J5=N) 1190,1190,1200
1190 J4 = N
  GO TO 1210
1200 J4 = J2(N)-1
1210 IF(J3.GT.J4) GO TO 1240
  DO 1230 IJ = J3,J4
    IK = J4+J3-IJ
    IL = IK+1
    KK6 = KK6*KK6(IK)
    IF(IK.EQ.LAYER) PKK6 = KK6
    EXPO=-X*T2(IL)
    IF(EXPO.LT.-70,0)GO TO 1212
    EXP1=EXP(EXPO)
    GO TO 1214
1212 EXP1=0,0
1214 DO 1220 I=1,4
      DO 1220 K = 1,2
1220 RH(I,K,IK)=(W(I,1,IK)*RR(1,K,IL)+W(I,2,IK)*HR(2,K,IL))
      *EXP1+W(I,3,IK)*RR(3,K,IL)+W(I,4,IK)*RR(4,K,IL)
1230 CONTINUE
1240 NN = N-1
  EXPO=-X*T2(J3)
  IF(EXPO.LT.-70,0)GO TO 1242
  EXP2=EXP(EXPO)
  GO TO 1244
1242 EXP2=0,0
1244 DO 1250 I=1,2
  DO 1250 K = 1,2
1250 P(I,K) = (GG(I,1,N)*RR(1,K,J3)+GG(I,2,N)*RR(2,K,J3))
      *EXP2+HH(I,1,N)*RR(3,K,J3)+HH(I,2,N)*RR(4,K,J3)
      PROD = P(1,1)*P(2,2)
      DET = PROD-P(1,2)*P(2,1)
C-----MATH2680
C TEST MATRIX CONDITION BEFORE INVERSION. MATH2690
C-----MATH2700
IF(ABS(DET).LT.1.0E-7*ABS(PROD)/ACCUR(3)) GO TO 2000
QKK6 = KK6/DET
PP(1,1) = P(2,2)*QKK6
PP(1,2) = -P(1,2)*QKK6
PP(2,1) = -P(2,1)*QKK6
PP(2,2) = P(1,1)*QKK6
IF(N.EQ.1) GO TO 1310
DO 1260 I = 1,2
  DO 1260 K = 1,2

```



```

1260      NJ(I,K,NN)=PP(I,1)*DD(1,K,NN)+PP(I,2)*DD(2,K,NN)      MATR280U
      DO 1270 I = 1,4      MATR281U
      DO 1270 K = 1,2      MATR282U
1270      P(I,K) =(HR(I,1,J3)*NJ(1,K,NN)+HR(I,2,J3)*NJ(2,K,NN))/KK6 MATR283U
      DO 1280 I = 1,2      MATR284U
      PP(1,1)=(P(1,1)+E012(NN)*P(2,1))*EXP2+FF(1,1,NN)      MATR285U
      *P(3,1)+FF(1,2,NN)*P(4,1)      MATR286U
1280      PP(2,1)=P(2,1)*EXP2+FF(2,1,NN)*P(3,1)+FF(2,2,NN)*P(4,1) MATR287U
      DO 1290 I = 1,2      MATR289U
      DO 1290 K = 1,2      MATR290U
1290      RR(I,K,J3-1) = CC(I,K,NN)+PP(I,K)      MATR291U
      RR(3,1,J3-1) = 1.0      MATR292U
      HR(3,2,J3-1) = 0.0      MATR293U
      HR(4,1,J3-1) = 0.0      MATR294U
      HR(4,2,J3-1) = 1.0      MATR295U
1300 CONTINUE      MATR296U
1310 IF(NTELL,EQ,2) GO TO 100      MATR297U
      IF(LABEL,GT,1) GO TO 1330      MATR2971
1320 IF(LABEL,EQ,0) RETURN      MATR298U
      NP(1,1) = PP(1,1)      MATR299U
      NP(2,1) = PP(2,1)      MATR300U
      GO TO 1340      MATR301U
1330 NP(1,1) = PP(1,2)      MATR302U
      NP(2,1) = PP(2,2)      MATR303U
1340 IF(J1,EQ,0) GO TO 1390      MATR304U
      DO 1350 I = 1,J1      MATR305U
      J = J1+1-I      MATR306U
      IF(LAYER,GT,J2(J)) GO TO 1360      MATR307U
1350 CONTINUE      MATR308U
      J5 = 1      MAT-30 U
      GO TO 1390      MATR310U
1360 DO 1380 I = 1,J      MATR311U
      IM = I+1      MATR312U
      DO 1370 K = 1,2      MATR313U
1370      NP(K,IM) = NJ(K,1,I)*NP(1,I)+NJ(K,2,I)*NP(2,I) .      MATR314U
1380 CONTINUE      MATR315U
      J5 = J+1      MATR316U
1390 J = LAYER      MATR317U
      S =(HR(1,1,J)*NP(1,J5)+HR(1,2,J)*NP(2,J5))/PKK6      MATR318U
      U =(HR(2,1,J)*NP(1,J5)+HR(2,2,J)*NP(2,J5))/PKK6      MATR319U
      T =(HR(3,1,J)*NP(1,J5)+HR(3,2,J)*NP(2,J5))/PKK6      MATR320U
      V =(HR(4,1,J)*NP(1,J5)+HR(4,2,J)*NP(2,J5))/PKK6      MATR321U
      IF(LABEL,GT,1) GO TO 1400      MATR322U
      TO = T      MATR323U
      SO = S      MATR324U
      UO = U      MATR325U
      VO = V      MATR326U
      RETURN      MATR327U
1400 S1 = S      MATR328U
      T1 = T      MATR329U
      U1 = U      MATR330U
      V1 = V      MATR331U
      LABEL = LABEL+2      MATR332U
      GO TO 1320      MATR333U
-----MATR334U
C      ARRIVAL HERE MEANS THAT SOLUTION OF THE      MATR335U
C      CHARACTERISTIC FUNCTIONS HAS BEEN STOPPED      MATR336U
C      PREMATURELY BECAUSE OF ILL MATRIX CONDI-      MATR337U
C      TION MET DURING SOLUTION PROCESS.      MATR338U
C-----MATR339U
2000 WRITE(NOUT,9000)X

```



```

      NTELL = 1
      RETURN
9000 FORMAT(' ILL-CONDITIONED DETERMINANT FOR X=',E15,7)
      END
      SUBROUTINE FPIGRA (IL,X)
-----
C      THIS SUBROUTINE COMPUTES THE BESSELFUNC=
C      TION=PART OF THE INTEGRANDS FOR THE
C      INTEGRALS COMPUTED IN INGRAL,
C      FOR IL=1 THIS PART IS JO(XR)*J1(X)
C      FOR IL=2 THIS PART IS J1(XR)*J1(X)
C      COMPUTED RESULTS ARE DELIVERED AS FPIGR,
C      EXP1 AND EXP2 IN COMMON/IGRAN/
C      THE SUBROUTINE CALLS IN FUNCTION BESS,
-----
      REAL LOAD,NU,ACCUR(3),K5
      COMMON/ASDT/LAYER,NLAYS,M,R,Z,NU(10),ACCUR,LOAD,HOSTRS,NZEROS,H(9)
      1,K5(10),E(10),AL(9),THICK(9),RADIUS(10)
      COMMON/IGRAN/TO,V0,S0,U0,T1,V1,S1,U1,TQ1,SQ1,FPIGR,EXP1,EXP2
      IF(LAYER,NE,1) GO TO 20
      TO = TO+2.0*NU(1)
      V0 = V0+1.0
      T1 = T1+1.0+2.0*NU(1)
      V1 = V1+1.0
      TQ1 = TQ1+1.0
20  IF(H,LT,ACCUR(1)) GO TO 40
      IF(IL,EQ,2) GO TO 30
      FPIGR = BESS(0,X*R)*BESS(1,X)/X
      GO TO 60
30  FPIGR = BESS(1,X*R)*BESS(1,X)/(X*R)
      GO TO 60
40  IF(IL,EQ,2) GO TO 50
      FPIGR = BESS(1,X)/X
      GO TO 60
50  FPIGR = 0.5*BESS(1,X)
60  IF(NLAYS,EQ,LAYER) GO TO 70
      IF(ABS(X*(2.0*M(LAYER)-Z)),GT,70.0)GO TO 70
      EXP1 = EXP(-X*(2.0*M(LAYER)-Z))
      IF((X*Z),GT,70.0)GO TO 90
      EXP2 = EXP(-X*Z)
      GO TO 100
70  IF((X*Z),GT,70.0)GO TO 80
      EXP1 = 0.0
      EXP2 = EXP(-X*Z)
      GO TO 100
80  EXP1 = 0.0
90  EXP2 = 0.0
100 RETURN
      END
      FUNCTION BESS(N,X)
-----
C      THE BESSEL FUNCTIONS JO(X) AND J1(X) ARE
C      EVALUATED FROM THEIR CHEBYSHEV SERIES,
C      (SEE CLENSHAW,MATH, TABLES=VOL,5,
C      CHEBYSHEV SERIES FOR MATH, FUNCTIONS
C      NPL=DSIR),
C      THIS PROGRAM SELECTS THE APPROPRIATE
C      CHEBYSHEV CONSTANTS ACCORDING TO WHETHER
C      N=0 OR N=1 AND WHETHER X IS GREATER OR
C      LESS THAN 8.0 AND CALLS IN FUNCTION CHEB
C      TO SUM THE SERIES,
-----

```



```

C-----BESS0130
DOUBLE PRECISION B(12,2),BP(5,2),BQ(5,2),Z
DATA B /-.3D=8,.76D=7,-.1762D=5,.32460D=4,-.460626D=3,.4819180D=2,
1=.34893769D=1,.158067102D+0,.370094994D+0,.265178613D+0,
2=.8723442D=2,.315455943D+0,-.1D=8,.29D=7,-.762D=6,.15887D=4,
3=.260444D=3,.3240270D=2,-.29175525D=1,.177709117D+0,-.661443934D+0
4,1.28799410D+0,-1.19180116D+0,1.29671754D+0/
DATA BP/.2D=8,-.52D=7,.3075D=5,-.536522D=3,1.99892070D+0,
1=.2D=8,.62D=7,-.3987D=5,.898990D=3,2.00180608D+0/
DATA BQ/-.1D=8,.18D=7,-.741D=6,.68385D=4,-.31111709D=1,
1.1D=8,-.21D=7,.914D=6,-.96277D=4,.93555574D=1/
M = N+1
IF(X=8,0) 1,1,2
1 Z = X*X*0.0625=2,0
BESS = CHEB(B(1,M),12,Z)
IF(N,EQ,1) BESS = 0.125*X*BESS
RETURN
2 Z = 256,0/(X*X)=2,0
XI = X-0.78539816
IF(N,EQ,1) XI = XI-1.5707963
BESS = (0.79788456/SQRT(X))*(CHEB(BP(1,M),5,Z)*COS(XI)-8,0*
1 CHEB(BQ(1,M),5,Z)*SIN(XI)/X)
RETURN
END
FUNCTION CHEB(A,N,Z)
C-----CHEB0020
C THIS SUBPROGRAM EVALUATES THE CHEBYSHEV CHEB0030
C SERIES USING THE RECURRENCE RELATION CHEB0040
C TECHNIQUE (SEE CLENSHAW NPL MATH, TABLES CHEB0050
C VOLUME 5 PAGE 9). CHEB0060
C-----CHEB0070
DOUBLE PRECISION A(1),B(14),Z
B(1)=0,00+0
B(2)=0,00+0
DO 1 I=1,N
B(I+2)=Z*B(I+1)-B(I)+A(I)
1 CONTINUE
CHEB = 0,5D0*(B(N+2)-B(N))
RETURN
END
REAL FUNCTION IGRAND (X,LABEL)
C-----IGRA0020
C THIS SUBROUTINE COMPUTES THE INTEGRANDS IGRA0030
C FOR THE INTEGRALS COMPUTED IN INGRAL, IGRA0040
C USE IS MADE OF THE RESULTS OF FPIGRA AND IGRA0050
C MATRIX STORED IN COMMON/IGRAN/. IGRA0060
C-----IGRA0070
REAL LOAD,NU,ACCUR(3),K5
COMMON/ASDT/LAYER,NLAYS,M,R,Z,NU(10),ACCUR,LOAD,HOSTRS,NZEROS,H(9)
1,K5(10),E(10),AL(9),THICK(9),RADIUS(10)
COMMON/IGRAN/T0,V0,S0,U0,T1,V1,S1,U1,TQ1,SQ1,FPIGR,EXP1,EXP2
GO TO (10,20,30,40,50,60,70,80,90,100,110,120,130,140,150,160,170)
1,LABEL
10 IGRAND =FPIGR*X*((U0*(K5(LAYER)-X*Z)-S0)*EXP1+(T0+V0*(K5(LAYER)+X*
12))*EXP2)
RETURN
20 IGRAND =FPIGR*X*(U0*EXP1+V0*EXP2)
RETURN
30 IGRAND =FPIGR*((U0*(2,0*K5(LAYER)-X*Z)-S0)*EXP1-(T0+V0*(2,0*K5(LAY
1ER)+X*Z))*EXP2)
RETURN
IGRA0210

```







	V( 3)=FT*RADI*INT( 3)	CALC0300
	IF(RLOW) GO TO 30	CALC0310
	V( 3)=V( 3)+FT*R*RADI*CT*((2,0=2,0*MU)*INT(11)-INT(10))	CALC0320
30	IF(,NOT,STRESS( 4)) GO TO 40	CALC0330
	V( 4)=CT*(INT( 8)+2,0*MU*INT( 9))+INT( 1)+INT( 4)=2,0*INT( 2)	CALC0340
	IF(RLOW) GO TO 40	CALC0350
	V( 4)=V( 4)-CT*FCT	CALC0360
40	IF(,NOT,STRESS( 5)) GO TO 50	CALC0370
	V( 5)=CT*2,0*MU*INT( 9)-2,0*MU*INT( 2)-INT( 4)	CALC0380
	IF(RLOW) GO TO 50	CALC0390
	V( 5)=V( 5)+CT*FCT	CALC0400
50	IF(,NOT,STRESS( 7)) GO TO 60	CALC0410
	V( 7)=ST*INT(15)	CALC0420
	IF(RLOW) GO TO 60	CALC0430
	V( 7)=V( 7)-ST*FCT	CALC0440
60	IF(,NOT,STRESS(10)) GO TO 70	CALC0450
	V(10)=FT*(CT*INT( 8)+INT( 1)+INT( 4)-(2,0=2,0*MU)*INT( 2))	CALC0460
	IF(RLOW) GO TO 70	CALC0470
	V(10)=V(10)-FT*CT*FCT	CALC0480
70	IF(,NOT,STRESS(11)) GO TO 80	CALC0490
	V(11)=FT*INT( 4)	CALC0500
	IF(RLOW) GO TO 80	CALC0510
	V(11)=V(11)+FT*CT*FCT	CALC0520
80	IF(STRESS(12)) V(12)=FT*(CT*((2,0=4,0*MU)*INT( 9)-INT( 8))+	CALC0530
	2,0*MU*INT( 2)-INT( 1))	CALC0540
	IF(Z,LT,ACC) GO TO 90	CALC0550
	IF(STRESS( 6)) V( 6)=CT*((2,0=2,0*MU)*INT( 9)-INT( 8))-INT( 1)	CALC0560
	IF(STRESS( 8)) V( 8)=CT*(INT(16)+INT(10)-INT( 6))-INT( 5)	CALC0570
	IF(STRESS( 9)) V( 9)=ST*(INT(16)-INT(13)+INT(10))	CALC0580
	GO TO 110	CALC0590
90	IF(ABS(R=1,0),LT,ACC) GO TO 100	CALC0600
	IF(R,GT,1,0) GO TO 110	CALC0610
	IF(STRESS( 6)) V( 6)=LOAD	CALC0620
	IF(STRESS( 8)) V( 8)=H0STRS*COS(P5I0)	CALC0630
	IF(STRESS( 9)) V( 9)=H0STRS*SIN(P5I0)	CALC0640
	GO TO 110	CALC0650
100	IF(STRESS( 6)) V( 6)=0,5*LOAD	CALC0660
	IF(STRESS( 8)) V( 8)=0,5*H0STRS*COS(P5I0)	CALC0670
	IF(STRESS( 9)) V( 9)=0,5*H0STRS*SIN(P5I0)	CALC0680
110	IF(STRESS(13)) V(13)=FT*V( 7)	CALC0690
	IF(STRESS(14)) V(14)=FT*V( 8)	CALC0700
	IF(STRESS(15)) V(15)=FT*V( 9)	CALC0710
	DO 120 I=2,18	CALC0720
120	FM(I)=T(8)	CALC0730
	DO 130 I=4,16,3	CALC0740
130	FM(I)=FMT(3)	CALC0750
	K=0	CALC0760
	J=0	CALC0770
	DO 210 I=1,15	CALC0780
	J=J+1	CALC0790
	IF(I=4) 190,160,140	CALC0800
140	IF(I=10) 190,150,190	CALC0810
150	IF(K,EQ,0) GO TO 180	CALC0820
	WRITE(NOUT,9010) (T(J),J=5,8)	CALC0830
	WRITE(NOUT,FM) (C(J),J=1,K)	CALC0840
	GO TO 170	CALC0850
160	IF(K,EQ,0) GO TO 180	CALC0860
	WRITE(NOUT,9000) (T(J),J=1,4)	CALC0870
	WRITE(NOUT,FM) (C(J),J=1,K)	CALC0880
170	K=0	CALC0890
180	J=1	CALC0900



190	M=3*J	CALC0910
	IF(,NOT,STRESS(I)) GO TO 200	CALC0920
	K=K+1	CALC0930
	C(K)=V(I)	CALC0940
	FM(M-1)=FMT(1)	CALC0950
	FM(M )=FMT(2)	CALC0960
	GO TO 210	CALC0970
200	FM(M-1)=FMT(4)	CALC0980
	FM(M )=FMT(5)	CALC0990
210	CONTINUE	CALC1000
	IF(K,EQ,0) RETURN	CALC1010
	WRITE(NOUT,9010) (T(J),J=9,12)	CALC1020
	WRITE(NOUT,FM) (C(J),J=1,K)	CALC1030
	RETURN	CALC1040
9000	FORMAT(1X,4A4/5X,"RADIAL",12X,"TANGENTIAL",14X,"VERTICAL")	CALC1050
9010	FORMAT(1X,4A4/5X,"RADIAL",12X,"TANGENTIAL",14X,"VERTICAL",12X,"RAD	CALC1060
	+,/TANG.",11X,"RAD,/VERT.",12X,"TANG,/VERT.")	CALC1070
	END	CALC1080
	SUBROUTINE OUTPUT(EPS,C,K,L)	OUTP0010
C	-----	OUTP0020
C	THIS SUBROUTINE OUTPUTS BY MEANS OF THREE	OUTP0030
C	SUBSEQUENT CALLS FROM THE MAIN PROGRAM	OUTP0040
C	THE TOTAL STRESSES,STRAINS AND SISPLACE-	OUTP0050
C	MENTS,	OUTP0060
C	-----	OUTP0070
	INTEGER FM(16),FMT(8)	OUTP0080
	LOGICAL EPS(6)	OUTP0090
	DIMENSION C(6),TKST(6,4)	OUTP0100
	COMMON/TAPE/NOUT	OUTP0110
	DATA TKST/	OUTP0120
	1" T O", " T A", " L ", "S T ", "R E ", "S S ",	OUTP0130
	2" T O", " T A", " L ", "S T ", "R A ", "I N ",	OUTP0140
	3" T O", " T A", " L ", "D I ", "S P ", "L A ",	OUTP0150
	4"C E ", "M E ", "N T ", " ", " ", " ", " "	OUTP0160
	DATA FMT,FM(16)/	OUTP0170
	1"(6A4",",12X", " ",",E12",",3 ",,"(12A",",4,48",",X ",") "/	OUTP0180
	IF(L,NE,3) GO TO 10	OUTP0190
	FM(1)=FMT(6)	OUTP0200
	FM(2)=FMT(7)	OUTP0210
	FM(3)=FMT(8)	OUTP0220
	GO TO 20	OUTP0230
10	FM(1)=FMT(1)	OUTP0240
	FM(2)=FMT(3)	OUTP0250
	FM(3)=FMT(3)	OUTP0260
20	N=0	OUTP0270
	M=2*K+2	OUTP0280
	DO 40 I=4,M,2	OUTP0290
	J=I/2-1	OUTP0300
	IF(,NOT,EPS(J)) GO TO 30	OUTP0310
	FM(I)=FMT(4)	OUTP0320
	FM(I+1)=FMT(5)	OUTP0330
	N=N+1	OUTP0340
	C(N)=C(J)	OUTP0350
	GO TO 40	OUTP0360
30	FM(I)=FMT(2)	OUTP0370
	FM(I+1)=FMT(3)	OUTP0380
40	CONTINUE	OUTP0390
	IF(L,EQ,3) GO TO 60	OUTP0400
	IF(N,EQ,0) GO TO 50	OUTP0410
	WRITE(NOUT,FM) (TKST(I,L),I=1,6),(C(I),I=1,N)	OUTP0420
	RETURN	OUTP0430



```

50 WRITE(NOUT,FM) (TKST(I,L),I=1,6)
RETURN
60 DO 70 I=10,15
70 FM(I)=FMT(3)
IF(N,EQ,0) GO TO 80
WRITE(NOUT,FM) (TKST(I,3),I=1,6),(TKST(I,4),I=1,6),(C(I),I=1,N)
RETURN
80 WRITE(NOUT,FM) (TKST(I,3),I=1,6),(TKST(I,4),I=1,6)
RETURN
END
SUBROUTINE JACOBI (H,U,ND,N,IVEC,W,IQ)
-----
C SUBROUTINE JACOBI TO COMPUTE EIGENVALUES AND EIGENVECTORS OF A SYMMETRIC MATRIX, H IS THE GIVEN MATRIX, THE DIAGONAL OF WHICH CONTAINS AFTER THE ITERATION THE EIGENVALUES OF H, U IS THE MATRIX, THE COLUMNS OF WHICH ARE THE EIGENVECTORS OF H, N AND ND ARE THE DIMENSIONS OF THE ACTUAL MATRIX AND THE ONE USED IN THE DIMENSION STATEMENT OF THE CALLINGPROGRAM RESPECTIVELY, IVEC=0 IF NO EIGENVECTORS ARE REQUIRED, IVEC=1 IF THE EIGENVECTORS SHOULD BE CALCULATED, THE ACCURACY OF THE EIGENVALUES IS ABOUT 1.0E-6, THE ACCURACY OF AN EIGENVECTOR IS ABOUT 1.0E-6/D, WHERE D IS THE MINIMUM DISTANCE OF THE CORRESPONDING EIGENVALUE FROM THE OTHER EIGENVALUES, W AND IQ ARE WORKINGSPACES, WHICH SHOULD BE DIMENSIONED IN THE CALLING PROGRAM.
-----
REAL H(ND,ND),U(ND,ND),W(ND)
INTEGER IQ(ND)
DOUBLE PRECISION TA,SI,CO,Z,Y,HTE,UTE
AN =N
NMI1=N-1
IF(IVEC=1) 60,10,60
10 DO 50 I=1,N
DO 40 J=1,N
IF(I=J) 30,20,30
20 U(I,J)=1,0
GO TO 40
30 U(I,J)=0,0
40 CONTINUE
50 CONTINUE
60 DO 90 I=1,NMI1
W(I)=0,0
IPL1=I+1
DO 80 J=IPL1,N
IF(W(I)=ABS(H(I,J))) 70,70,80
70 W(I)=ABS(H(I,J))
IQ(I)=J
80 CONTINUE
90 CONTINUE
100 DO 120 I=1,NMI1
IF(I,EQ,1) GO TO 110
IF(XMAX,GE,W(I)) GO TO 120
110 XMAX=W(I)

```



	IPIV=I	JACO0510
	JPIV=IQ(I)	JACO0520
120	CONTINUE	JACO0530
	IF(XMAX=1,E=12/M) 170,170,130	JACO0540
130	Z =H(IPIV,IPIV)-H(JPIV,JPIV)	JACO0550
	Y = 2,000*DBLE(I*(IPIV,JPIV))	JACO0560
	TA =Y/(DABS(Z)+DSQRT(Z*Z+Y*Y))	JACO0570
	IF(Z.LT.0,000) TA=-TA	JACO0580
	CO =1,00/DSQRT(1,00+TA*TA)	JACO0590
	SI =TA*CO	JACO0600
	HII=H(IPIV,IPIV)	JACO0610
	HJJ=H(JPIV,JPIV)	JACO0620
	HIJ=H(IPIV,JPIV)	JACO0630
	DO 140 K=1,N	JACO0640
	HTE=H(K,IPIV)	JACO0650
	H(K,IPIV)=DBLE(H(K,IPIV))*CO+DBLE(H(K,JPIV))*SI	JACO0660
	H(K,JPIV)=DBLE(H(K,JPIV))*CO-HTE*SI	JACO0670
	H(IPIV,K)=H(K,IPIV)	JACO0680
	H(JPIV,K)=H(K,JPIV)	JACO0690
140	CONTINUE	JACO0700
	H(IPIV,JPIV)=0,0	JACO0710
	H(JPIV,IPIV)=0,0	JACO0720
	AA=DBLE(HIJ)*TA	JACO0730
	H(IPIV,IPIV)=HII+AA	JACO0740
	H(JPIV,JPIV)=HJJ-AA	JACO0750
	IF(IVEC) 60,60,150	JACO0760
150	DO 160 K=1,N	JACO0770
	UTE=U(K,IPIV)	JACO0780
	U(K,IPIV)=DBLE(U(K,IPIV))*CO+DBLE(U(K,JPIV))*SI	JACO0790
	U(K,JPIV)=DBLE(U(K,JPIV))*CO-UTE*SI	JACO0800
160	CONTINUE	JACO0810
	GO TO 60	JACO0820
170	RETURN	JACO0830
	END	JACO0840
	SUBROUTINE ESORT (H,U,ND,N,IVEC,W,IQ)	ESOR0010
C	-----	ESOR0020
C	SUBROUTINE ESORT.	ESOR0030
C	THIS ROUTINE SORTS EIGENVALUES (AND EIGEN	ESOR0040
C	VECTORS) OBTAINED FROM SUBROUTINE JACOBI.	ESOR0050
C	H = ORIGINAL MATRIX(ND,ND).	ESOR0060
C	U = EIGENVECTORMATRIX(ND,ND).	ESOR0070
C	ND = MAX. DIMENSION OF MATRICES.	ESOR0080
C	N = ACTUAL DIMENSION OF MATRICES.	ESOR0090
C	IVEC=1 WITH EIGENVECTORS,	ESOR0100
C	=0 NO EIGENVECTORS.	ESOR0110
C	W = WORKINGSPACE(ND).	ESOR0120
C	IQ = WORKINGSPACE(ND).	ESOR0130
C	-----	ESOR0140
	REAL H(ND,ND),U(ND,ND),W(ND),DUMMY	ESOR0150
	INTEGER N,IQ(ND),FDUMMY,I,J,K,IVEC	ESOR0160
	LOGICAL LOGIC	ESOR0170
C		ESOR0180
	DO 10 I=1,N	ESOR0190
	W(I)=H(I,I)	ESOR0200
10	IQ(I)=I	ESOR0210
	J=N	ESOR0220
20	LOGIC=.FALSE.	ESOR0230
	K=J	ESOR0240
	DO 30 I=2,K	ESOR0250
	IF(W(I-1).GE.W(I)) GO TO 30	ESOR0260
	LOGIC=.TRUE.	ESOR0270



```

DUMMY=W(I-1)
W(I-1)=W(I)
W(I)=DUMMY
FDUMMY=IQ(I-1)
IQ(I-1)=IQ(I)
IQ(I)=FDUMMY
J=I-1
30 CONTINUE
IF (LOGIC) GO TO 20
IF (IVEC, EQ, 0) GO TO 60
DO 40 I=1, N
  K=IQ(I)
  DO 40 J=1, N
    40 H(J, I)=U(J, K)
  DO 50 I=1, N
    DO 50 J=1, N
      U(I, J)=H(I, J)
    50 H(I, J)=0.0
  60 DO 70 I=1, N
    70 H(I, I)=W(I)
RETURN
END
BLOCK DATA
-----BLDA0010
C-----BLDA0020
C IN THE BLOCK DATA ARE STORED SUBSEQUENTLY*BLDA0030
C -THE ABSCISSAE FOR THE LEGENDRE-GAUSS BLDA0040
C QUADRATURE, STARTING IN A WITH THE 2=ND BLDA0050
C ORDER AND ENDING IN N WITH THE 15=TH BLDA0060
C ORDER. BLDA0070
C -THE ABSCISSAE FOR THE JACOBI-GAUSS BLDA0080
C QUADRATURE OF THE 8=TH ORDER IN O. BLDA0090
C -THE WEIGHTS FOR THE LEGENDRE-GAUSS BLDA0100
C QUADRATURE, STARTING IN P WITH THE 2=ND BLDA0110
C ORDER AND ENDING IN CC WITH THE 15=TH BLDA0120
C ORDER. BLDA0130
C -THE WEIGHTS FOR THE JACOBI-GAUSS QUADRA= BLDA0140
C TURE OF THE 8=TH ORDER IN DD. BLDA0150
C -THE FIRST 149 ZEROS OF J0 IN EE AND FF BLDA0160
C -THE FIRST 149 ZEROS OF J1 IN GG AND HH BLDA0170
C-----BLDA0180
REAL I, J, K, L, M, N BLDA0190
DIMENSION A(2), B(3), C(4), D(5), E(6), F(7), G(8), H(9), I(10), J(11), K(12) BLDA0200
1), L(13), M(14), N(15), O( 8), P(2), Q(3), R(4), S(5), T(6), U(7), V(8), W(9), BLDA0210
2X(10), Y(11), Z(12), AA(13), BB(14), CC(15), DD( 8), EE(119), FF(30), GG(11) BLDA0220
39), HH(30) BLDA0230
COMMON/GAUSS/AGAUSS(16, 16), HGAUSS(16, 16) BLDA0240
COMMON/GEDATA/BZEROS(149, 2), ZEROS(298) BLDA0250
EQUIVALENCE (AGAUSS(1, 2), A(1)), (AGAUSS(1, 3), B(1)), BLDA0260
1(AGAUSS(1, 4), C(1)), (AGAUSS(1, 5), D(1)), (AGAUSS(1, 6), E(1)), BLDA0270
2(AGAUSS(1, 7), F(1)), (AGAUSS(1, 8), G(1)), (AGAUSS(1, 9), H(1)), BLDA0280
3(AGAUSS(1, 10), I(1)), (AGAUSS(1, 11), J(1)), (AGAUSS(1, 12), K(1)), BLDA0290
4(AGAUSS(1, 13), L(1)), (AGAUSS(1, 14), M(1)), (AGAUSS(1, 15), N(1)), BLDA0300
5(AGAUSS(1, 16), O(1)), (HGAUSS(1, 2), P(1)), (HGAUSS(1, 3), Q(1)), BLDA0310
6(HGAUSS(1, 4), R(1)), (HGAUSS(1, 5), S(1)), (HGAUSS(1, 6), T(1)), BLDA0320
7(HGAUSS(1, 7), U(1)), (HGAUSS(1, 8), V(1)), (HGAUSS(1, 9), W(1)), BLDA0330
8(HGAUSS(1, 10), X(1)), (HGAUSS(1, 11), Y(1)), (HGAUSS(1, 12), Z(1)), BLDA0340
9(HGAUSS(1, 13), AA(1)), (HGAUSS(1, 14), BB(1)), (HGAUSS(1, 15), CC(1)), BLDA0350
T(HGAUSS(1, 16), DD(1)), (BZEROS(1, 1), EE(1)), (BZEROS(120, 1), FF(1)), BLDA0360
1(BZEROS(1, 2), GG(1)), (BZEROS(120, 2), HH(1)) BLDA0370
DATA A, B, C, D, E, F, G, H, I, J, K, L, M BLDA0380
N/=, 4472136, 0.4472136, =0.6546537, 0.0000000, 0.6546537, =0.7650554, BLDA0390

```



1=0.2852315, 0.2852315, 0.7650553, -0.8302239, -0.4688488, 0.0000000, HLDA0400  
 2 0.4688488, 0.8302239, -0.8717402, -0.5917003, -0.2092993, 0.2092991, BLDA0410  
 3 0.5917001, 0.8717400, -0.8997580, -0.6771863, -0.3631175, 0.0000000, BLDA0420  
 4 0.3631175, 0.6771863, 0.8997580, -0.9195339, -0.7387739, -0.4779250, BLDA0430  
 5=0.1652790, 0.1652789, 0.4779249, 0.7387738, 0.9195338, -0.9340014, BLDA0440  
 6=0.7844836, -0.5652354, -0.2957582, 0.0000000, 0.2957581, 0.5652353, BLDA0450  
 7 0.7844834, 0.9340014, -0.9448975, -0.8192815, -0.6328754, -0.3995310, BLDA0460  
 8=0.1365529, 0.1365529, 0.3995309, 0.6328753, 0.8192813, 0.9448975, BLDA0470  
 9=0.9533069, -0.8463538, -0.6861843, -0.4829108, -0.2492869, 0.0000000, BLDA0480  
 T 0.2492868, 0.4829106, 0.6861842, 0.8463537, 0.9533068, -0.9599299, BLDA0490  
 1=0.8678104, -0.7288621, -0.5506417, -0.3427235, -0.1163319, 0.1163318, BLDA0500  
 2 0.3427235, 0.5506415, 0.7288620, 0.8678104, 0.9599298, -0.9652544, BLDA0510  
 3=0.8850636, -0.7635341, -0.6062477, -0.4206389, -0.2153539, 0.0000000, HLDA0520  
 4 0.2153538, 0.4206389, 0.6062477, 0.7635341, 0.8850635, 0.9652544, BLDA0530  
 5=0.9695861, -0.8991729, -0.7920153, -0.6523931, -0.4860575, -0.2998304, BLDA0540  
 6=0.1013263, 0.1013262, 0.2998304, 0.4860575, 0.6523930, 0.7920151, BLDA0550  
 7 0.8991728, 0.9695860/ BLDA0560  
 DATA N,O BLDA0570  
 N/=0.9731405, -0.9108602, -0.8157166, -0.6910172, -0.5413883, -0.3721744, BLDA0580  
 1=0.1895120, 0.0000000, 0.1895119, 0.3721744, 0.5413882, 0.6910170, BLDA0590  
 2 0.8157164, 0.9108602, 0.9731404, -0.9602899, -0.7966665, -0.5255324, BLDA0600  
 3=0.1834346, 0.1834346, 0.5255324, 0.7966665, 0.9602899/ BLDA0610  
 DATA P,Q,R,S,T,U,V,W,X,Y,Z,AA,BB BLDA0620  
 N/0.8333334, 0.8333331, 0.5444443, 0.7111111, 0.5444444, 0.3784749, BLDA0630  
 1 0.5548583, 0.5548581, 0.3784750, 0.2768261, 0.4317453, 0.4876190, BLDA0640  
 2 0.4317455, 0.2768261, 0.2107044, 0.3411230, 0.4124591, 0.4124591, BLDA0650  
 3 0.3411230, 0.2107046, 0.1654953, 0.2745391, 0.3464290, 0.3715193, BLDA0660  
 4 0.3464290, 0.2745388, 0.1654955, 0.1333061, 0.2248897, 0.2920431, BLDA0670  
 5 0.3275404, 0.3275403, 0.2920429, 0.2248897, 0.1333061, 0.1096126, BLDA0680  
 6 0.1871701, 0.2480485, 0.2868792, 0.3002176, 0.2868798, 0.2480485, BLDA0690  
 7 0.1871700, 0.1096126, 0.0916847, 0.1579750, 0.2125089, 0.2512758, BLDA0700  
 8 0.2714060, 0.2714060, 0.2512759, 0.2125089, 0.1579748, 0.0916846, BLDA0710  
 9 0.0778019, 0.1349820, 0.1836473, 0.2207679, 0.2440163, 0.2519308, BLDA0720  
 T 0.2440165, 0.2207679, 0.1836473, 0.1349820, 0.0778019, 0.0668373, BLDA0730  
 1 0.1165870, 0.1600221, 0.1948268, 0.2191266, 0.2316136, 0.2316138, BLDA0740  
 2 0.2191266, 0.1948268, 0.1600223, 0.1165869, 0.0668375, 0.0580301, BLDA0750  
 3 0.1016605, 0.1405119, 0.1727902, 0.1969877, 0.2119743, 0.2170480, BLDA0760  
 4 0.2119743, 0.1969876, 0.1727903, 0.1405120, 0.1016601, 0.0580301, BLDA0770  
 5 0.0508505, 0.0893939, 0.1242559, 0.1540275, 0.1774924, 0.1936907, BLDA0780  
 6 0.2019594, 0.2019594, 0.1936906, 0.1774925, 0.1540275, 0.1242554, BLDA0790  
 7 0.0893940, 0.0508506/ BLDA0800  
 DATA CC,DD BLDA0810  
 N/0.0449221, 0.0791985, 0.1105931, 0.1379879, 0.1603954, 0.1770052, BLDA0820  
 1 0.1872171, 0.1906618, 0.1872172, 0.1770049, 0.1603951, 0.1379883, BLDA0830  
 2 0.1105928, 0.0791985, 0.0449221, 0.1012285, 0.2223810, 0.3137067, BLDA0840  
 3 0.3626838, 0.3626838, 0.3137067, 0.2223810, 0.1012285/ BLDA0850  
 DATA EE /2.404826, 5.520078, 8.653728, 11.79153, 14.93092, BLDA0860  
 1 18.07106, 21.21164, 24.35247, 27.49348, 30.63461, 33.77582, BLDA0870  
 2 36.91710, 40.05843, 43.19979, 46.34119, 49.48261, 52.62405, BLDA0880  
 3 55.76551, 58.90698, 62.04847, 65.18996, 68.33147, 71.47298, BLDA0890  
 4 74.61450, 77.75603, 80.89756, 84.03909, 87.18063, 90.32217, BLDA0900  
 5 93.46372, 96.60527, 99.74682, 102.8883, 106.0299, 109.1715, BLDA0910  
 6 112.3131, 115.4546, 118.5962, 121.7377, 124.8793, 128.0209, BLDA0920  
 7 131.1624, 134.3040, 137.4456, 140.5872, 143.7287, 146.8703, BLDA0930  
 8 150.0119, 153.1535, 156.2950, 159.4366, 162.5782, 165.7198, BLDA0940  
 9 168.8613, 172.0029, 175.1445, 178.2861, 181.4277, 184.5692, BLDA0950  
 T 187.7108, 190.8524, 193.9940, 197.1356, 200.2772, 203.4187, BLDA0960  
 1 206.5603, 209.7019, 212.8435, 215.9850, 219.1267, 222.2682, BLDA0970  
 2 225.4098, 228.5514, 231.6930, 234.8346, 237.9762, 241.1178, BLDA0980  
 3 244.2593, 247.4009, 250.5425, 253.6841, 256.8257, 259.9673, BLDA0990  
 4 263.1089, 266.2504, 269.3920, 272.5336, 275.6752, 278.8168, BLDA1000



5281,9584,	285,1000,	288,2416,	291,3831,	294,5247,	297,6663,	BLDA1010
6300,8079,	303,9495,	307,0911,	310,2327,	313,3743,	316,5159,	BLDA1020
7319,6574,	322,7990,	325,9406,	329,0822,	332,2238,	335,3654,	BLDA1030
8338,5070,	341,6486,	344,7902,	347,9317,	351,0733,	354,2149,	BLDA1040
9357,3565,	360,4981,	363,6397,	366,7813,	369,9229,	373,0645,	BLDA1050
DATA FF /	376,2061,	379,3476,	382,4892,	385,6308,	388,7724,	BLDA1060
1391,9140,	395,0556,	398,1972,	401,3388,	404,4804,	407,6220,	BLDA1070
2410,7635,	413,9051,	417,0467,	420,1883,	423,3299,	426,4715,	BLDA1080
3429,6131,	432,7547,	435,8963,	439,0379,	442,1794,	445,3210,	BLDA1090
4448,4626,	451,6042,	454,7458,	457,8874,	461,0290,	464,1706,	BLDA1100
5467,3122/						BLDA1110
DATA GG	73,831706,	7,015587,	10,17347,	13,32369,	16,47063,	BLDA1120
1 19,61586,	22,76008,	25,90367,	29,04683,	32,18968,	35,33231,	BLDA1130
2 38,47477,	41,61709,	44,75932,	47,90146,	51,04354,	54,18555,	BLDA1140
3 57,32753,	60,46946,	63,61136,	66,75323,	69,89507,	73,03690,	BLDA1150
4 76,17870,	79,32049,	82,46226,	85,60402,	88,74577,	91,88750,	BLDA1160
5 95,02923,	98,17095,	101,3127,	104,4544,	107,5961,	110,7376,	BLDA1170
6113,8794,	117,0211,	120,1628,	123,3045,	126,4461,	129,5878,	BLDA1180
7132,7295,	135,8711,	139,0128,	142,1544,	145,2961,	148,4377,	BLDA1190
8151,5794,	154,7210,	157,8626,	161,0043,	164,1459,	167,2876,	BLDA1200
9170,4292,	173,5708,	176,7125,	179,8541,	182,9957,	186,1374,	BLDA1210
T189,2790,	192,4206,	195,5622,	198,7038,	201,8455,	204,9871,	BLDA1220
1208,1287,	211,2703,	214,4120,	217,5536,	220,6952,	223,8368,	BLDA1230
2226,9784,	230,1200,	233,2616,	236,4033,	239,5449,	242,6865,	BLDA1240
3245,8281,	248,9697,	252,1113,	255,2529,	258,3945,	261,5362,	BLDA1250
4264,6778,	267,8194,	270,9610,	274,1026,	277,2442,	280,3858,	BLDA1260
5283,5274,	286,6690,	289,8106,	292,9522,	296,0938,	299,2354,	BLDA1270
6302,3771,	305,5187,	308,6603,	311,8019,	314,9435,	318,0851,	BLDA1280
7321,2267,	324,3683,	327,5099,	330,6515,	333,7931,	336,9347,	BLDA1290
8340,0763,	343,2179,	346,3595,	349,5011,	352,6427,	355,7843,	BLDA1300
9358,9259,	362,0675,	365,2091,	368,3507,	371,4923,	374,6339,	BLDA1310
DATA HH /	377,7755,	380,9171,	384,0587,	387,2003,	390,3419,	BLDA1320
1393,4835,	396,6251,	399,7667,	402,9083,	406,0499,	409,1919,	BLDA1330
2412,3331,	415,4747,	418,6163,	421,7579,	424,8995,	428,0411,	BLDA1340
3431,1827,	434,3243,	437,4659,	440,6075,	443,7491,	446,8907,	BLDA1350
4450,0323,	453,1739,	456,3155,	459,4570,	462,5987,	465,7403,	BLDA1360
5468,8819/						BLDA1370
END						BLDA1380



# INPUT GUIDE

The input guide is listed in Tables F1-F8.

Tables F1, F2, and F3

Table 1: Title

TEXT	2 0 A 4
------	---------



Table 2:

Columns 1-2 NSYS = number of problems

Table 3:

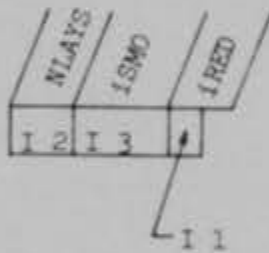
Columns 1-2 NLAYS = number of layers in pavement system

Columns 3-5 ISMO = 0 request for rough computational procedure

ISMO = 1 request for smooth computational procedure (see Note 1)

Column 6 IRED = 0 AK(i) is input in Table 4 or

IRED = 1 ALK(i) is input in Table 4



F-45

NOTE (1): The smooth calculation procedure is more stable but less efficient than the rough procedure and is used for systems with frictionless slip between the layers or for cases where numerical instabilities are expected.



# Table F4

Table 4: Layer Information: One card for each layer (see Note 2)  
 Columns 1-10 E(i) = moduli of layer i  
 Columns 11-20 NU(i) = Poisson's ratio  
 Columns 21-30 Thick(i) = thickness of layer i  
 Columns 31-40 AK(i) = interface compliance  
 or ALK(i) = reduced interface compliance (see Note 3)

Note (2): Columns 21-40 left blank for last layer

(3): AK(i) values are generally very small thus it may be more

desirable to use ALK(i) where  $ALK(i) = \frac{E_i}{1 + \nu_i} \cdot AK(i)$

for complete adhesion between layers i and i + 1 set  $AK(i) = ALK(i) = 0$

for almost frictionless slip between layers set  $\frac{E_i}{1 + \nu_i} AK(i) = ALK(i) \geq 1000$

F-46

Cards for layers i=1 thru NLAYS - 1

E(i)	NU(i)	THICK(i)	AK(i) or ALK(i)
F10.0	F10.0	F10.0	F10.0

Card for layer i = NLAYS

E(i)	NU(i)
F10.0	F10.0

Tables F5 and F6



Table 5:

Columns 1-2 NLOAD = number of loaded areas

Table 6: Load information: One card for each load

- Columns 1-10 LDSTRS(1) = vertical load in units of load for loaded area 1
- Columns 11-20 RADIUS(1) = radius of loaded area 1
- Columns 21-30 X(1) = abscissa of center of loaded area
- Columns 31-40 Y(1) = ordinate of center of loaded area
- Columns 41-50 HOSTR(1) = horizontal load in units of load for loaded area 1
- Columns 51-60 PSI(1) = angle of HOSTR(1) with respect to positive X-axis in degrees

F-47

LDSTRS	RADIUS	X	Y	HOSTR	PSI
F10.0	F10.0	F10.0	F10.0	F10.0	F10.0



Tables F7 and F8

Table 7:

Columns 1-2 NPOS = the number of position for which stress, strains, and displacements are to be computed



Table 8: Position data; one card for each position

Columns 1-2 LAYER(i) = layer number for position i  
 Columns 11-20 AX(i) = abscissa of position  
 Columns 21-30 AY(i) = ordinate of position  
 Columns 31-40 Depth(i) = depth from pavement surface to position  
 Columns 41-50 ETA(i) = angle from which position is observed with respect to the direction of the tangential loading



AX	AY	DEPTH	ETA
F10.0	F10.0	F10.0	F10.0

If another problem is needed return to Table 3 and repeat input thru Table 8.

F-48

## EXAMPLE PROBLEM

The example problem is for the computation of the tensile stress at two locations at the bottom of a PCC slab which is subjected to the loading of a dual-wheel aircraft gear. Figure F1 shows the pavement section, the characteristics of the applied load, and the locations at which the stress is computed. The coded data for the example problem are given in Table F9, and the output in Table F10.

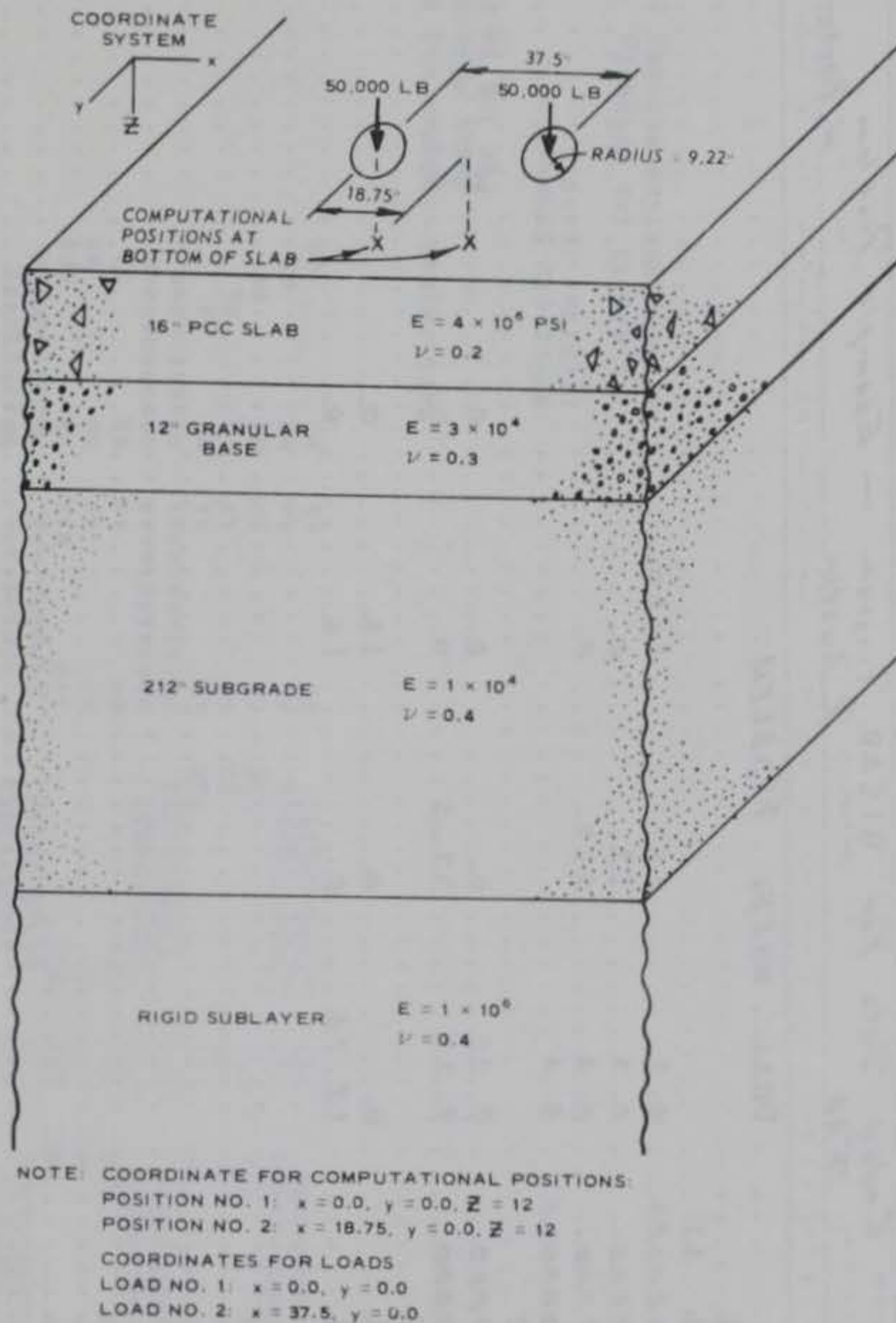


Figure F1. Diagram for example problem



Table F9

Coded Data for BISAR Program - Example Problem

GENERAL PURPOSE DATA FORM

Coded Data For BISAR Program - Example Problem				DATE
REQ. ORDER BY		PREPARED BY	APPROVED BY	8/1/78
FAA		R. Austin	W. Barker	1
DUAL WHEEL PROBLEM				
1				
4	1.1			
40.000.00	0.2	1.6	1.00.0.	
3.00.00	0.3	1.2	0.	
1.00.00	0.4	2.1.2	0.	
1.00.00.00	0.4			
2				
50.00.0.	9.2.2	0.	0.	0.
50.00.0.	9.2.2	3.7.5	0.	0.
2				
1	0.	0.	1.6	0.
1	1.8.7.5	0.	1.6	0.

F-50

Table F10

Output for Example Problem

```
BBBBBBB BBBB      III  SSSSSSSSSSSS      AAAAAAAAAA      RRRRRRRRRRRR
BBBBBBB BBBB      III  SSSSSSSSSSSS      AAAAAAAAAA      RRRRRRRRRRRR
BB      BBB      III  SSS      AAA      AAA      RR      RRH
BB      BB      III  SS      AA      AA      RR      RH
BB      BBB      III  SSS      AA      AA      RR      RR
BBBBBBB BBBB      III  SSSSSSSSSSSS      AAAAAAAAAA      RRRRRRRRRRRR
BBBBBBB BBBB      III  SSSSSSSSSSSS      AAAAAAAAAA      RRRRRRRRRRRR
BB      BBB      III  SSS      AA      AA      RR      RR
BB      BB      III  SS      AA      AA      RR      RR
BB      BBB      III  SSS      AA      AA      RR      RR
BBBBBBB BBBB      III  SSSSSSSSSSSS      AAAAAAAAAA      RRRRRRRRRRRR
BBBBBBB BBBB      III  SSSSSSSSSSSS      AAAAAAAAAA      RRRRRRRRRRRR
```

F-51

THIS 'BISAR' PROGRAM WAS BEEN OBTAINED FROM  
SHELL RESEARCH B.V.  
FOR THE SOLE USE OF

SHELL OIL COMPANY  
HOUSTON, TEXAS

ALL RIGHTS ARE RESERVED. USE OF THIS PROGRAM  
BY UNAUTHORIZED PERSONS IS PROHIBITED



DUAL WHEEL PROBLEM

SYSTEM NUMBER 1

LAYER NUMBER	CALCULATION METHOD	YOUNG'S MODLLS	POISSON'S RATIO	THICKNESS	REDUCED SPRINGCOMPL
1	SMOOTH	0.4000E 07	0.2000E 00	0.1600E 02	0.1000E 04
2	SMOOTH	0.3000E 05	0.3000E 00	0.1200E 02	0.
3	SMOOTH	0.1000E 05	0.4000E 00	0.2120E 03	0.
4		0.1000E 07	0.4000E 00		

LOAD NUMBER	NORMAL STRESS	SHEAR STRESS	RADIUS OF LOADED AREA	LOAD - POSITION		SHEAR DIRECTION
				X	Y	
1	0.1872E 03	0.	0.9220E 01	0.	0.	0.
2	0.1872E 03	0.	0.9220E 01	0.3750E 02	0.	0.

P-52

POSITION NUMBER 1

LAYER NUMBER 1

COORDINATES

X 0. Y 0. Z 0.1600E 02

DISTANCE TO LOAD-AXIS( 1)

THETA

DISPLACEMENTS

RADIAL

TANGENTIAL

VERTICAL

STRESSES

RADIAL

TANGENTIAL

VERTICAL

RAD./TANG.

RAD./VERT.

TANG./VERT.

STRAINS

RADIAL

TANGENTIAL

VERTICAL

RAD./TANG.

RAD./VERT.

TANG./VERT.

DISTANCE TO LOAD-AXIS( 2)

THETA

DISPLACEMENTS

RADIAL

TANGENTIAL

VERTICAL

STRESSES

RADIAL

TANGENTIAL

VERTICAL

RAD./TANG.

RAD./VERT.

TANG./VERT.

STRAINS

RADIAL

TANGENTIAL

VERTICAL

RAD./TANG.

RAD./VERT.

TANG./VERT.

	XX	YY	ZZ	YZ	KZ	XY	UX	UY	UZ
TOTAL STRESS	0.303E-03	0.368E-03	-0.509E-01	0.	0.645E-00	0.			
TOTAL STRAIN	0.576E-04	0.770E-04	-0.348E-04	0.	0.193E-06	0.			
TOTAL DISPLACEMENT							0.876E-03	0.	0.314E-01

PRINCIPAL VALUES AND DIRECTIONS OF TOTAL STRESSES AND STRAINS

	NORMAL STRESS	NORMAL STRAIN	SHEAR STRESS	SHEAR STRAIN	X COMPONENT	Y COMPONENT	Z COMPONENT
MAXIMUM	0.368E-03	0.770E-04			0.	1.000	0.
MINIMAX	0.303E-03	0.576E-04			1.000	0.	0.002
MINIMUM	-0.509E-01	-0.348E-04			-0.002	0.	1.000
MAXIMUM			0.148E-03	0.559E-04	0.001	0.707	-0.707
MINIMAX	0.141E-03		0.179E-03	0.462E-04	-0.001	0.707	0.707
MINIMUM	0.149E-03		0.324E-02	0.971E-05	0.709	0.	-0.706
MAXIMUM					0.706	0.	0.709
MINIMUM	0.335E-03				-0.707	0.707	-0.001
					0.707	0.707	0.001

STRAIN ENERGY 0.2297E-01  
STRAIN ENERGY OF DISTORTION 0.1190E-01

F-53



POSITION NUMBER 2

LAYER NUMBER 1

COORDINATES

X 0.1875E 02 Y 0. Z 0.1600E 02

DISTANCE TO LOAD-AXIS( 1)  
0.1875E 02

THETA  
0.

DISPLACEMENTS						
RADIAL	TANGENTIAL	VERTICAL				
0.6985E-03	0.	0.1613E-01				
STRESSES						
RADIAL	TANGENTIAL	VERTICAL	RAD./TANG.	RAD./VERT.	TANG./VERT.	
0.1043E-03	0.1094E-03	-0.2292E-01	0.	-0.7379E-00	0.	
STRAINS						
RADIAL	TANGENTIAL	VERTICAL	RAD./TANG.	RAD./VERT.	TANG./VERT.	
0.1771E-04	0.3725E-04	-0.1426E-04	0.	-0.2214E-06	0.	

DISTANCE TO LOAD-AXIS( 2)  
0.1875E 02

THETA  
0.3142E 01

DISPLACEMENTS						
RADIAL	TANGENTIAL	VERTICAL				
0.6985E-03	0.	0.1613E-01				
STRESSES						
RADIAL	TANGENTIAL	VERTICAL	RAD./TANG.	RAD./VERT.	TANG./VERT.	
0.1043E-03	0.1094E-03	-0.2292E-01	0.	-0.7379E-00	0.	
STRAINS						
RADIAL	TANGENTIAL	VERTICAL	RAD./TANG.	RAD./VERT.	TANG./VERT.	
0.1771E-04	0.3725E-04	-0.1426E-04	0.	-0.2214E-06	0.	

TOTAL STRESS	XX	YY	ZZ	YZ	KZ	XZ	UX	UY	UZ
	0.209E-03	0.339E-03	-0.458E-01	0.	0.	0.	0.	0.	0.323E-01
TOTAL STRAIN	0.354E-04	0.745E-04	-0.285E-04	0.	0.	0.			
TOTAL DISPLACEMENT									

PRINCIPAL VALUES AND DIRECTIONS OF TOTAL STRESSES AND STRAINS

	NORMAL STRESS	NORMAL STRAIN	SHEAR STRESS	SHEAR STRAIN	X COMPONENT	Y COMPONENT	Z COMPONENT
MAXIMUM	0.339E 03	0.745E-04			0.	1.000	0.
MINIMAX	0.209E 03	0.354E-04			1.000	0.	0.
MINIMUM	-0.458E 01	-0.285E-04			0.	0.	1.000
MAXIMUM	0.167E 03		0.172E 03	0.515E-04	0.	0.707	-0.707
MINIMAX	0.102E 03		0.107E 03	0.320E-04	0.707	0.	0.707
MINIMUM	0.274E 03		0.671E 02	0.195E-04	0.707	0.	-0.707
					-0.707	0.707	0.
					0.707	0.707	0.

STRAIN ENERGY 0.1638E-01  
STRAIN ENERGY OF DISTORTION 0.9015E-02

F-54



## APPENDIX G: REFERENCES

1. Department of Transportation, Federal Aviation Administration, "Airport Pavement Design and Evaluation," Advisory Circular AC 150/5320-6B, May 1974, Washington, D. C.
2. Headquarters, Department of the Army, "Army Airfield and Heliport Rigid and Overlay Pavement Design," Technical Manual TM 5-823-3, Oct 1968, Washington, D. C.
3. \_\_\_\_\_, "Rigid Pavements for Airfields Other Than Army," Technical Manual TM 5-824-3 or Air Force Manual 88-6, Chapter 4, Nov 1970, Washington, D. C.
4. Department of the Navy, Naval Facilities Engineering Command, "Airfield Pavements," Design Manual NAVFAC DM-21, Jun 1973, Alexandria, Va.
5. Packard, Robert G., "Design of Concrete Airport Pavement," Engineering Bulletin 050.03P, 1973, Portland Cement Association, Skokie, Ill.
6. Winkler, E., Die Lehre von Elastizität und Festigkeit (On Elasticity and Fixity), Prague, 1867.
7. Westergaard, H. M., "Stresses in Concrete Pavements Computed by Theoretical Analyses," Public Roads, Vol 7, No. 2, Apr 1926, pp. 25-35.
8. Department of Defense, "Test Methods for Pavement, Subgrade, Sub-base, and Base-Course Materials," Military Standard No. MIL-STD-621A, Method 104, Dec 1964, Washington, D. C.
9. American Society for Testing and Materials, "Standard Method for Nonrepetitive Static Plate Load Tests of Soils and Flexible Pavement Components, for Use in Evaluation and Design of Airport and Highway Pavements," Designation D 1196-64, 1975 Annual Book of ASTM Standards, Part 19, 1975, Philadelphia, Pa.
10. Barker, W. R. and Brabston, W. N., "Development of a Structural Design Procedure for Flexible Airport Pavements," Report No. FAA-RD-74-199 (also designated TR S-75-17, U. S. Army Engineer Waterways Experiment Station), Sep 1975, Federal Aviation Administration, Washington, D. C.
11. Burmister, D. M., "The Theory of Stresses and Displacements in Layered Systems and Application to the Design of Airport Runways," Proceedings, Highway Research Board, Vol 23, 1943.



12. Crawford, J. E. and Katona, M. G., "State-of-the-Art for Prediction of Pavement Response," Report No. FAA-RD-75-183 (also designated CR S-75-8, U. S. Army Engineer Waterways Experiment Station), Oct 1975, Federal Aviation Administration, Washington, D. C.
13. Hudson, W. R. and Matlock, H., "Discontinuous Orthotropic Plates and Pavement Slabs," Research Report 56-6, May 1966, Center for Highway Research, Austin, Tex.
14. Saxena, S. K., "Pavement Slabs Resting on Elastic Foundation," Highway Research Record No. 466, 1973, pp. 163-1978.
15. Huang, Y. H. and Wang, S. T., "Finite-Element Analysis of Concrete Slabs and Its Implications for Rigid Pavement Design," Highway Research Record No. 466, 1973, pp. 55-69.
16. Eberhardt, A. C., "Aircraft-Pavement Interaction Studies Phase I: A Finite-Element Model of a Jointed Concrete Pavement on a Non-Linear Viscous Subgrade," Preliminary Report S-19, Jun 1973, Construction Engineering Research Laboratory, CE, Champaign, Ill.
17. Eberhardt, A. C. and Willmer, J. L., "Computer Program for the Finite Element Analysis of Concrete Airfield Pavements," Technical Report S-26, Nov 1973, Construction Engineering Research Laboratory, CE, Champaign, Ill.
18. Pickett, G. et al., "Deflections, Moments, and Reactive Pressures for Concrete Pavements." Bulletin No. 65, Oct 1951, Kansas State College, Manhattan, Kans.
19. Pickett, G. and Ray, G. K., "Influence Charts for Concrete Pavements," Transactions, American Society of Civil Engineers, Vol 116, 1951, pp. 49-73.
20. Peutz, M. G. F., "BISTRO: Computer Program for Layered Systems Under Normal Surface Loads," 1968, Koninklijke/Shell Laboratorium, Amsterdam, Holland.
21. Michelow, J., "Analysis of Stresses and Displacements in an n-Layered Elastic System Under a Load Uniformly Distributed on a Circular Area," Sep 1963, California Research Corporation, Richmond, Calif.
22. Harrison, W. J. et al., "Computer Programs for Circle and Strip Loads on Layered Anisotropic Media," 1972, Division of Applied Geomechanics, Commonwealth Scientific and Industrial Research Organization, Melbourne, Australia.
23. Koninklijke/Shell Laboratorium, "BISAR Users Manual; Layered System Under Normal and Tangential Loads," Jul 1972, Amsterdam, Holland.



24. Headquarters, Department of the Army, "Airfield Flexible Pavements - Air Force," Technical Manual TM 5-824-2 or Air Force Manual 88-6, Chapter 4, Feb 1969, Washington, D. C.
25. Chou, Y. T., "Engineering Behavior of Pavement Materials; State of the Art," Report No. FAA-RD-77-37 (also designated TR S-77-9, U. S. Army Engineer Waterways Experiment Station), Feb 1977, Federal Aviation Administration, Washington, D. C.
26. Department of Transportation, Federal Aviation Administration, "Standard Specifications for Construction of Airports," Advisory Circular 150/5370-1A, May 1968, Washington, D. C.
27. Departments of the Army, Navy, and Air Force, "Military Construction Guide Specification, Bituminous-Stabilized Base Course, Subbase, or Subgrade," MCGS 02693, Mar 1976, Washington, D. C.
28. \_\_\_\_\_, "Military Construction Guide Specification, Lime-Stabilized Base Course, Subbase, or Subgrade," MCGS 02695, Mar 1976, Washington, D. C.
29. \_\_\_\_\_, "Military Construction Guide Specification, Portland Cement-Stabilized Base or Subbase Course for Airfields, Roads, and Streets," MCGS 02694, Jul 1976, Washington, D. C.
30. Yimprasert, P. and McCullough, B. F., "Fatigue and Stress Analysis Concepts for Modifying the Rigid Pavement Design System," Research Report 123-16, Jan 1973, Center for Highway Research, Austin, Tex.
31. Phillippe, R. R. and Mellinger, F. M., "Structural Behavior of Heavy-Duty Concrete Airfield Pavements," Proceedings, Highway Research Board, Vol 31, 1952.
32. Mellinger, F. M. and Sale, J. P., "The Design of Non-Rigid Overlays for Concrete Airfield Pavements," Proceedings, American Society of Civil Engineers, Vol 82, 1956.
33. Hutchinson, R. L., "Basis for Rigid Pavement Design for Military Airfields," Miscellaneous Paper No. 5-7, May 1966, U. S. Army Corps of Engineers, Ohio River Division Laboratories, Mariemont, Ohio.
34. Mellinger, F. M., Sale, J. P., and Wathen, T. R., "Heavy Wheel Load Traffic on Concrete Airfield Pavements," Proceedings, Highway Research Board, Vol 36, 1957.
35. Ahlvin, R. G. et al., "Multiple-Wheel Heavy Gear Load Pavement Tests," AFWL-TR-70-113, Vols I-IV (also designated TR S-71-17, U. S. Army Engineer Waterways Experiment Station), Nov 1971, Air Force Weapons Laboratory, Kirtland AFB, N. Mex.



36. Brown, D. N. and Thompson, O. O., "Lateral Distribution of Aircraft Traffic," Miscellaneous Paper S-73-56, Jul 1973, U. S. Army Engineer Waterways Experiment Station, CE, Vicksburg, Miss.
37. U. S. Army Corps of Engineers, Ohio River Division Laboratories, "A Method for Estimating the Life of Rigid Airfield Pavements," Technical Report No. 4-23, Mar 1962, Cincinnati, Ohio.
38. Grau, R. W., "Strengthening of Keyed Longitudinal Construction Joints in Rigid Pavements," Report No. FAA-RD-72-106 (also designated MP S-72-43, U. S. Army Engineer Waterways Experiment Station), Aug 1972, Federal Aviation Administration, Washington, D. C.
39. Burns, C. D. et al., "Comparative Performance of Structural Layers in Pavement Systems; Vol I: Design, Construction, and Behavior Under Traffic of Pavement Test Sections," Report No. FAA-RD-73-198-I (also designated TR S-74-8-I, U. S. Army Engineer Waterways Experiment Station), Jun 1974, Federal Aviation Administration, Washington, D. C.
40. U. S. Army Corps of Engineers, Ohio River Division Laboratories, "Design and Construction Report: Lockbourne Test Track," Jun 1944, Mariemont, Ohio.
41. \_\_\_\_\_, "Lockbourne No. 1 Test Track; Report of Reconstruction," Jan 1945, Mariemont, Ohio.
42. \_\_\_\_\_, "Lockbourne No. 1 Test Track: Final Report," Mar 1946, Mariemont, Ohio.
43. \_\_\_\_\_, "Lockbourne No. 2; 300,000 Pound Experimental Mat: Report of Construction," Jun 1945, Mariemont, Ohio.
44. \_\_\_\_\_, "Lockbourne No. 2; Experimental Mat: Final Report," May 1950, Mariemont, Ohio.
45. \_\_\_\_\_, "Lockbourne No. 3, Overlay Mat Pavement Investigation: Report of Construction," Jun 1948, Mariemont, Ohio.
46. \_\_\_\_\_, "Lockbourne No. 3, Pavement Overlay Investigation: Final Report," Mar 1951, Mariemont, Ohio.
47. \_\_\_\_\_, "Channelized Test Tracks, Sharonville, Ohio: Report of Construction," Technical Report No. 4-7, Mar 1957, Mariemont, Ohio.
48. \_\_\_\_\_, "Heavy-Load Test Tracks: Report of Construction," Technical Report No. 4-17, Feb 1961, Mariemont, Ohio.



49. Brabston, W. N., Barker, W. R., and Harvey, G. G., "Development of a Structural Design Procedure for All-Bituminous Concrete Pavements for Military Roads," Technical Report S-75-10, Jul 1975, U. S. Army Engineer Waterways Experiment Station, CE, Vicksburg, Miss.
50. Chou, Y. T., "Evaluation of Nonlinear Resilient Moduli of Unbound Granular Materials from Accelerated Traffic Test Data," Technical Report S-76-12, Aug 1976, U. S. Army Engineer Waterways Experiment Station, CE, Vicksburg, Miss.
51. Chisolm, E. E. and Townsend, F. C., "Behavioral Characteristics of Gravelly Sand and Crushed Limestone for Pavement Design," Report No. FAA-RD-75-117 (also designated TR S-76-17, U. S. Army Engineer Waterways Experiment Station), Sep 1976, Federal Aviation Administration, Washington, D. C.
52. Hicks, R. G., Factors Influencing the Resilient Properties of Granular Materials, Ph.D. Dissertation, 1970, University of California, Berkeley, Calif.
53. Hutchinson, R. L. and Wathen, T. R., "Strengthening Existing Airport Pavements," Proceedings, American Society of Civil Engineers, Vol 88, 1962.
54. Philippe, R. R., "Use of Reinforcement in Concrete Pavements," Proceedings, Highway Research Board, Vol 28, 1948.
55. American Society for Testing and Materials, "Standard Method of Obtaining and Testing Drilled Cores and Sawed Beams of Concrete," Designation: C 42-68, 1975 Annual Book of ASTM Standards, Part 14, 1975, Philadelphia, Pa.
56. U. S. Army Engineer Waterways Experiment Station, CE, Handbook for Concrete and Cement, Aug 1949 (with quarterly supplements), Vicksburg, Miss.
57. American Society for Testing and Materials, "Standard Method of Test for Flexural Strength of Concrete (Using Simple Beam With Third-Point Loading)," Designation: C 78-75, 1975 Annual Book of ASTM Standards, Part 14, 1975, Philadelphia, Pa.
58. \_\_\_\_\_, "Standard Method of Test for Splitting Tensile Strength of Cylindrical Concrete Specimens," Designation: C 496-71, 1975 Annual Book of ASTM Standards, Part 14, 1975, Philadelphia, Pa.
59. Hammitt, G. M., II, "Concrete Strength Relationships," Miscellaneous Paper S-74-3, Dec 1974, U. S. Army Engineer Waterways Experiment Station, CE, Vicksburg, Miss.



60. Raithby, K. D. and Whiffin, A. C., "Failure of Plain Concrete Under Fatigue Loading - A Review of Current Knowledge," Report LR 231, 1968, Road Research Laboratory, Ministry of Transport, Crowthorne, Great Britain.
61. Forrest, J. B., Katona, M. G., and Griffin, D. F., "Layered Pavement Systems - Part II: Fatigue of Plain Concrete," Technical Report R-763, Apr 1972, Naval Civil Engineering Laboratory, Port Hueneme, Calif.
62. Hutchinson, R. L. and Vedros, P. J., "Performance of Heavy-Load Portland Cement Concrete (Rigid) Airfield Pavements," Proceedings, International Conference on Concrete Pavement Design, Feb 1977, Purdue University, pp. 187-203.
63. Ledbetter, R. H., "Pavement Response to Aircraft Dynamic Loads, Vol II, Presentation and Analysis of Data," Report No. FAA-RD-74-39-II (also designated TR S-75-11, U. S. Army Engineer Waterways Experiment Station), Sep 1975, Federal Aviation Administration, Washington, D. C.
64. Lysmer, J. and Duncan, J. M., "Stresses and Deflections in Foundations and Pavements," Fourth Edition, 1969, Institute of Transportation and Traffic Engineering, University of California, Berkeley, Calif.
65. American Society for Testing and Materials, "Standard Method of Making and Curing Soil-Cement Compression and Flexural Test Specimens in the Laboratory," Designation: D 1632-63, 1975 Annual Book of ASTM Standards, Part 19, 1975, Philadelphia, Pa.
66. \_\_\_\_\_, "Standard Recommended Practice for Preparation of Bituminous Mixture Beam Specimens by Means of the California Kneading Compactor," Designation: D 3202-73, 1975 Annual Book of ASTM Standards, Part 15, 1975, Philadelphia, Pa.
67. Office, Chief of Engineers, Department of the Army, "Laboratory Soils Testing," Engineer Manual EM 1110-2-1906, 30 Nov 1970, Washington, D. C.
68. \_\_\_\_\_, "Soil Sampling," Engineer Manual EM 1110-2-1907, Mar 1972, Washington, D. C.

In accordance with letter from DAEN-RDC, DAEN-ASI dated 22 July 1977, Subject: Facsimile Catalog Cards for Laboratory Technical Publications, a facsimile catalog card in Library of Congress MARC format is reproduced below.

Parker, Frazier

Development of a structural design procedure for rigid airport pavements / by Frazier Parker ... [et al.]. Vicksburg, Miss. : U. S. Waterways Experiment Station ; Springfield, Va. : available from National Technical Information Service, 1979.

vi, 110, [183] p. : ill. ; 27 cm. (Technical report - U. S. Army Engineer Waterways Experiment Station ; GL-79-4)

Prepared for Office, Chief of Engineers, U. S. Army, Washington, D. C., under Project Nos. 4A762719AT04 and 4A161102B52E and Federal Aviation Administration, Washington, D. C., under Inter-Agency Agreement No. DOT-FA78WAI-377.

Report No. FAA-RD-77-81.

References: p. G-1 - G-6.

1. Airport pavements. 2. Pavement design. 3. Rigid pavements. I. United States. Army. Corps of Engineers. II. United States. Federal Aviation Administration. III. Series: United States. Waterways Experiment Station, Vicksburg, Miss. Technical report ; GL-79-4.

TA7.W34 no.GL-79-4